

# Field Study of Compaction Monitoring Systems: Self-Propelled Non-Vibratory 825G and Vibratory Smooth Drum CS-533E Rollers



**Final Report**  
**April 2007**

**Sponsored by**  
Caterpillar Inc.



**IOWA STATE**  
**UNIVERSITY**

## **About the PGA**

The mission of the Partnership for Geotechnical Advancement is to increase highway performance in a cost-effective manner by developing and implementing methods, materials, and technologies to solve highway construction problems in a continuing and sustainable manner.

## **Disclaimer Notice**

The contents of this report reflect the views of the authors, who are responsible for the facts and the accuracy of the information presented herein. The opinions, findings and conclusions expressed in this publication are those of the authors and not necessarily those of the sponsors.

The sponsors assume no liability for the contents or use of the information contained in this document. This report does not constitute a standard, specification, or regulation.

The sponsors do not endorse products or manufacturers. Trademarks or manufacturers' names appear in this report only because they are considered essential to the objective of the document.

## **Non-discrimination Statement**

Iowa State University does not discriminate on the basis of race, color, age, religion, national origin, sexual orientation, gender identity, sex, marital status, disability, or status as a U.S. veteran. Inquiries can be directed to the Director of Equal Opportunity and Diversity, (515) 294-7612.

**Technical Report Documentation Page**

<b>1. Report No.</b>	<b>2. Government Accession No.</b>	<b>3. Recipient's Catalog No.</b>	
<b>4. Title and Subtitle</b> Field Study of Compaction Monitoring Systems: Self-Propelled Non-Vibratory 825G and Vibratory Smooth Drum CS-533E Rollers		<b>5. Report Date</b> April 2007	
		<b>6. Performing Organization Code</b>	
<b>7. Authors</b> David J. White, Mark J. Thompson, Pavana Vennapusa		<b>8. Performing Organization Report No.</b>	
<b>9. Performing Organization Name and Address</b> Center for Transportation Research and Education Iowa State University 2711 South Loop Drive, Suite 4700 Ames, IA 50010-8664		<b>10. Work Unit No. (TRAVIS)</b>	
		<b>11. Contract or Grant No.</b>	
<b>12. Sponsoring Organization Name and Address</b> Caterpillar Inc. 100 NE Adams Street Peoria, IL 61629		<b>13. Type of Report and Period Covered</b> Final Report	
		<b>14. Sponsoring Agency Code</b>	
<b>15. Supplementary Notes</b>			
<b>16. Abstract</b> A field study comprised of experimental testing and statistical analyses was conducted to evaluate the Caterpillar machine drive power (MDP) and Geodynamik compaction meter value (CMV) compaction monitoring technologies applied to Caterpillar rollers. The study was comprised of three projects, all of which were conducted at the Caterpillar Edwards Demonstration facility near Peoria, IL. The first project investigated the feasibility of using MDP applied to a Caterpillar self-propelled non-vibratory 825G roller. A test strip was constructed, compacted using the prototype 825G roller, and tested with in situ test devices. The second project also consisted of experimental testing on one-dimensional test strips. This project, however, used five cohesionless base materials, which were compacted using a CS-533E vibratory smooth drum roller with both MDP and CMV measurement capabilities. The independent roller measurements were compared and described in terms of soil engineering properties. The final project was conducted with only one cohesionless material. Four test strips (three uniform strips at different moisture contents and one with variable lift thickness) were constructed and tested to develop relationships between roller measurements and soil engineering properties. Using the material of the test strips, two-dimensional test areas with variable lift thickness and moisture content were then tested. Spatial analyses of the in situ measurements were performed to identify the spatial distribution of soil properties. The interpretation of the ground condition was then compared to machine output for evaluating the roller measurement systems and the proposed roller calibration procedure.			
<b>17. Key Words</b> compaction monitoring—earthwork construction—intelligent compaction— machine energy—quality control/quality assurance—soil compaction		<b>18. Distribution Statement</b> No restrictions.	
<b>19. Security Classification (of this report)</b> Unclassified.	<b>20. Security Classification (of this page)</b> Unclassified.	<b>21. No. of Pages</b> 231	<b>22. Price</b> NA



# **FIELD STUDY OF COMPACTION MONITORING SYSTEMS: SELF-PROPELLED NON-VIBRATORY 825G AND VIBRATORY SMOOTH DRUM CS-533E ROLLERS**

**Final Report  
April 2007**

## **Principal Investigator**

David J. White  
Assistant Professor

Department of Civil, Construction, and Environmental Engineering, Iowa State University

## **Research Assistants**

Mark J. Thompson and Pavana Vennapusa

## **Authors**

David J. White, Mark J. Thompson, and Pavana Vennapusa

Sponsored by  
Caterpillar Inc.

A report from  
**Center for Transportation Research and Education**

**Iowa State University**

2711 South Loop Drive, Suite 4700

Ames, IA 50010-8664

Phone: 515-294-8103

Fax: 515-294-0467

[www.ctre.iastate.edu](http://www.ctre.iastate.edu)



## TABLE OF CONTENTS

ACKNOWLEDGMENTS .....	XIII
EXECUTIVE SUMMARY .....	XV
INTRODUCTION .....	1
Problem Statement .....	1
Research Objectives.....	1
Project Scope .....	2
Phase I Summary .....	2
Phase II Summary .....	3
RESEARCH METHODOLOGY.....	6
Description of Compaction Monitoring Technologies .....	6
In Situ Test Measurements .....	8
Design of Experimental Testing .....	9
PROJECT 1. EDWARDS FACILITY, SELF-PROPELLED NON-VIBRATORY 825G ROLLER.....	10
Project Description and Objectives.....	10
Construction and Testing Operations .....	11
Material Properties.....	14
Compaction Monitor and In Situ Measurements .....	15
Linear Regression Analyses.....	19
Project Observations .....	20
PROJECT 2. EDWARDS FACILITY, CS-533 VIBRATORY SMOOTH DRUM .....	21
Project Description and Objectives.....	21
Construction and Testing Operations .....	22
Material Properties.....	23
Compaction Monitoring and In Situ Measurements.....	29
Regression Analyses .....	52
Project Observations .....	68
PROJECT 3. EDWARDS FACILITY, CS-533 VIBRATORY SMOOTH DRUM .....	70
Project Description and Objectives.....	70
Construction and Testing Operations .....	73
Material Properties.....	80
Machine Calibration Using Regression Analysis .....	81
Analysis of Strip 2 .....	84
Spatial Area 1.....	93
Spatial Area 2.....	101
Spatial Area 3.....	138
Project Observations .....	146
PROJECT SUMMARY .....	147

RECOMMENDATIONS FOR FUTURE RESEARCH.....	149
REFERENCES .....	151
APPENDIX A. PROJECT 1 IN SITU TEST DATA .....	A-1
APPENDIX B. PROJECT 1 DCP PROFILES .....	B-1
APPENDIX C. PROJECT 2 IN SITU TEST DATA.....	C-1
APPENDIX D. PROJECT 2 DCP PROFILES.....	D-1
APPENDIX E. PROJECT 2 PLATE LOAD TEST LOAD-DEFLECTION CURVES.....	E-1
APPENDIX F. PROJECT 3 IN SITU TEST DATA .....	F-1

## LIST OF FIGURES

Figure 1. Machine calibration procedure.....	7
Figure 2. Caterpillar self-propelled non-vibratory 825G roller.....	10
Figure 3. Moisture conditioning test strip.....	11
Figure 4. Reclamation of test strip material.....	12
Figure 5. Compaction of test strip using 825G roller (cont.).....	13
Figure 6. Moisture and density measurement using nuclear moisture-density gauge.....	13
Figure 7. Soil strength measurement using dynamic cone penetrometer.....	13
Figure 8. Edwards till particle size distribution.....	14
Figure 9. Edwards till standard and modified Proctor moisture-density relationships.....	14
Figure 10. Screen captures at two viewing scales for coverage and MDP with the test strip outlined.....	15
Figure 11. MDP compaction history at ten (X, Y) points along the test strip.....	16
Figure 12. Compaction monitoring and field measurement data.....	17
Figure 13. Distribution plots of compaction monitoring and field measurements.....	18
Figure 14. Linear regression results for predicting (a) dry unit weight from MDP, (b) DCP index from MDP.....	19
Figure 15. Caterpillar CS-533 vibratory smooth drum roller.....	21
Figure 16. Test Strips 1-5 (left to right) comprised of base materials.....	22
Figure 17. In situ test performance on Strip 2.....	23
Figure 18. RAP particle size distribution.....	24
Figure 19. CA6-C particle size distribution.....	25
Figure 20. CA5-C particle size distribution.....	25
Figure 21. FA6 particle size distribution.....	26
Figure 22. CA6-G particle size distribution.....	26
Figure 23. RAP standard Proctor moisture-density relationship.....	27
Figure 24. CA6-C standard Proctor moisture-density relationship.....	27
Figure 25. FA6 standard Proctor moisture-density relationship.....	28
Figure 26. CA6-G standard Proctor moisture-density relationship.....	28
Figure 27. Screen captures for RAP after 1, 4, and 11 passes.....	30
Figure 28. Screen captures for CA6-C after 1, 4, and 12 passes.....	31
Figure 29. Screen captures for CA5-C after 1, 4, and 12 passes.....	32
Figure 30. Screen captures for FA6 after 1, 4, and 12 passes.....	33
Figure 31. Screen captures for CA6-G after 1, 4, and 12 passes.....	34
Figure 32. MDP, dry density, DCP index, CIV, and $E_{PFWD}$ data for RAP.....	35
Figure 33. CMV, dry density, DCP index, CIV, and $E_{PFWD}$ data for RAP.....	36
Figure 34. MDP, dry density, DCP index, CIV, and $E_{PFWD}$ data for CA6-C.....	37
Figure 35. CMV, dry density, DCP index, CIV, and $E_{PFWD}$ data for CA6-C.....	38
Figure 36. MDP, dry density, DCP index, CIV, and $E_{PFWD}$ data for CA5-C.....	39
Figure 37. CMV, dry density, DCP index, CIV, and $E_{PFWD}$ data for CA5-C.....	40
Figure 38. MDP, dry density, DCP index, CIV, and $E_{PFWD}$ data for FA6.....	41
Figure 39. CMV, dry density, DCP index, CIV, and $E_{PFWD}$ data for FA6.....	42
Figure 40. MDP, dry density, DCP index, CIV, and $E_{PFWD}$ data for CA6-G.....	43
Figure 41. CMV, dry density, DCP index, CIV, and $E_{PFWD}$ data for CA6-G.....	44
Figure 42. Final pass CMV and subgrade CBR for (a) RAP, (b) CA6-C, (c) CA5-C, (d) FA6, and (e) CA6-G.....	45

Figure 43. Compaction curves for average roller and field measurements for Strip 1 (RAP) .....	47
Figure 44. Compaction curves for average roller and field measurements for Strip 2 (CA6-C)...	48
Figure 45. Compaction curves for average roller and field measurements for Strip 3 (CA5-C)...	49
Figure 46. Compaction curves for average roller and field measurements for Strip 4 (FA6) .....	50
Figure 47. Compaction curves for average roller and field measurements for Strip 5 (CA6-G) ..	51
Figure 48. MDP regression analysis results for Strip 1 (RAP) using average of 10 tests .....	53
Figure 49. CMV regression analysis results for Strip 1 (RAP) using average of 10 tests.....	54
Figure 50. MDP regression analysis results for Strip 2 (CA6-C) using average of 10 tests .....	55
Figure 51. CMV regression analysis results for Strip 2 (CA6-C) using average of 10 tests.....	56
Figure 52. MDP regression analysis results for Strip 3 (CA5-C) using average of 10 tests .....	57
Figure 53. CMV regression analysis results for Strip 3 (CA5-C) using average of 10 tests.....	58
Figure 54. MDP regression analysis results for Strip 4 (FA6) using average of 10 tests.....	59
Figure 55. CMV regression analysis results for Strip 4 (FA6) using average of 10 tests .....	60
Figure 56. MDP regression analysis results for Strip 5 (CA6-G) using average of 10 tests .....	61
Figure 57. CMV regression analysis results for Strip 5 (CA6-G) using average of 10 tests.....	62
Figure 58. MDP-CMV moving average correlation at various length scales for Strip 1 (RAP): (a) 0.2 m, (b) 1 m, (c) 5 m, and (d) 10 m.....	64
Figure 59. MDP-CMV moving average correlation at various length scales for Strip 2 (CA6-C): (a) 0.2 m, (b) 1 m, (c) 5 m, (d) 10 m.....	65
Figure 60. MDP-CMV moving average correlation at various length scales for Strip 3 (CA5-C): (a) 0.2 m, (b) 1 m, (c) 5 m, (d) 10 m.....	66
Figure 61. MDP-CMV moving average correlation at various length scales for Strip 4 (FA6): (a) 0.2 m, (b) 1 m, (c) 5 m, (d) 10 m .....	67
Figure 62. Relationship between averaging length and MDP-CMV regression correlation .....	68
Figure 63. Caterpillar CS-533 vibratory smooth drum roller .....	70
Figure 64. Calibration strip testing program.....	71
Figure 65. Testing plan for Spatial 2 .....	72
Figure 66. Testing plan for Spatial 2 .....	73
Figure 67. Compacting Strip 1.....	73
Figure 68. Excavation for Strip 2.....	74
Figure 69. Placement of fill in Strip 2 excavation .....	75
Figure 70. Excavations for Spatial 2 test area .....	76
Figure 71. Compaction of Spatial 2 .....	77
Figure 72. In situ testing of Spatial 2.....	78
Figure 73. Spatial 3 test area (outlined in white).....	79
Figure 74. Compaction of Spatial 3 .....	79
Figure 75. CA6-G particle size distribution.....	81
Figure 76. CA6-G standard Proctor moisture-density relationship .....	81
Figure 77. Multiple regression analysis results for Strip 1 (a-c) .....	83
Figure 78. MDP and CMV for Passes 1, 2, and 8 on Strip 2.....	84
Figure 79. Strip 2 DCP profiles for Passes 0, 1, and 2 .....	85
Figure 80. Strip 2 DCP profiles for Passes, 4, 8, and 16 .....	86
Figure 81. Compaction curves for six lift thicknesses (Strip 2) .....	87
Figure 82. PFWD test in an excavated trench .....	88
Figure 83. DCP index and $E_{PFWD}$ profiles for Strip 2 after 16 roller passes.....	89
Figure 84. $E_{PFWD}$ and dry unit weight profiles for Strip 2 after 16 roller passes .....	89
Figure 85. DCP index and dry unit weight profiles for Strip 2 after 16 roller passes .....	90

Figure 86. Relationship between mean CMV and MDP, and mean $E_{PFWD}$ , DCP index, and dry unit weight along Strip 2 at different test locations.....	92
Figure 87. Preparation and compaction of spatial test area 1 .....	94
Figure 88. Compaction monitor views for trial spatial analysis: (a) MDP, (b) CMV .....	95
Figure 89. Location of the 144 measurements taken within the study area.....	96
Figure 90. DCP index variogram, surface plot, and contour plot of kriged DCP index.....	97
Figure 91. CIV variogram, surface plot, and contour plot of kriged CIV .....	98
Figure 92. MDP variogram, surface plot, and contour plot of kriged MDP.....	99
Figure 93. CMV variogram, surface plot, and contour plot of kriged CMV .....	100
Figure 94. Distribution plots of compaction monitoring and field measurements for 200 mm and 510 mm lift thicknesses (Pass 2).....	102
Figure 95. Distribution plots of MDP for 200 mm and 510 mm lift thicknesses (all passes) .....	103
Figure 96. Distribution plots of CMV for 200 mm and 510 mm lift thicknesses (all passes).....	104
Figure 97. MDP (kJ/s) output at (a) Pass 1, (b) Pass 2, (c) Pass 3, and (d) Pass 4.....	106
Figure 98. MDP (kJ/s) output at (a) Pass 5, (b) Pass 6, (c) Pass 7, and (d) Pass 8.....	107
Figure 99. MDP (kJ/s) output at (a) Pass 9, (b) Pass 10, (c) Pass 11, and (d) Pass 12.....	108
Figure 100. CMV output at (a) Pass 1, (b) Pass 2, (c) Pass 3, and (d) Pass 4 .....	109
Figure 101. CMV output at (a) Pass 5, (b) Pass 6, (c) Pass 7, and (d) Pass 8 .....	110
Figure 102. CMV output at (a) Pass 9, (b) Pass 10, (c) Pass 11, and (d) Pass 12 .....	111
Figure 103. Roller elevation difference at (a) Pass 1, (b) Pass 2, (c) Pass 3, and (d) Pass 4 .....	112
Figure 104. Roller elevation difference at (a) Pass 5, (b) Pass 6, (c) Pass 7, and (d) Pass 8.....	113
Figure 105. Roller elevation difference at (a) Pass 9, (b) Pass 10, (c) Pass 11, and (d) Pass 12.....	114
Figure 106. Experimental variograms (points) and variogram models (lines) for MDP.....	116
Figure 107. MDP cross-validation results (measured versus estimated observations) .....	117
Figure 108. Experimental variograms (points) and variogram models (lines) for CMV .....	119
Figure 109. CMV cross-validation results (measured versus estimated observations).....	120
Figure 110. Kriged MDP (kJ/s) for (a) Pass 1, (b) Pass 2, (c) Pass 3, (d) Pass 4.....	122
Figure 111. Kriged MDP (kJ/s) for (a) Pass 5, (b) Pass 6, (c) Pass 7, (d) Pass 8.....	123
Figure 112. Kriged MDP (kJ/s) for (a) Pass 9, (b) Pass 10, (c) Pass 11, (d) Pass 12.....	124
Figure 113. Kriged CMV for (a) Pass 1, (b) Pass 2, (c) Pass 3, (d) Pass 4 .....	125
Figure 114. Kriged CMV for (a) Pass 5, (b) Pass 6, (c) Pass 7, (d) Pass 8 .....	126
Figure 115. Kriged CMV for (a) Pass 9, (b) Pass 10, (c) Pass 11, (d) Pass 12 .....	127
Figure 116. Experimental (points) and model (lines) variograms for in situ measurements of Spatial 2 .....	129
Figure 117. Cross validation results (measured versus estimated observations) for in situ properties at Spatial 2 .....	130
Figure 118. Moisture content for Spatial 2 at Pass 2.....	131
Figure 119. In situ measurement results: (a) dry density, (b) $E_{PFWD}$ , (c) DCP index, and (d) Clegg impact value.....	133
Figure 120. Levels of compaction monitoring technology use .....	134
Figure 121. Quality acceptance maps based on calibration for (a) MDP data, (b) CMV data, (c) MDP kriged surface, and (d) CMV kriged surface.....	136
Figure 122. Quality acceptance maps based on calibration for (a) dry unit weight, (b) $E_{PFWD}$ , (c) DCP index, and (d) 20-kg CIV .....	137
Figure 123. MDP (kJ/s) output for Spatial 3 at (a) Pass 1 and (b) Pass 4 .....	138
Figure 124. Kriged MDP (kJ/s) at (a) Pass 1 (n = 592) and (b) Pass 4 (n = 1725) .....	138
Figure 125. CMV output for Spatial 3 at (a) Pass 1 and (b) Pass 4.....	139

Figure 126. Kriged CMV at (a) Pass 1 (n = 592) and (b) Pass 4 (n = 1725).....	139
Figure 127. Experimental (points) and model (lines) variograms for in situ measurements of Spatial 2 .....	141
Figure 128. In situ measurement cross-validation results (estimated versus measured observations).....	142
Figure 129. Moisture content for Spatial 2 at Pass 1 .....	143
Figure 130. Field measurement results: (a) dry density, (b) $E_{PFWD}$ , (c) surface DCP index, and (d) 20-kg Clegg impact value.....	144
Figure 131. Edwards till: (a) Pt 1, (b) Pt 2, (c) Pt 3, (d) Pt 4, (e) Pt 5 .....	B-1
Figure 132. Edwards till: (a) Pt 6, (b) Pt 7, (c) Pt 8, (d) Pt 9, (e) Pt 10.....	B-2
Figure 133. Edwards till: (a) Pt 11, (b) Pt 12, (c) Pt 13, (d) Pt 14, (e) Pt 15 .....	B-3
Figure 134. Edwards till: (a) Pt 16, (b) Pt 17, (c) Pt 18, (d) Pt 19, (e) Pt 20 .....	B-4
Figure 135. Strip 1: (a) Pt 1, (b) Pt 2, (c) Pt 3, (d) Pt 4, and (e) Pt 5.....	D-1
Figure 136. Strip 1: (a) Pt 6, (b) Pt 7, (c) Pt 8, (d) Pt 9, and (e) Pt 10.....	D-2
Figure 137. Strip 2: (a) Pt 1, (b) Pt 2, (c) Pt 3, (d) Pt 4, and (e) Pt 5.....	D-3
Figure 138. Strip 2: (a) Pt 6, (b) Pt 7, (c) Pt 8, (d) Pt 9, and (e) Pt 10.....	D-4
Figure 139. Strip 3: (a) Pt 1, (b) Pt 2, (c) Pt 3, (d) Pt 4, and (e) Pt 5.....	D-5
Figure 140. Strip 3: (a) Pt 6, (b) Pt 7, (c) Pt 8, (d) Pt 9, and (e) Pt 10.....	D-6
Figure 141. Strip 4: (a) Pt 1, (b) Pt 2, (c) Pt 3, (d) Pt 4, and (e) Pt 5.....	D-7
Figure 142. Strip 4: (a) Pt 6, (b) Pt 7, (c) Pt 8, (d) Pt 9, and (e) Pt 10.....	D-8
Figure 143. Strip 5: (a) Pt 1, (b) Pt 2, (c) Pt 3, (d) Pt 4, and (e) Pt 5.....	D-9
Figure 144. Strip 5: (a) Pt 6, (b) Pt 7, (c) Pt 8, (d) Pt 9, and (e) Pt 10.....	D-10
Figure 145. Plate load test load-deflection curves: (a) RAP, (b) CA6-C, (c) CA5-C, (d) FA6, and (e) CA6-G.....	E-1

## LIST OF TABLES

Table 1. Project 1 testing program.....	10
Table 2. Project 1 testing material .....	15
Table 3. Project 2 testing program.....	21
Table 4. Project 2 testing materials.....	24
Table 5. Correlation coefficients ( $R^2$ ) for linear regression analyses with MDP as independent variable.....	63
Table 6. Correlation coefficients ( $R^2$ ) for linear regression analyses with CMV as independent variable.....	63
Table 7. Pilot Project 3 testing materials .....	80
Table 8. Coefficients for machine calibration regression analysis .....	82
Table 9. Comparison of roller measurements and in situ spot test measurements .....	91
Table 10. Summary of MDP variogram modeling .....	115
Table 11. Summary of CMV variogram modeling.....	118
Table 12. Summary of in situ measurement variogram modeling.....	131
Table 13. Summary of variogram parameters for in situ measurements .....	140
Table 14. In situ measurement summary of Edwards till, 0 roller passes .....	A-1
Table 15. In situ measurement summary of Edwards till, 1 roller pass.....	A-2
Table 16. In situ measurement summary of Edwards till, 2 roller passes .....	A-2
Table 17. In situ measurement summary of Edwards till, 4 roller passes .....	A-3
Table 18. In situ measurement summary of Edwards till, 8 roller passes .....	A-3
Table 19. In situ measurement summary of Edwards till, 12 roller passes .....	A-3
Table 20. Moisture and density summary of RAP, Strip 1, 0 roller passes.....	C-1
Table 21. Stiffness and strength summary of RAP, Strip 1, 0 roller passes .....	C-1
Table 22. Moisture and density summary of RAP, Strip 1, 1 roller pass .....	C-2
Table 23. Stiffness and strength summary of RAP, Strip 1, 1 roller pass .....	C-2
Table 24. Moisture and density summary of RAP, Strip 1, 2 roller passes.....	C-3
Table 25. Stiffness and strength summary of RAP, Strip 1, 2 roller passes .....	C-3
Table 26. Moisture and density summary of RAP, Strip 1, 3 roller passes.....	C-4
Table 27. Stiffness and strength summary of RAP, Strip 1, 3 roller passes .....	C-4
Table 28. Moisture and density summary of RAP, Strip 1, 4 roller passes.....	C-5
Table 29. Stiffness and strength summary of RAP, Strip 1, 4 roller passes .....	C-5
Table 30. Moisture and density summary of RAP, Strip 1, 8 roller passes.....	C-6
Table 31. Stiffness and strength summary of RAP, Strip 1, 8 roller passes .....	C-6
Table 32. Moisture and density summary of RAP, Strip 1, 12 roller passes.....	C-7
Table 33. Stiffness and strength summary of RAP, Strip 1, 12 roller passes .....	C-7
Table 34. Moisture and density summary of CA6-C, Strip 2, 0 roller passes .....	C-8
Table 35. Stiffness and strength summary of CA6-C, Strip 2, 0 roller passes .....	C-8
Table 36. Moisture and density summary of CA6-C, Strip 2, 1 roller pass .....	C-9
Table 37. Stiffness and strength summary of CA6-C, Strip 2, 1 roller pass.....	C-9
Table 38. Moisture and density summary of CA6-C, Strip 2, 2 roller passes .....	C-10
Table 39. Stiffness and strength summary of CA6-C, Strip 2, 2 roller passes .....	C-10
Table 40. Moisture and density summary of CA6-C, Strip 2, 4 roller passes .....	C-11
Table 41. Stiffness and strength summary of CA6-C, Strip 2, 4 roller passes .....	C-11
Table 42. Moisture and density summary of CA6-C, Strip 2, 8 roller passes .....	C-12
Table 43. Stiffness and strength summary of CA6-C, Strip 2, 8 roller passes .....	C-12

Table 44. Moisture and density summary of CA6-C, Strip 2, 12 roller passes .....	C-13
Table 45. Stiffness and strength summary of CA6-C, Strip 2, 12 roller passes .....	C-13
Table 46. Moisture and density summary of CA5-C, Strip 3, 0 roller passes .....	C-14
Table 47. Stiffness and strength summary of CA5-C, Strip 3, 0 roller passes .....	C-14
Table 48. Moisture and density summary of CA5-C, Strip 3, 1 roller pass .....	C-15
Table 49. Stiffness and strength summary of CA5-C, Strip 3, 1 roller pass.....	C-15
Table 50. Moisture and density summary of CA5-C, Strip 3, 2 roller passes .....	C-16
Table 51. Stiffness and strength summary of CA5-C, Strip 3, 2 roller passes .....	C-16
Table 52. Moisture and density summary of CA5-C, Strip 3, 4 roller passes .....	C-17
Table 53. Stiffness and strength summary of CA5-C, Strip 3, 4 roller passes .....	C-17
Table 54. Moisture and density summary of CA5-C, Strip 3, 8 roller passes .....	C-18
Table 55. Stiffness and strength summary of CA5-C, Strip 3, 8 roller passes .....	C-18
Table 56. Moisture and density summary of CA5-C, Strip 3, 12 roller passes .....	C-19
Table 57. Stiffness and strength summary of CA5-C, Strip 3, 12 roller passes .....	C-19
Table 58. Moisture and density summary of FA6, Strip 4, 0 roller passes.....	C-20
Table 59. Stiffness and strength summary of FA6, Strip 4, 0 roller passes.....	C-20
Table 60. Moisture and density summary of FA6, Strip 4, 1 roller pass .....	C-21
Table 61. Stiffness and strength summary of FA6, Strip 4, 1 roller pass .....	C-21
Table 62. Moisture and density summary of FA6, Strip 4, 2 roller passes.....	C-22
Table 63. Stiffness and strength summary of FA6, Strip 4, 2 roller passes.....	C-22
Table 64. Moisture and density summary of FA6, Strip 4, 4 roller passes.....	C-23
Table 65. Stiffness and strength summary of FA6, Strip 4, 4 roller passes.....	C-23
Table 66. Moisture and density summary of FA6, Strip 4, 8 roller passes.....	C-24
Table 67. Stiffness and strength summary of FA6, Strip 4, 8 roller passes.....	C-24
Table 68. Moisture and density summary of FA6, Strip 4, 12 roller passes.....	C-25
Table 69. Stiffness and strength summary of FA6, Strip 4, 12 roller passes.....	C-25
Table 70. Moisture and density summary of CA6-G, Strip 5, 0 roller passes .....	C-26
Table 71. Stiffness and strength summary of CA6-G, Strip 5, 0 roller passes .....	C-26
Table 72. Moisture and density summary of CA6-G, Strip 5, 1 roller pass .....	C-27
Table 73. Stiffness and strength summary of CA6-G, Strip 5, 1 roller pass .....	C-27
Table 74. Moisture and density summary of CA6-G, Strip 5, 2 roller passes .....	C-28
Table 75. Stiffness and strength summary of CA6-G, Strip 5, 2 roller passes .....	C-28
Table 76. Moisture and density summary of CA6-G, Strip 5, 4 roller passes .....	C-29
Table 77. Stiffness and strength summary of CA6-G, Strip 5, 4 roller passes .....	C-29
Table 78. Moisture and density summary of CA6-G, Strip 5, 8 roller passes .....	C-30
Table 79. Stiffness and strength summary of CA6-G, Strip 5, 8 roller passes .....	C-30
Table 80. Moisture and density summary of CA6-G, Strip 5, 12 roller passes .....	C-31
Table 81. Stiffness and strength summary of CA6-G, Strip 5, 12 roller passes .....	C-31
Table 82. Summary of Spatial 2 in situ test data .....	F-1
Table 83. Summary of Spatial 2 in situ test data .....	F-2
Table 84. Summary of Spatial 2 in situ test data .....	F-3
Table 85. Summary of Spatial 2 in situ test data .....	F-4
Table 86. Summary of Spatial 2 in situ test data .....	F-5
Table 87. Summary of Spatial 3 in situ test data .....	F-6
Table 88. Summary of Spatial 3 in situ test data .....	F-7
Table 89. Summary of Spatial 3 in situ test data .....	F-8
Table 90. Summary of Spatial 3 in situ test data .....	F-9

## **ACKNOWLEDGMENTS**

This study was funded by Caterpillar Inc. (CAT). Further, this material is based upon work supported by a National Science Foundation Graduate Research Fellowship. This support is greatly appreciated. E. Tom Cackler of the Center for Transportation Research and Education helped organized this research effort. Paul Corcoran, Tom Congdon, Donald Hutchen, Allen DeClerk, and Glen Feather of CAT provided assistance with field testing. The authors would also like to acknowledge the assistance of Heath Gieselmann, Muhannad Suleiman, Lifeng Li, Allison Moyer, Jeremy McIntyre, Mike Kruse, and Amy Heurung for providing assistance with field testing.



## **EXECUTIVE SUMMARY**

Compaction monitoring technologies have recently been incorporated into quality control practices of transportation earthwork projects in the United States, and the use of such technology is anticipated to increase in upcoming years. Transportation agencies and contractors are implementing this technology with the expectation that the systems will (1) improve construction efficiency, (2) streamline quality management programs of earthwork projects, (3) better link quality acceptance parameters and documentation with pavement design, and (4) improve the performance of compacted materials.

To realize these expectations and accelerate the implementation of compaction monitoring technology into practice, detailed and statistically robust field studies leading to improved understanding of the relationships between machine parameters and soil engineering properties are needed. The empirical relationships between roller-generated data and soil engineering properties, which are influenced by the operating conditions of the various machines (e.g., roller size, vibration amplitude and frequency, velocity) and soil conditions (e.g., soil type, moisture content, lift thickness, underlying layer stiffness), are identified using experimental testing and statistical analysis methods with special consideration for the nature and variability of the measurement systems.

### **Research Summary**

A field study comprised of experimental testing and statistical analyses was conducted to evaluate the Caterpillar Inc. machine drive power (MDP) and Geodynamik compaction meter value (CMV) compaction monitoring technologies applied to Caterpillar rollers. The study consisted of three projects, all of which were conducted at the Caterpillar Edwards Demonstration facility near Peoria, Illinois.

The first project investigated the feasibility of using MDP applied to a Caterpillar self-propelled non-vibratory 825G roller. A test strip was constructed, compacted using the prototype 825G roller, and tested with in situ test devices.

The second project also consisted of experimental testing on one-dimensional test strips. This project, however, used five cohesionless base materials, which were compacted using a CS-533E vibratory smooth drum roller with both MDP and CMV measurement capabilities. The independent roller measurements were compared and described in terms of soil engineering properties.

The final project was conducted with only one cohesionless material. Four test strips (three uniform strips at different moisture contents and one with variable lift thickness) were constructed and tested to develop relationships between roller measurements and soil engineering properties. Using the material of the test strips, two-dimensional test areas with variable lift thickness and moisture content were then tested. Spatial analyses of the in situ measurements were performed to identify the spatial distribution of soil properties. The

interpretation of the ground condition was then compared to machine output for evaluating the roller measurement systems and the proposed calibration procedure.

## **Research Conclusions**

Some of the significant conclusions drawn from this investigation are as follows:

- Validation of MDP technology for alternative roller configurations has broad implications for earthwork construction practice.
- Testing a single test point does not provide a high level of confidence for being representative of the average material characteristics, particularly when dealing with variable compaction monitoring data and variable soil conditions. In the case of comparing machine parameters to field measurements, soil property variation and measurement influence area must be considered. For performing statistical analyses, data were averaged over the test strip area at each stage of compaction.
- The effect of soil compaction on roller machine-ground interaction is to decrease MDP (rolling resistance) and increase CMV (soil stiffness response). The change in compaction monitoring data with each roller pass can be described in terms of compaction measurements through logarithmic or linear relationships. Correlation coefficients (i.e.,  $R^2$  values) for the regressions often exceed 0.90.
- The local variation in MDP is generally greater than that of CMV for soils tested during this field study. Coefficients of variation and standard deviations for CMV and MDP, respectively, vary between test strips (soil types), despite being within a relatively narrow range for an individual test strip.
- MDP was shown to be locally variable, but repeatable for multiple passes. The measurement was noted to be significantly affected by the soil characteristics of the compaction layer. For a two-dimensional test area, MDP provided some indication of differential lift thickness.
- CMV accurately identified the regions of thick lift on a two-dimensional test area with variable lift thickness and moisture content.
- Several challenges in generating a precise and reliable map of a compaction measurement based on compaction monitoring data and a calibration equation were identified, including (1) measurement influence depth, (2) variable compaction monitoring measurements, and (3) influences of underlying soil layers on machine response.

## **Recommendations for Implementation**

For this research study, MDP technology was evaluated on a Caterpillar 825G roller to indicate compaction of Edwards till material. The ability of the roller to identify the state of the soil was verified with in situ testing. The feasibility of using this compaction monitoring technology for alternative roller configurations should continue to be studied because such an effort would have broad implications for earthwork construction. Specifically, the mechanical performance of various machines should be investigated with the goal of identifying machine internal loss coefficients for correcting gross power output for net power. Then, more calibration strip testing may be performed to identify the relationships between MDP and soil engineering properties for the various machines.

Developing tools for managing and analyzing compaction monitoring data is an ongoing effort. These tools will be particularly important and necessary for inspectors of earthwork construction. Geostatistics have recently been used to analyze and view compaction monitoring data. Further investigation should be conducted to evaluate whether this approach to interpreting near-continuous data is appropriate and valid. Other methods for representing spatial data should be investigated. Such tools may include software for handheld computers, such that inspectors may see what roller operators see on the onboard compaction monitor. The software may also include features for performing statistical analyses using raw data without the need for an engineer to post-process the data.



## **INTRODUCTION**

### **Problem Statement**

Compaction monitoring technologies have been incorporated into quality control practices of transportation earthwork projects in the United States. The use of such technology is anticipated to increase in upcoming years. Transportation agencies are implementing compaction monitoring technology with the expectation that the systems will (1) improve construction efficiency, (2) streamline quality management programs, (3) link quality acceptance parameters with pavement design, and (4) improve the performance of the compacted materials. To realize these expectations and accelerate the implementation of compaction monitoring technology into practice, detailed field studies leading to improved understanding of the relationships between machine parameters and soil engineering properties are needed. The empirical relationships between machine data and soil properties, which are influenced by operating conditions of the various machines and soil conditions, are identified using experimental testing and statistical analysis methods with consideration of the nature of the measurement systems.

### **Research Objectives**

Widespread use of compaction monitoring technologies requires the applicability of the technologies to a wide range of soil types and field conditions, roller configurations, and operating conditions. Therefore, the following research objectives were established for this study:

- Investigate the feasibility of using machine drive power (MDP) with various roller configurations, including vibratory smooth drum and impact rollers. Static and vibratory padfoot rollers had been used for previous studies.
- Collect data to contribute to ongoing population of a database of intelligent compaction results applied to different soil types and roller machines.
- Evaluate and compare MDP and compaction meter value (CMV) for several cohesionless base materials using vibratory smooth drum roller.
- Describe MDP and CMV in terms of soil engineering properties, including dry density, moisture content, dynamic cone penetration index, Clegg impact value, Geogauge soil stiffness, static plate load test modulus, and light weight deflectometer elastic modulus.
- Evaluate MDP and CMV on two-dimensional areas that incorporate variable stiffness properties and moisture conditions.
- Conduct spatial analyses of in situ measurements to compare with machine data in order to indicate how the results from various measurement systems are related, considering the variability and spatial distribution of soil properties.
- Evaluate the applicability of test strip calibration relationships to two-dimensional areas.
- Document recommendations for future research using compaction monitoring technologies, namely MDP and CMV.

## **Project Scope**

This report summarizes experimental testing programs, field measurements, and statistical analyses performed to evaluate the MDP compaction monitoring technology developed by Caterpillar Inc. and the Geodynamik CMV compaction monitoring technology applied to Caterpillar rollers. The study is comprised of three projects, all of which were conducted at the Caterpillar Edwards Demonstration Arena near Peoria, Illinois.

The first project investigated the feasibility of using MDP applied to a Caterpillar 825G roller. A test strip was constructed, compacted using the prototype 825G roller, and tested with in situ test devices. The second project was also comprised of experimental testing on one-dimensional test strips. This project, however, used five cohesionless base materials, which were compacted using a vibratory smooth drum roller with both MDP and CMV measurement capabilities. The independent roller measurements (MDP and CMV) were compared and described in terms of soil engineering properties. The final project was conducted with only one cohesionless material. Four test strips (three uniform strips at different moisture contents and one with variable lift thickness) were constructed and tested to develop relationships between roller measurements and soil engineering properties. Using the material of the test strips, two-dimensional tests areas with variable lift thickness and moisture content were then tested. Spatial analyses of the in situ measurements were performed to identify the spatial distribution of soil properties. The interpretation of the ground condition was then compared to machine output in order to evaluate the roller measurement systems and the proposed calibration procedure.

## **Phase I Summary**

Phase I was initiated in 2003 to begin evaluating the compaction monitoring technology developed by Caterpillar Inc. The technology consists of an instrumented prototype padfoot roller that monitors changes in machine power output resulting from soil compaction and the corresponding changes in machine-soil interaction. The roller, diagrammed, is additionally fitted with a global positioning system (GPS) so that coverage (i.e., history of the roller location) and machine power are mapped and viewed in real-time during compaction operations. The specific objectives of Phase I included (1) a literature review of current compaction monitoring technologies, (2) data collection using the compaction monitoring system and in situ testing devices for comparing machine power to physical soil properties (e.g., density, strength, stiffness), (3) identification of modifications to be made to the technological and communication systems, and (4) identification of the benefits to contractors and owners who may use the technology.

The Phase I report summarized preliminary analyses of data collected during pilot studies at Caterpillar Inc. facilities in Peoria, Illinois, and on an actual earthwork project in West Des Moines, Iowa. At the sites, in situ tests were conducted using currently accepted practices to evaluate the technology. The field measurements of soil density, moisture content, strength, and stiffness showed a high level of promise for the technology output (machine power) to indicate soil compaction.

The significant research findings from Phase I (White et al. 2004) are summarized as follows:

- Multiple linear regression analyses were performed using machine power and various field measurements (nuclear moisture and density, dynamic cone penetrometer index, Clegg impact value). The  $R^2$  values of the models indicated that compaction energy accounts for more variation in dry unit weight than dynamic cone penetrometer (DCP) index or Clegg impact values (CIV).
- Incorporating moisture content in the regression analyses improved model  $R^2$  values for DCP index and CIV, indicating the influence of moisture content on strength and stiffness.
- The compaction monitoring technology showed a high level of promise for use as a quality control/quality assurance (QC/QA) tool, but was demonstrated for a relatively narrow range of field conditions.

The results of this proof-of-concept study provided evidence that machine power may reliably indicate soil compaction with the advantages of 100% coverage and real-time results. Additional field trials were recommended, however, to expand the range of correlations to other soil types, roller configurations, lift thicknesses, and moisture contents. The observed promise for using such compaction monitoring technology in earthwork QC/QA practices also required developing guidelines for its use, considering a statistical framework for analyzing the near-continuous data.

## **Phase II Summary**

Primary research tasks for the Phase II study involved (1) performing experimental testing and statistical analyses to evaluate machine power in terms of engineering properties of the compacted soil (e.g., density, strength, stiffness) and (2) developing recommendations for using the compaction monitoring technology in practice. For this study, data were collected at three test sites. The first two projects (February and May 2005) were conducted at Caterpillar Inc. facilities near Peoria, Illinois, and included constructing and testing relatively uniform test strips using different soil types, moisture contents, and lift thicknesses. The data collected facilitated linear and multiple linear regression analyses with moisture content, lift thickness, and soil type as regression parameters. The third test site (June 2005) was conducted at an earthwork construction project for the TH 14 bypass near Janesville, Minnesota. For this final project, the ability of the compaction monitoring technology to identify localized areas of weak or poorly-compacted soil was demonstrated by mapping select locations of the project and comparing to the test rolling.

For all test projects, in situ testing of soil density (nuclear moisture-density gauge), strength (DCP, Clegg impact hammer), and stiffness (GeoGauge, light weight deflectometer, plate load test) provided data to characterize the soil at various stages of compaction (i.e., roller passes). For each test strip (i.e., uniform soil type and moisture content) or test area (variable conditions), in situ soil properties were compared directly to machine power values to establish statistical relationships. Using a physical model developed from laboratory compaction energy-dry unit weight moisture content measurements as a basis, statistical models were developed to predict soil density, strength, and stiffness from the machine power values. Field data for multiple test strips (i.e., multiple moisture contents, lift thicknesses, and/or soil types) were evaluated. The  $R^2$  correlation coefficient was generally used to assess the quality of the regressions.

The established research objectives were achieved because the testing methods and operations generated usable data for evaluating machine power in terms of soil compaction measures. Machine power and field measurements were collected at various levels of compaction, including soft, intermediate, and hard materials. Also, using a variety of in situ testing devices to characterize soil density, strength, and stiffness facilitated multiple interpretations about machine power response, not just the conventional approach of determining relative compaction. Future research to investigate compaction monitoring technology may use similar testing procedures, but will isolate other variables affecting machine-soil response (e.g., speed, slope, accelerations, turning radius, etc.).

The major findings from previous studies of the MDP system (White et al. 2006) include the following:

- Using averaged machine power and field measurement data, strong correlations ( $R^2 \geq 0.9$ ) were developed to characterize the machine-soil interaction. These correlations (i.e., models) were initially derived from laboratory compaction data relating compaction energy, moisture content, and dry unit weight. The final models for each combination of soil type, lift thickness, and test device show that machine power is statistically significant in predicting various soil properties. Since the initial physical model was derived from moisture-density relationships, predictions of dry unit weight were often more accurate than predictions of soil strength or stiffness. The complexity of soil strength and stiffness requires that a more complicated physical model be used. Nevertheless, by incorporating moisture content and moisture-energy (i.e., machine power) interaction terms into the regressions, high correlations were achieved and indicate the promise of using such compaction monitoring technology as a tool for earthwork quality control.
- The compaction monitoring technology identified “wet” and “soft” spots incorporated into a test strip, evidenced by relatively high net power values observed at these locations and displayed on the compaction monitor. The difference in net power observed between these locations and the rest of the test strip was considerable; this observation reflects the extreme conditions (i.e., high lift thickness and moisture content) built into the strip design. Future testing may be required to determine and quantify the roller sensitivity to these changes in moisture content and soil lift thickness resulting from variation in construction operations (e.g., fill placement, moisture conditioning, existing site conditions) for a wider range of soil types and for larger test areas.
- The compaction monitoring technology may identify areas of weak or poorly compacted soil with real-time readings and 100% coverage. Two-dimensional spatial mapping trials conducted at the TH 14 bypass earthwork pilot project showed that in situ test measurements and proof rolling verified the compaction monitoring output for cohesive subgrade soils, but showed less certainty in some areas for fine sandy soils.
- The research program revealed that a single in situ test point does not provide a high level of confidence for being representative of the average soil engineering property value over a given area. Rather, variation always exists, and several samples must be tested to determine the soil properties with any confidence. In the case of comparing compaction monitoring output to field measurements, soil property variation and measurement influence area must be considered.
- Investigating the influence of lift thickness on the machine power output data provided

important insight into the factors affecting machine-soil response. The summary of  $R^2$  values for multiple linear regression analyses per soil showed that correlation coefficients for thicker lifts were consistently higher than for the thin lifts. The relative change in  $R^2$  values between thin and thick lifts suggests that the depth influencing machine power response exceeds representative lift thicknesses encountered in field conditions. While the depth to a stabilized base (e.g., any soil layer with differing stiffness properties) affects the field measurements to some degree, the measurement influence depth affects the roller response (higher weight and contact area than in situ test devices) to a greater extent than the in situ tests.

## RESEARCH METHODOLOGY

### Description of Compaction Monitoring Technologies

#### *Machine Drive Power*

The use of MDP as a measure of soil compaction is a concept originating from study of vehicle-terrain interaction. MDP, which relates to the soil properties controlling drum sinkage, uses the concepts of rolling resistance and sinkage to determine the stresses acting on the drum and the energy necessary to overcome the resistance to motion. Using MDP to describe soil compaction, where higher power indicates soft or weak material and lower power indicates compact or stiff material, is documented by White et al. (2004) and White et al. (2006). The net MDP required to propel the machine over a layer of soil can be represented as

$$MDP = P_g - WV \left( \sin \theta + \frac{a}{g} \right) - (mV + b) \quad (1)$$

where  $P_g$  is the gross power needed to move the machine,  $W$  is the roller weight,  $V$  is the roller velocity,  $\theta$  is a slope angle,  $a$  is acceleration of the machine,  $g$  is acceleration of gravity, and  $m$  and  $b$  are machine internal loss coefficients specific to a particular machine (White et al. 2006). The second and third terms of Equation 1 account for the machine power associated with sloping grade and internal machine loss, respectively.

The procedure for calibrating machine power, shown in Figure 1, consists of three steps. Machine power calibration is begun by identifying the orientation of the pitch sensor on the machine (Step 1). The roller is parked on a sloping surface with a known inclination (facing uphill), and the pitch reading is noted (positive slope). The roller is then rotated to face downhill, and the new pitch sensor is noted (negative slope). The average pitch reading for these cases is the offset applied to all sensor readings. The internal loss coefficients ( $m$  and  $b$  in Equation 1) are then determined by operating the roller on a relatively uniform reference surface (i.e., net power is a relative value referencing the physical properties of this surface, with positive values indicating a less compact state). Gross power and slope compensation are then monitored while operating the roller at 3.2, 4.8, and 6.4 kph in both forward and reverse directions (Step 2). At each roller speed, the difference between the gross power output and slope compensation is the internal loss (i.e., propel power). Plotting the slope-compensated machine power against roller speed then provides a linear relationship from which the internal loss coefficients are calculated (Step 3). Application of the pitch offset and internal loss coefficients to Equation 1 thus gives net power readings of about zero for roller operation on the calibration surface.

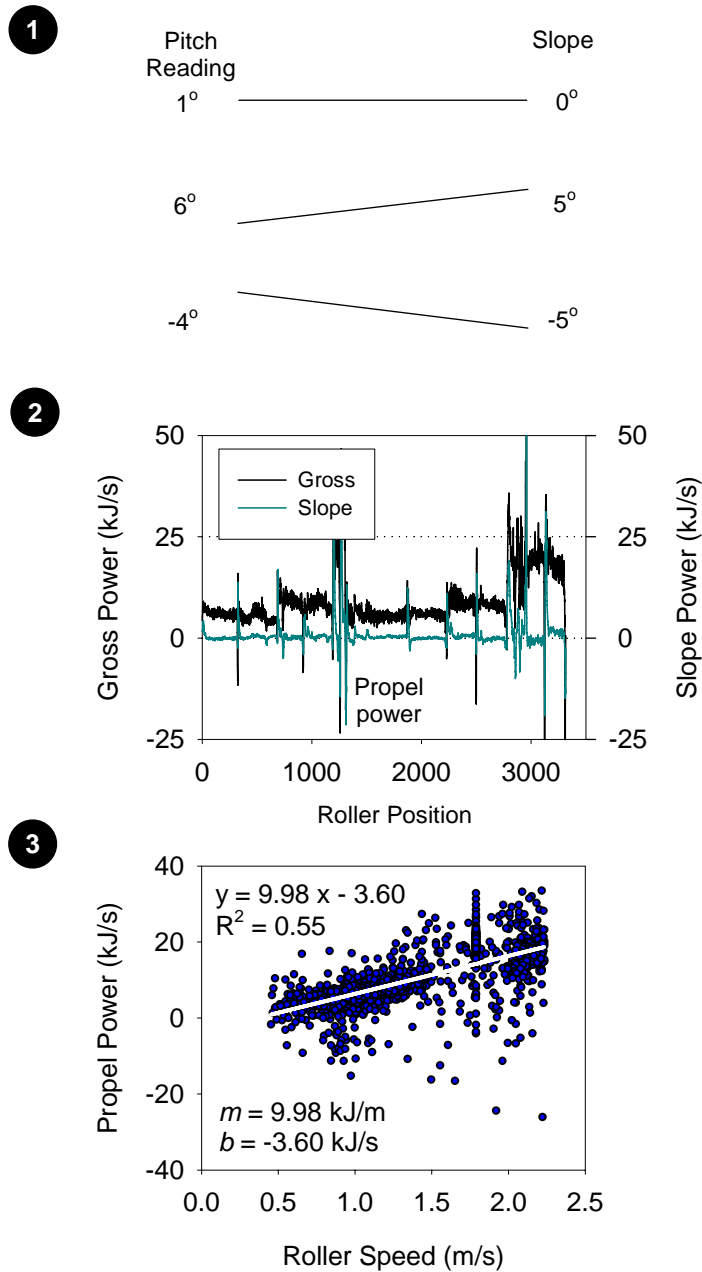


**Figure 1. Machine calibration procedure**

*Compaction Meter Value*

Intelligent vibratory compaction is an equipment-based technology that uses instrumentation to track roller drum accelerations in response to soil behavior during compaction operations. The dynamic response measurements of a vibrating roller drum on soil has been likened to dynamic plate load tests. By installing accelerometers on a roller drum, the force of the drum acting on the soil can be estimated using the first harmonic of the vertical drum acceleration, and drum

displacement can be calculated by integrating the fundamental acceleration. Soil modulus and CMV can be calculated as

$$E_c = c_1 \cdot \frac{F}{h} = c_2 \cdot \frac{1}{\omega^2} \cdot \frac{A_1}{A_0} \quad (2)$$

$$\text{CMV} = C \cdot \frac{A_1}{A_0} \quad (3)$$

where  $E_c$  is cylinder deformation modulus,  $c$  is constant,  $F$  is applied force by the roller drum,  $h$  is drum displacement obtained from the double integral of the fundamental acceleration,  $\omega$  is fundamental angular frequency of the vibration,  $C$  is constant (about 300),  $A_1$  is acceleration of the first harmonic component of the vibration, and  $A_0$  is acceleration of the fundamental component of the vibration (Sandström and Pettersson 2004). The constant in Equation 3 is determined during calibration to give a full-scale reading of 100. Since CMV is determined using dynamic roller response, results are related primarily to the deformation characteristics of soil. As a result, Sandström and Pettersson (2004) advise that CMV should not be expected to correspond directly to either density or percent compaction, particularly for fine-grained soils at above-optimum moisture contents. Finally, CMV is a dimensionless value that depends on roller dimensions (e.g., drum diameter, weight) and roller operation parameters (e.g., frequency, amplitude, speed). In European earthworks practice, each roller with CMV measurement capabilities is calibrated for each project soil type using plate loading tests.

One dataset in Adam (1997) shows CMV values ranging from about 10 to 60. For the production area, the threshold for sufficient compaction was 30. A compaction control chart with a CMV range from 20 to 40 was also documented, suggesting that establishing a lower limit without calibrating CMV to another measured soil property is subject to interpretation. Another example calibration diagram is shown in Adam (1997), with CMV strongly (and linearly) correlated to initial modulus from plate loading tests. The data show a modulus ranging from 35 to 90 MPa and CMV ranging from 20 to 120.

Turner and Sandström (1980) present CMV data for intentionally heterogeneous gravel and subgrade. For both soils, CMV ranges from about 2 to 80. Another dataset for 15-cm thick gravel shows CMV for up to 15 roller passes. For the initial pass, CMV ranged from 5 to 15; for the final pass, CMV ranged from 5 to 60.

## **In Situ Test Measurements**

### *Moisture and Density*

The nuclear moisture-density gauge was incorporated into the testing program to provide a rapid measurement of density and moisture. These tests provided an average measurement over the compaction layer, generally about 200 mm.

## *Soil Strength and Stiffness*

Soil strength and modulus were determined using the Clegg impact hammer, DCP (compaction layer), soil stiffness gauge (SSG), portable falling weight deflectometer (PFWD), and plate load tests (PLT). CIVs have been empirically related to California bearing ratio (CBR). DCP tests were performed to develop strength profiles with depth. For test strips, DCP index values for the compaction layer were used in regressions with MDP and CMV. Determining DCP index values for spatial areas is discussed in the respective report sections. The soil stiffness gauge determined in situ deformation properties of soil, giving both soil stiffness and elastic modulus. SSG stiffness and SSG modulus ( $E_{SSG}$ ) are related linearly, such that only  $E_{SSG}$  was used in performing statistical analyses. The PFWD is equipped with a load sensor and geophone and determines applied load and plate deflection for either a 200- or 300 mm steel plate. The result of this test is elastic modulus.

### **Design of Experimental Testing**

An earlier research project (White et al. 2006) evaluated MDP applied to static and vibratory padfoot rollers for indicating compaction of cohesive soils. Experimental testing for the project described in this report addresses MDP applied to alternative roller configurations for cohesive and cohesionless soils. As before, the experimental designs consider (1) state of soil compaction (i.e., roller pass or percent compaction), (2) soil type, (3) lift thickness, and (4) moisture content.

For Projects 1 and 2, relatively uniform test strips were constructed, with lengths ranging from 25 to 30 m, and were compacted using Caterpillar self-propelled non-vibratory 825G and CS-533 vibratory smooth drum rollers, respectively. MDP (and also CMV for Project 2) were monitored throughout the compaction process. For each test strip, in situ measurements of soil density, strength, and modulus were also collected at various stages of compaction (e.g., 1, 2, 4, 8, and 12 roller passes). The various measurements were then statistically treated and compared for describing machine data in terms of soil engineering properties.

Project 3 initially incorporated one-dimensional test strips that were constructed and tested to develop material- and roller-specific relationships between MDP, CMV, and soil engineering properties. This testing demonstrated the proposed roller calibration procedure that accounts for moisture content. Testing was then conducted on two-dimensional areas to evaluate the applicability of calibration correlations. The spatial testing was also designed to exercise the ability of a roller to identify localized areas of either variable moisture content or lift thickness. Understanding how rollers with integrated compaction monitoring technology identify soil properties is necessary to develop effective quality statements for implementing the technology into earthworks practice.

Details of experimental testing for the three projects are provided in the respective report chapters.

# PROJECT 1. EDWARDS FACILITY, SELF-PROPELLED NON-VIBRATORY 825G ROLLER

## Project Description and Objectives

Establishing the feasibility of applying MDP technology to various roller configurations in order to indicate soil compaction has significant implications for earthwork construction practice. First, validating MDP as an indicator of soil properties broadens the current scope of intelligent compaction and compaction monitoring technology to include non-vibratory systems. Further, MDP applied to alternative roller configurations expands the number of applications for which the technology may be used (e.g., compaction of municipal waste).

Project 1 was conducted at the Caterpillar Edwards Facility from June 28 to June 30, 2005. The testing program for the project consisted of one test strip, which was constructed with Edwards till material at optimum moisture content and compacted using a Caterpillar 825G roller. This 32,734-kg roller has drum diameters of 1.30 m, drum widths of 1.13 m, and a wheelbase of 3.7 m. For this project, the roller was additionally fitted with a GPS system to monitor roller coverage during compaction operation. The testing program is summarized in Table 1. The impact roller is shown in Figure 2.

**Table 1. Project 1 testing program**

Soil type	Strip no.	Loose lift thickness (mm)	Moisture content (%)	Moisture deviation (%) <sup>a</sup>
Till	1	200	12	-1

<sup>a</sup> Moisture deviation from optimum, based on standard Proctor test ( $w - w_{opt}$ )



**Figure 2. Caterpillar self-propelled non-vibratory 825G roller**

MDP measurement capability has recently been introduced to the 825G roller. Therefore, the mechanical performance of the roller has not yet been fully characterized. The reported magnitude of machine power output is accordingly uncertain and acknowledged to be significantly higher than MDP observed during previous studies. Nevertheless, the feasibility of using MDP with alternative roller configurations was successfully investigated.

## Construction and Testing Operations

At the test site, loose Edwards till material was placed over existing, relatively stiff Edwards till subgrade. The material was moisture conditioned to optimum moisture content (12%) using a water truck (see Figure 3). The soil was then mixed in situ using a reclaimer, set to give a nominal loose lift thickness of about 200 mm (see Figure 4). Immediately following construction, the test strip was compacted using the 825G roller, as shown in Figure 5.

For testing, ten test points were established at about 2.5 m intervals in the center of each roller wheel path. At each length interval (either left or right), density and moisture content of the soil were determined using a nuclear moisture-density gauge (see Figure 6). Soil strength was determined with DCP testing, as shown in Figure 7. For this project, the mean DCP index at the bottom of the compaction layer was used for analysis. This parameter is calculated as follows

$$\text{DCP Index} = \frac{\text{PI}_1 z_1 + \text{PI}_2 z_2 + \dots + \text{PI}_n z_n}{\sum_{i=1}^n z_i} \quad (4)$$

where PI is penetration index (penetration per blow) for a set of drops, and z is penetration for the same set of drops. Soil testing with in situ devices followed Passes 1, 2, 4, 8, and 12.



**Figure 3. Moisture conditioning test strip**



**Figure 4. Reclamation of test strip material**



**Figure 5. Compaction of test strip using 825G roller**



**Figure 5. Compaction of test strip using 825G roller (cont.)**



**Figure 6. Moisture and density measurement using nuclear moisture-density gauge**



**Figure 7. Soil strength measurement using dynamic cone penetrometer**

## Material Properties

Testing was conducted using Edwards glacial till material. This moderately plastic soil is fine grained and classifies as CL Sandy lean clay. Figure 8 shows the particle size distribution curve.

Moisture-density tests were performed following the Standard and Modified Proctor test methods (ASTM D 698-00 and ASTM D 1557-98, respectively). The moisture-density curves are provided in Figure 9. The Standard maximum dry unit weight was about  $18.6 \text{ kN/m}^3$ , with optimum moisture content at approximately 13.0%. The Modified maximum dry unit weight was about  $19.9 \text{ kN/m}^3$ , with optimum moisture content at approximately 7.0%. Engineering properties for the material are provided in Table 2.

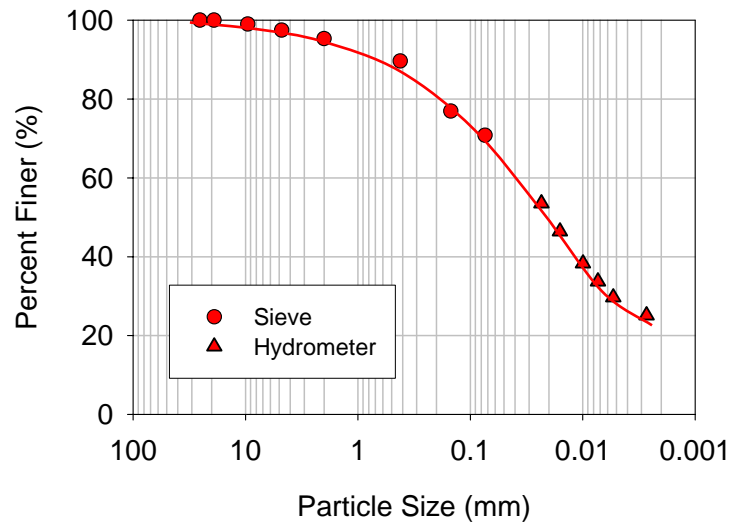


**Figure 8. Edwards till particle size distribution**

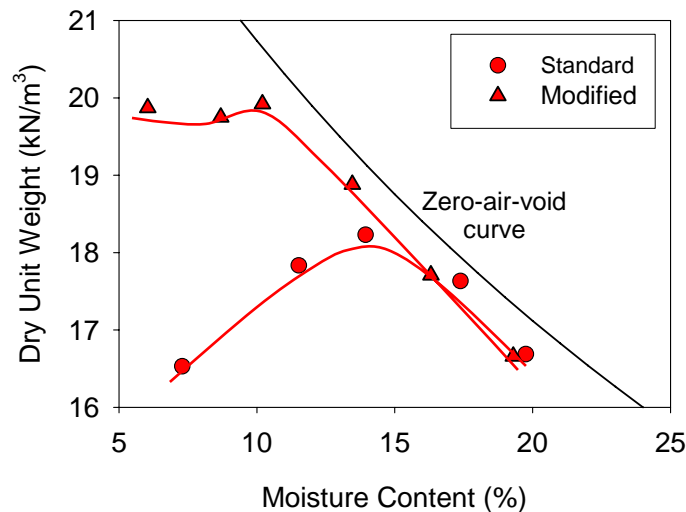


**Figure 9. Edwards till standard and modified Proctor moisture-density relationships**

**Table 2. Project 1 testing material**

Soil property	Edwards till
USCS:	
Symbol	CL
Name	Sandy lean clay
$G_s$	2.75
$F_{200}$ (%)	68
LL (PI)	29 (12)
Standard Proctor:	
$\gamma_{d, \max}$ ( $\text{kN/m}^3$ ) <sup>a</sup>	18.6
$w_{\text{opt}}$ (%) <sup>a</sup>	13.0
Modified Proctor:	
$\gamma_{d, \max}$ ( $\text{kN/m}^3$ ) <sup>b</sup>	19.9
$w_{\text{opt}}$ (%) <sup>b</sup>	10.0

### Compaction Monitor and In Situ Measurements

Compaction monitoring technology output is summarized in Figure 10 using screen captures from the Caterpillar Viewer program. Compaction history at ten 3 m spaced locations along the test strip is shown in Figure 11, also obtained from the Caterpillar Viewer program.

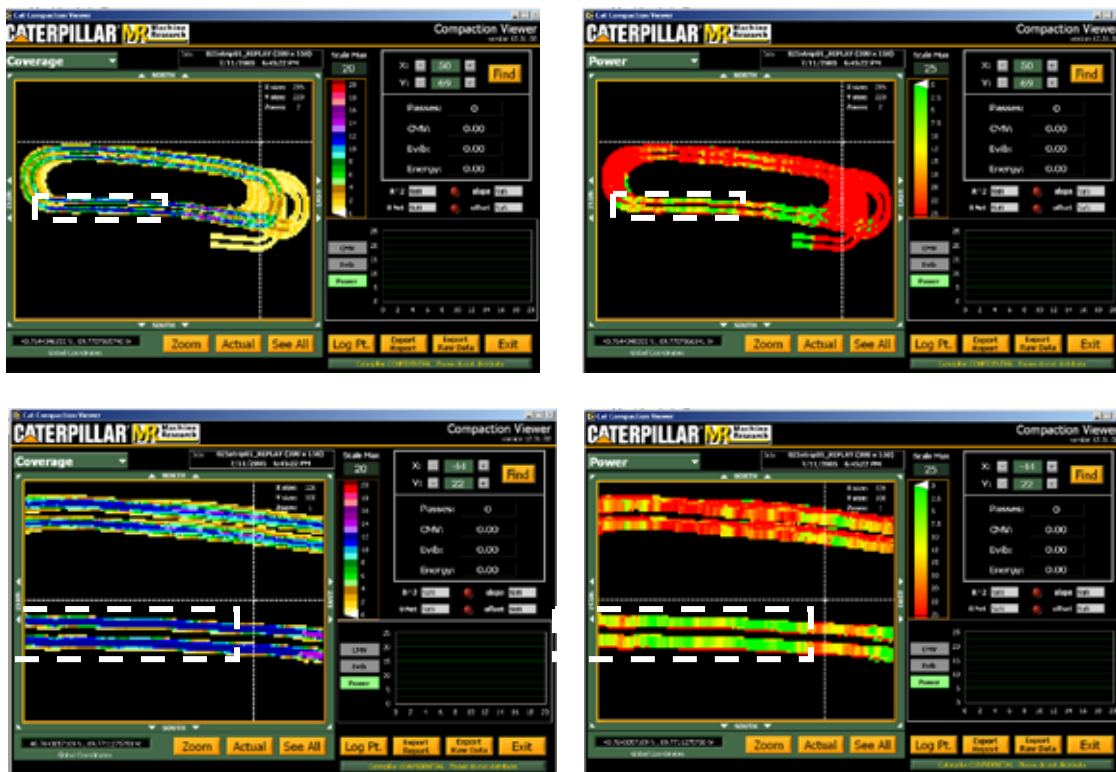


**Figure 10. Screen captures at two viewing scales for coverage and MDP with the test strip outlined**

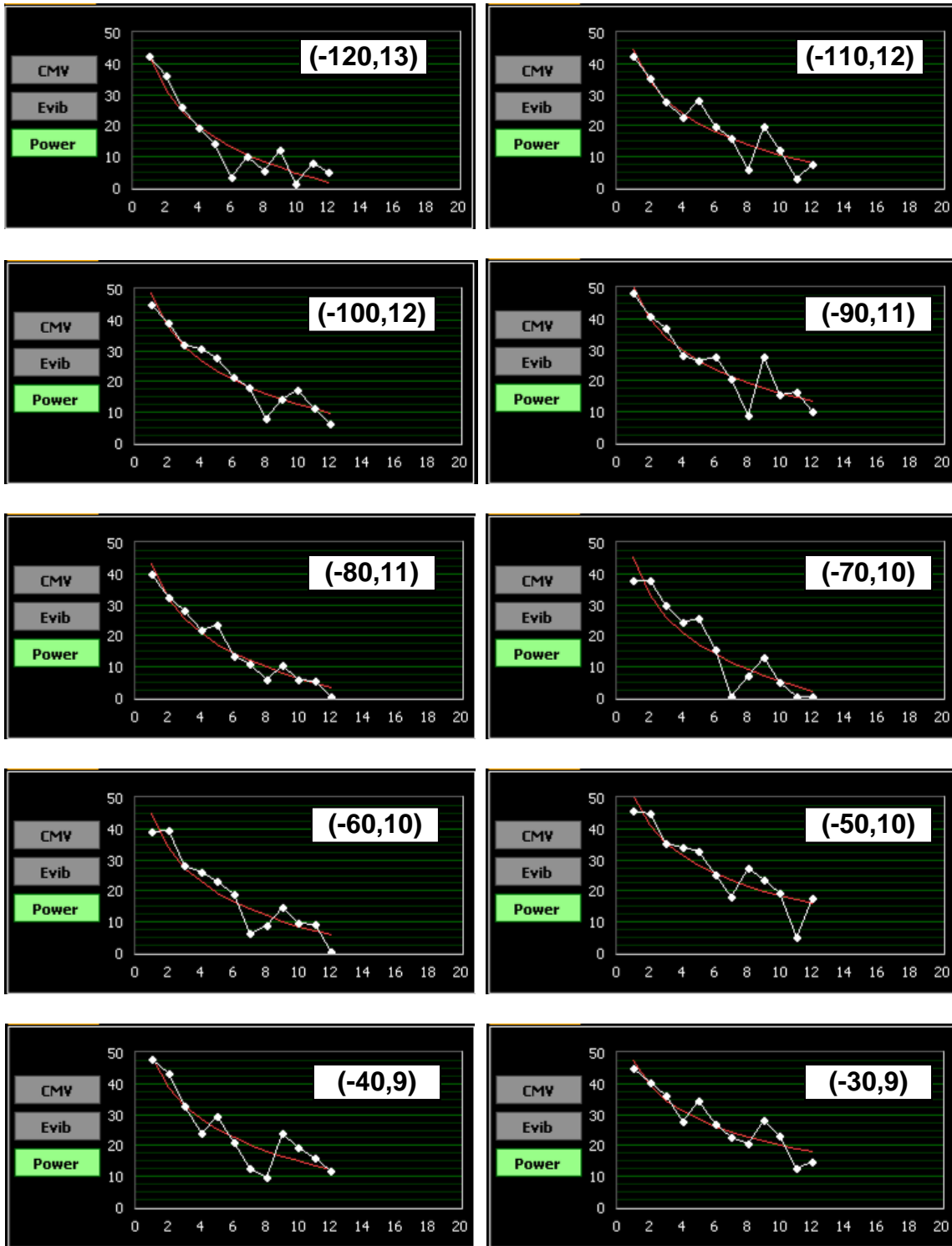
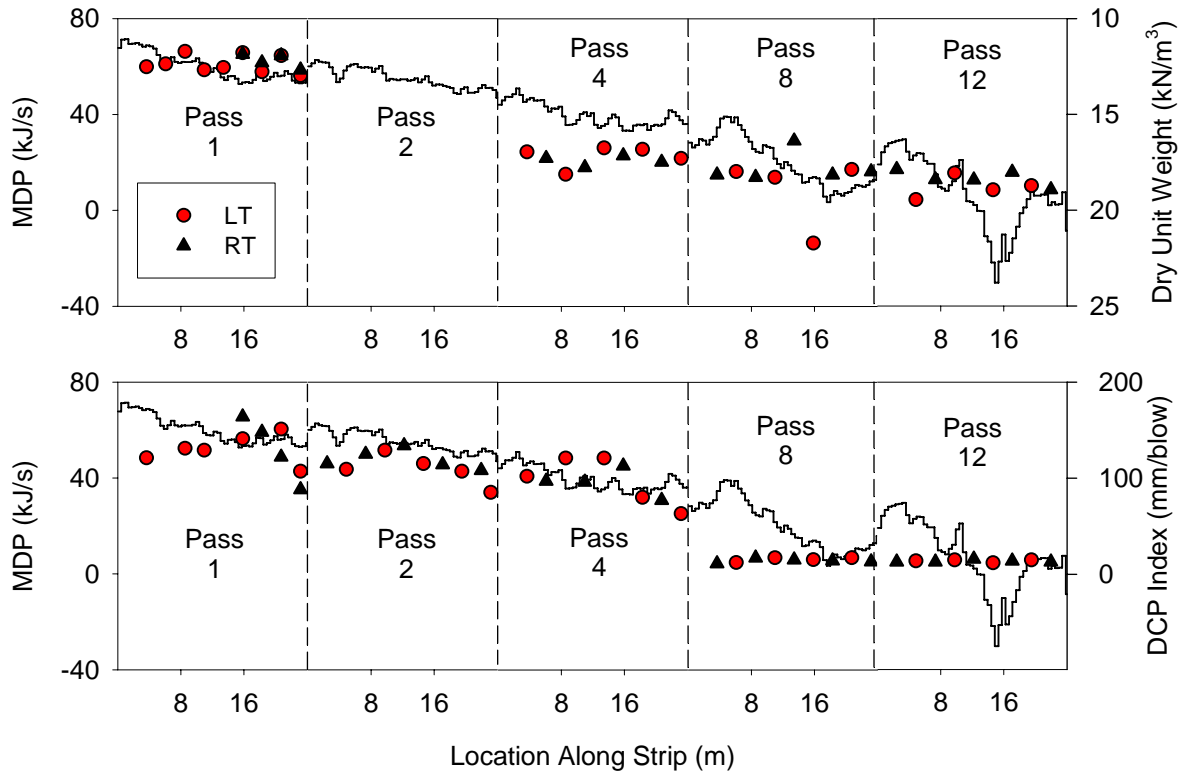


Figure 11. MDP compaction history at ten (X, Y) points along the test strip

In situ measures of soil density and strength were collected concurrent with MDP. MDP and in situ test data are plotted with the test strip location in Figure 12 for all passes. MDP, which ranges from 0 to 70 kJ/s throughout the compaction process, is observed to decrease with increasing roller passes. And, for each roller pass, MDP is higher at the beginning of the test strip than at the end, indicating a heterogeneous condition. Since this trend was not observed with the in situ measurements of the compaction layer, the source of variation may be variable subgrade conditions.



**Figure 12. Compaction monitoring and field measurement data**

Following the findings of previous studies, frequency distribution plots were created to investigate the nature of the respective measurements (see Figure 13). MDP, as previously observed, decreases with the increasing number of roller passes, which is consistent with compaction of the material and less resistance to mechanical motion. The standard deviation of the data, however, increases. The reclaimed and uncompacted material is likely to be quite uniform. As the soil is compacted, the soil deviates from this condition to give progressively variable measurements.

Just as MDP provides an indication of soil compaction, dry density and DCP index show the effect of increasing roller passes on the respective soil properties. Dry density increases from about 12.3 kN/m<sup>3</sup> after 1 roller pass to about 18.3 kN/m<sup>3</sup> (98% compaction) following 12 roller passes. DCP index decreases from about 130 to 15 mm/blow. Coefficients of variation ( $C_v$ ) for dry density ranged from 2% to 8%, while  $C_v$  for DCP index ranged from 12% to 21%.

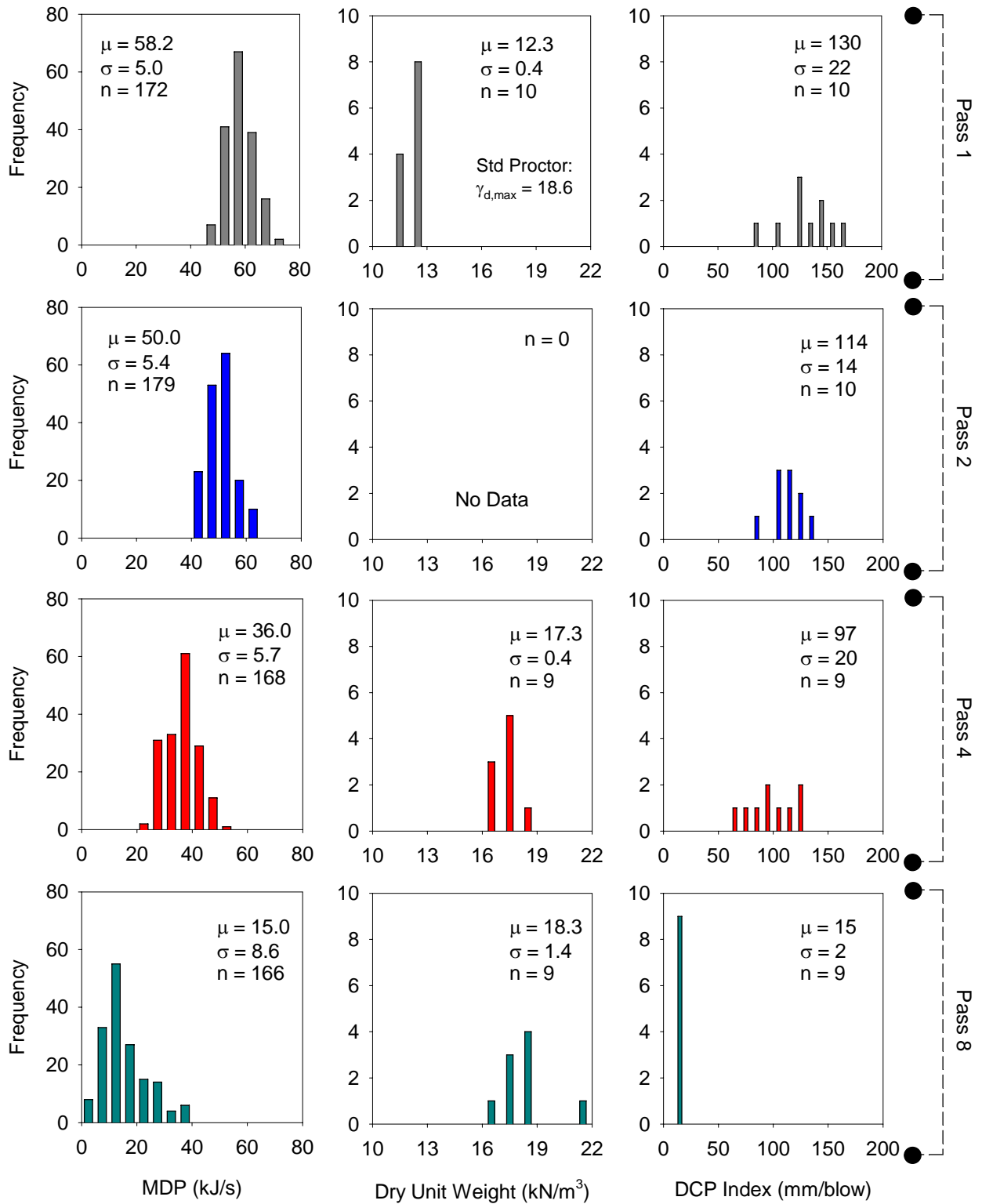


**Figure 13. Distribution plots of compaction monitoring and field measurements**

## Linear Regression Analyses

To further support MDP as a quantifiable indicator of soil compaction and change in soil condition, the relationships between roller and in situ spot measurements were investigated. The averages of data along the test strip were used to develop scatter plots relating MDP and in situ measurements, with each point representing the average measurement following a given roller pass. Averaging the data clearly minimizes the observed scatter in these relationships and mitigates the effect of variable measurements. Predictions of dry density and DCP index from MDP are shown in Figure 14. A negative relationship is observed between dry density and MDP. The linear relationship is largely controlled by the first data point (MDP of about 60). A strong linear relationship is observed between MDP and DCP index, with an  $R^2$  value of 0.96.

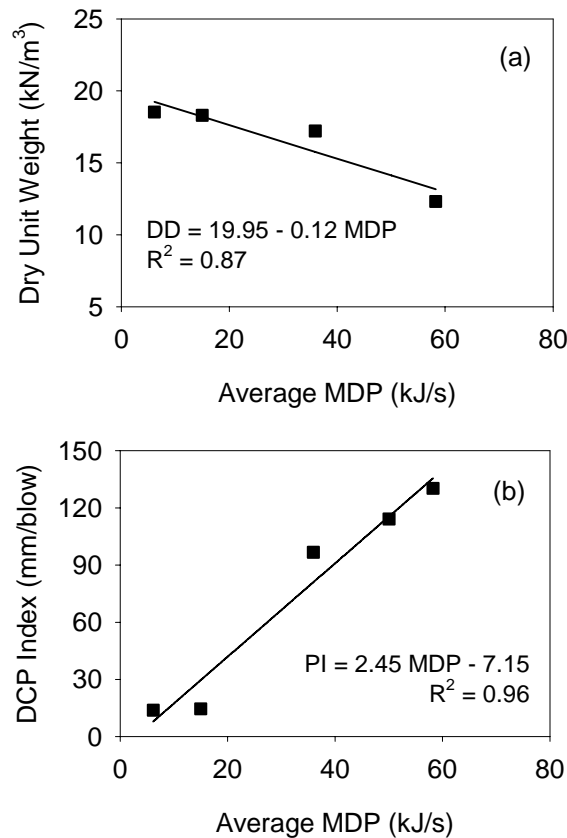


**Figure 14. Linear regression results for predicting (a) dry unit weight from MDP, (b) DCP index from MDP**

## Project Observations

The following observations were made from Project 1 testing and analysis:

- Validation of MDP technology for alternative roller configurations has broad implications for earthwork construction practice.
- Variation of MDP measurements observed for a test strip was attributed to variable subgrade conditions, as in situ measurements did not show the same trends.
- The mean MDP measurement decreased with increasing roller passes, which is consistent with reducing the rolling resistance during the soil compaction process. The standard deviation of MDP increased with roller passes, as the soil condition deviated from a uniform initial condition.
- Similar compaction was achieved by both the left- and right-side wheels of the impact roller, evidenced by similar density and strength measurements at the various stages of compaction. MDP is derived from machine-ground interaction from all wheels.
- A moderately-strong ( $R^2 = 0.87$ ) correlation was observed between MDP and dry unit weight. The relationship, however, was strongly influenced by a single data point. A strong relationship ( $R^2 = 0.96$ ) was observed between MDP and DCP index.

## PROJECT 2. EDWARDS FACILITY, CS-533 VIBRATORY SMOOTH DRUM

### Project Description and Objectives

Project 2 was conducted from August 1 to August 4, 2005, to evaluate both MDP and CMV for vibratory compaction of five cohesionless soil types. The experimental testing plan of this study, comprised of five test strips for the respective soils, is provided in Table 3. The specific objective of experimental testing and subsequent analyses was to investigate relationships between MDP, CMV, and soil properties, including soil density, moisture content, strength, and deformation characteristics.

**Table 3. Project 2 testing program**

Soil type	Strip no.	Loose lift thickness (mm)	Moisture content (%)	Moisture deviation <sup>a</sup> (%)
RAP	1	350	8	0
CA6-C	2	280	4	+4 <sup>b</sup>
CA5-C	3	300	4	---
FA6	4	360	6	-2
CA6-G	5	340	8	-2

<sup>a</sup> Moisture deviation from optimum, based on standard Proctor test ( $w - w_{opt}$ )

<sup>b</sup> Within bulking moisture range

The roller used for this project was a prototype CS-533 vibratory smooth drum roller, shown in Figure 15. The 9,960-kg roller had a drum diameter of 1.52 m, a drum width of 2.13 m, and a rear wheel-to-drum length of 2.90 m. The roller was additionally fitted with a GPS system, such that coverage (i.e., history of the roller location), MDP, and CMV were each mapped and viewed in real-time during compaction operations.



**Figure 15. Caterpillar CS-533 vibratory smooth drum roller**

## Construction and Testing Operations

Five 30 m long test strips were constructed using five different cohesionless subbase materials. The test strips were constructed with widths of approximately 3.0 m, slightly wider than the roller drum. The soils were placed on well-compacted subgrade at approximately natural moisture content, varying by soil type, with loose lift thicknesses ranging from 280 mm to 360 mm between test strips. Additional material was placed at the ends of the test strips to transition from the existing ground surface to the test strip elevations. Constructed test strips are shown in Figure 16.

Soil was compacted using the prototype CS-533 vibratory roller at the “high” amplitude (1.70 mm) setting. The frequency of drum vibration (31.9 Hz) was also constant throughout the field study. During this compaction operation, machine power and CMV measurements were collected approximately every 20 cm along the test strip. Near-continuous roller location information was also obtained from GPS measurements.



**Figure 16. Test Strips 1-5 (left to right) comprised of base materials**

To determine the properties of the compacted soil, field measurements were obtained at each of ten 2.5 m spaced test points. Field measurements of density, moisture content, strength, and modulus were obtained for the uncompacted material and following 1, 2, 4, 8, and 12 roller passes over the test strip. GPS measurements were additionally collected at each test location using a rover to allow pairing of the field measurement results with spatially nearest intelligent compaction data. Considering the relative influence and sensitivity of soil disturbance on test results, the order in which tests were performed was predetermined as follows: (1) nuclear moisture and density using a calibrated nuclear moisture-density gauge, (2) SSG, (3) PFWD, (4) Clegg impact test, and (5) DCP. As in Project 1, the mean DCP index at the bottom of the compaction layer was calculated using Equation 4 and subsequently used for analysis. A single 300 mm diameter plate load test was conducted at the end of the test strip next to the tenth test point. Upon completion of testing, the characteristics of the compacted subbase materials, defined using MDP, CMV, and in situ measures of soil density, strength, and stiffness, were available for the full range of soil compaction states.

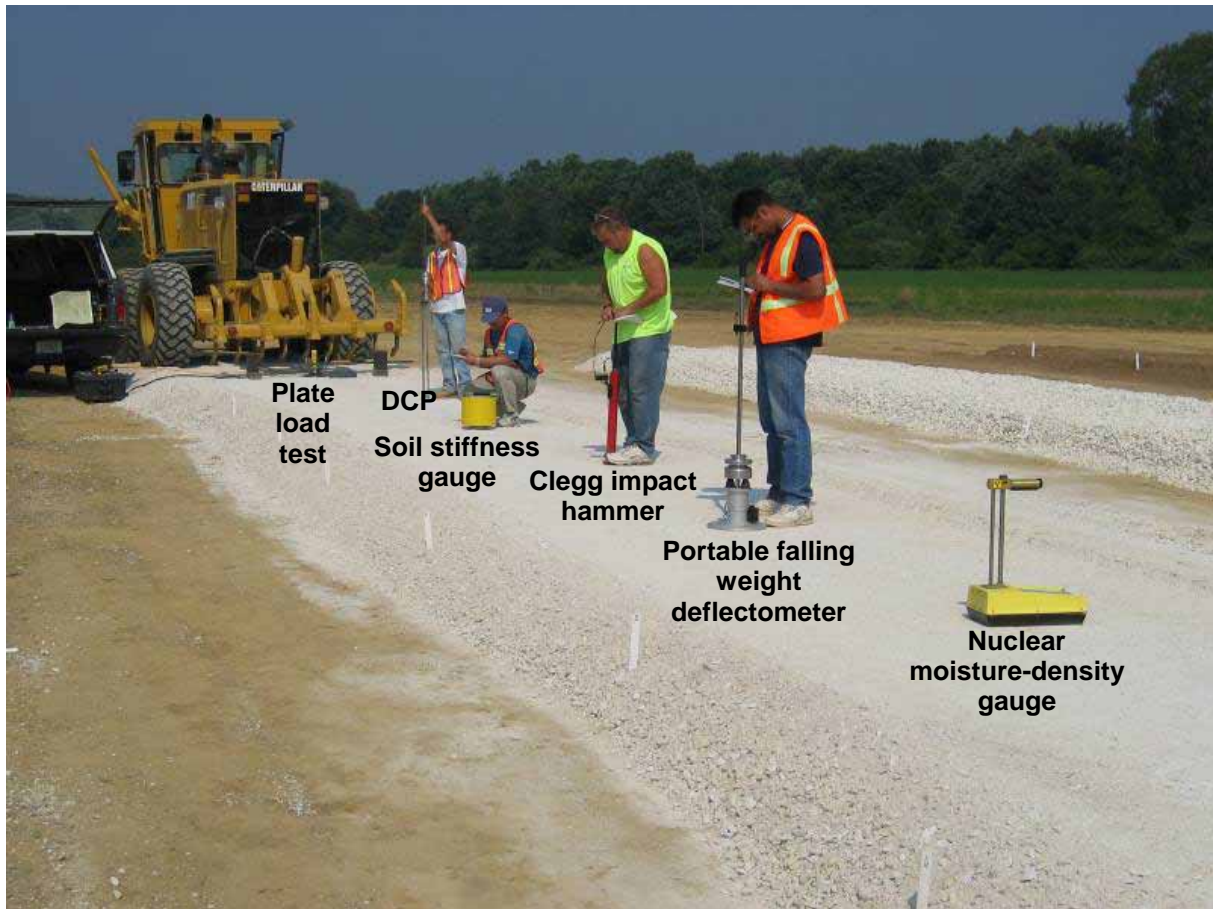


**Figure 17. In situ test performance on Strip 2**

## **Material Properties**

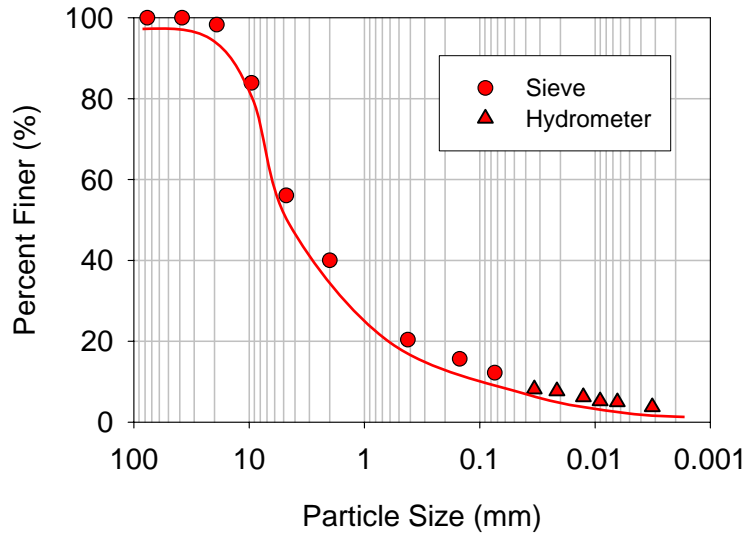
Evaluating the applicability of intelligent compaction technology to various cohesionless soil types was an important aspect of the current field study. As a result, experimental testing involved compaction and field testing of five soils. Recycled asphalt pavement (RAP), CA6-C, CA5-C, FA6, and CA6-G (Illinois DOT classifications) were obtained from local sources. Each soil was coarse-grained with low plasticity. Particle size distribution curves are shown from Figure 18 to Figure 22.

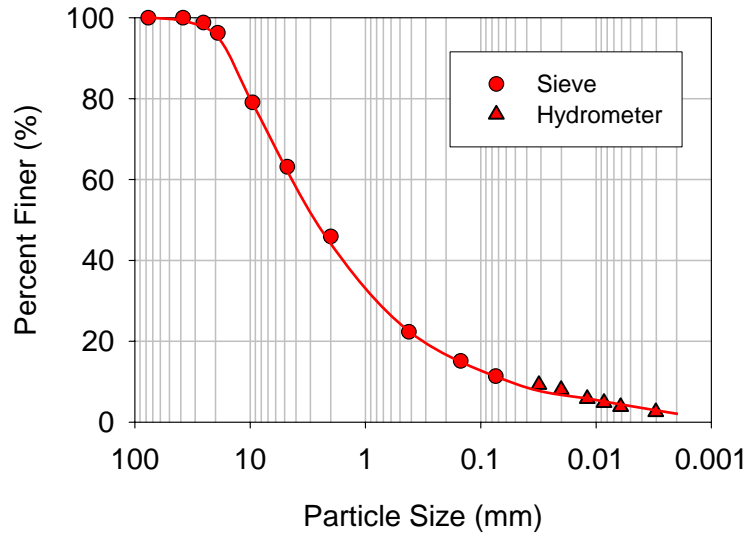
Moisture-density tests were performed following the Standard Proctor test method (ASTM D 698-78). An automated, calibrated mechanical rammer was provided for compaction. Moisture-density curves are shown from Figure 23 to Figure 26. Maximum dry unit weights and optimum moisture contents were observed for all materials, while only the CA6-C material (highest coarse fraction of tested soils) exhibited bulking behavior at low moisture contents. Since the coarse-grained soils were also free draining, relative density tests were performed following ASTM D 4253 (Maximum Index Density and Unit Weight of Soils Using a Vibrating Table). Soil classification and compaction properties of the testing materials are summarized in Table 4.

**Table 4. Project 2 testing materials**

Soil Property	RAP	CA6-C	CA5-C	FA6	CA6-G
USCS:	GM	SM	GP	SM	GC
AASHTO	A-1-b	A-1-a	A-1-a	A-2-4	A-2-6
$G_s$	2.52	2.69	2.75	2.68	2.67
$F_{3/4}$ (%)	98.3	96.2	3.4	99.4	91.9
$F_{3/8}$ (%)	83.9	79.0	3.4	98.3	70.7
$F_4$ (%)	56.1	63.1	3.4	90.8	63.1
$F_{200}$ (%)	14.4	11.3	0.0	21.3	31.7
Percent gravel	44	37	97	9	37
Percent sand	42	52	2	70	31
Percent silt	11	9	1	16	22
Percent clay	3	2	0	5	10
$C_c$	4.02	3.93	1.07	1.28	0.41
$C_u$	130.43	117.47	1.39	48.60	1977.03
Fineness modulus	4.27	4.11	7.73	2.04	3.24
LL (PI)	15 (NP)	14 (NP)	NP	17 (NP)	26 (12)
Standard Proctor:					
$\gamma_{d, \max}$ (kN/m <sup>3</sup> )	19.5	20.1	---	19.8	20.0
$w_{\text{opt}}$ (%)	8.2	0.0	---	7.6	10.1
Relative Density:					
$\gamma_{d, \max}$ (kN/m <sup>3</sup> )	19.22	19.78	14.12	18.99	18.63
$\gamma_{d, \min}$ (kN/m <sup>3</sup> )	14.38	15.19	11.84	15.76	13.54

--- No test performed





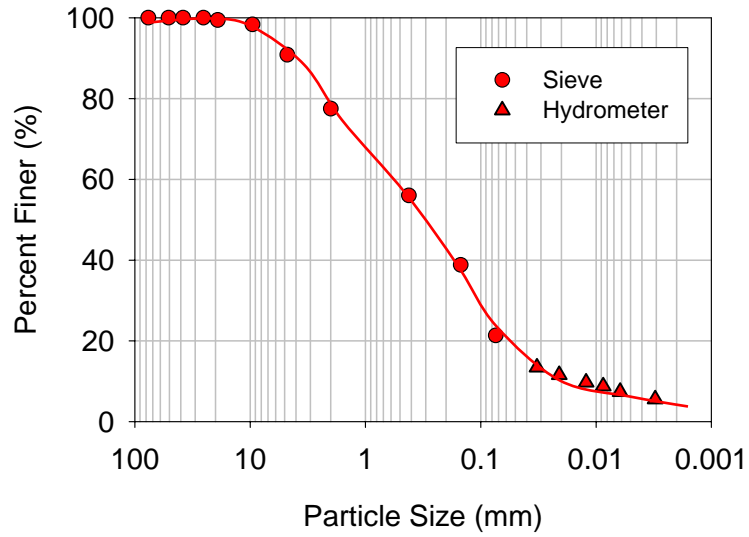


**Figure 21. FA6 particle size distribution**

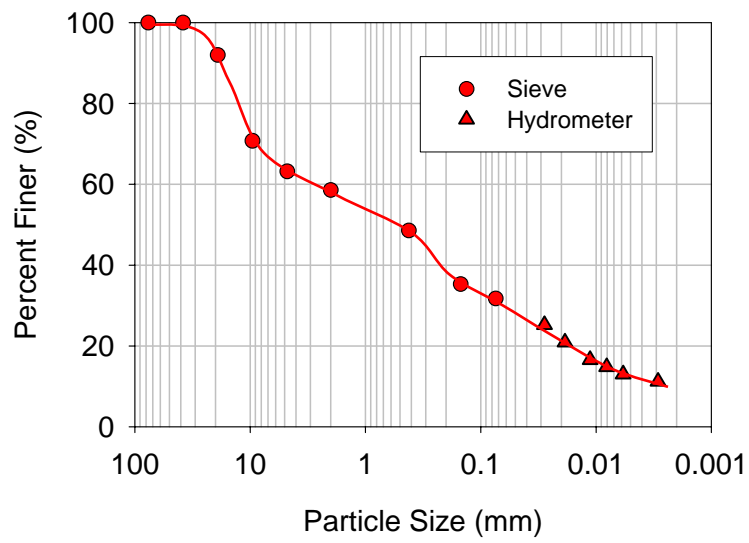


**Figure 22. CA6-G particle size distribution**

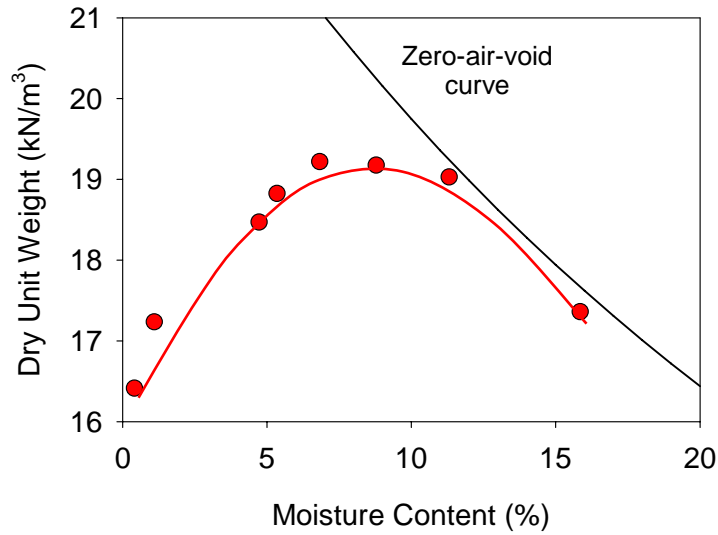


**Figure 23. RAP standard Proctor moisture-density relationship**

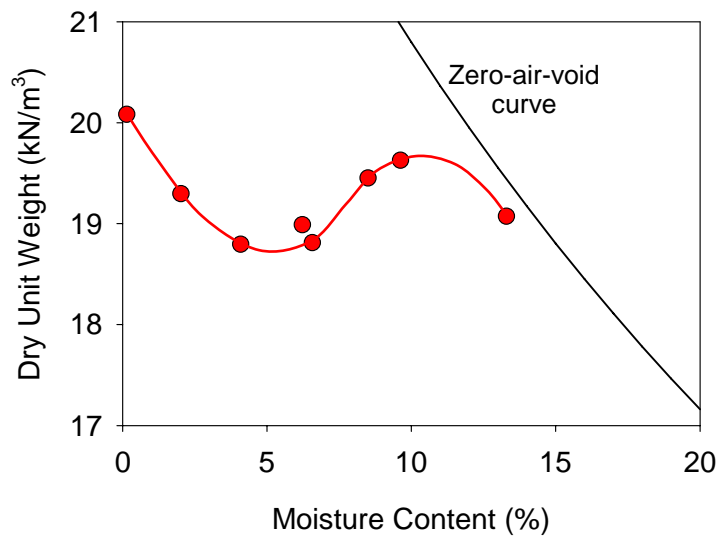


**Figure 24. CA6-C standard Proctor moisture-density relationship**

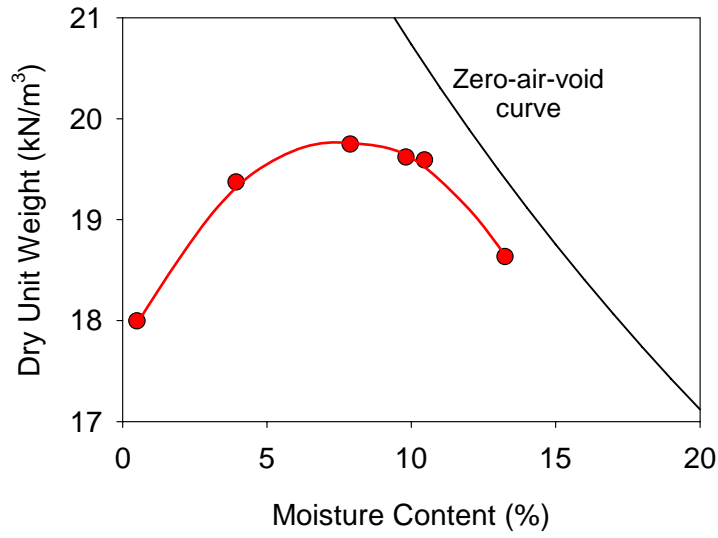


**Figure 25. FA6 standard Proctor moisture-density relationship**

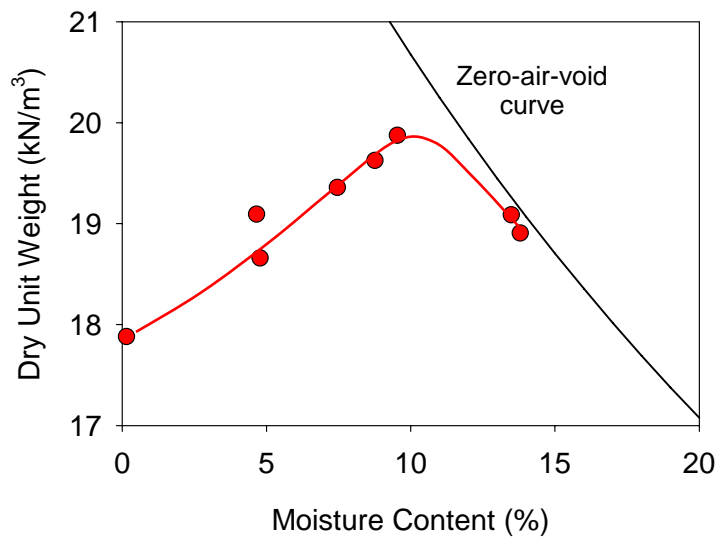


**Figure 26. CA6-G standard Proctor moisture-density relationship**

## Compaction Monitoring and In Situ Measurements

Screen captures from the Caterpillar Player program are shown from Figure 27 to Figure 31 for each test strip following 1, 4, and 12 roller passes.

The nuclear moisture-density gauge was incorporated into the testing program to provide a rapid measurement of density and moisture. For each test, density was determined for the full depth of the compacted soil layer (i.e., variable depth depending on state of compaction). Soil strength was determined using the Clegg impact hammer and DCP. Soil modulus was determined using the SSG, PFWD, and PLT.

The in situ measures of soil density, strength, and stiffness were collected concurrent with MDP and CMV on test strips of varying soil type. All statistical outliers of compaction monitoring data remained in the dataset for performing regression analyses. Data were initially plotted versus the location along each respective test strip from Figure 32 to Figure 41. In doing this, the general trends and potential correlations were observed for compaction monitoring data and in situ measurements. With an increasing number of roller passes, the CMV and dry unit weight increases, while MDP decreases. Considerable local variability in MDP was observed compared to both CMV and dry unit weight, which may be explained by the sensitivity and potentially unquantified error of measurements associated with machine performance. Machine power output indicates both the internal and external energy consumption of the roller, whereas CMV is related to the characterization of behavior only at the roller drum ground interface. Higher rates of compaction were observed at those locations of comparatively high stiffness following the initial roller pass, as evidenced by CMV output. This behavior was also observed by Thurner and Sandström (1980). The stiffness of the underlying soil at these locations may be higher, giving an initially higher stiffness response, and may promote more efficient (i.e., more rapid) compaction of the fill material. For each test strip, CMV is plotted with subgrade CBR calculated from DCP index, shown in Figure 42.

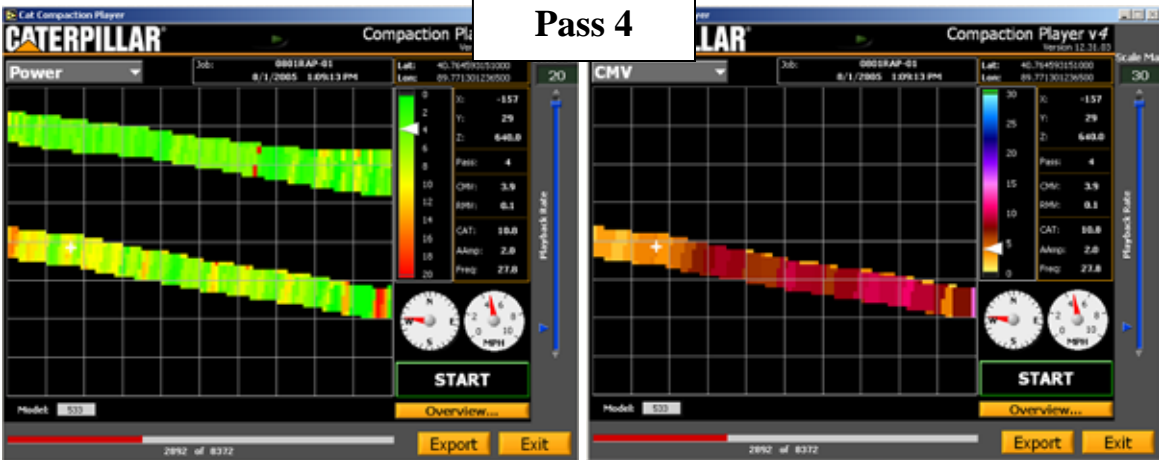
MDP

CMV

Pass 1



Pass 4



Pass 11



Figure 27. Screen captures for RAP after 1, 4, and 11 passes

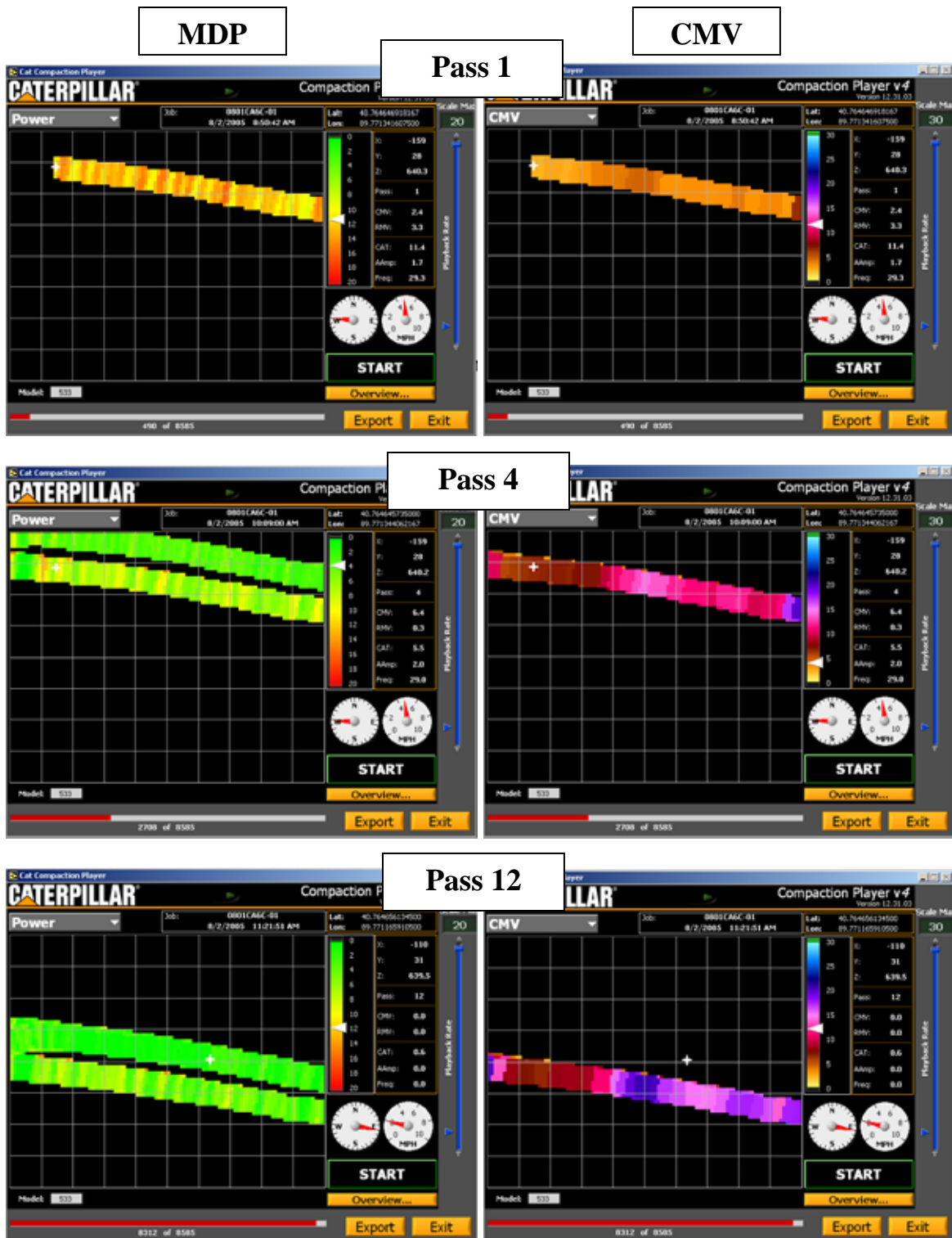


Figure 28. Screen captures for CA6-C after 1, 4, and 12 passes

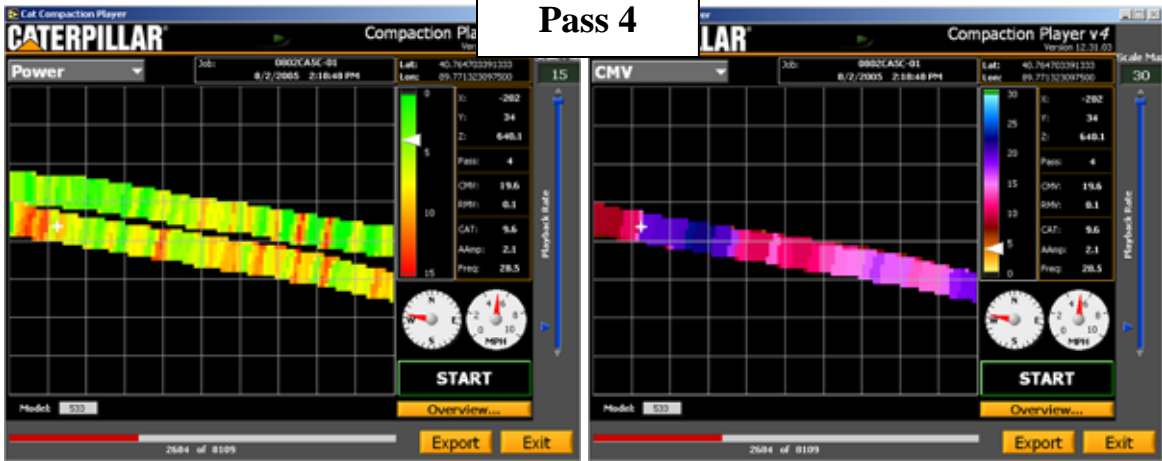
MDP

CMV

Pass 1



Pass 4



Pass 12

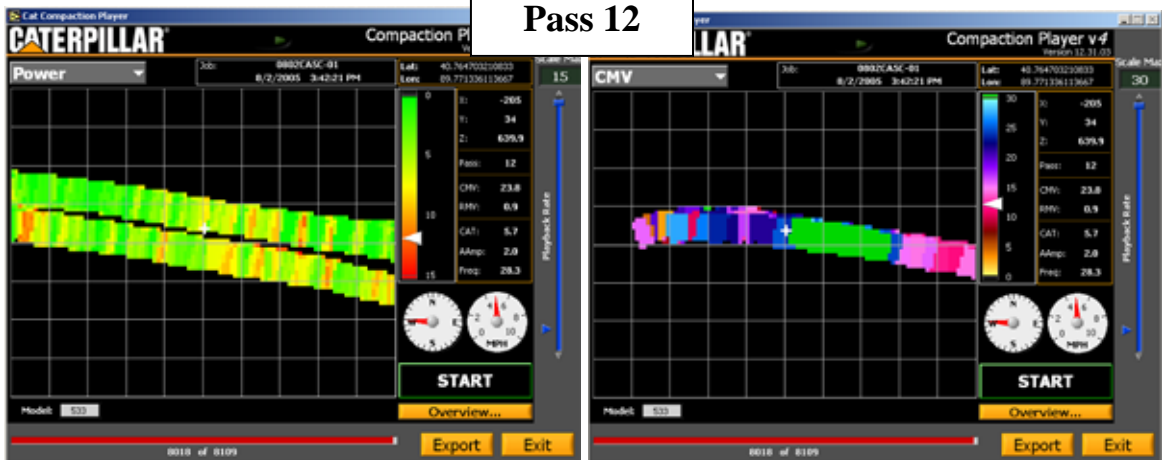


Figure 29. Screen captures for CA5-C after 1, 4, and 12 passes

MDP

CMV

Pass 1



Pass 4



Pass 12

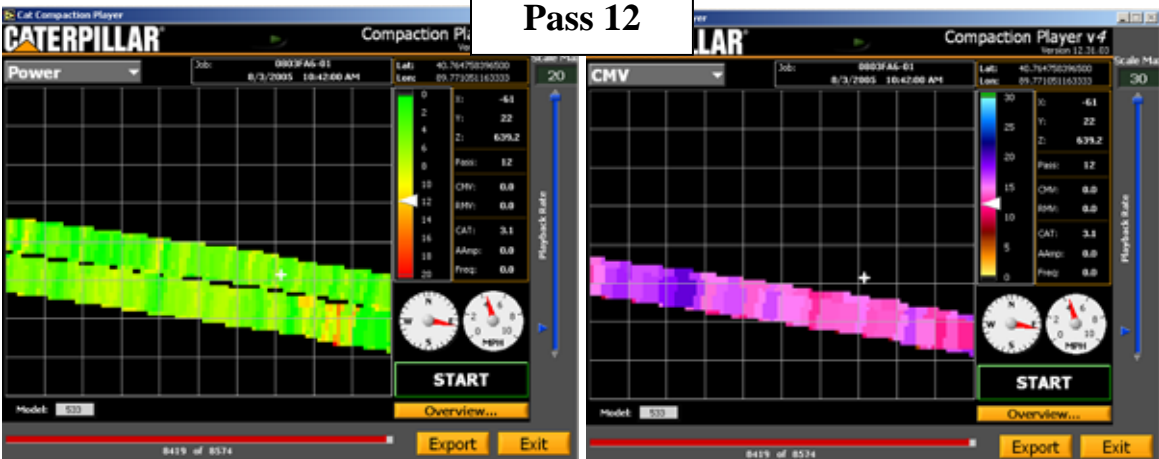


Figure 30. Screen captures for FA6 after 1, 4, and 12 passes

MDP

CMV

Pass 1



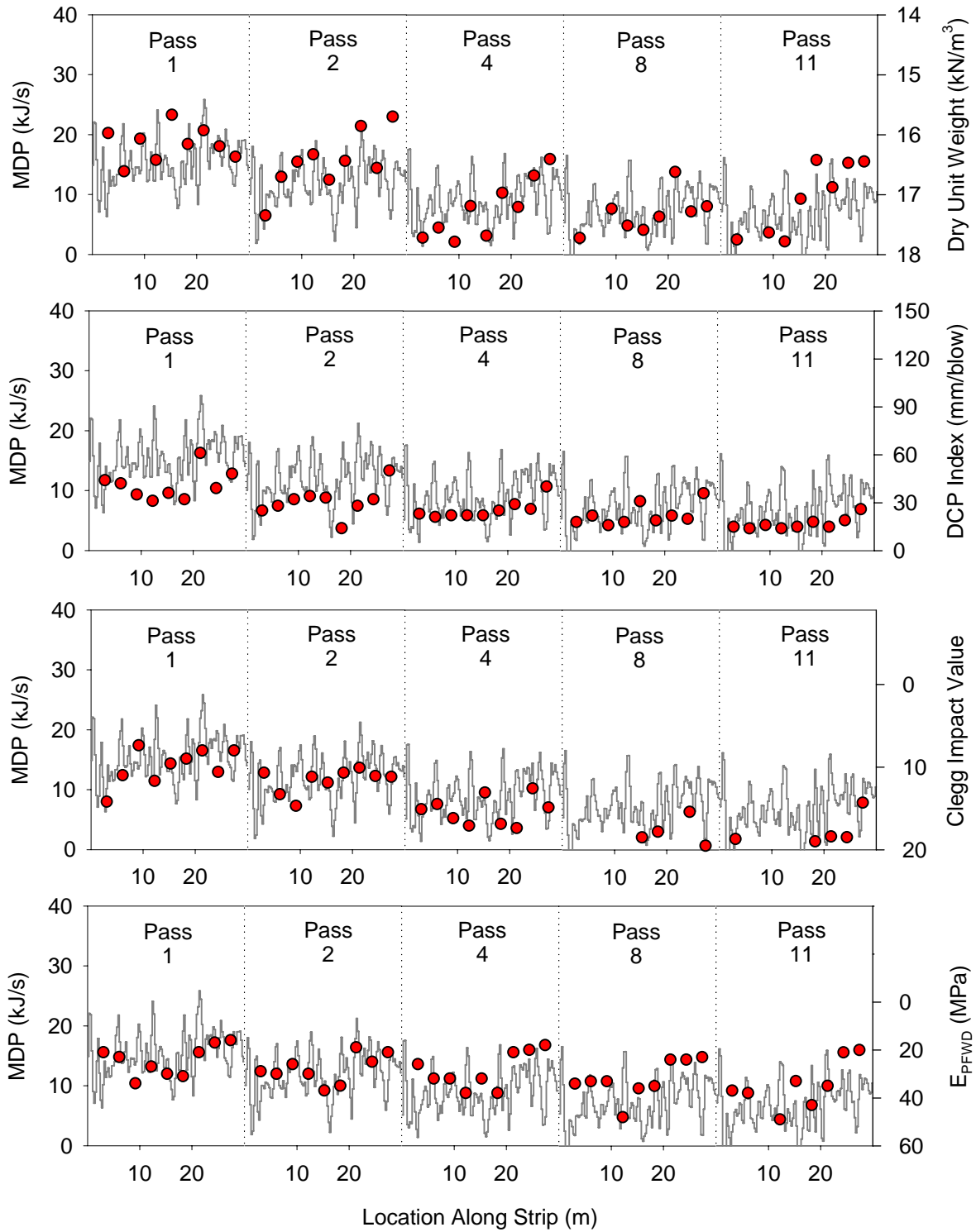
Pass 4



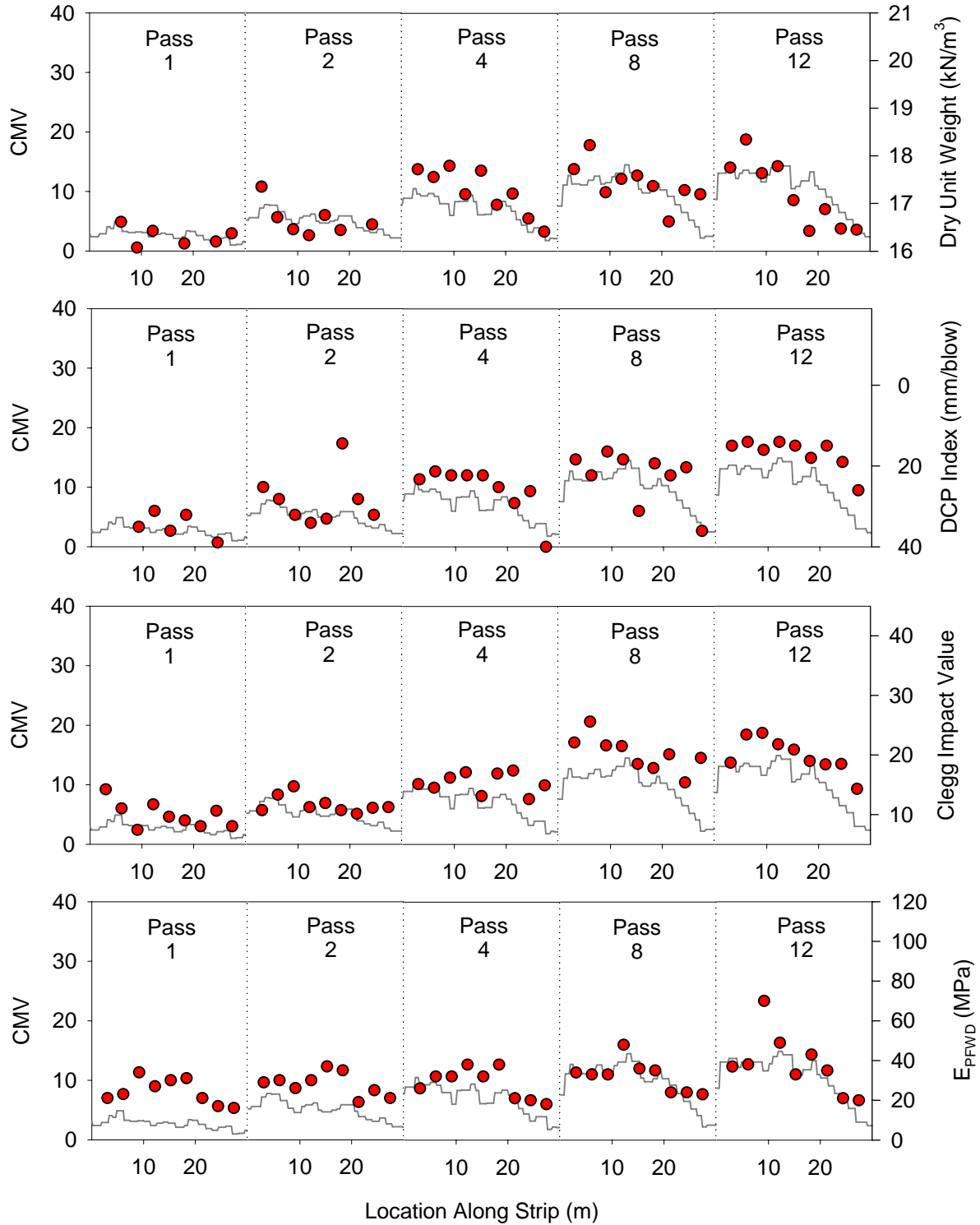
Pass 12



Figure 31. Screen captures for CA6-G after 1, 4, and 12 passes



**Figure 32. MDP, dry density, DCP index, CIV, and  $E_{PFW D}$  data for RAP**



**Figure 33. CMV, dry density, DCP index, CIV, and E<sub>PFD</sub> data for RAP**

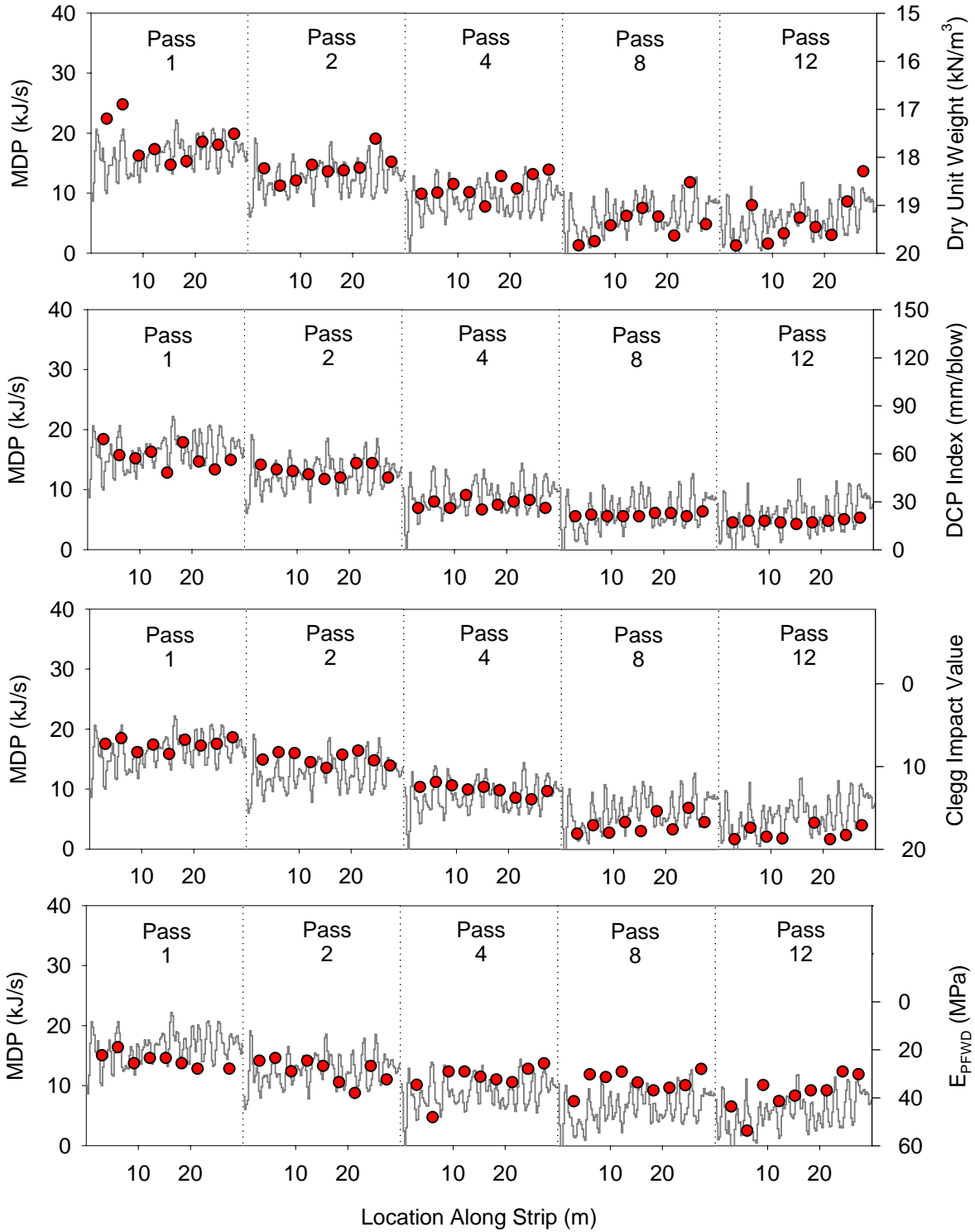


**Figure 34. MDP, dry density, DCP index, CIV, and  $E_{PFFWD}$  data for CA6-C**

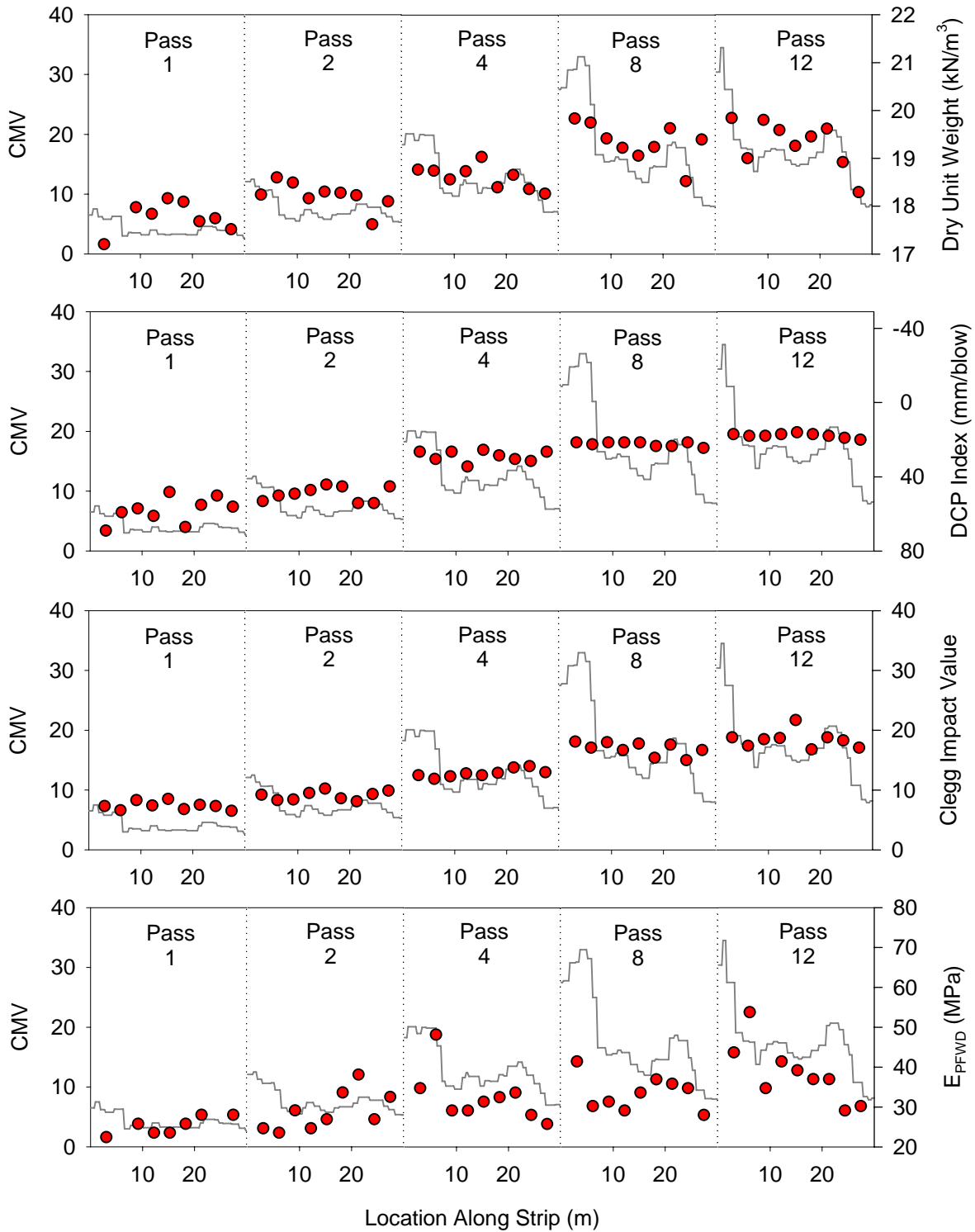
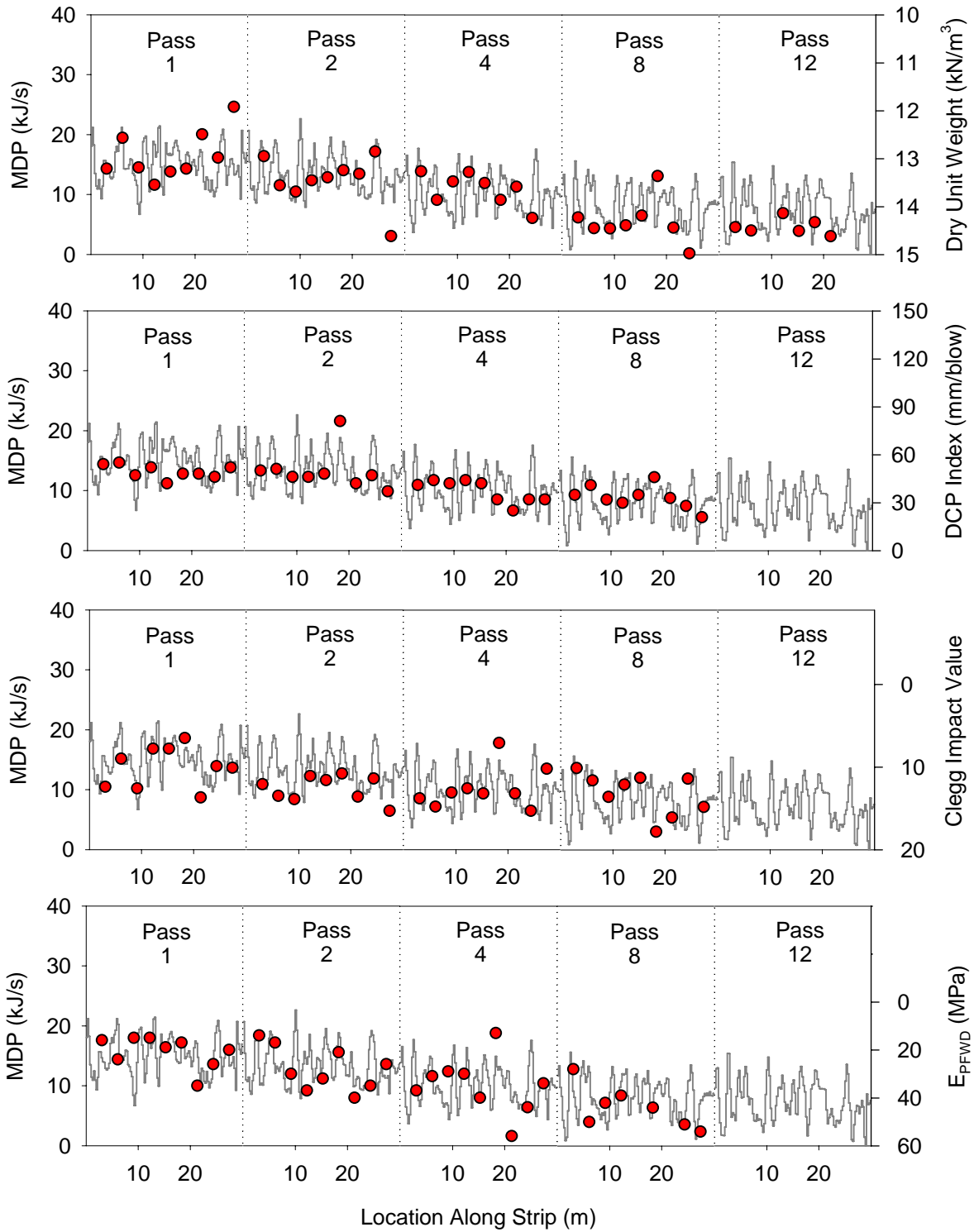
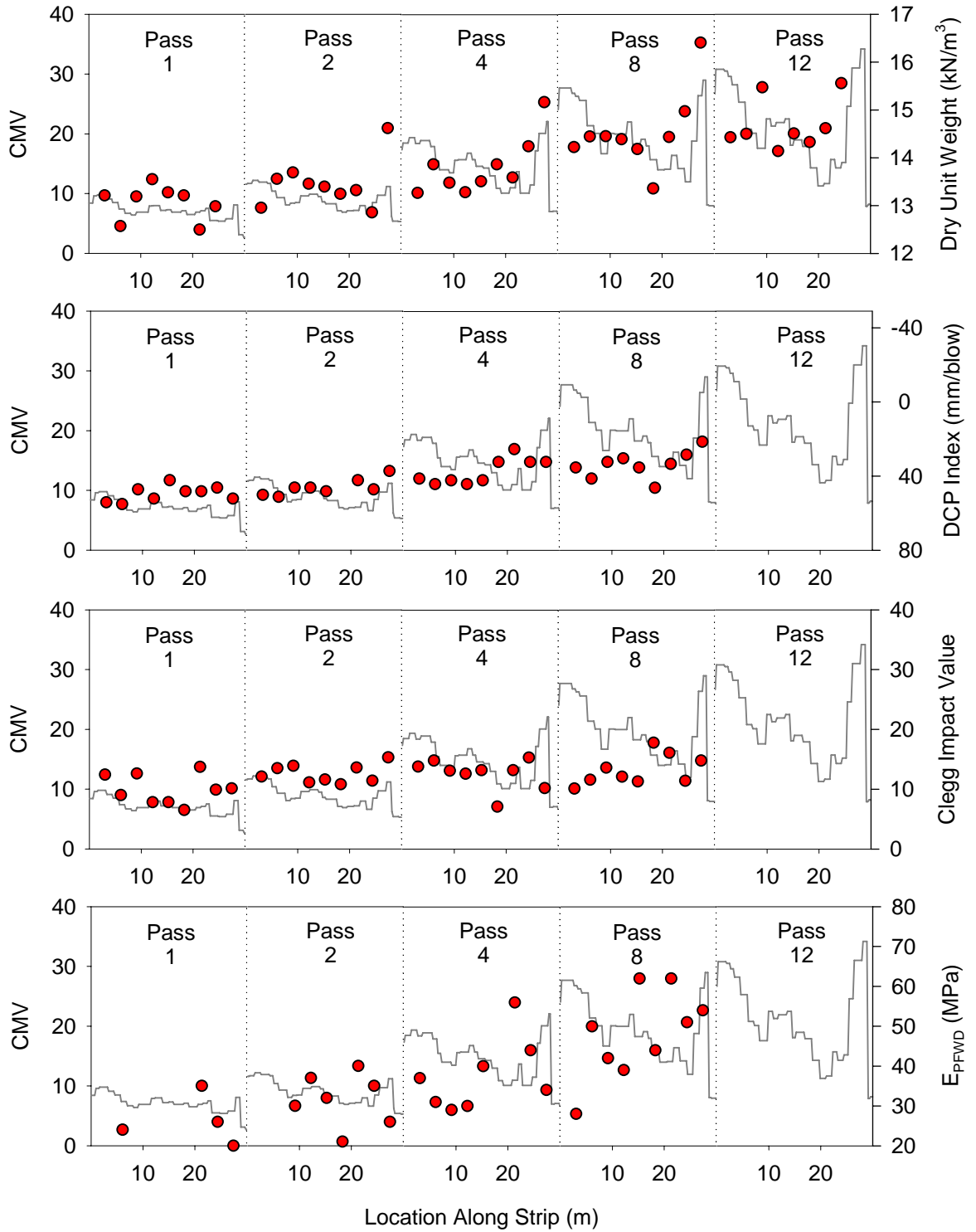


Figure 35. CMV, dry density, DCP index, CIV, and E<sub>PFWD</sub> data for CA6-C



**Figure 36. MDP, dry density, DCP index, CIV, and  $E_{PFFWD}$  data for CA5-C**



**Figure 37. CMV, dry density, DCP index, CIV, and E<sub>PFW D</sub> data for CA5-C**

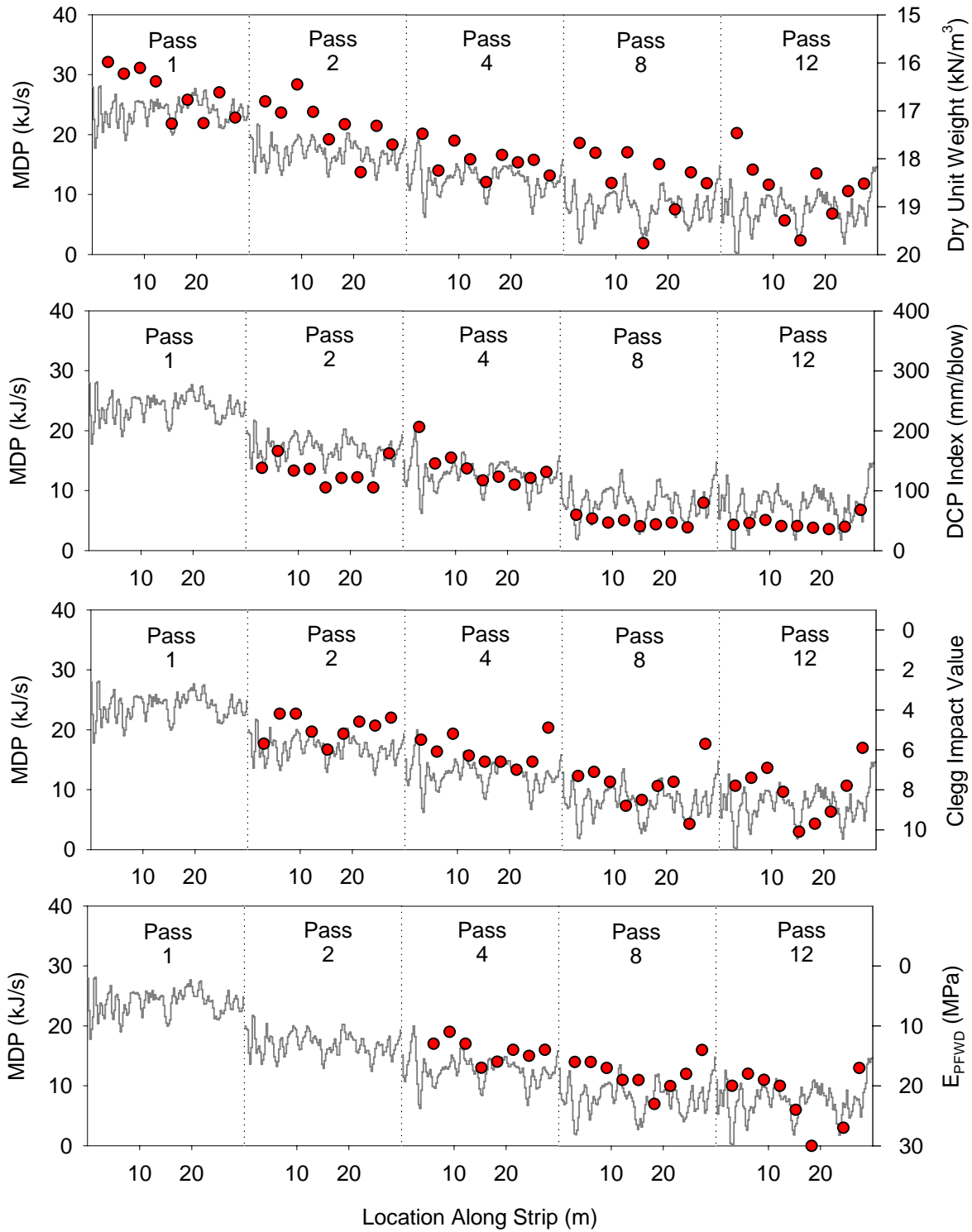


**Figure 38. MDP, dry density, DCP index, CIV, and E<sub>PFFWD</sub> data for FA6**

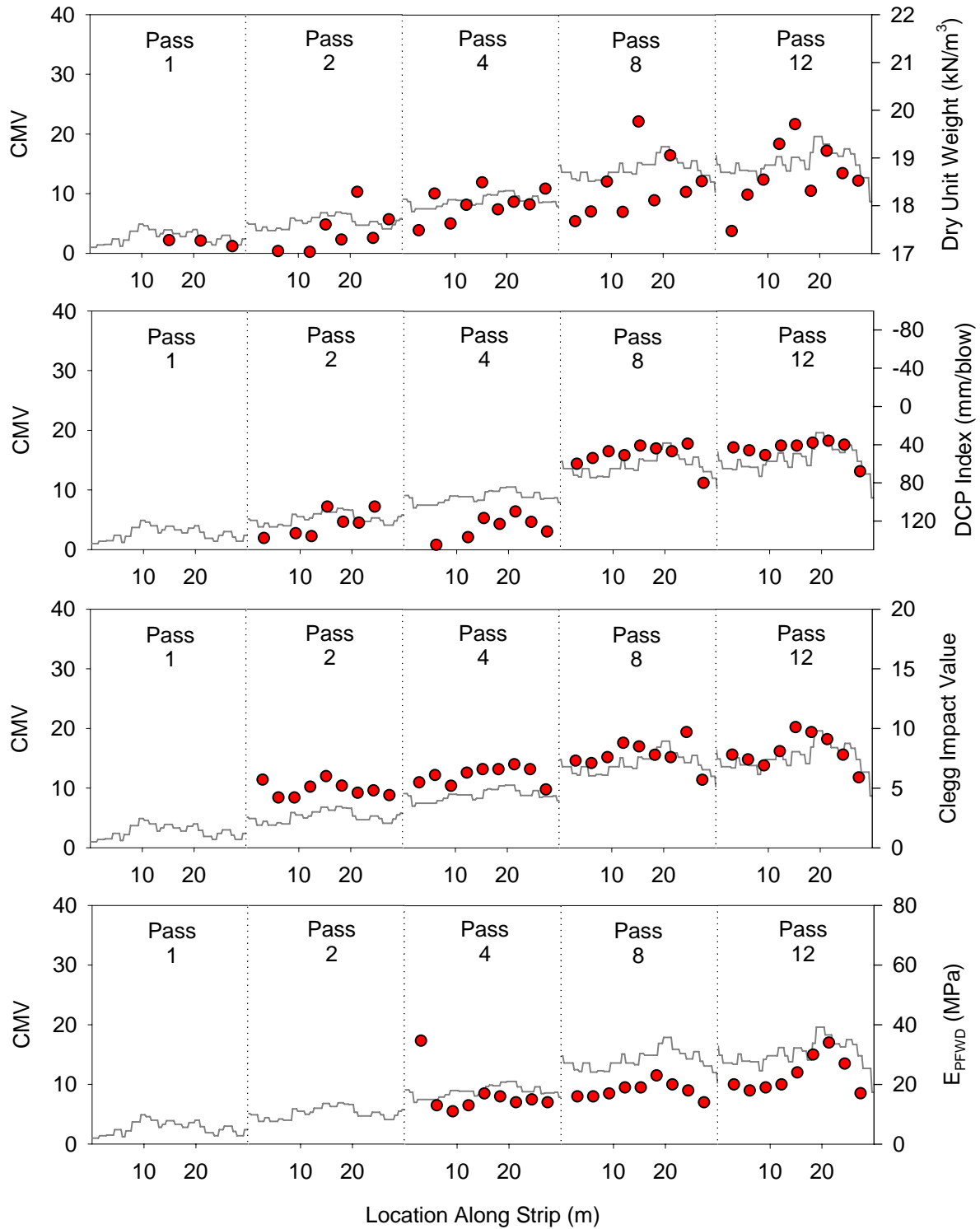


**Figure 39. CMV, dry density, DCP index, CIV, and E<sub>PFWD</sub> data for FA6**

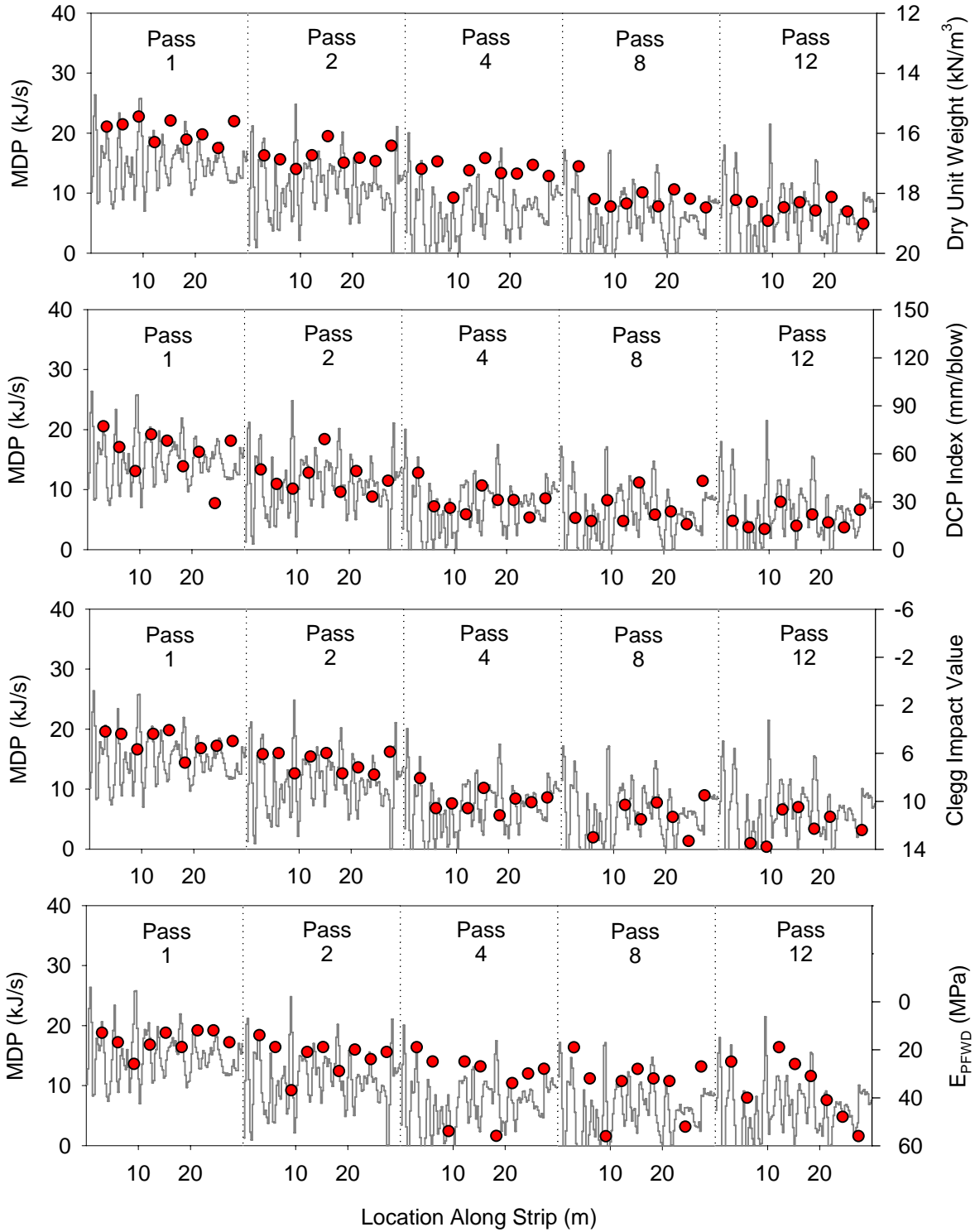


**Figure 40. MDP, dry density, DCP index, CIV, and  $E_{PFW}$  data for CA6-G**

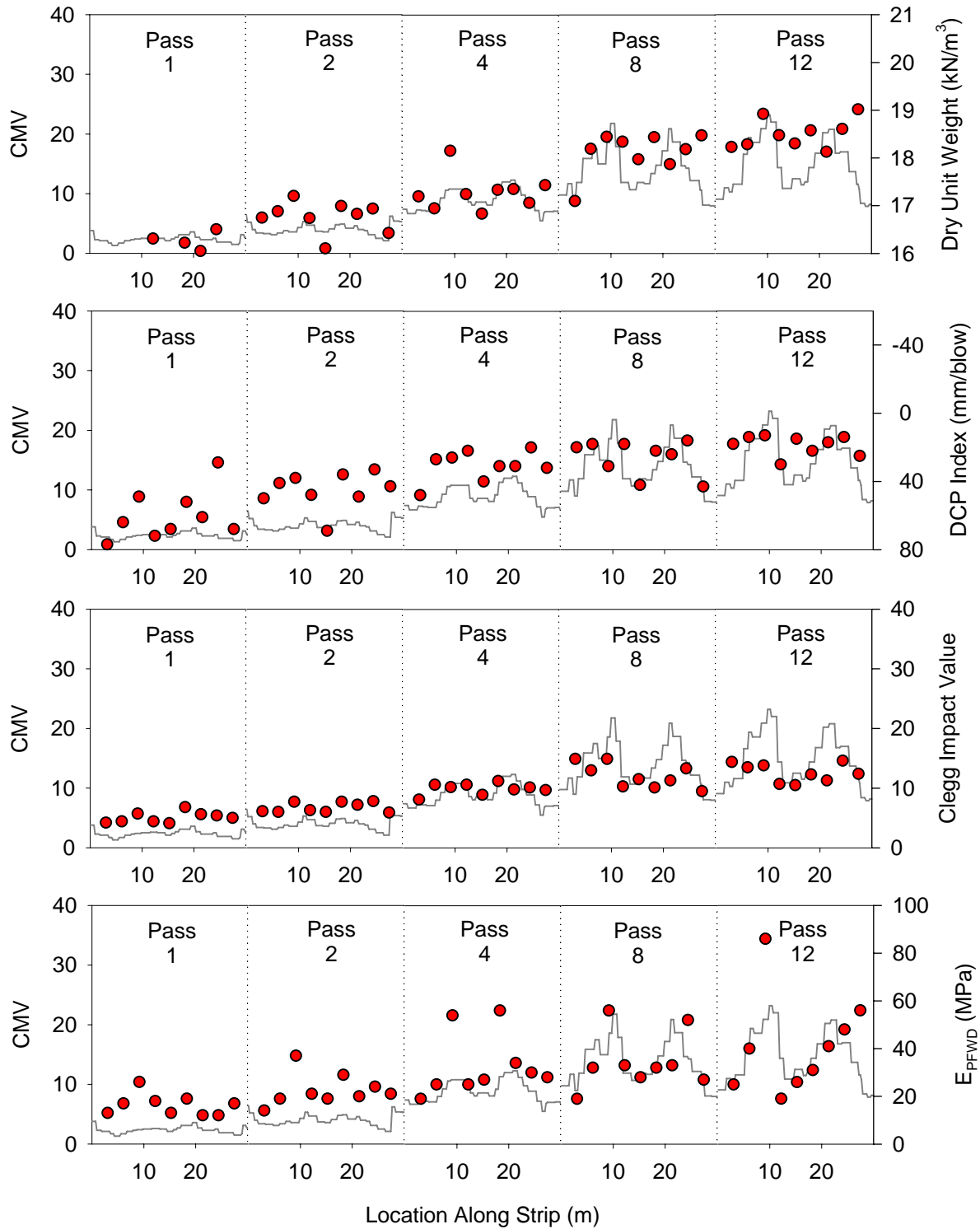


**Figure 41. CMV, dry density, DCP index, CIV, and  $E_{PFW D}$  data for CA6-G**

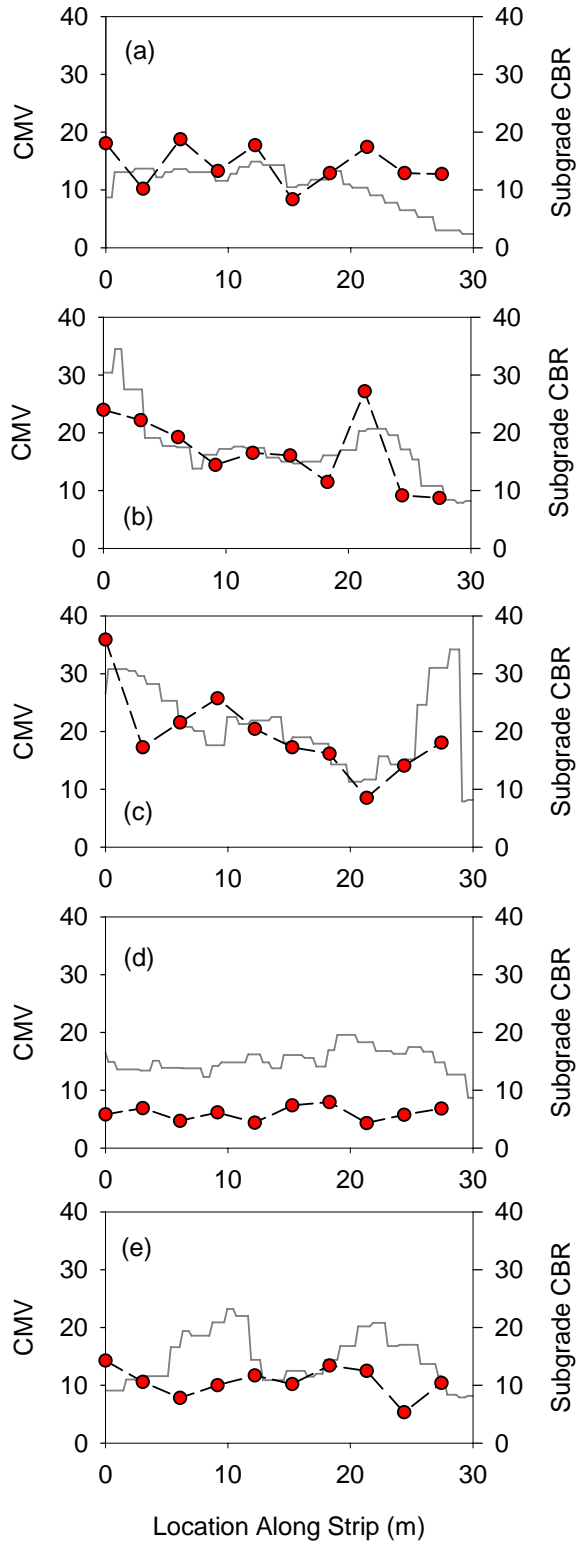


**Figure 42. Final pass CMV and subgrade CBR for (a) RAP, (b) CA6-C, (c) CA5-C, (d) FA6, and (e) CA6-G**

Scatterplots developed using field measurements and spatially nearest machine power values showed considerable scatter and generally provided relatively weak correlations. Possible sources of error in these scatter plots include (1) inherent soil variation, (2) location measurement error, (3) rear wheel-soil interaction at a different location from the location measurement, (4) machine measurement error, and (5) test device/measurement error (White et al. 2006). The experimental testing revealed that a single test point does not provide a high level of confidence for being representative of the average material characteristics, particularly when dealing with variable intelligent compaction data. Rather, variation always exists, and several data must be obtained to determine the soil properties with any confidence. In the case of comparing machine output to field measurements, soil property variation and measurement influence area must be considered, particularly for developing effective specifications and calibration procedures.

In recognizing that the test strips were constructed to be as uniform as may be expected under real field conditions and that multiple tests must be performed to find an engineering parameter representative of the tested soil, MDP, CMV, and in situ measurement values were averaged for each roller pass. Field compaction curves for MDP, CMV, and in situ measurements are shown from Figure 43 to Figure 47. Thurner and Sandström (1980) additionally used statistical means to present compaction curve data.

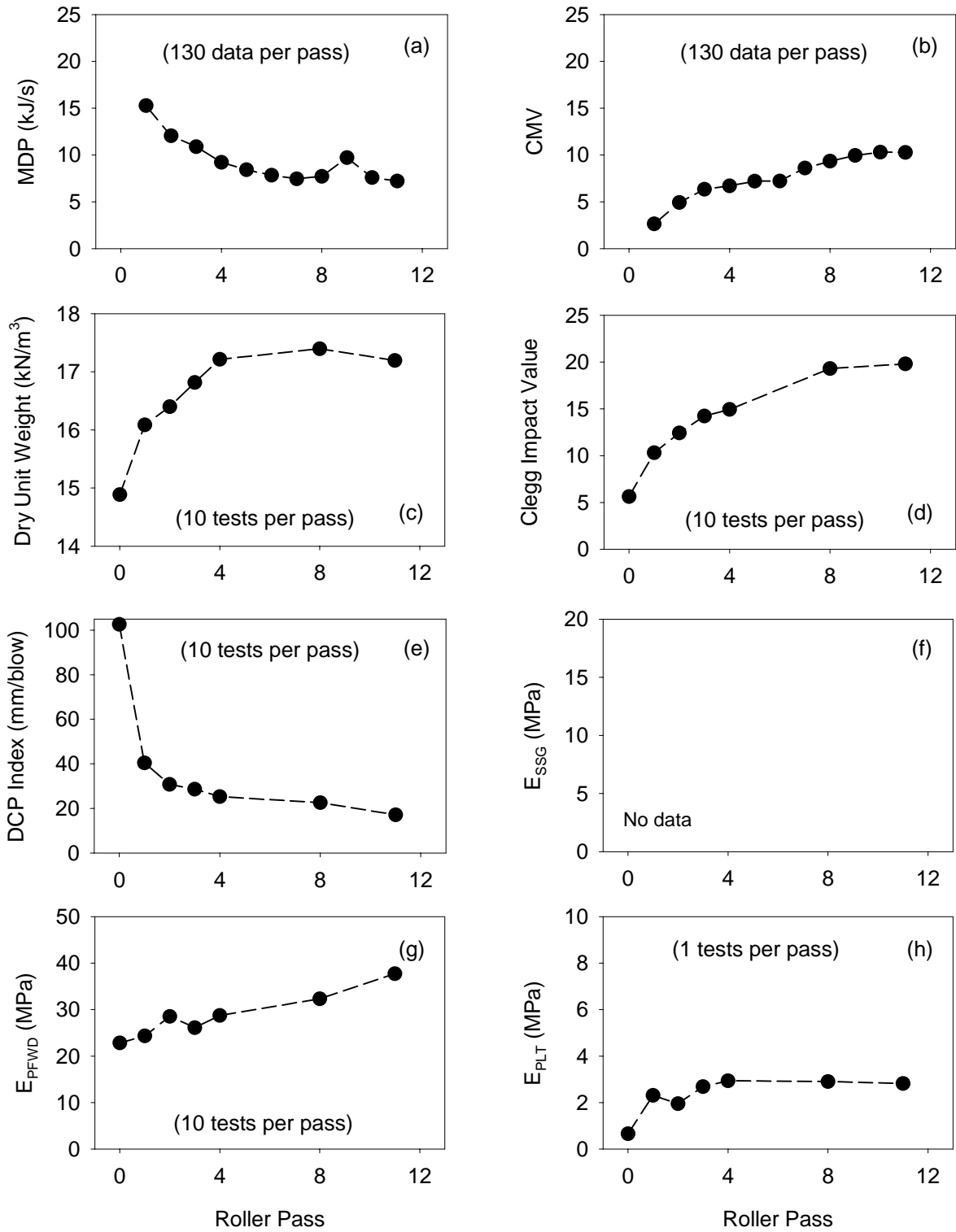
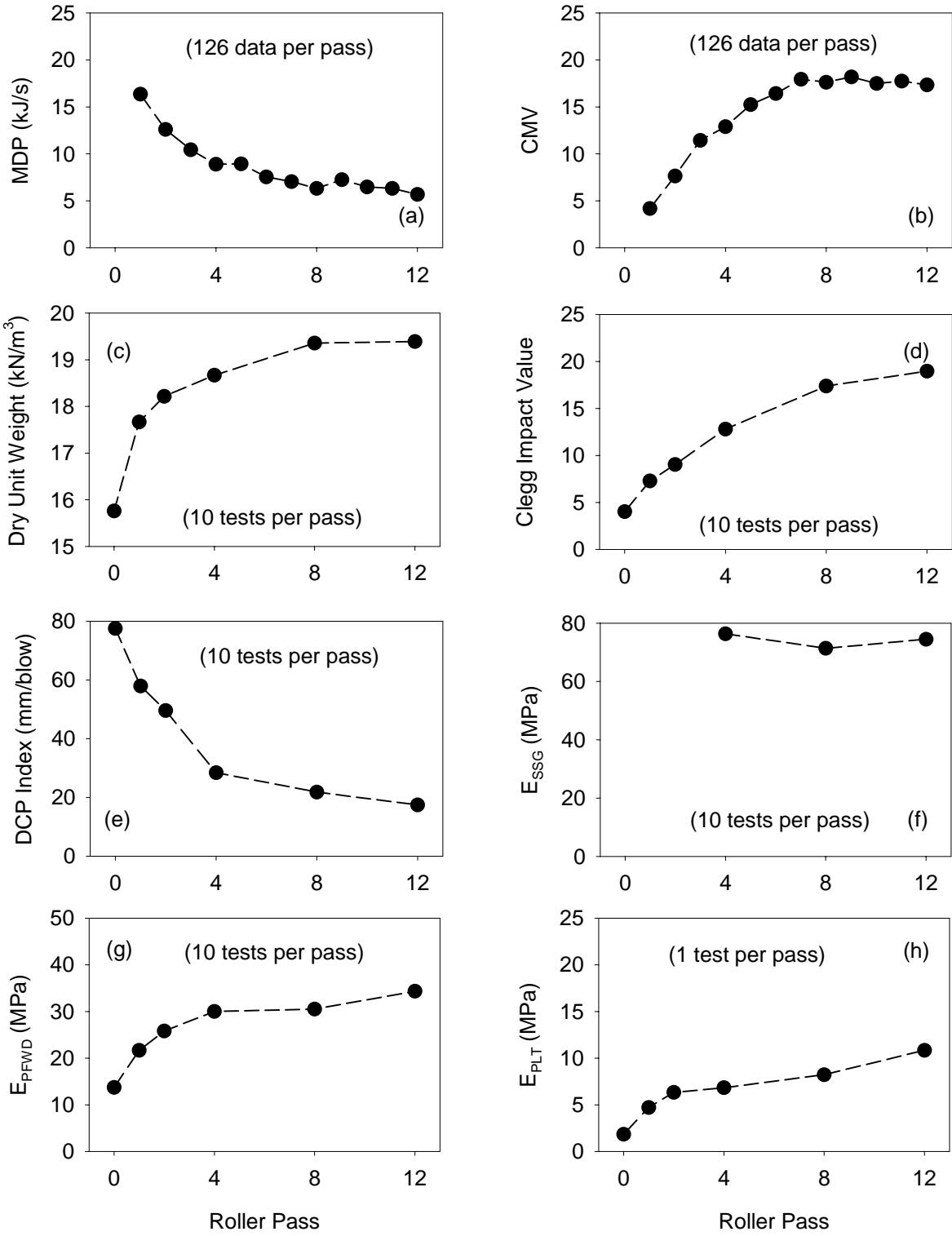
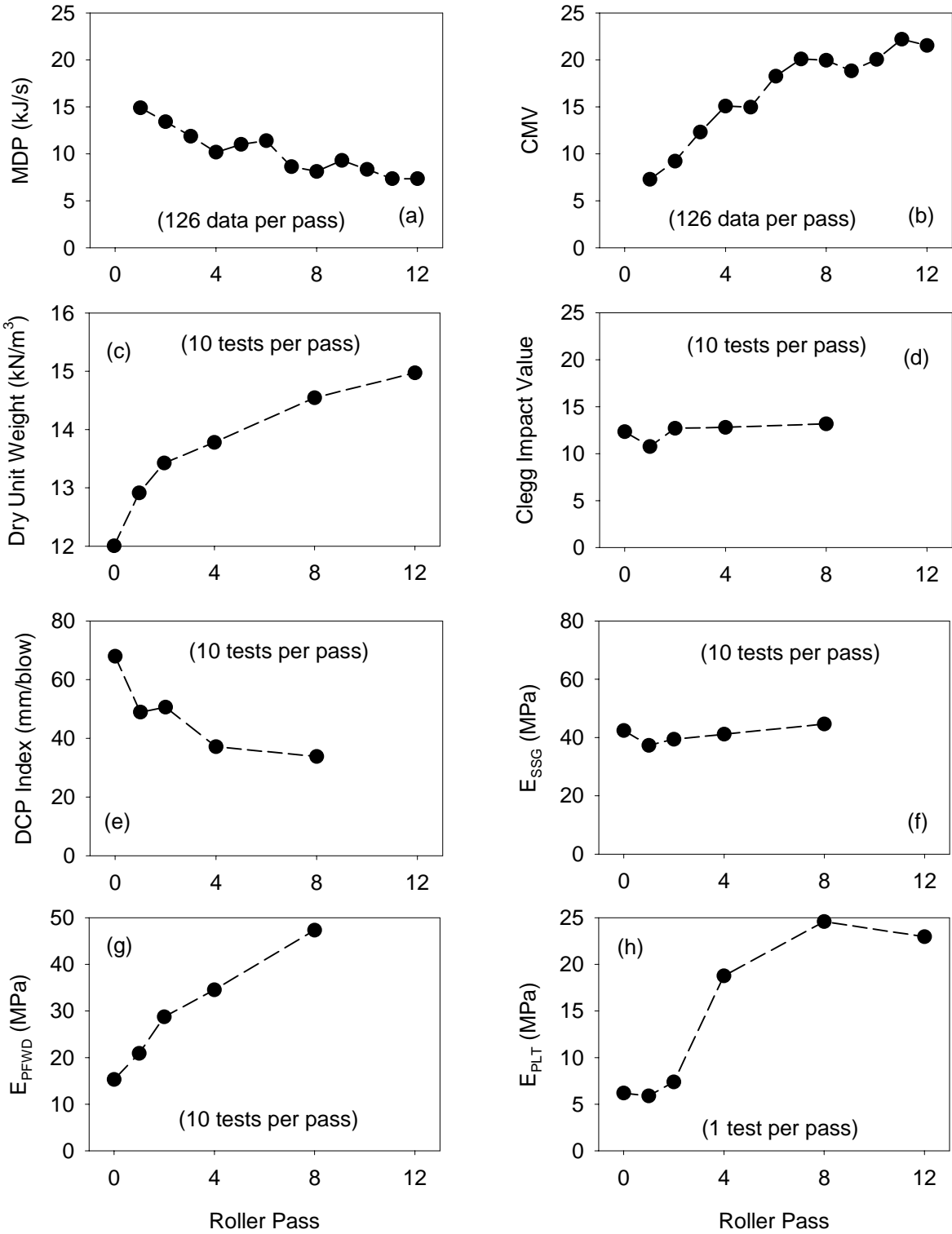


Figure 43. Compaction curves for average roller and field measurements for Strip 1 (RAP)



**Figure 44. Compaction curves for average roller and field measurements for Strip 2 (CA6-C)**



**Figure 45. Compaction curves for average roller and field measurements for Strip 3 (CA5-C)**

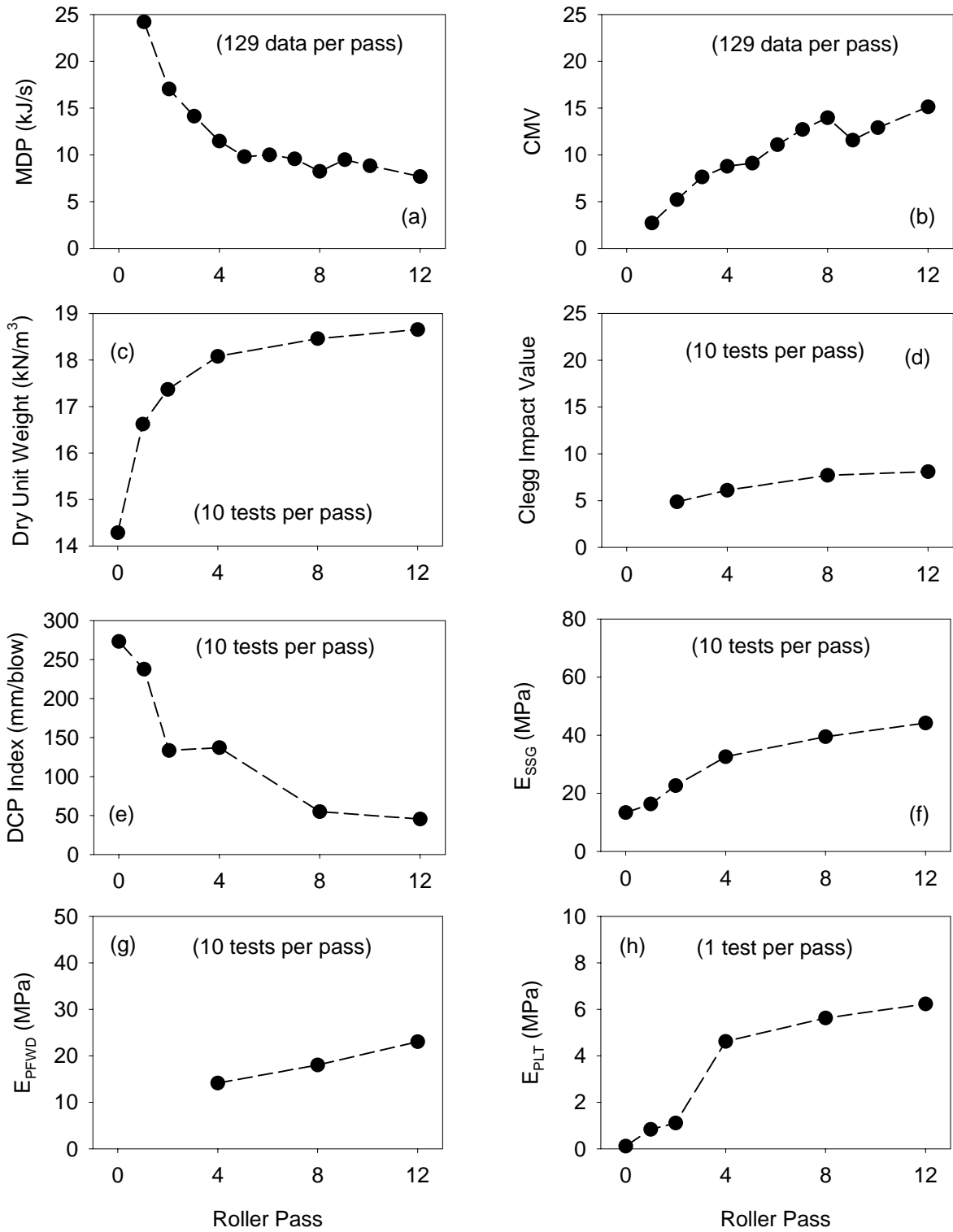


Figure 46. Compaction curves for average roller and field measurements for Strip 4 (FA6)

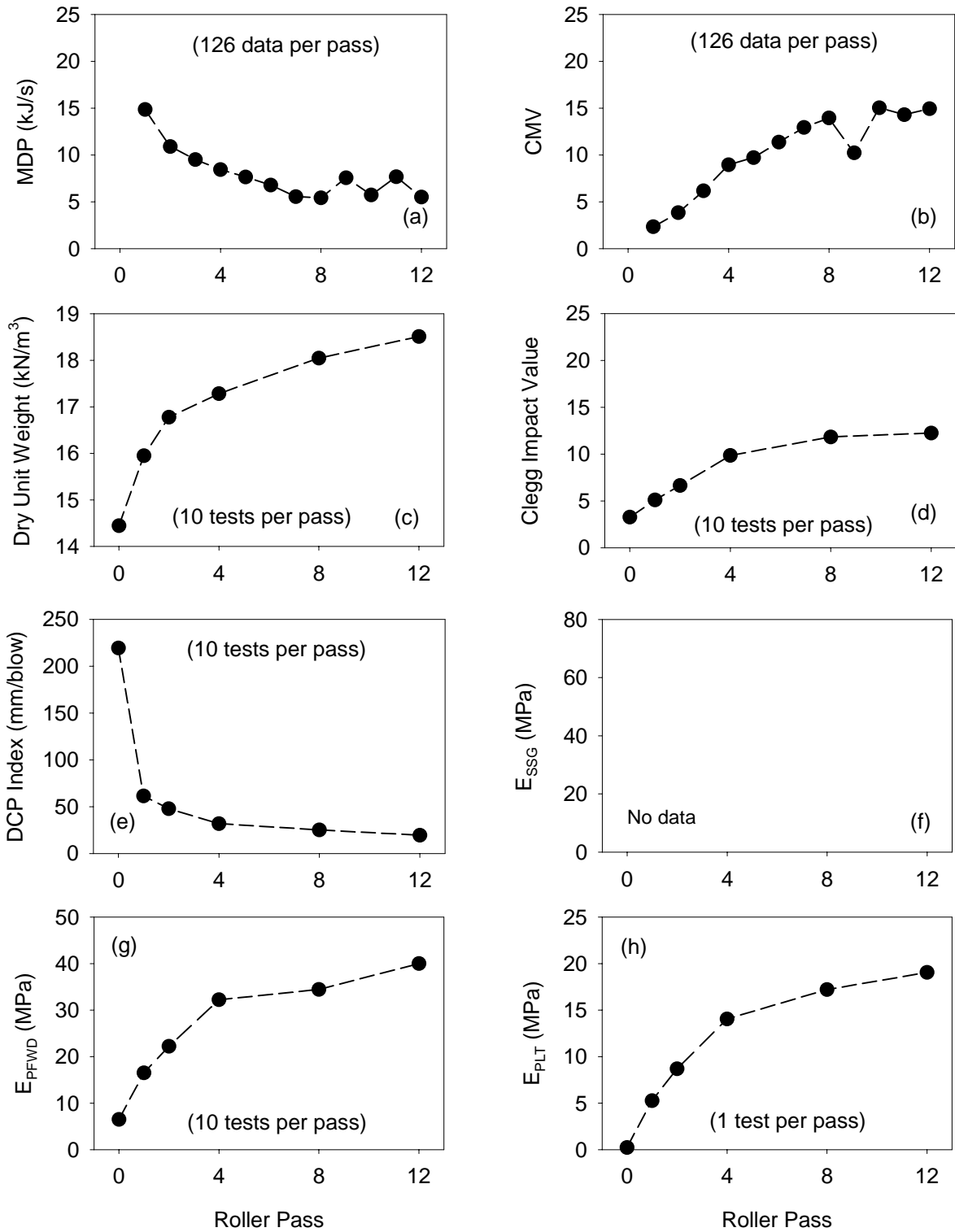


Figure 47. Compaction curves for average roller and field measurements for Strip 5 (CA6-G)

## Regression Analyses

The relationships between soil engineering properties, MDP, and CMV are shown from Figure 48 to Figure 57. These scatterplots are comprised of only five data points, with each data point representing the average measurement (from 10 tests) for the roller pass that was followed by field measurements (1, 2, 4, 8, and 12). Dry unit weight, CIV, DCP index, SSG modulus, PFWD modulus, and PLT modulus are all predicted from a logarithmic relationship with MDP. The soil properties show a linear relationship with CMV. To assess the quality of these relationships, correlation coefficients ( $R^2$ ) were calculated and provided in Table 5 for MDP and Table 6 for CMV. For MDP, about 82% (23 of 28) of the  $R^2$  values exceeded 0.90. Of the five values less than 0.90, four correlation coefficients were for predicting soil modulus, as opposed to soil density or strength. The relative difficulty in estimating soil modulus is likely related to the relative complexity of deformation characteristics and the variability associated with soil stiffness measurement. For CMV, about 71% (20 of 28) of the  $R^2$  values exceeded 0.90. The lowest observed correlation coefficient was 0.50 for predicting PLT modulus of RAP material. In this case, modulus determined by plate loading was nearly constant throughout the entire compaction process.

The recognition of “high” machine power for the initial roller pass over materials, which is the reason for using logarithmic relationships, applies also to relationships with physical soil properties. The highest MDP values for FA6 and CA6-G show a tendency to decrease the regression slope. The regressions, particularly the correlation coefficients, are also dependent on the measurements taken near full compaction. Slight decompaction was observed following 8 to 10 roller passes, evidenced by an increase in MDP and a decrease in CMV for the subsequent pass.

The presented linear relationships between physical soil properties and compaction monitoring results are limited to the respective five soil types and corresponding moisture conditions of the test strips. In an attempt to predict soil properties using compaction monitoring results independent of soil type, multiple regression analyses were performed with one composite dataset using compaction monitoring results, nominal moisture content, and soil indices as independent variables, with soil indices quantitatively representing soil type. To predict each in situ test measurement, roller output (CMV or MDP) and moisture content were statistically significant. Unfortunately, each cohesionless soil type was compacted and tested at only one moisture content, such that the influence of moisture content alone on test data could not be investigated. To predict select measurement results, combinations of fines content, percent gravel, percent sand, percent silt, and percent clay were significant, but still provided weak prediction models. A simple, consistent model for predicting soil density, strength, or stiffness independent of soil type was therefore not observed using the data from this field study.

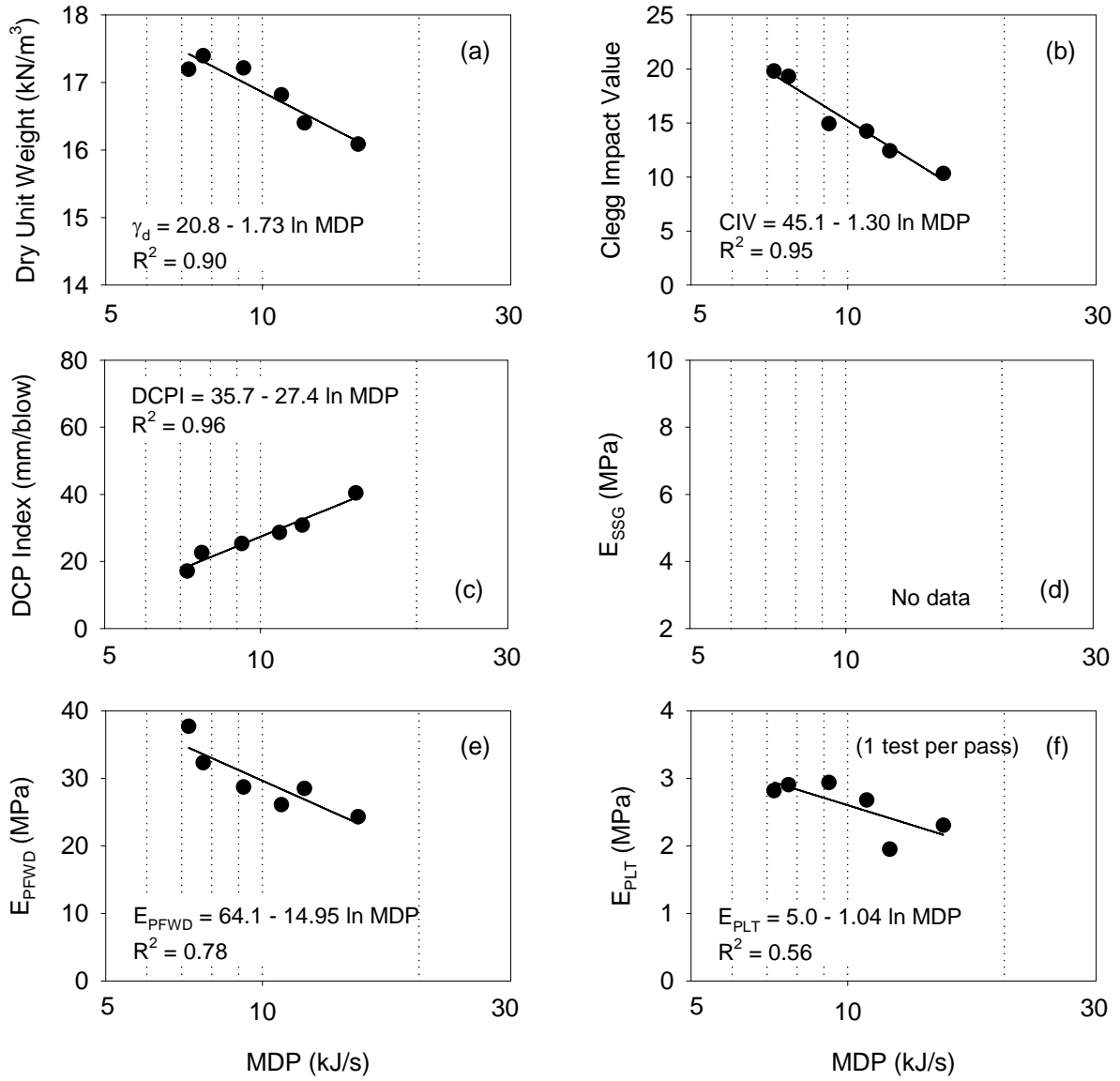


Figure 48. MDP regression analysis results for Strip 1 (RAP) using average of 10 tests

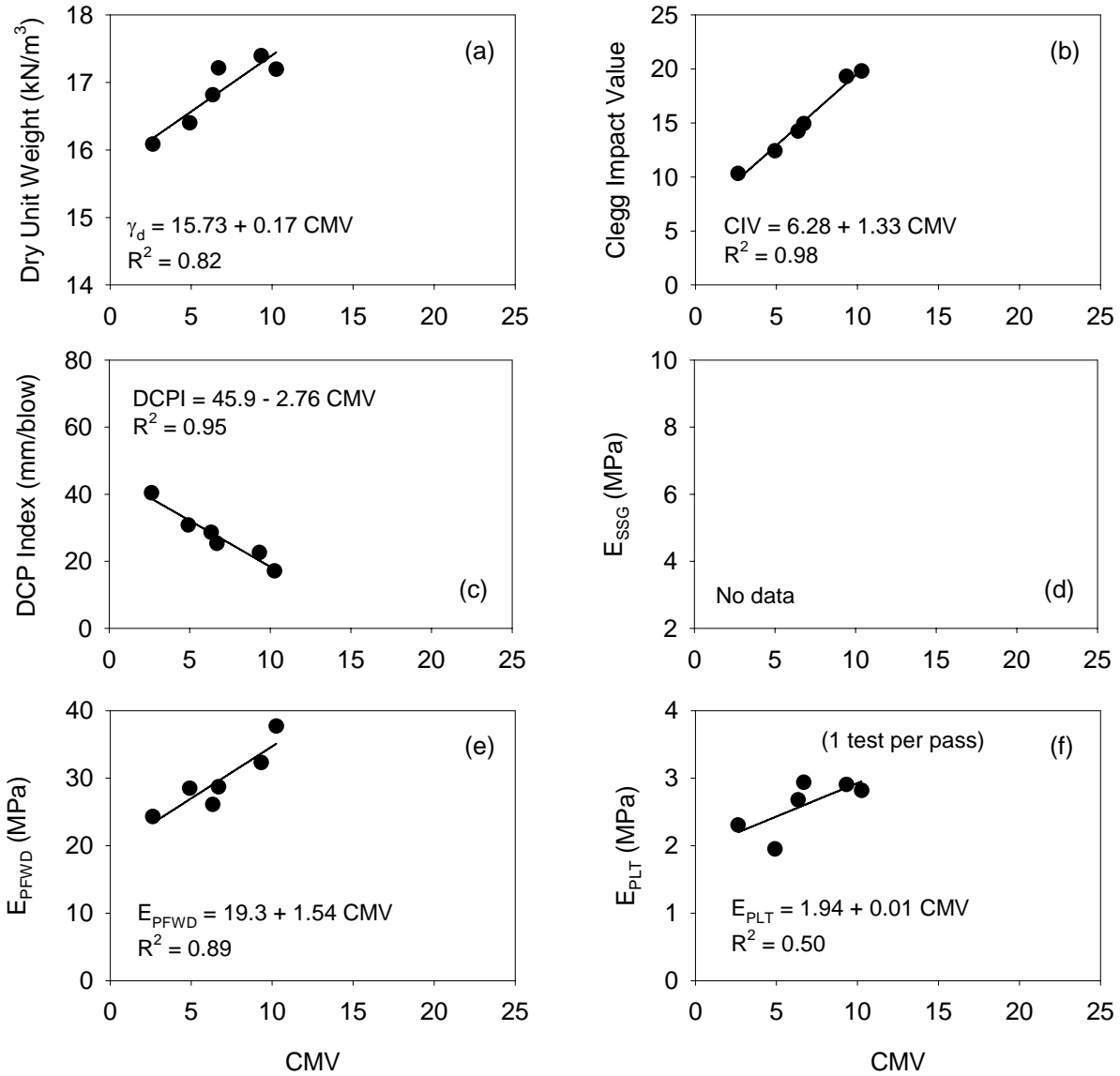


Figure 49. CMV regression analysis results for Strip 1 (RAP) using average of 10 tests

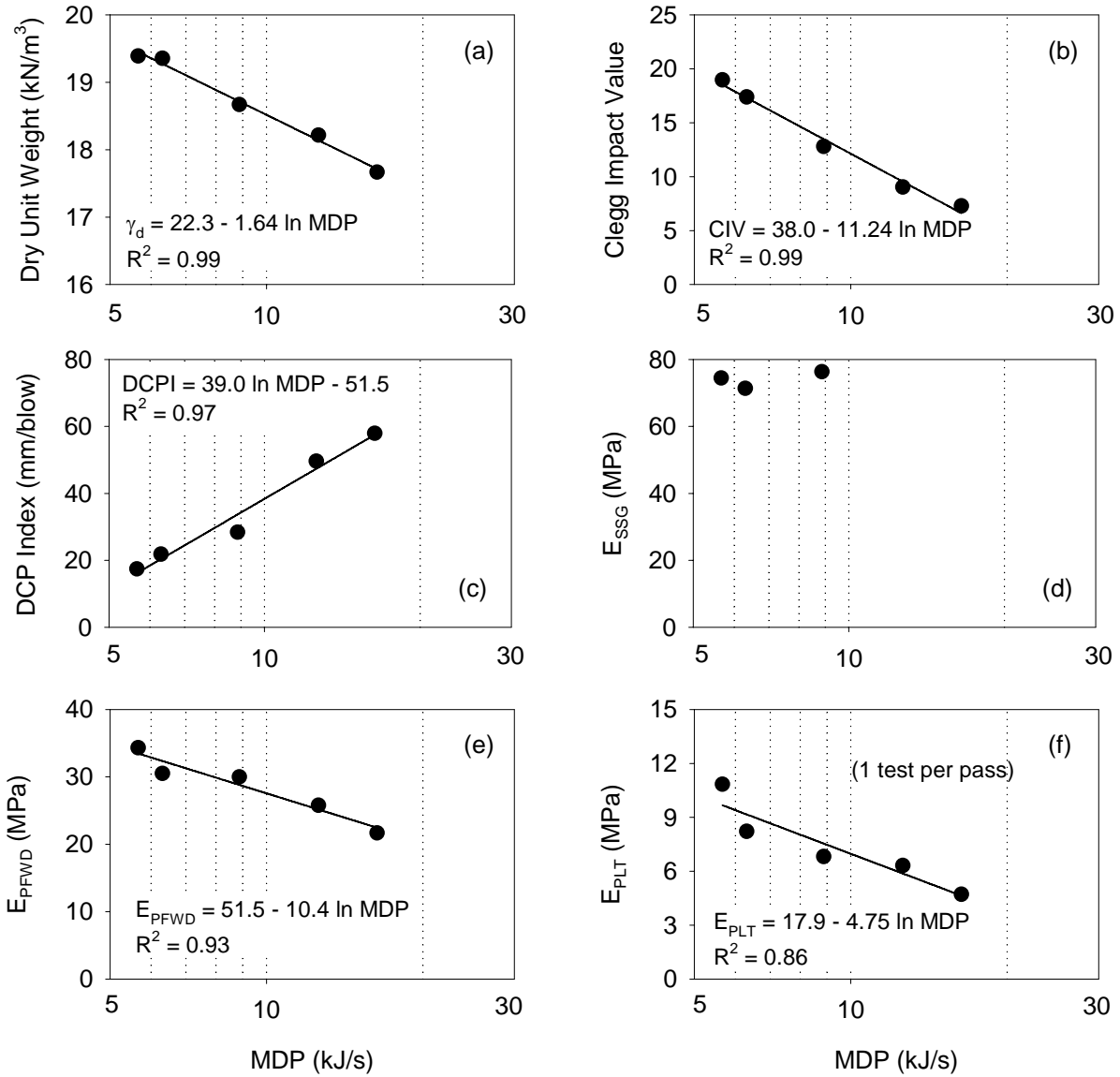


Figure 50. MDP regression analysis results for Strip 2 (CA6-C) using average of 10 tests

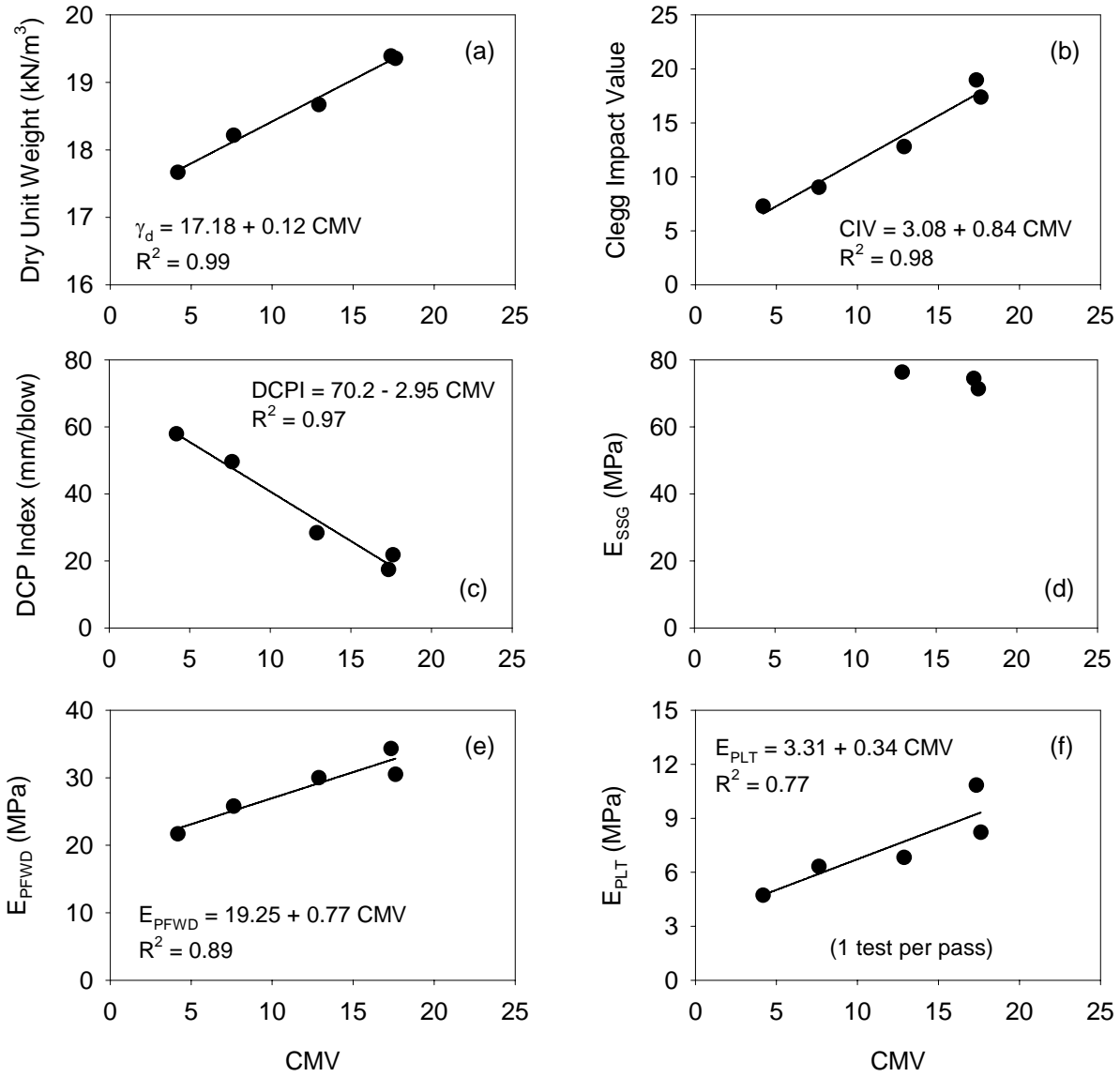


Figure 51. CMV regression analysis results for Strip 2 (CA6-C) using average of 10 tests

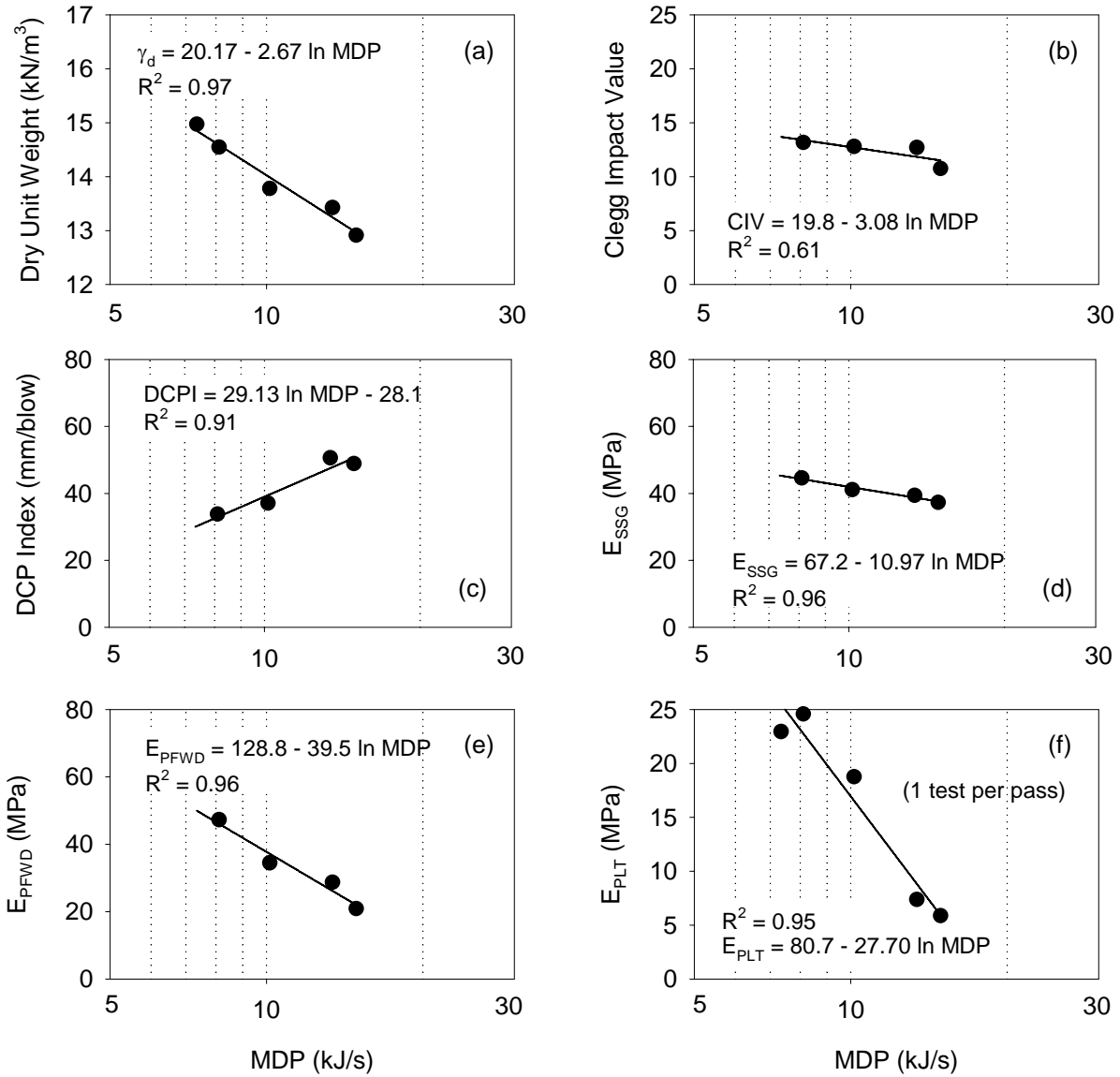


Figure 52. MDP regression analysis results for Strip 3 (CA5-C) using average of 10 tests

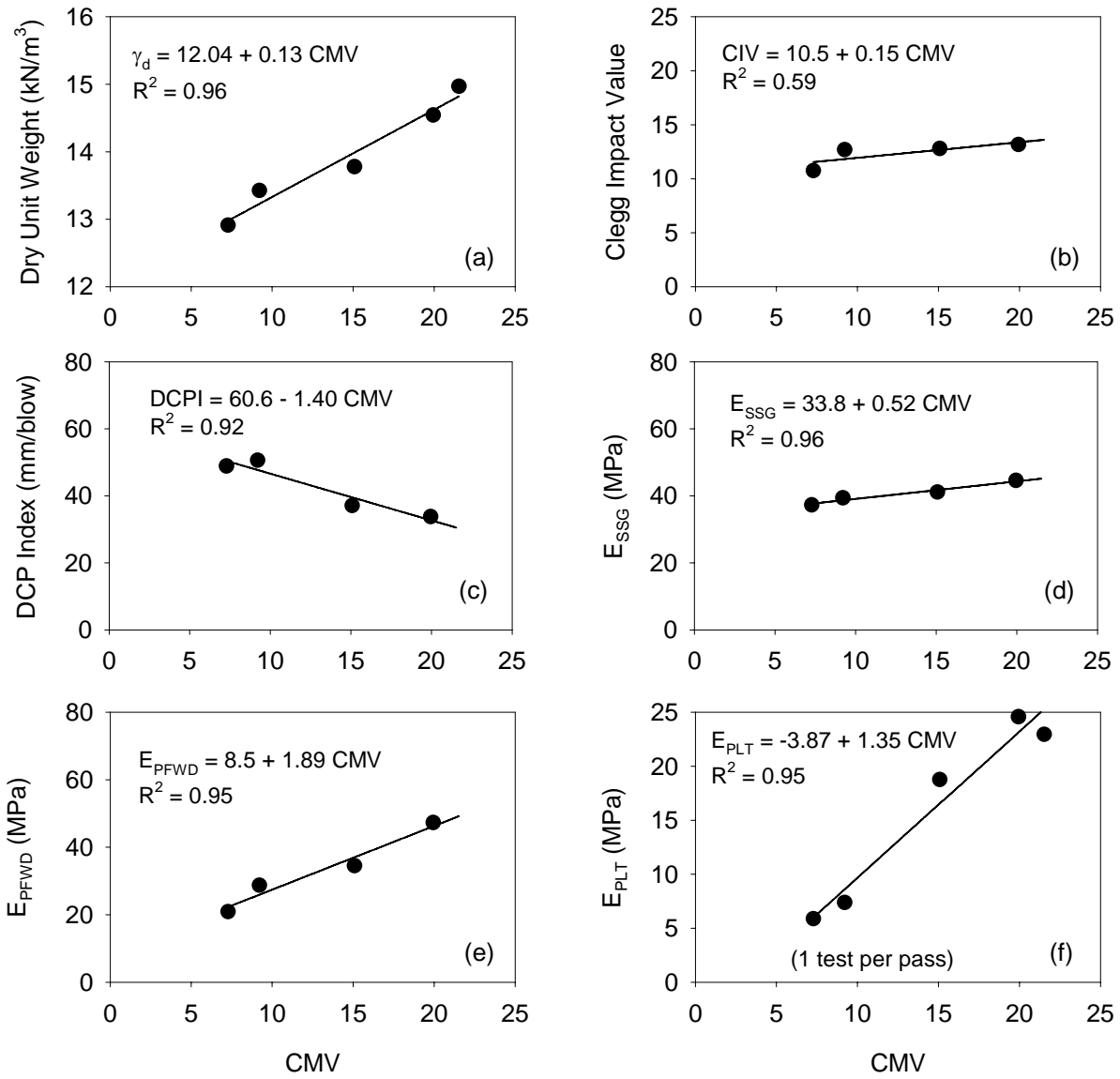


Figure 53. CMV regression analysis results for Strip 3 (CA5-C) using average of 10 tests

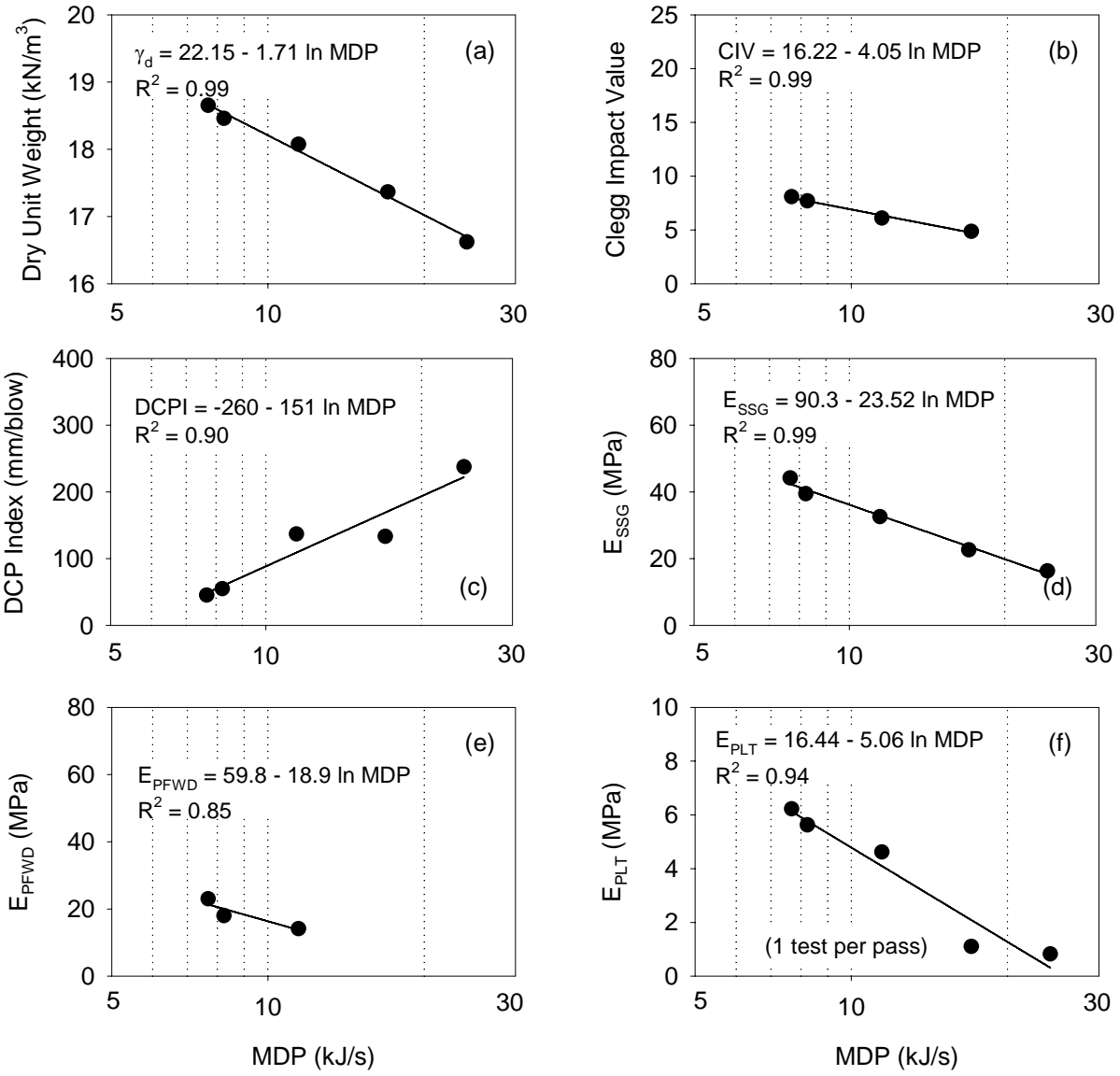


Figure 54. MDP regression analysis results for Strip 4 (FA6) using average of 10 tests

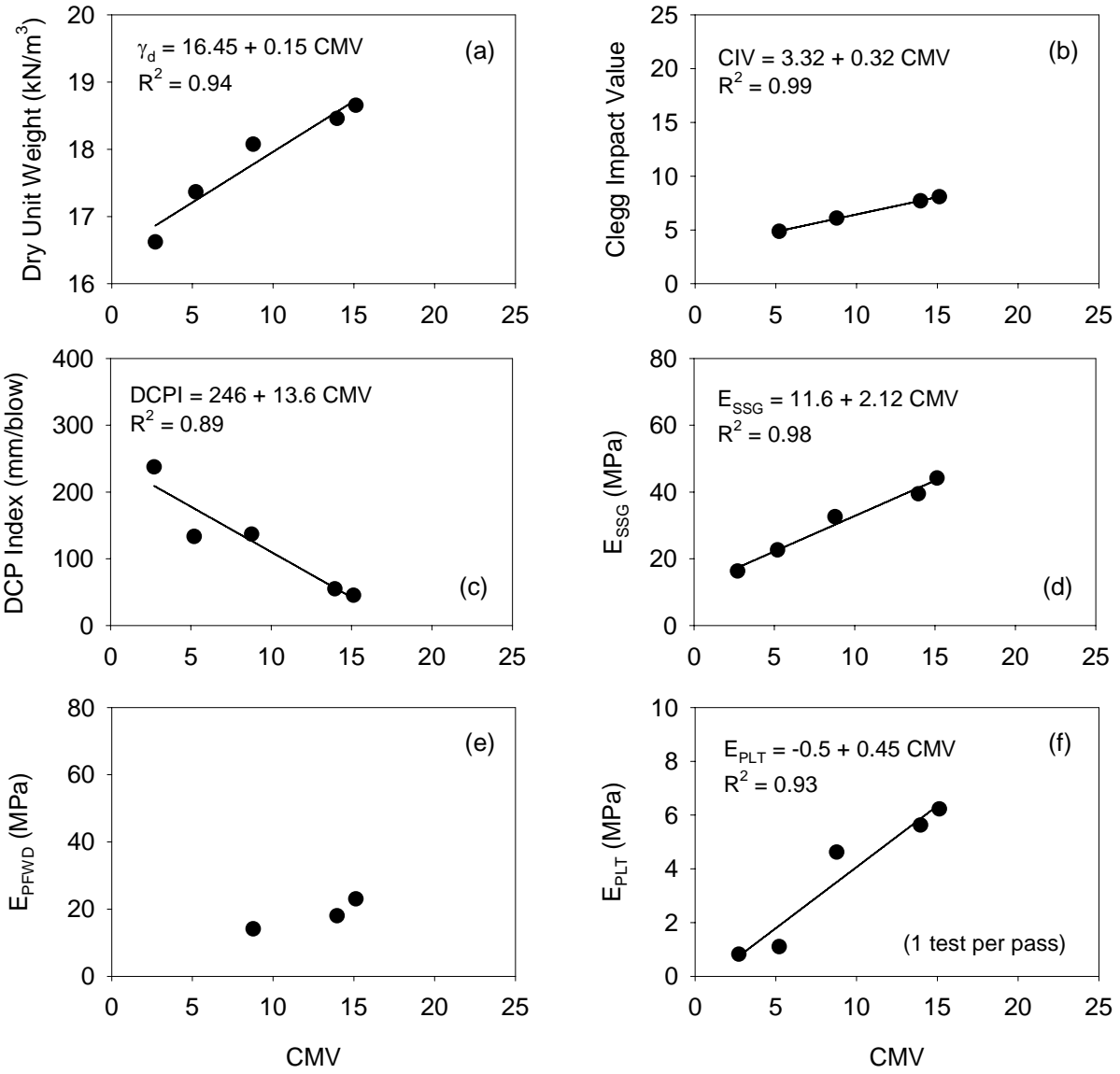


Figure 55. CMV regression analysis results for Strip 4 (FA6) using average of 10 tests

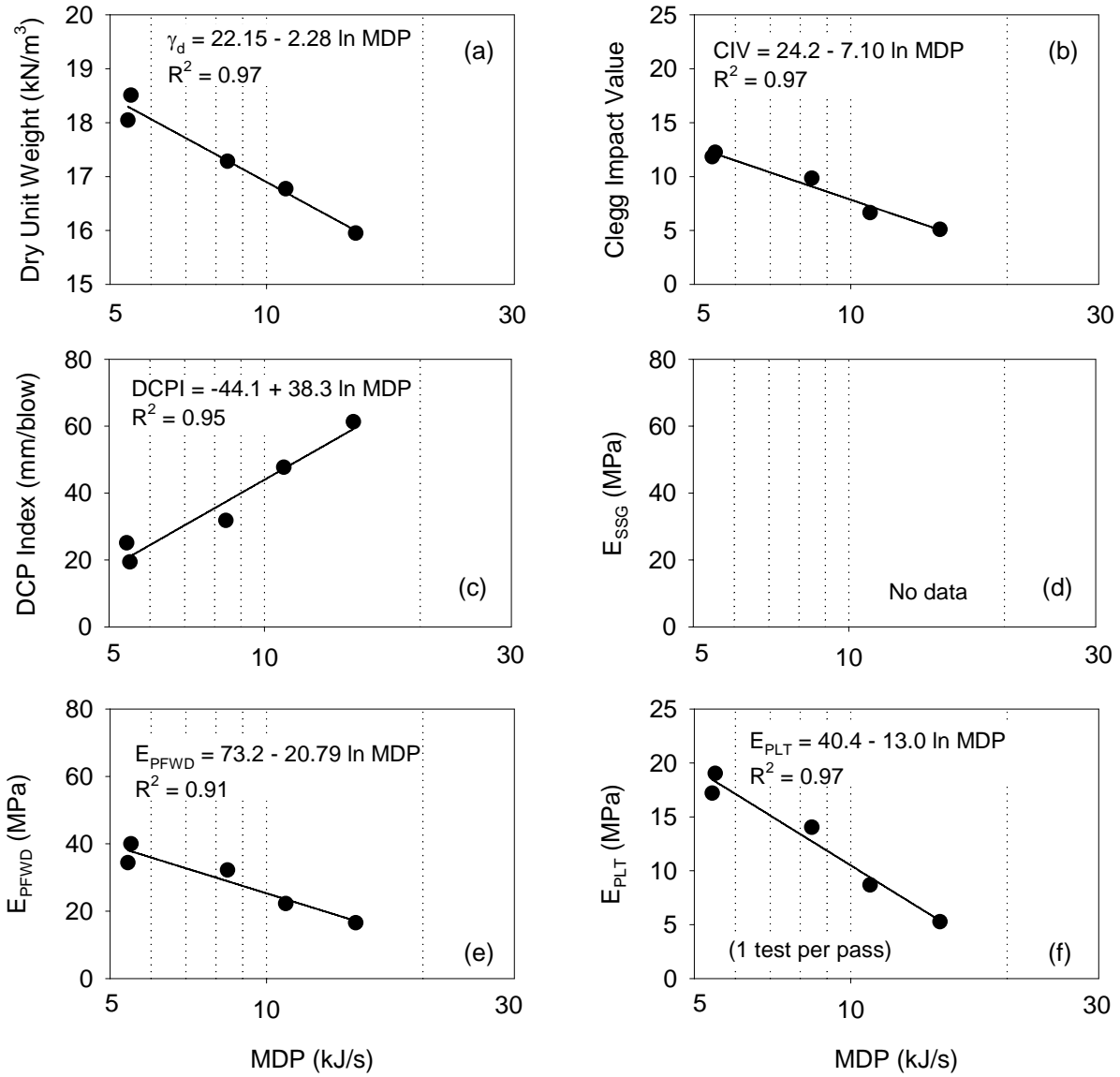


Figure 56. MDP regression analysis results for Strip 5 (CA6-G) using average of 10 tests

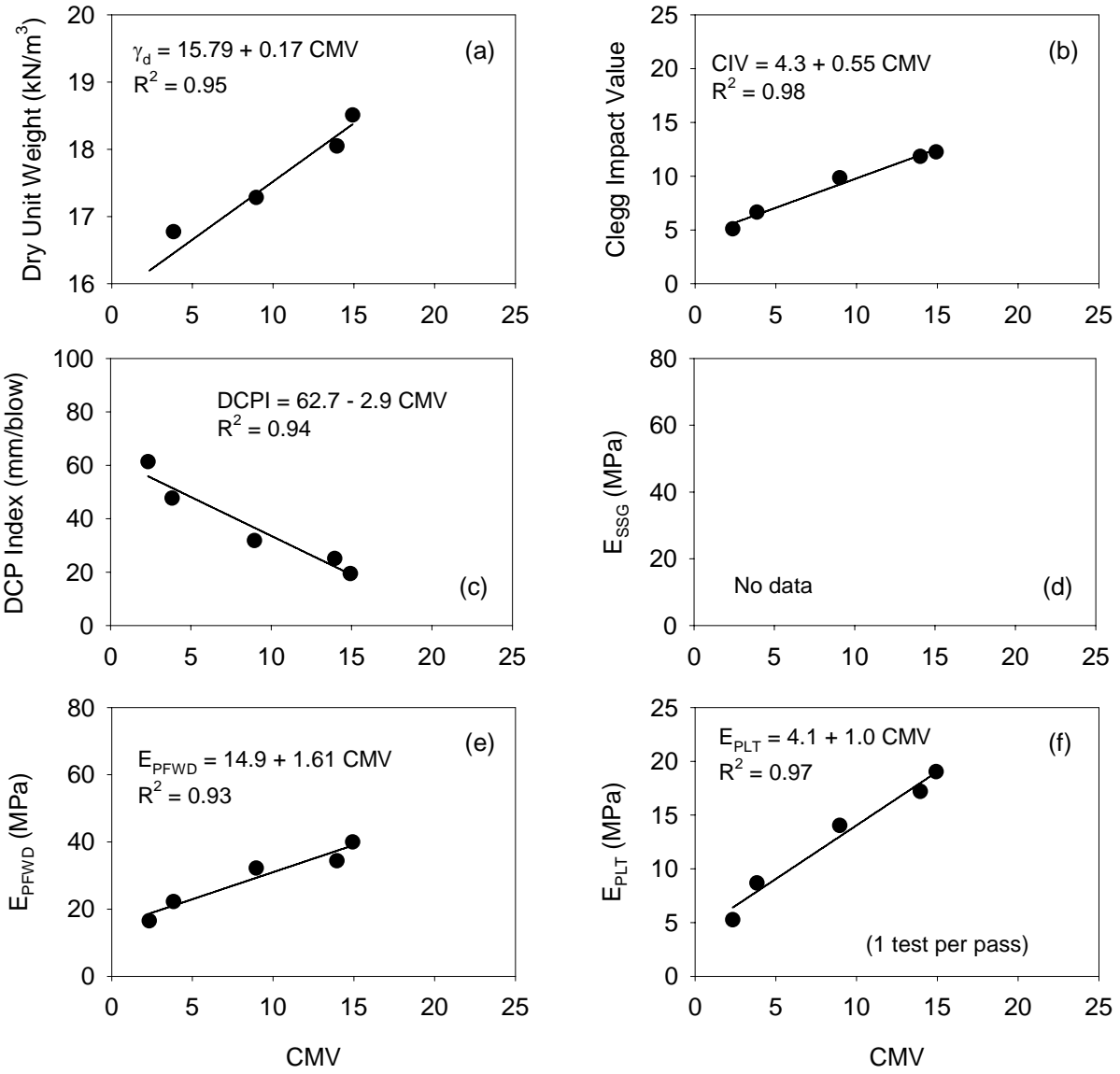


Figure 57. CMV regression analysis results for Strip 5 (CA6-G) using average of 10 tests

**Table 5. Correlation coefficients ( $R^2$ ) for linear regression analyses with MDP as independent variable**

<b>Soil property</b>	<b>RAP</b>	<b>CA6-C</b>	<b>CA5-C</b>	<b>FA6</b>	<b>CA6-G</b>
CMV	0.91	0.96	0.84	0.92	0.97
$\gamma_d$	0.90	0.99	0.97	0.99	0.97
CIV	0.95	0.99	0.61	0.99	0.97
DCP Index	0.96	0.97	0.91	0.90	0.95
$E_{GG}$	---	0.43	0.96	0.99	---
$E_{PFWD}$	0.78	0.93	0.96	0.85	0.91
$E_{PLT}$	0.56	0.86	0.95	0.94	0.97

**Table 6. Correlation coefficients ( $R^2$ ) for linear regression analyses with CMV as independent variable**

<b>Soil Property</b>	<b>RAP</b>	<b>CA6-C</b>	<b>CA5-C</b>	<b>FA6</b>	<b>CA6-G</b>
MDP	0.91	0.96	0.84	0.92	0.97
$\gamma_d$	0.82	0.99	0.96	0.94	0.95
CIV	0.98	0.98	0.59	0.99	0.98
DCP Index	0.95	0.97	0.92	0.89	0.94
$E_{GG}$	---	---	0.96	0.98	---
$E_{PFWD}$	0.89	0.89	0.95	0.83	0.93
$E_{PLT}$	0.50	0.77	0.95	0.93	0.97

Using averaged MDP and CMV data, logarithmic relationships were generally observed between the two compaction monitoring systems, as shown with squares from Figure 58 to Figure 61 for the cohesionless soils. The points shown as dots represent moving averages for “window” lengths of 0.2 (raw data), 1, 5, and 10 m. Scatter is observed in the MDP-CMV relationships for averaging lengths of less than 5 m. As a result, little confidence may be given to a single measurement value. Rather, multiple measurements must be statistically treated to increase the reliability of the measurement output. Even moving averages of 10 m produce a correlation with more scatter than averages over the entire strip length. The correlation coefficients ( $R^2$ ) for logarithmic relationships between MDP and CMV for moving averages of the different moving average window lengths are shown in Figure 62. The variability of both compaction monitoring measurements must be addressed in quality statements for implementing the technology into practice.

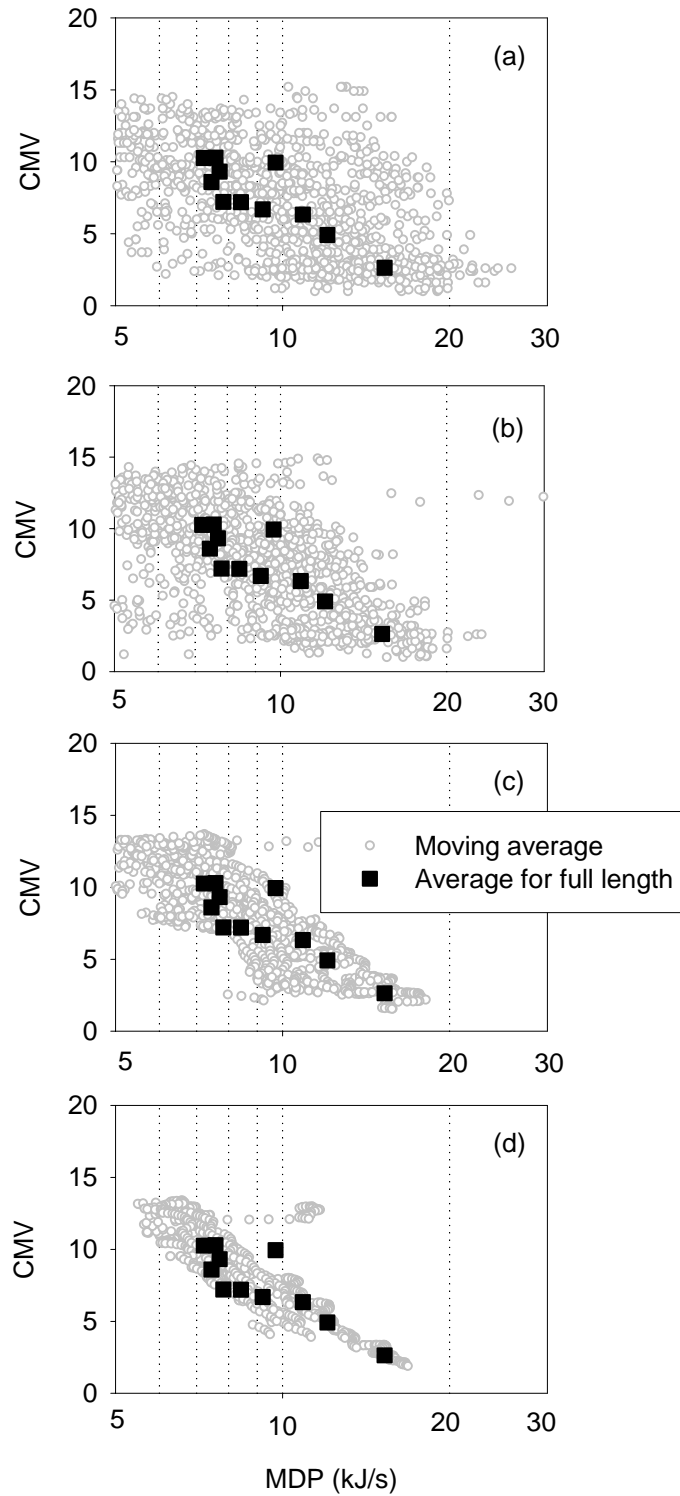


**Figure 58. MDP-CMV moving average correlation at various length scales for Strip 1 (RAP): (a) 0.2 m, (b) 1 m, (c) 5 m, and (d) 10 m**

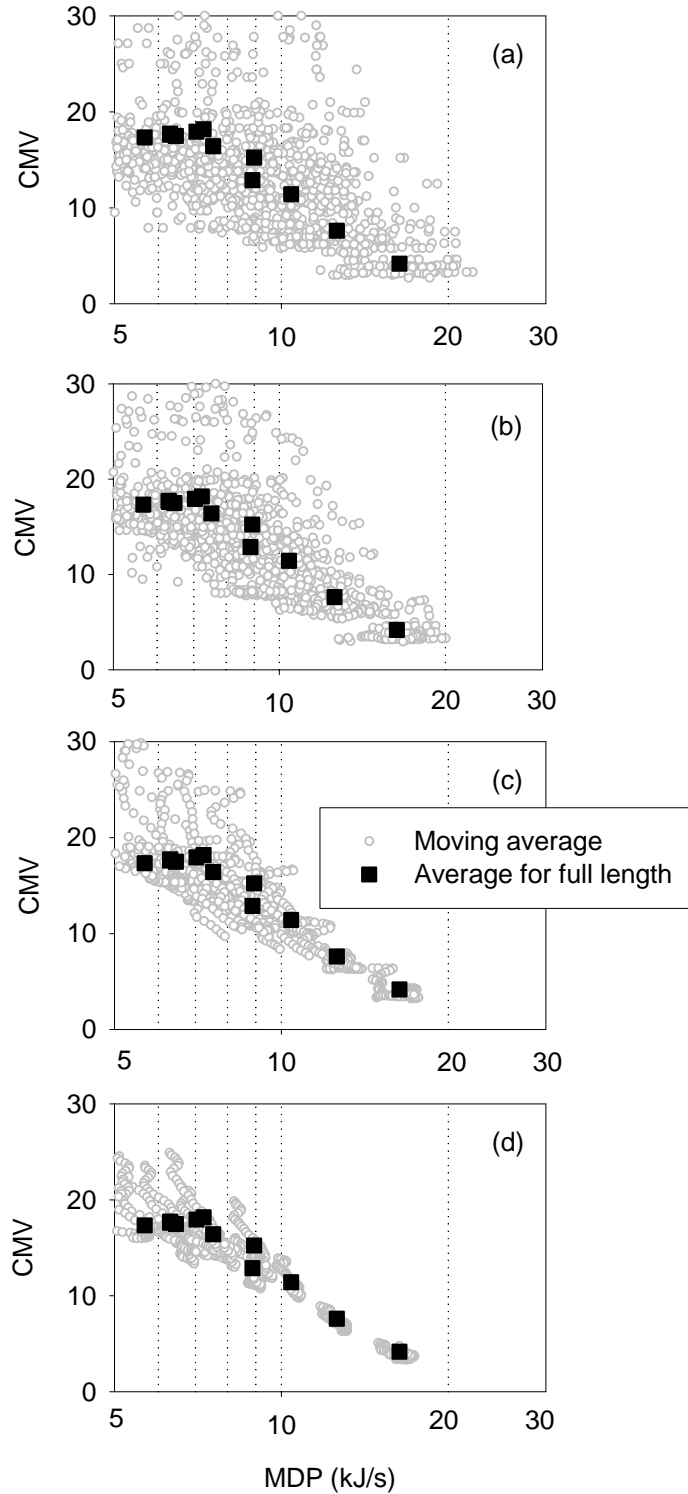


**Figure 59. MDP-CMV moving average correlation at various length scales for Strip 2 (CA6-C): (a) 0.2 m, (b) 1 m, (c) 5 m, (d) 10 m**

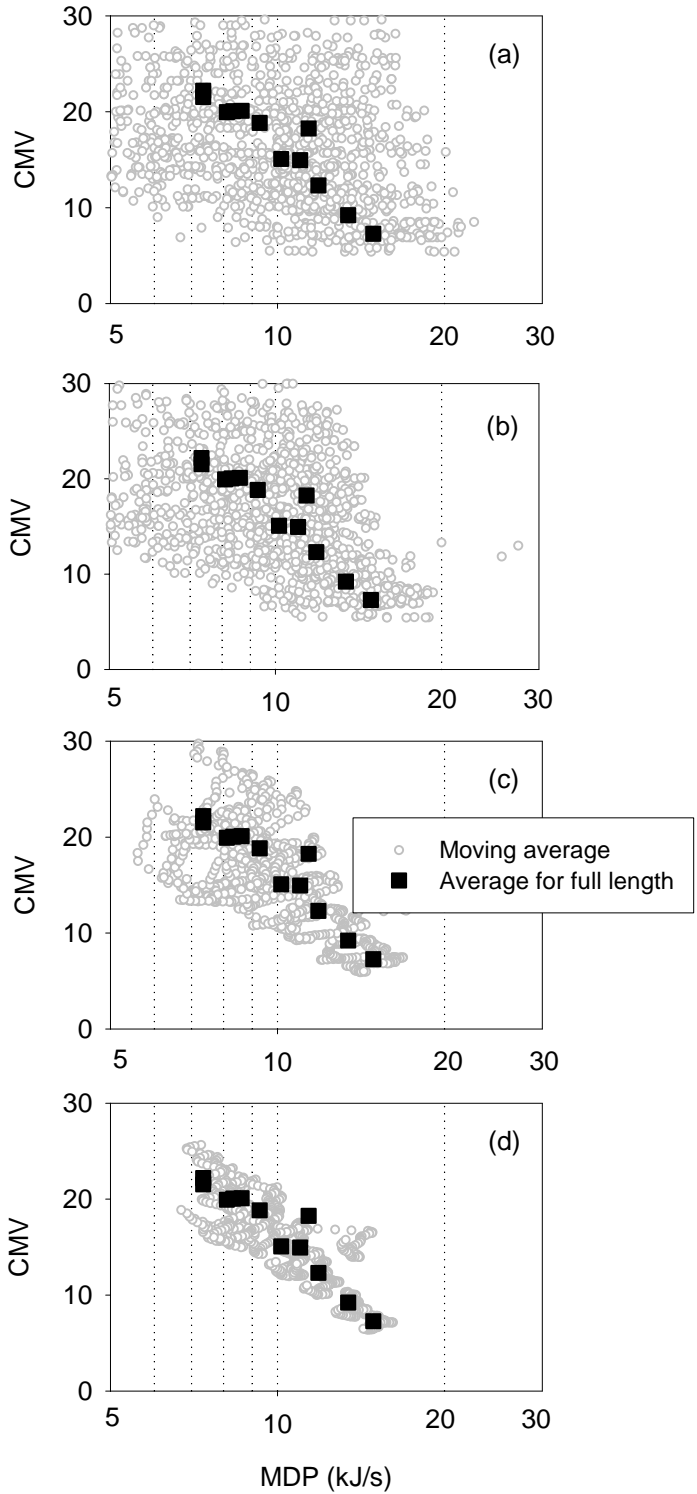


**Figure 60. MDP-CMV moving average correlation at various length scales for Strip 3 (CA5-C): (a) 0.2 m, (b) 1 m, (c) 5 m, (d) 10 m**

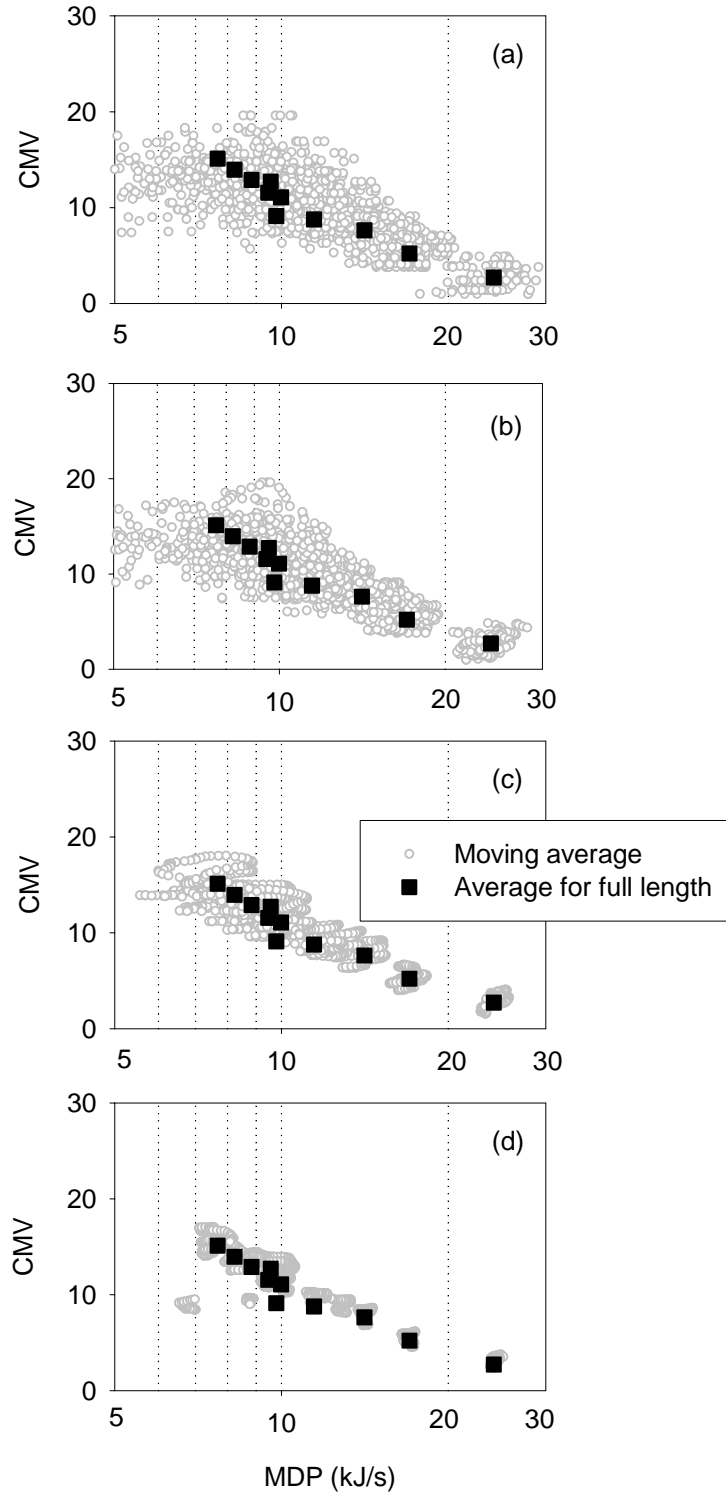


**Figure 61. MDP-CMV moving average correlation at various length scales for Strip 4 (FA6): (a) 0.2 m, (b) 1 m, (c) 5 m, (d) 10 m**

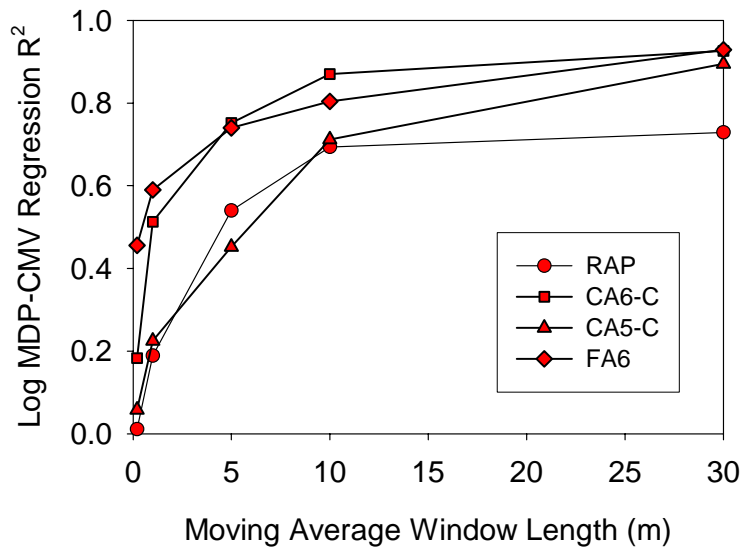


**Figure 62. Relationship between averaging length and MDP-CMV regression correlation**

### Project Observations

Experimental testing was conducted using a CS-533 vibratory smooth drum roller with integrated intelligent compaction technology to evaluate both MDP and CMV in terms of soil compaction and physical properties of compacted soil for five cohesionless soil types. In situ testing of soil density, strength, and deformation characteristics (i.e., soil modulus) provided data to characterize the soil at various stages (i.e., roller passes) of compaction.

The following conclusions were drawn from data and analysis in this study:

- Testing a single test point does not provide a high level of confidence for being representative of the average material characteristics, particularly when dealing with variable intelligent compaction data and variable soil conditions. In the case of comparing intelligent compaction results to field measurements, soil property variation and measurement influence area must be considered. For performing statistical analyses, data were averaged over the test strip area at each stage of compaction.
- The effect of soil compaction on roller machine-ground interaction is to decrease machine power (rolling resistance) and increase CMV (soil stiffness response). The change in intelligent compaction data with each roller pass can be described in terms of physical soil properties through linear relationships observed with dry unit weight, soil strength, and soil modulus. Correlation coefficients ( $R^2$  values) for the regressions generally exceed 0.90.
- The local variation in MDP is greater than for CMV for four of five soil types tested during this field study. Coefficients of variation and standard deviations for CMV and MDP, respectively, vary between test strips (soil types), despite being within a relatively narrow range for an individual test strip.

- Logarithmic relationships are generally observed between MDP and CMV compaction results, with different measurement influence depths acting for the two systems.
- In terms of predicting physical soil properties independent of soil type, both intelligent compaction results (CMV or MDP) and nominal moisture content are statistically significant. The limited dataset, however, did not provide a consistent model to improve the prediction of soil properties using soil indices as regression parameters to represent soil type.

## **PROJECT 3. EDWARDS FACILITY, CS-533 VIBRATORY SMOOTH DRUM**

### **Project Description and Objectives**

This section describes a project conducted from June 12 to June 15, 2006. Experimental testing and results are described to establish the applicability of using averaged roller data from one-dimensional calibration test strips to assess the compaction of a two-dimensional (i.e., spatial) area. Such an evaluation is necessary for verifying the reliability of using one-dimensional test strip calibrations as a specification component (see ISSMGE [2005]) for using compaction monitoring technologies. The specific objectives of this project included (1) collection of compaction monitoring results over a two-dimensional area that incorporates variable lift thickness and stiffness properties (2) documentation of how the result from two different compaction monitoring technologies are related, considering spatial variability of soil properties and measurement variability; (3) evaluation of how accurately two different compaction monitoring technologies predict soil properties compared to in situ compaction control tests; and (4) evaluation of previous research findings, such as using moisture content with machine compaction monitoring values to predict soil properties, for implementing the findings into quality statements or specifications.

The MDP and CMV compaction monitoring technologies were used for the project. The technologies were applied to a CS-533 vibratory smooth drum roller, shown in Figure 63. The 10,240-kg roller has a drum diameter of 1.55 m, a drum width of 2.13 m, and a rear wheel-to-drum width of 2.90 m. The roller was additionally fitted with a GPS to track roller coverage and apply compaction monitoring results to discrete locations over the project area (i.e., mapping).



**Figure 63. Caterpillar CS-533 vibratory smooth drum roller**

Field calibration testing was performed on the roller using four 30 m test strips. The initial test strips consisted of uniformly placed and moisture-conditioned material. To identify the influence of moisture content on machine response during compaction, the first test strip was compacted, tested, and then reconstructed at two additional moisture contents. For each of these test strips, five tests were conducted using each test device following 1, 2, 4, 8, and 12 roller passes. This compaction curve testing was used to develop statistical regressions relating MDP, CMV, and moisture content to the various in situ soil properties. The second test strip, which was constructed using well-graded subbase material at optimum moisture content, incorporated variable lift thickness (127 to 508 mm). Roller data from this test strip indicated the effect of lift thickness on machine response. The calibration strip testing program is shown in Figure 64.

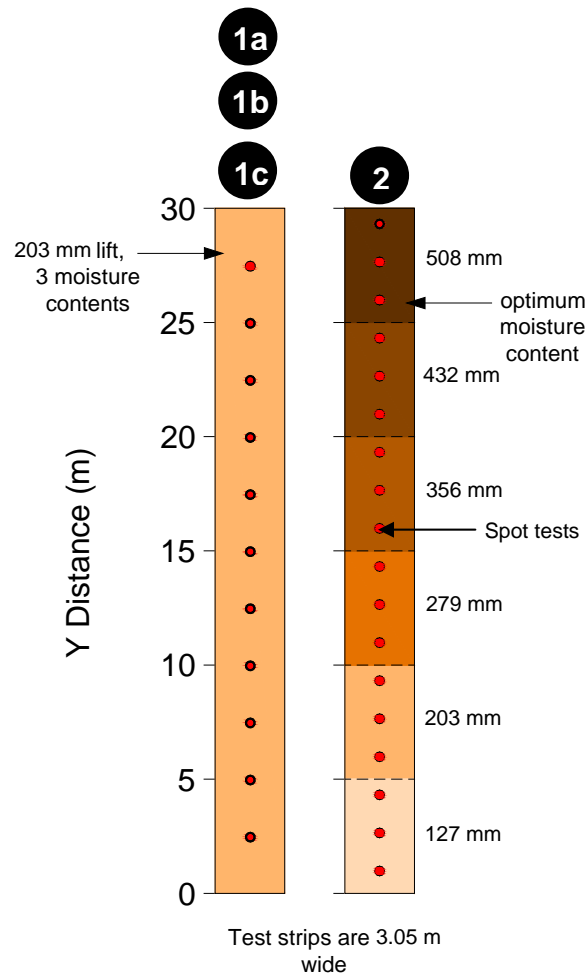


**Figure 64. Calibration strip testing program**

The second spatial testing plan (Spatial 2) was designed with dimensions of 30 m by 17.1 m, with increasing x-coordinates oriented in the North direction. The plan area, shown in Figure 65, was subdivided into eight roller widths. The testing used only one soil type and one nominal moisture content (optimum), but incorporated variable lift thickness (either 200 or 510 mm) to artificially achieve variation in soil stiffness properties. The test points for determining soil density, strength, and modulus are also shown in Figure 65. A stratified random testing design

was used, in which four random points were tested in each roller width every 5 m along the length of the test area, to give a total of 192 test locations.

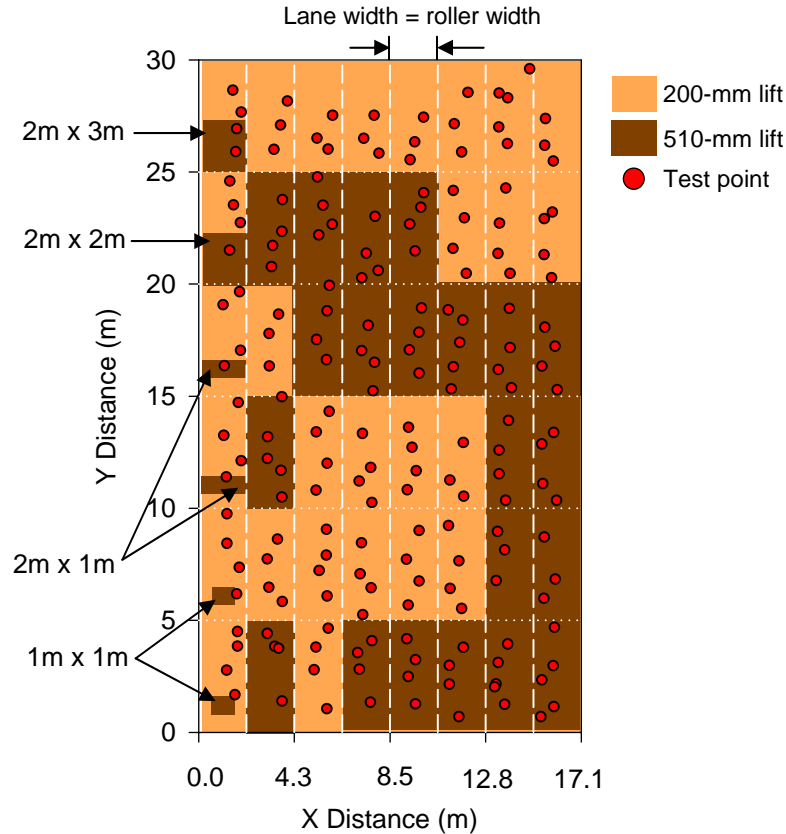


**Figure 65. Testing plan for Spatial 2**

The third spatial testing plan (Spatial 3) was designed with dimensions of 15 m by 17.1 m, with increasing x-coordinates oriented in the North direction. The plan area, shown in Figure 66, was also subdivided into eight roller widths. The testing area used the first 10 m of Spatial 1 (CA6-G material), but incorporated relatively stiff subgrade material to artificially achieve variation in soil stiffness properties. The test points for determining soil density, strength, and modulus are also shown in Figure 66. Six points were tested in each roller width every 5 m along the length of the test area, to give a total of 144 test locations. Four of these points defined the corners of each 5 m x 2.17 m “section,” with two additional measurements randomly oriented within these boundaries.

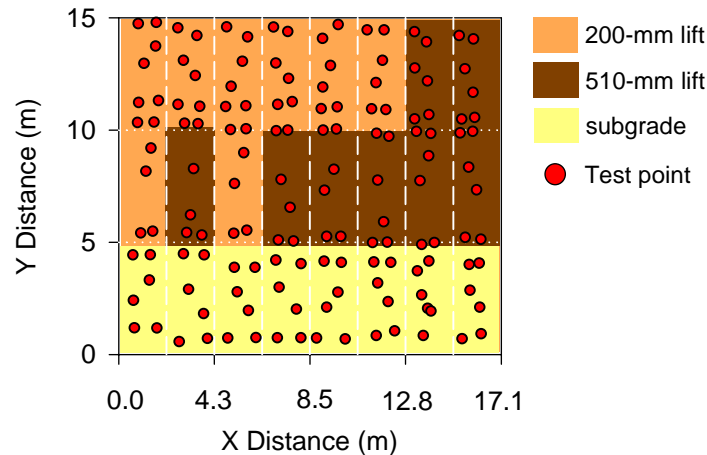


**Figure 66. Testing plan for Spatial 2**

### Construction and Testing Operations

The first test strip, shown in Figure 67, was constructed with a single nominal lift thickness (200 mm only), but incorporated variable soil moisture content. The soil of Strip 1a was drier than the Standard Proctor optimum, at about 5.4% moisture by weight; Strip 1b was moisture conditioned close to Standard Proctor optimum moisture content (8.2%); and Strip 1c was wetter than Standard Proctor optimum, at about 12.0%. For each test strip, spot testing followed 1, 2, 4, 8, and 12 roller passes. The second calibration test strip was constructed with progressively thicker loose lifts. The 30 m strip was comprised of 5 m sections of the following six nominal lift thicknesses: 127, 203, 279, 356, 432, and 508 mm. Variable lift thickness was achieved by first excavating the subgrade material in 76 mm steps, as shown in Figure 68. Placement of fill in Strip 2 is shown in Figure 69.



**Figure 67. Compacting Strip 1**



**Figure 68. Excavation for Strip 2**



**Figure 69. Placement of fill in Strip 2 excavation**

Construction of the Spatial 2 test area began by excavating select areas of the existing subgrade material to a depth of 310 mm. The excavated plan area is shown in Figure 70. The subgrade material was comparatively stiff at the soil surface, but decreased in stiffness with depth. After excavating the areas of thicker lift, base material (CA6-G) was placed to 200 mm above the original grade to give either 200 mm or 510 mm loose lift. Prior to compaction, several DCP tests were performed to ensure low strength throughout the entire vertical profile of loose fill.

After constructing the test area, the base material was compacted using the CS-533 vibratory smooth drum roller. The roller was operated at the “high” amplitude setting (about 1.70 mm), and the frequency of drum vibration was constant at about 32 Hz. Compaction of the test area is shown in Figure 71. For this project, the roller did not overlap its path, but rather traveled in

designated “lanes.” Near-continuous measurements of CMV and machine power were made approximately every 0.2 m along the length (in the y-direction) of the test area. GPS coordinates were collected with compaction monitoring measurements, such that results were mapped and viewed in real-time during compaction operations.

Soil testing was performed over the two-dimensional area following only the second roller pass to obtain the soil density, moisture content, DCP index, CIV, and  $E_{PFWD}$  at a total of 192 test locations, with the exact spatial location of these test points obtained using a GPS rover working off the same base station as the roller GPS system. DCP testing was conducted; the mean DCP index at 500 mm penetration was used throughout the analysis of Spatial 2. In situ spot testing is shown in Figure 72.



**Figure 70. Excavations for Spatial 2 test area**



**Figure 71. Compaction of Spatial 2**



**Figure 72. In situ testing of Spatial 2**

Spatial 3 was configured such that two-thirds of the area was comprised of CA6-G material and one-third of the area was comprised of existing Edwards till subgrade. The test area and compaction of the test area are shown in Figure 73 and Figure 74, respectively. In situ testing was conducted as it was for Spatial 2, except that DCP tests were conducted only to 200 mm penetration.

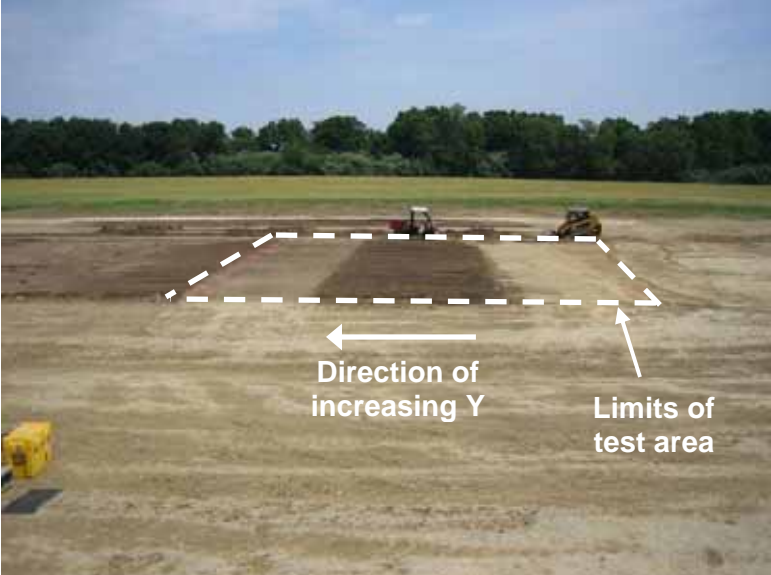


**Figure 73. Spatial 3 test area (outlined in white)**



**Figure 74. Compaction of Spatial 3**

## Material Properties

Compaction curve and spatial testing were conducted using CA6-G (Illinois DOT classification) from a local source. This non-plastic soil is coarse-grained ( $C_u = 30$ ,  $C_c = 2.7$ ) and classifies as SW-SM well-graded sand with silt and gravel according to USCE, and A-1-b according to AASHTO soil classification (see Table 7 and Figure 75).

Moisture-density tests were performed following the Standard and Modified Proctor test methods (ASTM D 698-00 and ASTM D 1557-98, respectively). The Standard maximum dry unit weight was about  $21.4 \text{ kN/m}^3$ , with optimum moisture content at approximately 8.0%. The Modified maximum dry unit weight was about  $21.8 \text{ kN/m}^3$ , with optimum moisture content at approximately 5.4% (see Table 7 and Figure 76). The minimum and maximum dry unit weights from relative density testing (ASTM D 4253-00) were approximately  $14.4$  and  $19.8 \text{ kN/m}^3$ , respectively, for oven-dry soil.

The underlying subgrade soil, a till material, classifies as CL sandy lean clay with moderate plasticity.

**Table 7. Pilot Project 3 testing materials**

Soil property	CA6-G
USCS:	
Symbol	SW-SM
Name	Well-graded sand with silt
$G_s$	2.75
$F_{200}$ (%)	68
LL (PI)	NP
Standard Proctor:	
$\gamma_{d, \max}$ ( $\text{kN/m}^3$ )	21.4
$w_{\text{opt}}$ (%)	8.0
Modified Proctor:	
$\gamma_{d, \max}$ ( $\text{kN/m}^3$ )	21.8
$w_{\text{opt}}$ (%)	5.4

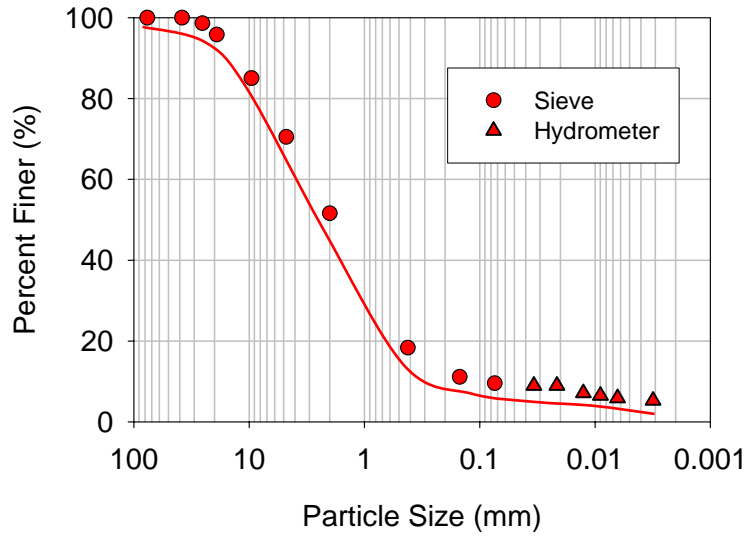


**Figure 75. CA6-G particle size distribution**

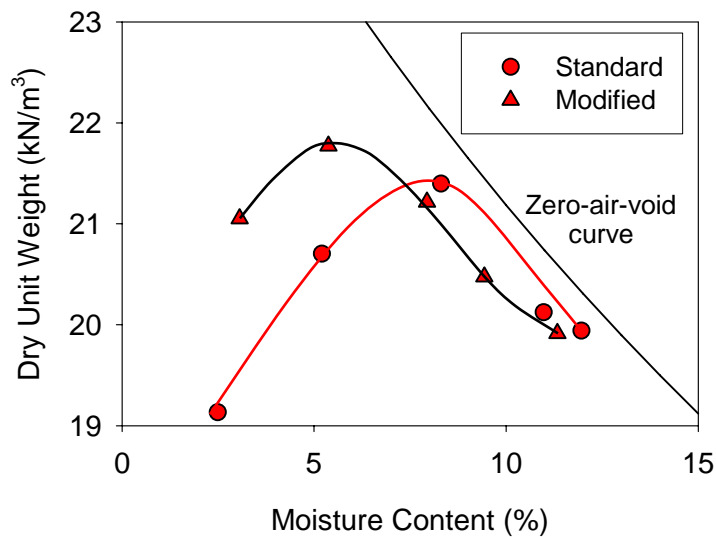


**Figure 76. CA6-G standard Proctor moisture-density relationship**

### Machine Calibration Using Regression Analysis

Calibration of CMV and MDP was accomplished using Strips 1 and 2 by correlating the collected roller data to the measured in situ soil properties. Considering the variability associated with the two compaction monitoring technology measurements, as well as the measurement variability of each in situ spot measurement, data were averaged along the length of the test strips to produce a single data point for each roller pass.

Preliminary target compaction monitoring values were selected from the nominal 203 mm lift thickness section of Strip 2. At 95% of the maximum dry unit weight (based on standard Proctor compaction energy), observed after four roller passes, the average MDP equaled 8.3 kJ/s and the average CMV equaled 8.0. This relatively simple method for determining quality criteria, while not providing a unified correlation that accounts for all variables affecting machine response, also does not require detailed statistical analyses.

Because the first test strip (1a, 1b, and 1c) was tested following 1, 2, 4, 8, and 12 roller passes, five data points were obtained per test strip to provide a total of 15 data points from which a correlation was developed to account for variable moisture content. The averaging and regression model development procedure is described in White et al. (2006). Multiple regression analysis results are presented in Table 8 and Figure 77, where the data points are the average measured values and the solid lines are predictions from the provided regression equations. In predicting DCP index, CIV, and  $E_{PFWD}$  from compaction monitoring results, the addition of moisture content as a second regression parameter yielded correlation coefficients ( $R^2$ ) that ranged from 0.85 to 0.95, with both MDP and CMV providing reliable results. In predicting soil density, the compaction monitoring technologies differed in that the regression model using MDP yielded a higher correlation coefficient (0.92) than CMV (0.68).

**Table 8. Coefficients for machine calibration regression analysis**

<b>Correlation</b>	<b>b<sub>0</sub></b>	<b>b<sub>1</sub></b>	<b>b<sub>2</sub></b>	<b>b<sub>3</sub></b>	<b>b<sub>4</sub></b>
Log MDP- $\gamma_d$	23.63 (kN/m <sup>3</sup> )	1.3 (kN/m <sup>3</sup> )	-1.2 (% <sup>-1</sup> ) kN/m <sup>3</sup>	0.1 (% <sup>-2</sup> ) kN/m <sup>3</sup>	-0.6 (% <sup>-1</sup> ) kN/m <sup>3</sup>
Log MDP-CIV	15.8	-7.3	-0.6 (% <sup>-1</sup> )	---	---
Log MDP-DCPI	-69.6 (mm/blow)	65.1 (mm/blow)	11.1 (% <sup>-1</sup> ) mm/blow	---	---
Log MDP- $E_{PFWD}$	60.1 (MPa)	-18.8 (MPa)	-2.6 (% <sup>-1</sup> ) MPa	---	---
CMV- $\gamma_d$	12.7 (kN/m <sup>3</sup> )	0.9 (kN/m <sup>3</sup> )	0.9 (% <sup>-1</sup> ) kN/m <sup>3</sup>	-0.12 (% <sup>-1</sup> ) kN/m <sup>3</sup>	---
CMV-CIV	7.5	0.5	-0.8 (% <sup>-1</sup> )	---	---
CMV-DCPI	13.1 (mm/blow)	-5.9 (mm/blow)	12.8 (% <sup>-1</sup> ) mm/blow	---	---
CMV- $E_{PFWD}$	31.1 (MPa)	2.3 (MPa)	-2.9 (% <sup>-1</sup> ) MPa	---	---

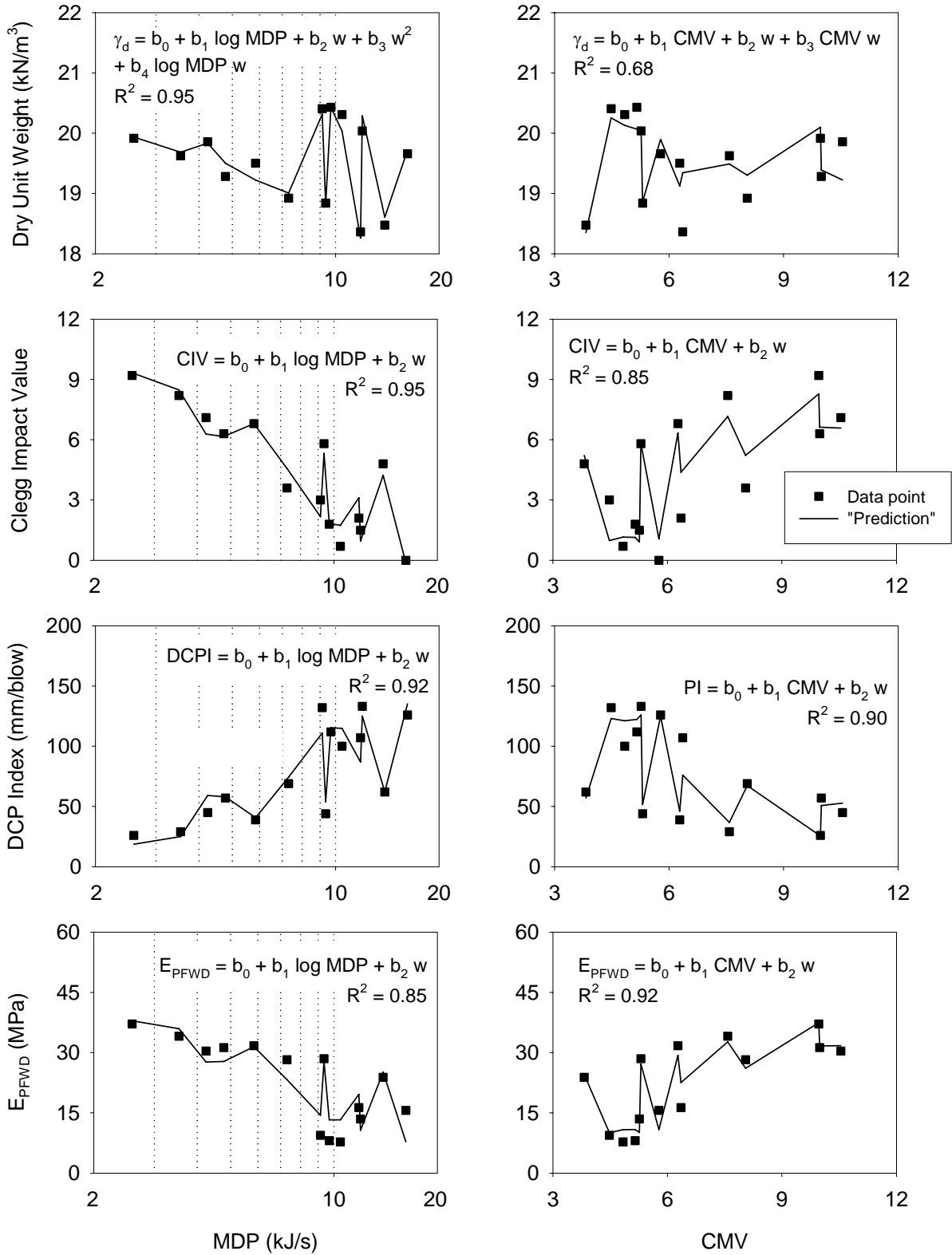


**Figure 77. Multiple regression analysis results for Strip 1 (a-c)**

## Analysis of Strip 2

### Machine Data and Compaction Curves

Machine data for Strip 2 is shown in Figure 78 for Passes 1, 2, and 8. Limits of the six nominal loose lift thicknesses are demarcated with dashed lines and labeled. The data show that thicker lifts result in higher MDP and lower CMV. However, with increasing roller passes, MDP still decreases and CMV still increases. DCP data collected on Strip 2 are shown in Figure 79 and Figure 80 for several roller passes to show the lift thicknesses that comprise the test strip. Field compaction curves for Strip 2 are then shown in Figure 81 for each roller and in situ measurement. For each measurement, compaction is observed with the increasing number of roller passes through a nonlinear relationship. The effect of lift thickness is also observed. The effect of increasing lift thickness is to increase MDP and to decrease CMV, as observed in the raw data. CIV and  $E_{PFWD}$  are observed to decrease with increasing lift thickness. Differential lift thickness has less effect on dry unit weight and DCP index. Based on data from the six nominal lift thickness sections, the lowest soil stiffness was observed for the 432 mm lift thickness.

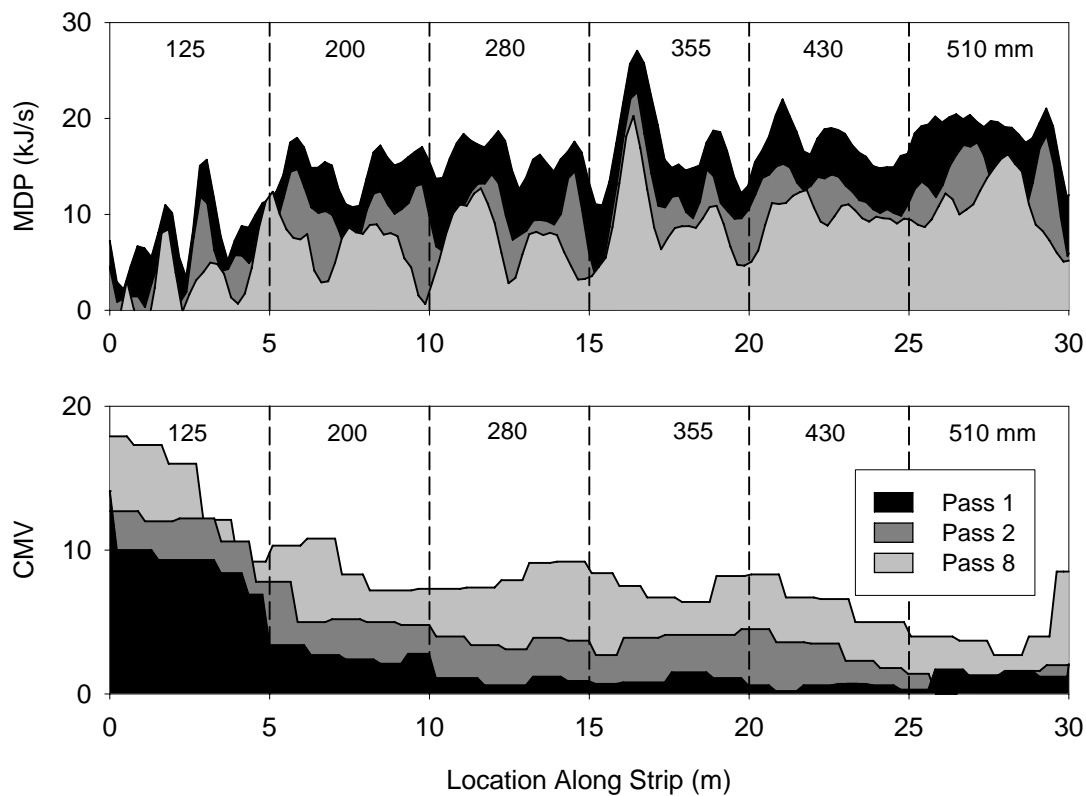
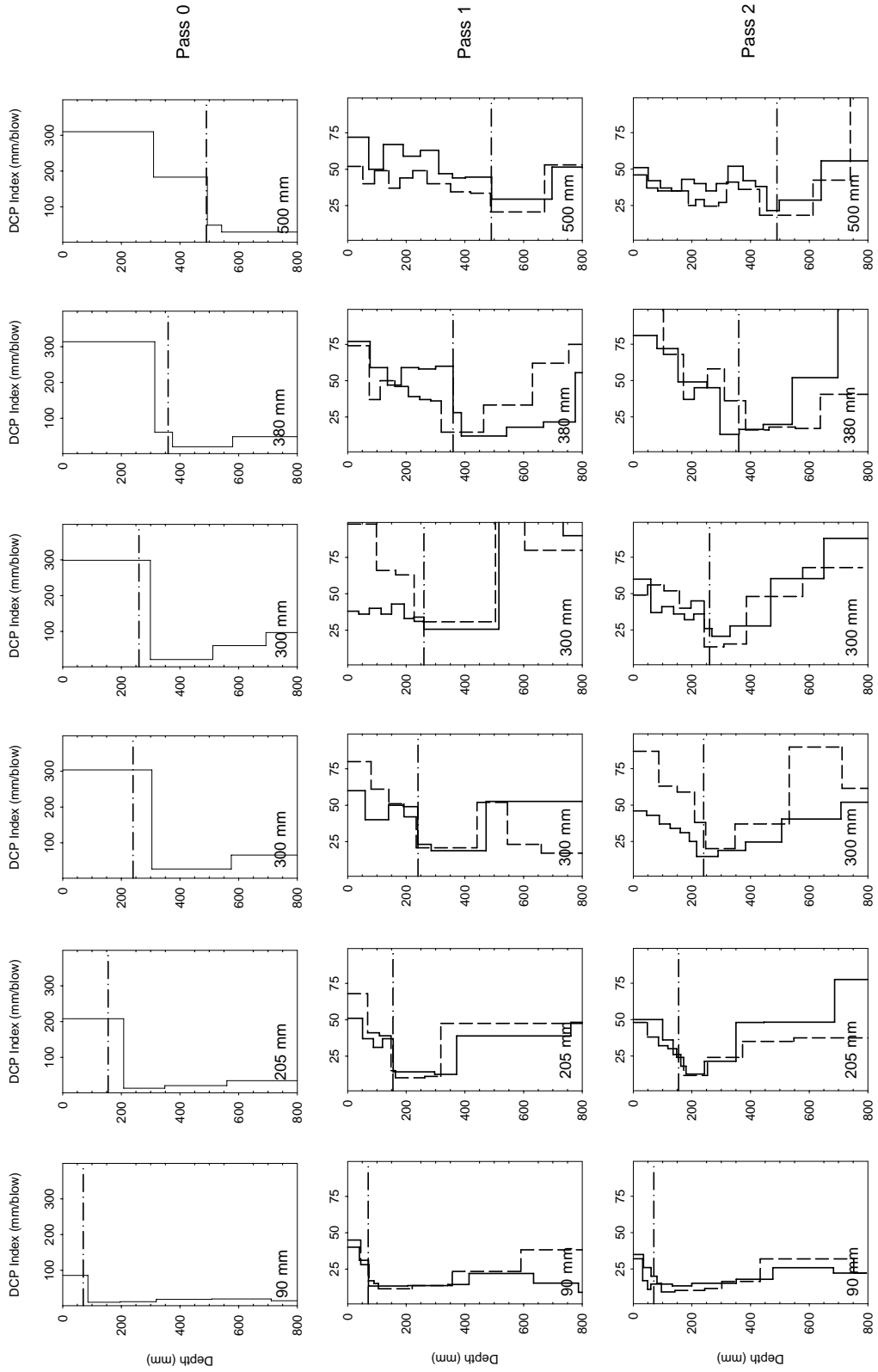
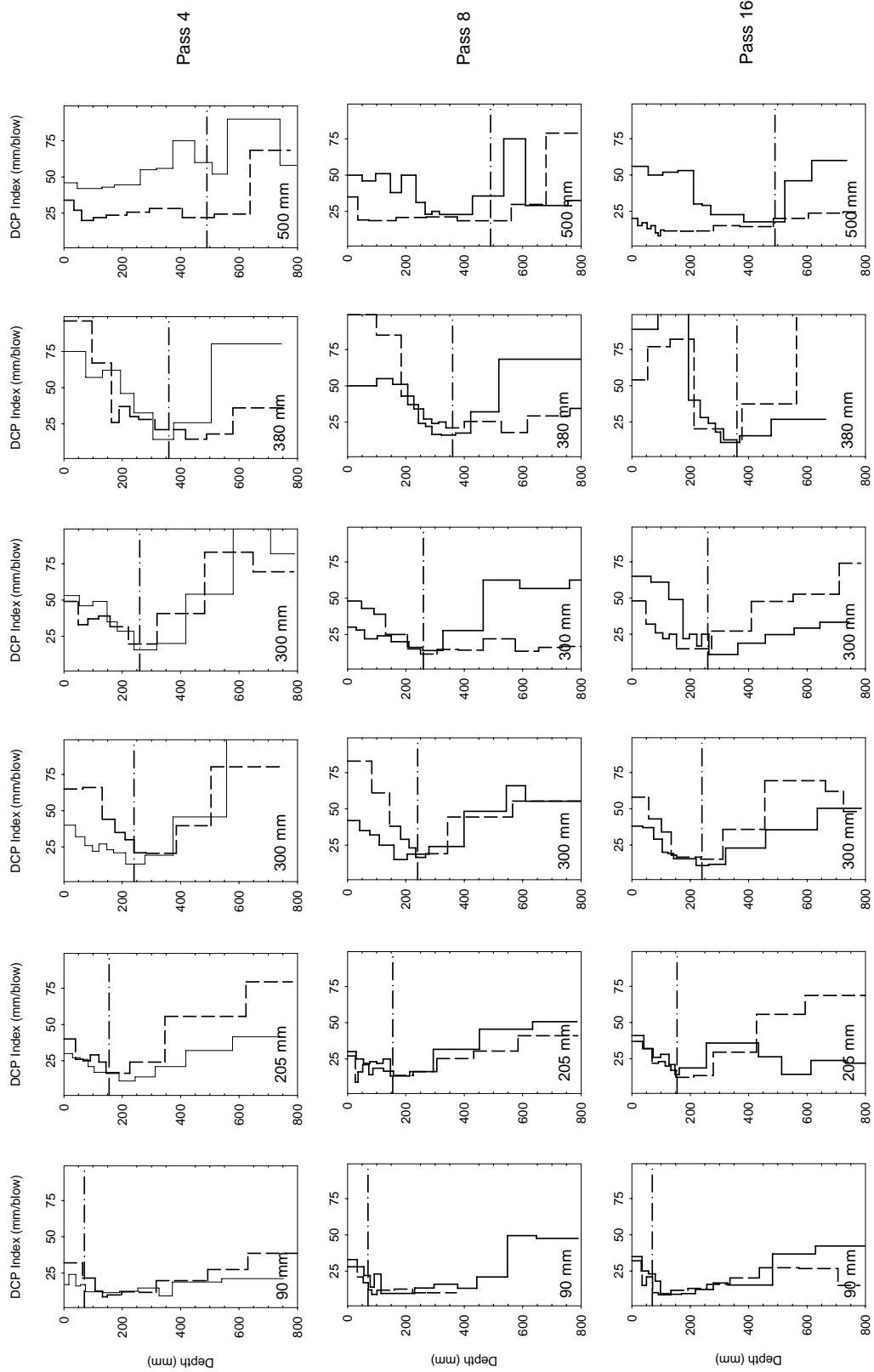


Figure 78. MDP and CMV for Passes 1, 2, and 8 on Strip 2



**Figure 79. Strip 2 DCP profiles for Passes 0, 1, and 2**



**Figure 80. Strip 2 DCP profiles for Passes, 4, 8, and 16**

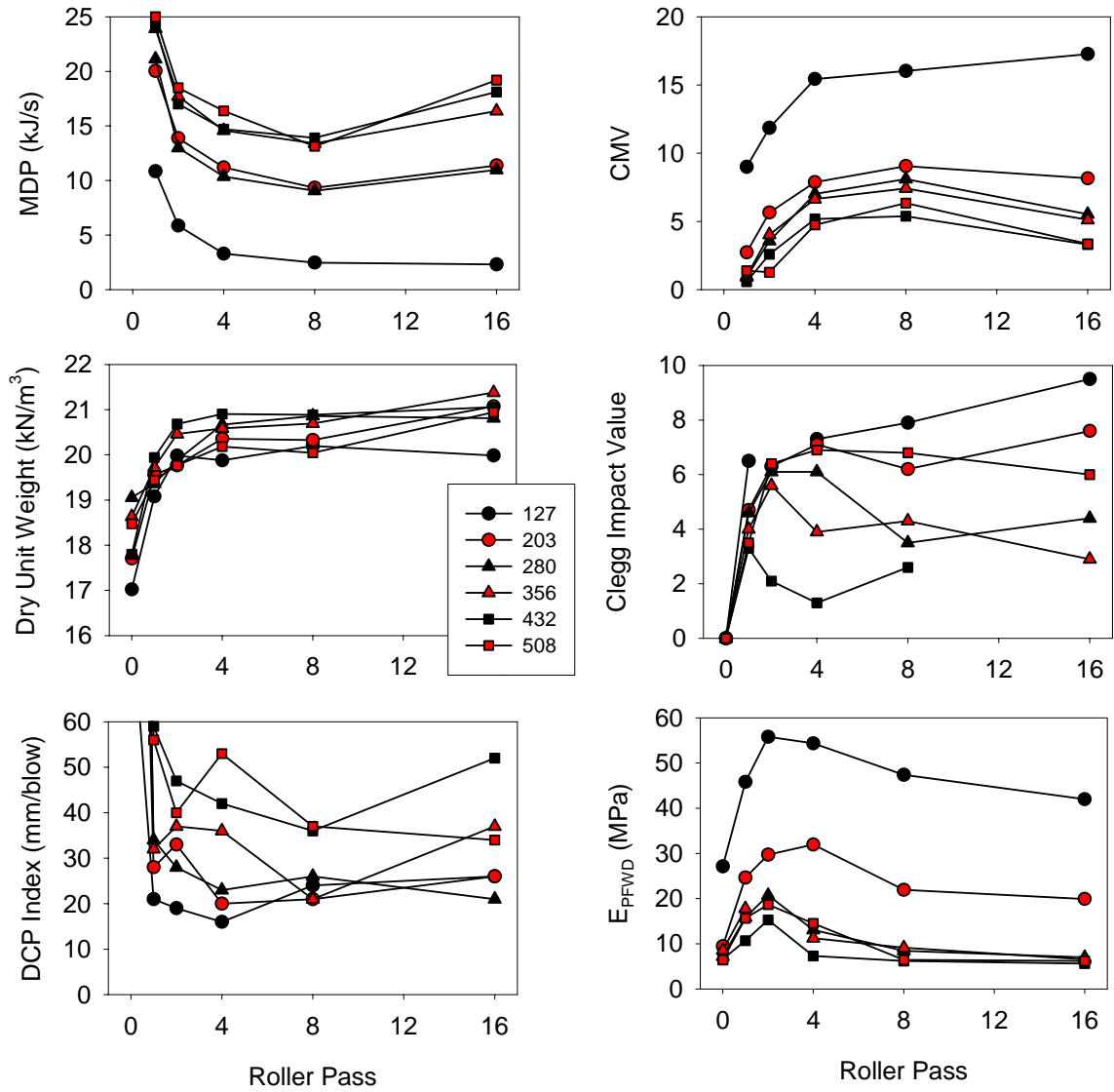


**Figure 81. Compaction curves for six lift thicknesses (Strip 2)**

*Preliminary Investigation of Roller Measurement Influence Depth*

In addition to the in situ test results described above for Strip 2, other tests were performed after 16 roller passes to investigate the relationship between the full-depth in situ engineering properties (both the compacted base material and underlying subgrade) and the roller CMV and MDP measurements. These additional tests included PFWD, DCP, and nuclear gauge density tests at four locations along Strip 2. These four locations consisted of different lift thicknesses and are identified in this part of the report by the thickness of the loose lift placed at that location (e.g., 508 mm lift section).

PFWD tests were performed on the final compacted surface, and at various depths below the surface, by excavating a trench down to the required depth (see Figure 82). Before performing PFWD tests, DCP and nuclear gauge density tests were performed at the surface of these test

locations. DCP tests were performed to penetration depths about 900 to 925 mm below the final surface by noting the depth of penetration per each blow. PFWD tests were performed at several locations, from the surface to depths about 660 mm to 860 mm below the final surface. Nuclear gauge density tests were performed at the surface by varying the probe penetration depth from 300 mm to 0 mm below the surface. The density test results performed in this manner provide an average density of the material between the surface and the probe penetration depth. Therefore, the dry unit weight measurements were corrected to estimate the density of the material at each probe penetration depth (identified as “corrected dry unit weight”).



**Figure 82. PFWD test in an excavated trench**

Figure 83 shows the variation in PFWD modulus and DCP index, with the measured depth, at the four test locations across Strip 2. Figure 84 and Figure 85 compare measured dry unit weight to soil stiffness measurements (modulus and DCP index) at these four test locations. Mean CMV and MDP values at each location after 16 roller passes are also noted on the figures for comparison.

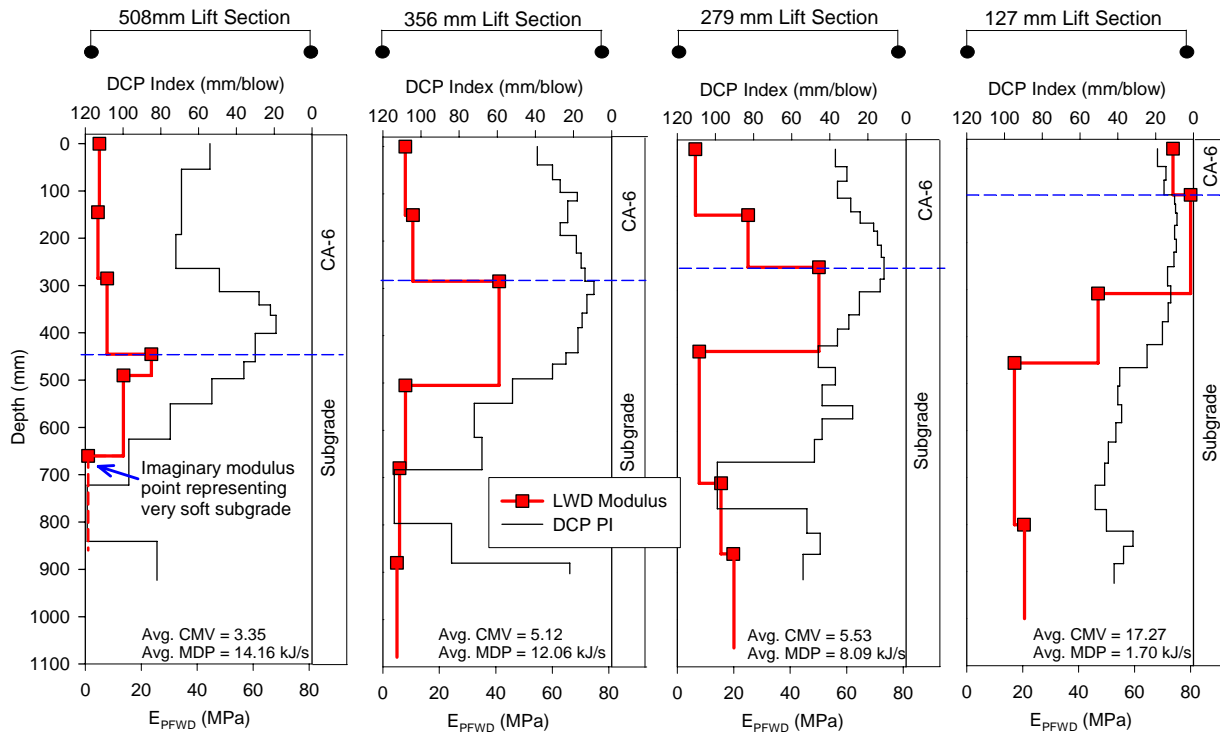


**Figure 83. DCP index and  $E_{PFW_D}$  profiles for Strip 2 after 16 roller passes**

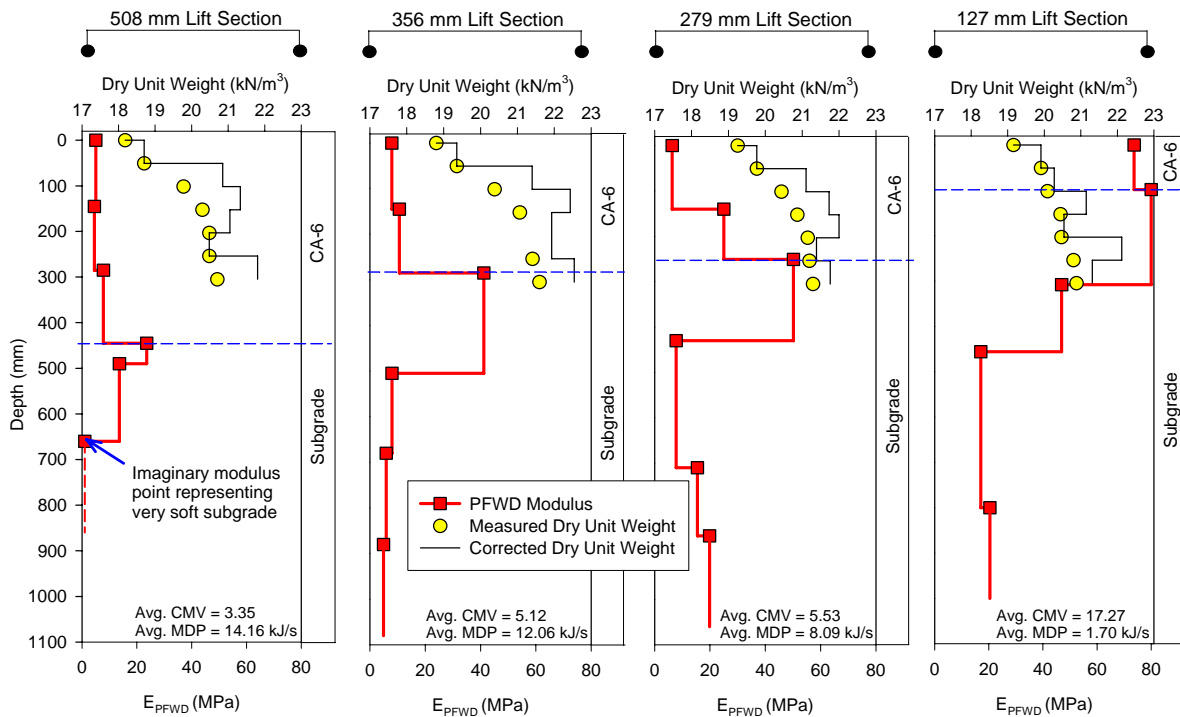


**Figure 84.  $E_{PFW_D}$  and dry unit weight profiles for Strip 2 after 16 roller passes**

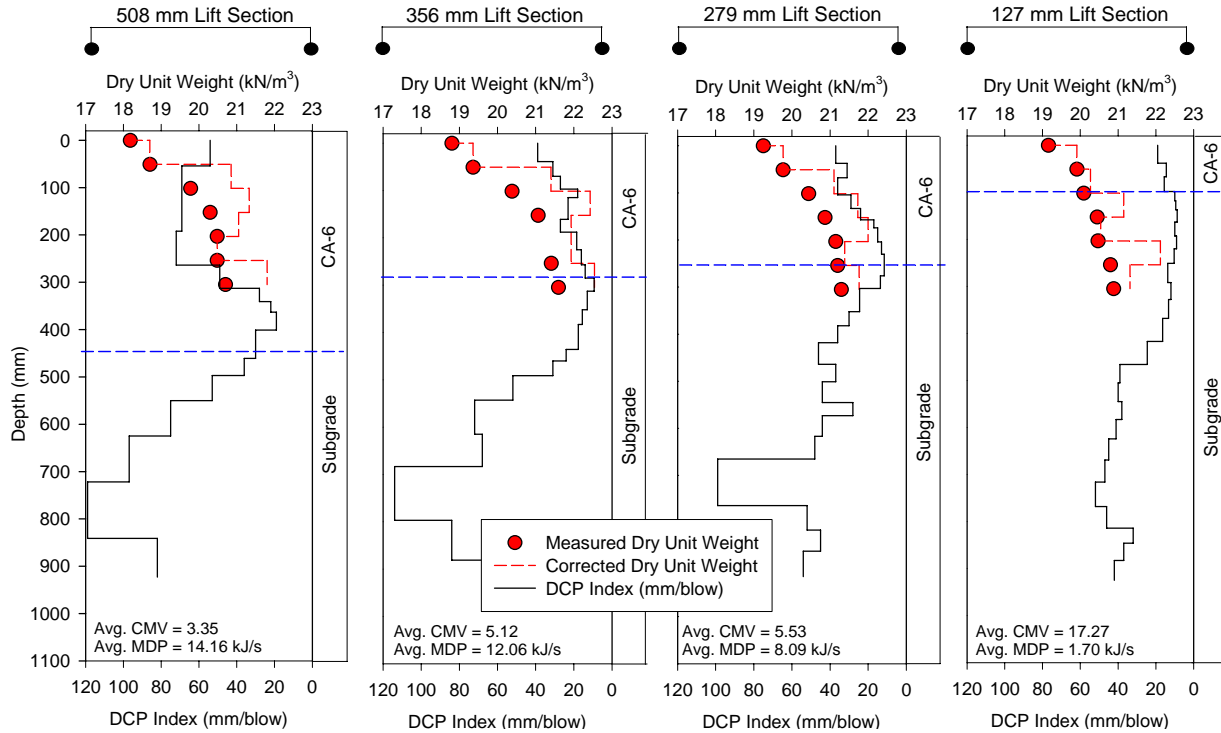


**Figure 85. DCP index and dry unit weight profiles for Strip 2 after 16 roller passes**

Table 9 presents the mean ( $\mu$ ) and standard deviation ( $\sigma$ ) of the roller CMV and MDP at the four test locations. The mean and standard deviation of these roller measurements are based on a number of data points obtained over each section along Strip 2 (e.g., 17 data points were obtained from the 508 mm loose lift thickness section). A weighted mean of the in situ spot test measurements are also included in the table. Note that the mean of the  $E_{PFWD}$  at a location is weighted for the difference in elevation (depth from the surface) between that location and its successive deeper location, except for the last measurement (deepest location). The last  $E_{PFWD}$  measurement was weighted for a depth of about 200 mm (it is assumed that the depth of influence is approximately equal to the diameter of the loading plate). The DCP index was weighted for the depth of total penetration. Table 9 also shows the mean modulus, DCP index, and dry unit weight at the surface and for the compaction layer (CA-6 base), as well as the modulus and DCP index for the full testing depth (which includes the compaction layer and the underlying subgrade). Based on the data presented in Table 9, Figure 86 was plotted to show the relationship between mean CMV and mean  $E_{PFWD}$ , DCP index, and dry unit weight measurements as compared to surface, compaction layer, and full testing depth measurements.

**Table 9. Comparison of roller measurements and in situ spot test measurements**

Test location	CMV	MDP (kJ/s)	Mean PFWD modulus (MPa)	Mean DCP index (mm/blow)	Mean dry unit weight (kN/m <sup>3</sup> )
508 mm	$\mu = 3.35$	$\mu = 14.16$	5.0 <sup>a</sup>	*62.0 <sup>a</sup>	18.2 <sup>a</sup>
	$\sigma = 1.99$	$\sigma = 3.58$	5.9 <sup>b</sup>	51.7 <sup>b</sup>	20.7 <sup>b</sup>
	n = 17	n = 17	7.2 <sup>c</sup>	69.2 <sup>c</sup>	
356 mm	$\mu = 5.12$	$\mu = 12.06$	6.4 <sup>a</sup>	*34.0 <sup>a</sup>	19.3 <sup>a</sup>
	$\sigma = 0.58$	$\sigma = 5.05$	9.3 <sup>b</sup>	24.2 <sup>b</sup>	21.4 <sup>b</sup>
	n = 25	n = 25	14.2 <sup>c</sup>	48.4 <sup>c</sup>	
279 mm	$\mu = 5.53$	$\mu = 8.09$	8.0 <sup>a</sup>	*35.0 <sup>a</sup>	18.8 <sup>a</sup>
	$\sigma = 1.01$	$\sigma = 5.18$	14.6 <sup>b</sup>	25.2 <sup>b</sup>	21.2 <sup>b</sup>
	n = 23	n = 23	19.9 <sup>c</sup>	41.9 <sup>c</sup>	
127 mm	$\mu = 17.27$	$\mu = 1.70$	73.7 <sup>a</sup>	*19.0 <sup>a</sup>	19.2 <sup>a</sup>
	$\sigma = 3.55$	$\sigma = 2.73$	73.7 <sup>b</sup>	16.6 <sup>b</sup>	20.1 <sup>b</sup>
	n = 24	n = 24	40.9 <sup>c</sup>	28.2 <sup>c</sup>	

Notes: Please refer to text for calculation of mean of the in situ spot test measurements

<sup>a</sup> measurement value at the surface

<sup>b</sup> measurement value for the compaction layer (CA-6 base)

<sup>c</sup> measurement value for the full depth (including compaction layer and underlying subgrade)

\* mean DCP index for the first two blows at the surface

The data presented in Table 9 and from Figure 83 to Figure 86 clearly indicate an increase in CMV and a decrease in MDP with a reduction in the thickness of loose lift placed at different sections across the strip. Similarly, a general increase in soil stiffness measurements (modulus and DCP index) with a reduction in the loose lift thickness can be observed from these figures. From Figure 86, it can also be inferred that there is a strong trend with a nonlinear relationship between roller measurements and soil stiffness measurements (DCP index and modulus). Interestingly, similar trends in the change in modulus and DCP index can be observed if measurements taken at the surface, compaction layer, and full depth are compared. In contrast, and as expected, it is observed that there is very little variation in dry unit weight values across the strip (18.2 to 19.3 kN/m<sup>3</sup> at the surface and 20.7 to 21.2 kN/m<sup>3</sup> for the compaction layer). This suggests that the dry unit weight may have had little influence on the stiffness measurements.

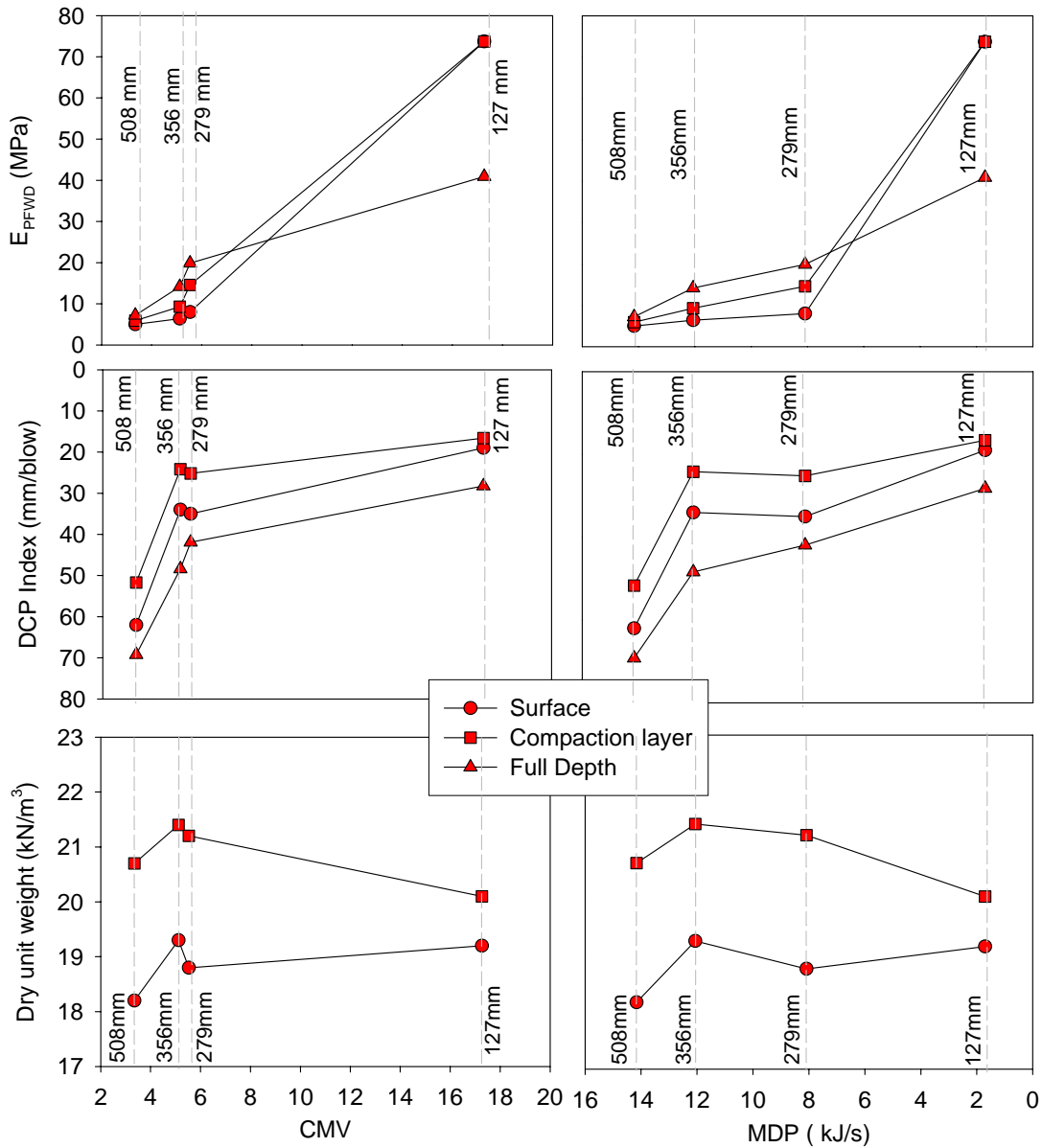


**Figure 86. Relationship between mean CMV and MDP, and mean  $E_{PFWD}$ , DCP index, and dry unit weight along Strip 2 at different test locations**

A fair relationship between the measured DCP index and PFWD modulus was observed, as shown in Figure 83, with a general increase in modulus with decrease in DCP index. This suggests the use of DCP as an effective tool for testing the soil stiffness properties at greater depths below the surface. No general trend was observed between dry unit weight and DCP index/ $E_{PFWD}$  (see Figure 84 and Figure 85).

From the data presented from Figure 83 to Figure 86, it is clear that the roller measurements are highly influenced by the stiffness of the compaction layer (CA-6), as there is no appreciable difference in the underlying subgrade stiffness properties. Therefore, a clear understanding of the

influence depth of the roller measurements is not possible with such limited data obtained from this preliminary investigation. However, the results have provided enough motivation to further investigate this relationship with some detailed testing in the future. Similar additional testing, along with testing on a strip consisting of a subgrade with significant variations in moisture, strength, and stiffness, overlaid by a relatively uniform compaction, would provide a better understanding of the influence depth of the roller CMV and MDP values.

## **Spatial Area 1**

The goal of this preliminary spatial analysis was to determine whether a known compaction pattern could be accurately estimated by spatial kriging of spot and machine measurements. The study area was approximately 32 m by 14 m in size. A “Z” shape was tilled in the existing subgrade material and the area was then compacted (see Figure 87). Compaction monitor views for MDP and CMV are shown in Figure 88. Soil strength testing at 144 locations followed compaction using the DCP and Clegg impact tester. The locations of these measurements are shown in Figure 89.

Kriging methods, specifically the variograms on which kriging is based, assume stationarity. Stationarity means that the variance of the difference in the process being modeled (e.g., DCP index) at two points is a function only of the distance between those two points. Thus, large-scale trends in the data (in this case, the known difference between the compacted and uncompact areas) violate this assumption. The usual procedure in spatial analysis is thus to separate the large-scale trends from the small-scale spatial variability, model the spatial variability using a variogram, then use both the large-scale trend and the spatial model for prediction.

The common methods of separating large-scale trend (model fitting or median polish) were not appropriate for this data set. Model fitting is used when there is a consistent spatial trend in one direction or another; a slope, for example. The shape of the compacted area in this study did not lend itself to this kind of analysis. Median polish is more flexible in the type of trends it can remove, but it requires the data to be spaced in a regular grid of rows and columns. While a rough grid can be imposed on randomly spaced data to allow median polishing to be used, the majority of the cells must be filled (ideally with only one data point) for median polishing to work well. Such a grid could not be imposed for this study. A coarse grid for which most of the cells were filled often had numerous data points in a cell, and the cells overlapped the edges of the compacted areas. A finer grid in which cells did not overlap the edges of the compacted areas, and where each cell contained no more than two data points, had too few cells filled for median polishing to work well. Therefore, it was decided to use only data within the compacted areas to determine the variogram, then use it to krig the entire study area.



**Figure 87. Preparation and compaction of spatial test area 1**

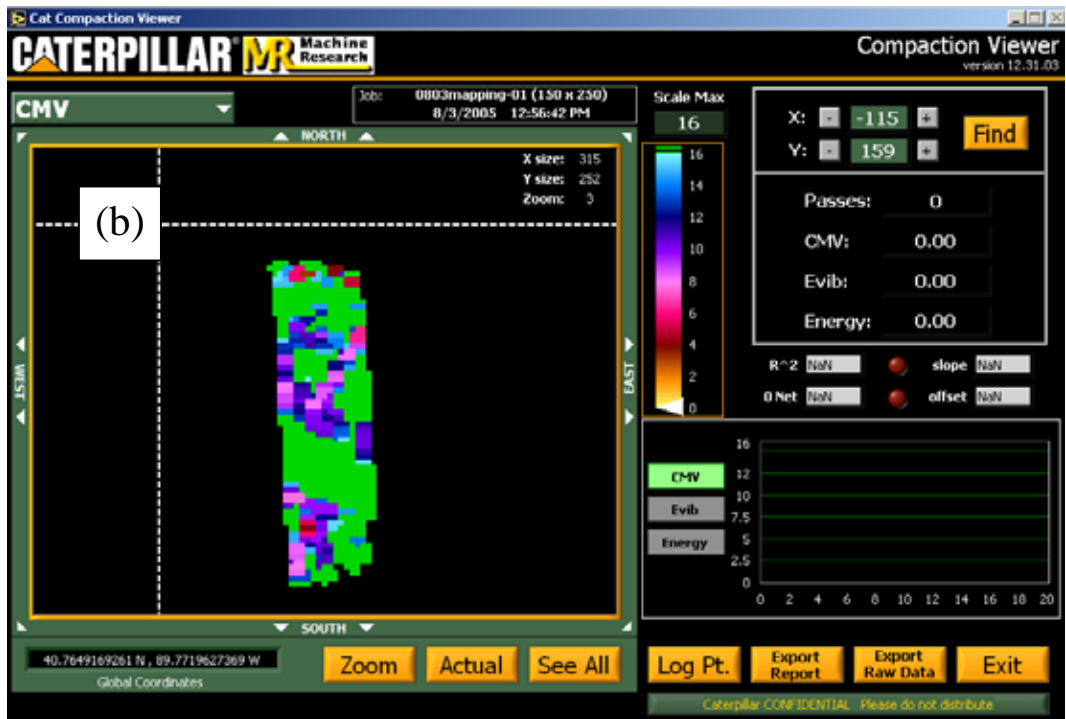
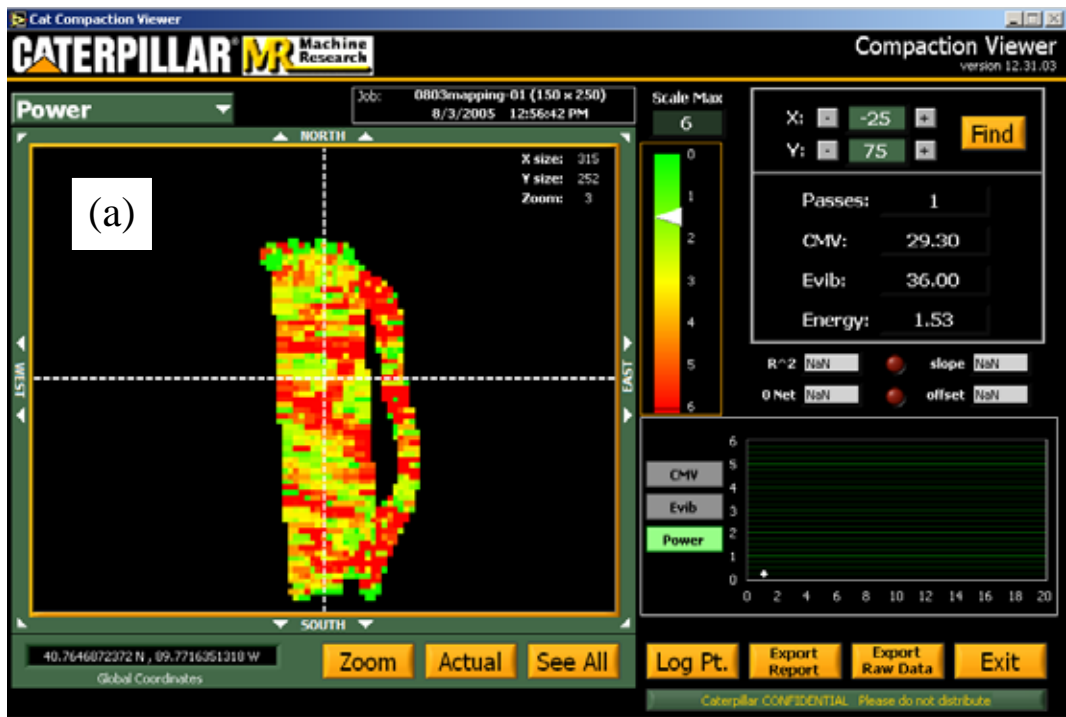
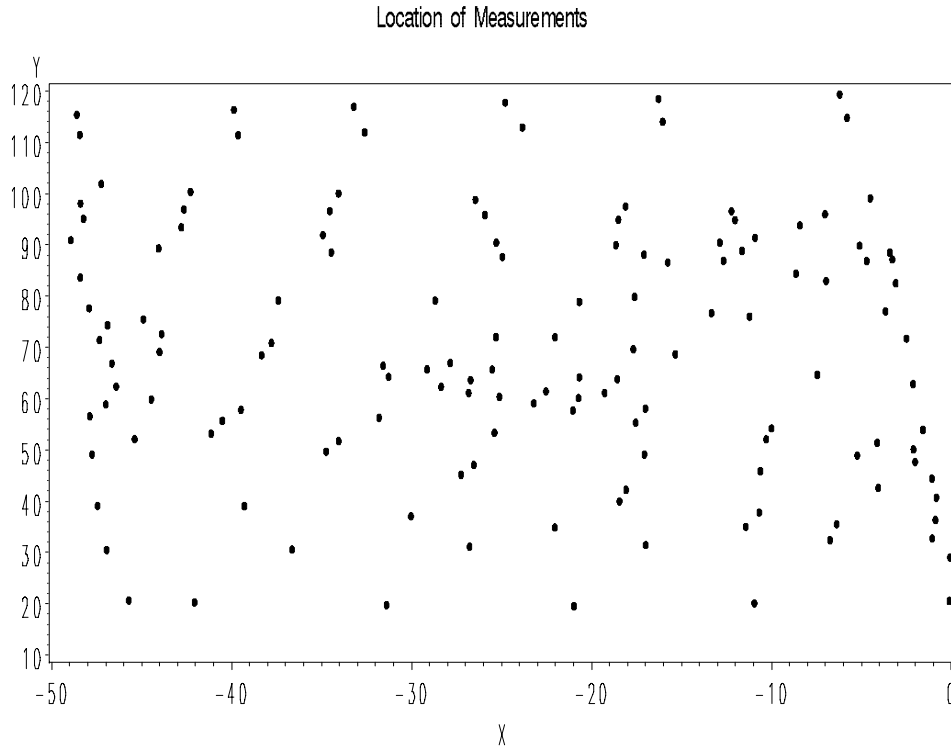
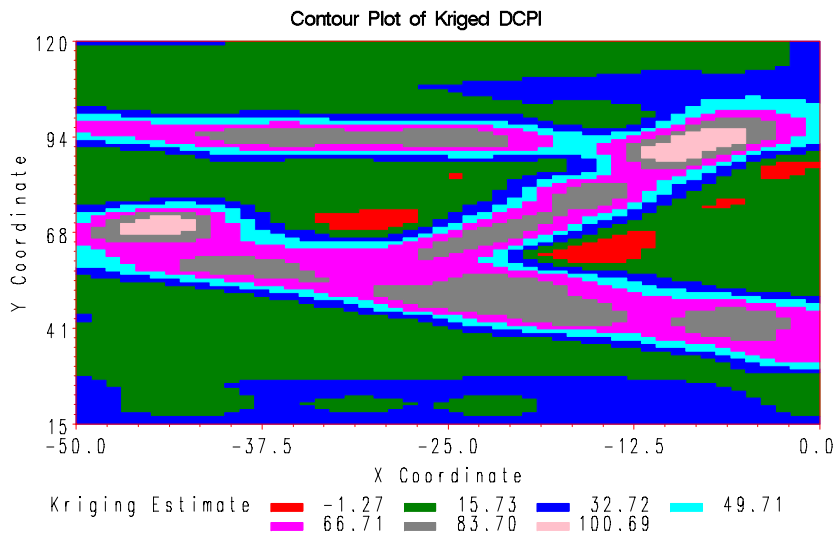
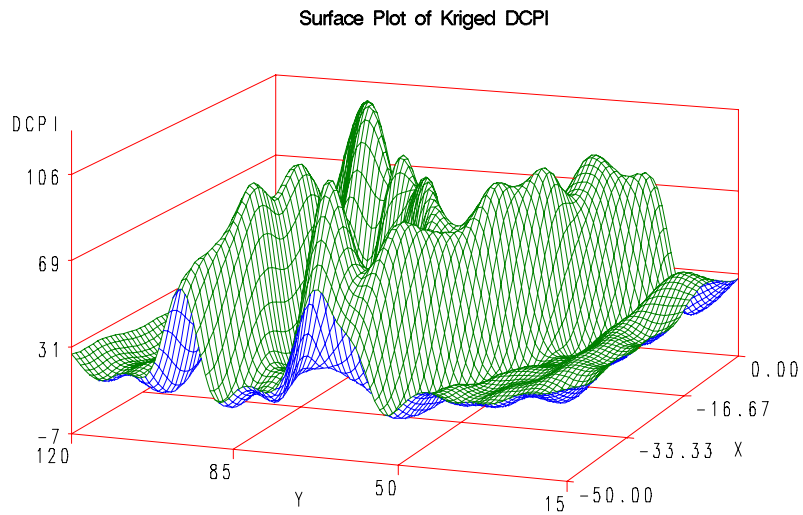
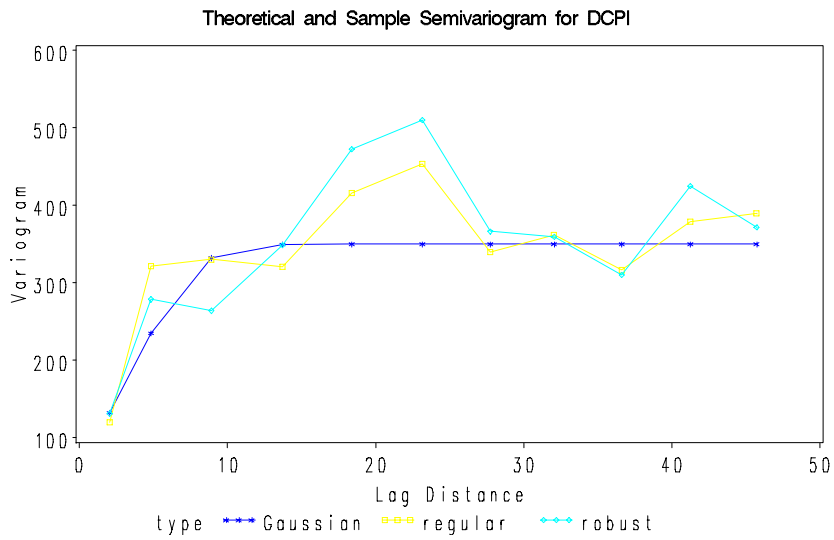


Figure 88. Compaaction monitor views for trial spatial analysis: (a) MDP, (b) CMV



**Figure 89. Location of the 144 measurements taken within the study area**

Variograms, surface plots, and contour plots of the kriging estimates for DCP index, CIV, CMV, and MDP are shown from Figure 90 to Figure 93. The compacted areas are more clearly delineated by the spot measurements (DCP index and CIV) than by the machine measurements (MDP and CMV). Additional data points for the machine measurements were available. Kriging estimates for CMV and MDP based on the larger dataset were obtained using the same method as for the original, smaller, dataset. However, kriging estimates for these data did not produce more clearly delineated plots; in fact, they were less clear.



**Figure 90. DCP index variogram, surface plot, and contour plot of kriged DCP index**

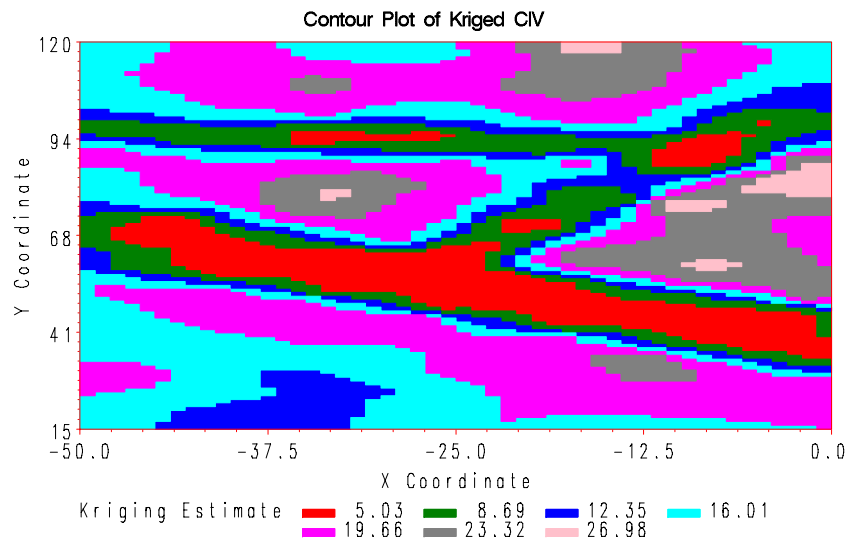
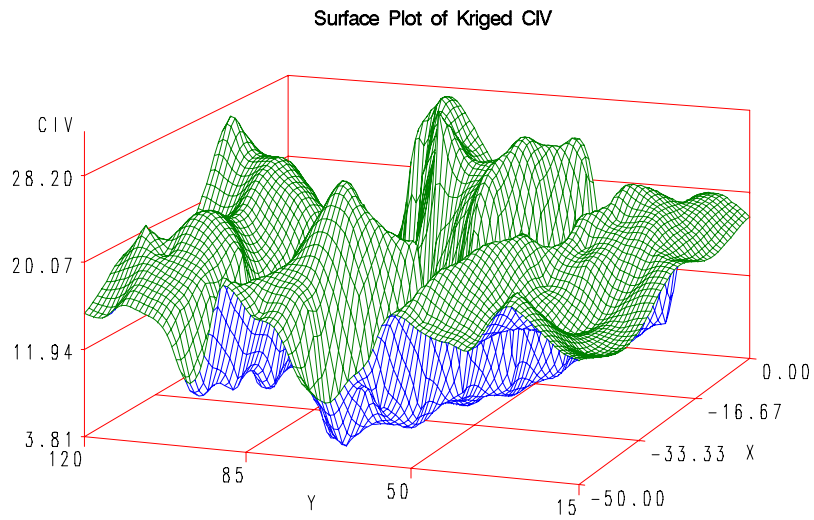
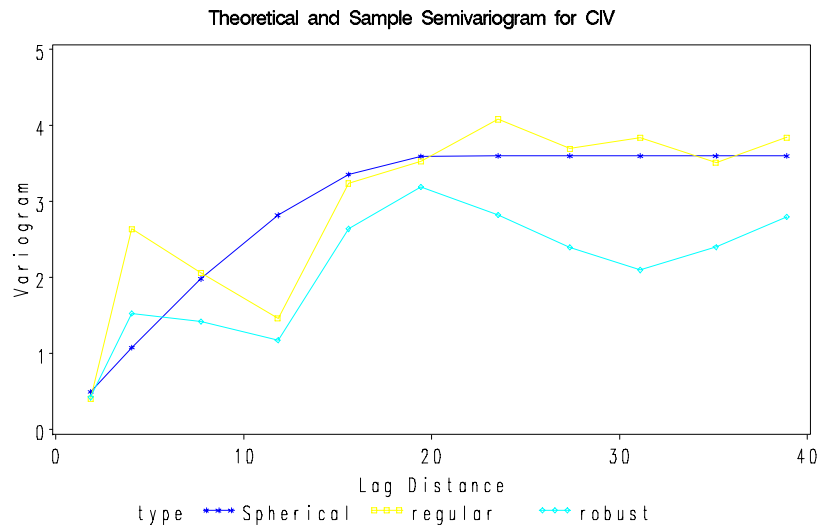


**Figure 91. CIV variogram, surface plot, and contour plot of kriged CIV**

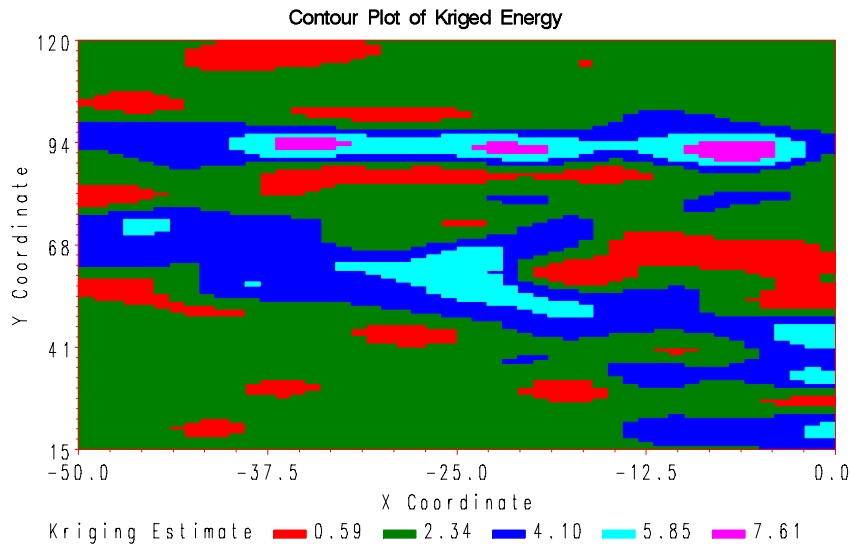
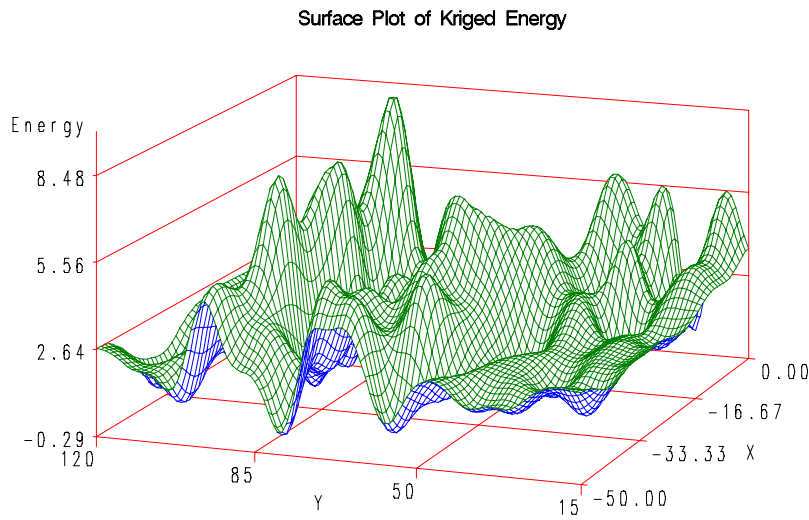
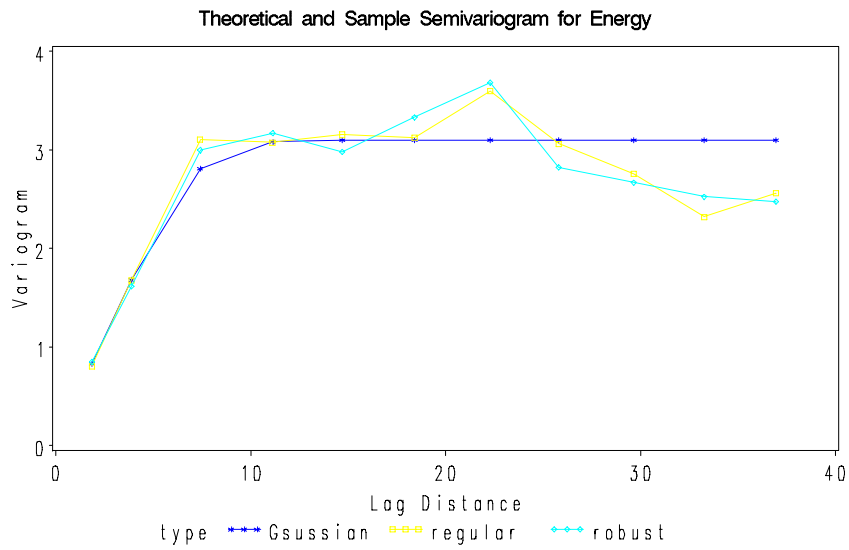


**Figure 92. MDP variogram, surface plot, and contour plot of kriged MDP**

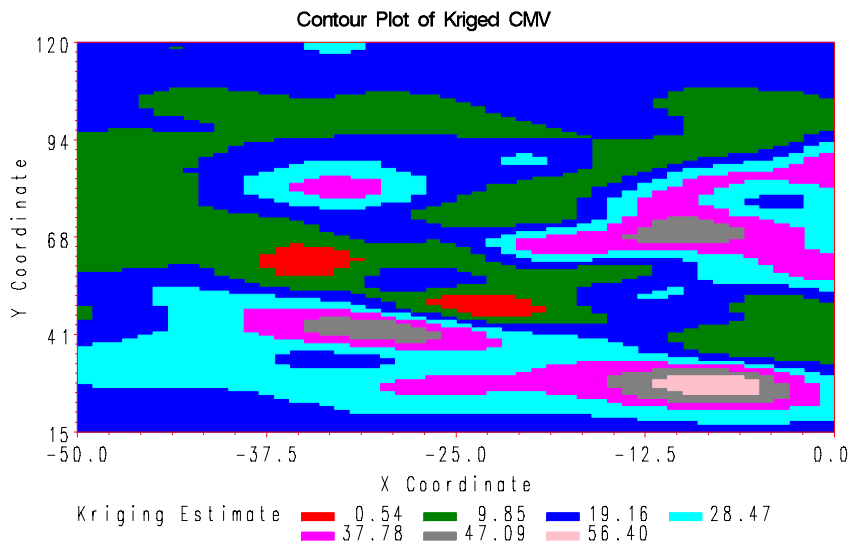
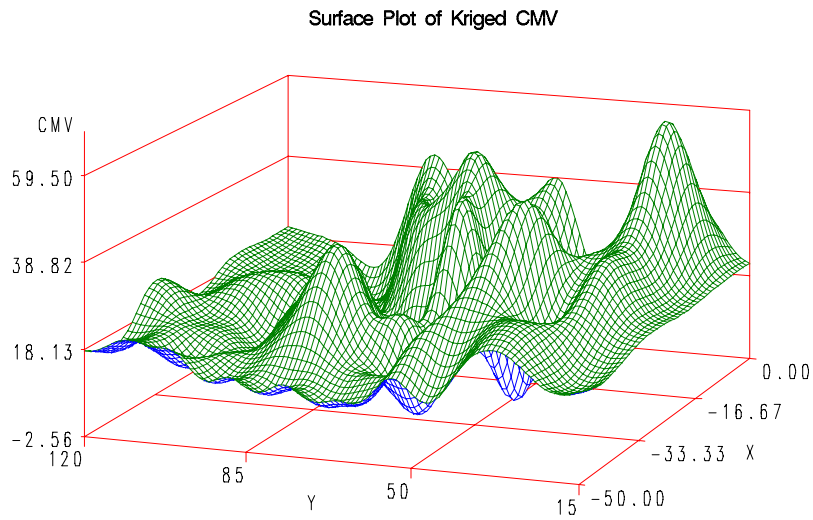
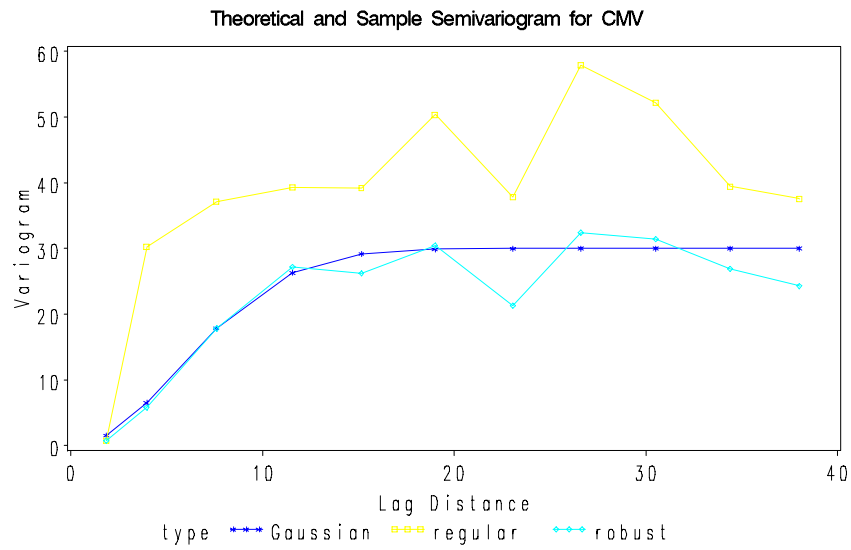


**Figure 93. CMV variogram, surface plot, and contour plot of kriged CMV**

## Spatial Area 2

### *Distribution Plots of Roller Data and Soil Engineering Properties*

The variation of soil property measurement results are shown with distribution plots in Figure 94. To indicate whether, after the second roller pass, the compaction monitoring technologies and the in situ spot tests consistently identified variable lift thickness, the distributions of test results are separated into results performed on a 200 mm or 510 mm lift. Mean values and coefficients of variation ( $C_v$ ) are additionally provided in Figure 94 for each measurement and for the two nominal lift thicknesses. CMV and full-depth DCP index clearly show the influence of variable lift thickness on the measurements, evidenced by two different distributions of data. MDP and the other compaction control test results, however, provide only a slight indication of a different soil condition. Throughout the compaction process, MDP for 200 mm lift thickness was consistently lower than MDP for 510 mm lift thickness (see Figure 95). CMV for 200 mm lift thickness was consistently higher than CMV for 510 mm lift thickness (see Figure 96).

Dry density and moisture content were within a relatively narrow range for the spatial test area. Moisture content of the test area ranged from 7% to 9%. Dry density varied from about 19.2 to 21.1 kN/m<sup>3</sup> (90% to 99% of the maximum dry unit weight). Soil modulus and strength measurements were generally more variable, with  $E_{PFWD}$  ranging from 6 to 30 MPa, mean DCP index ranging from 10 to 50 mm/blow, and Clegg impact value (CIV) ranging from 2 to about 8.

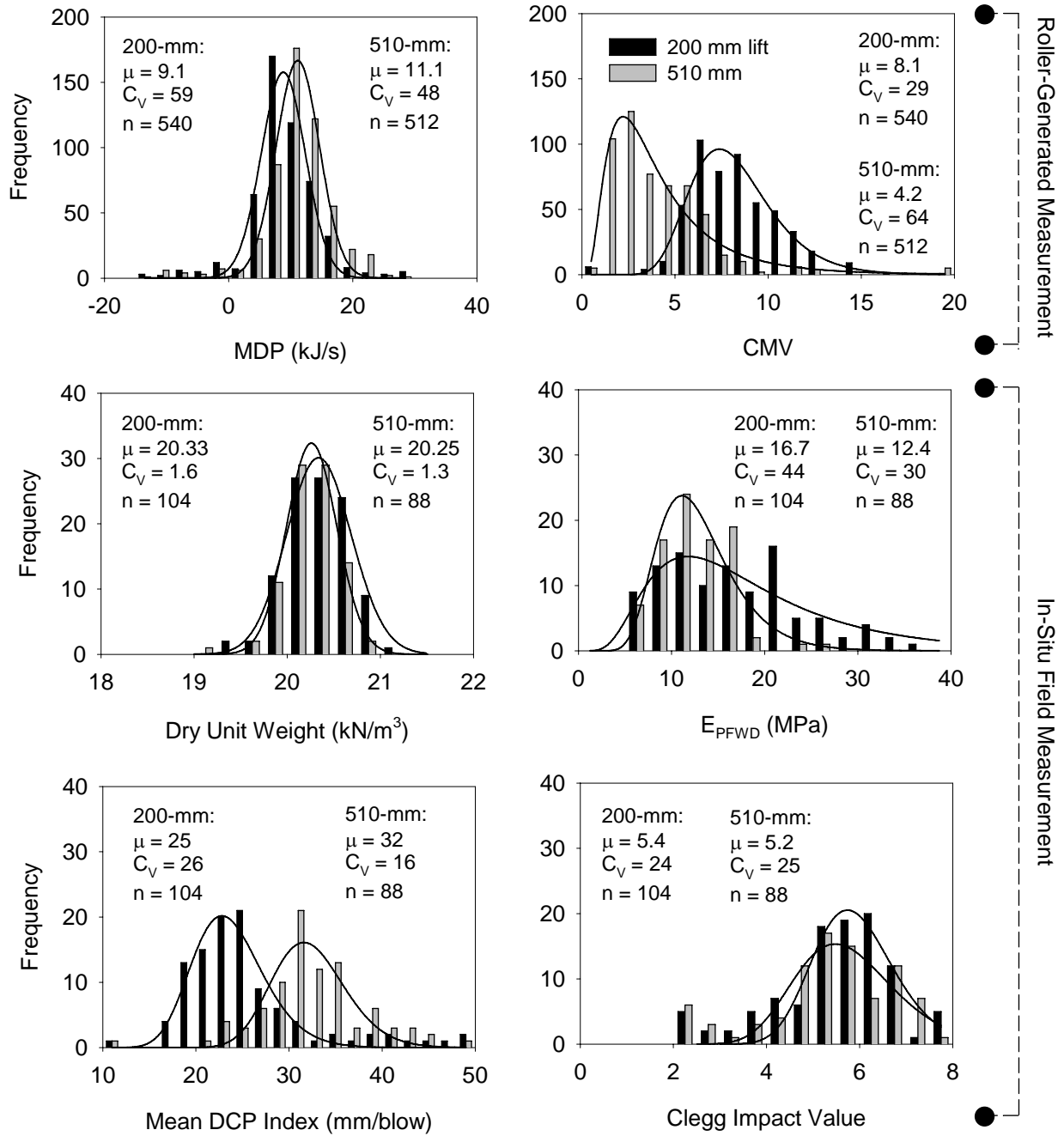


**Figure 94. Distribution plots of compaction monitoring and field measurements for 200 mm and 510 mm lift thicknesses (Pass 2)**

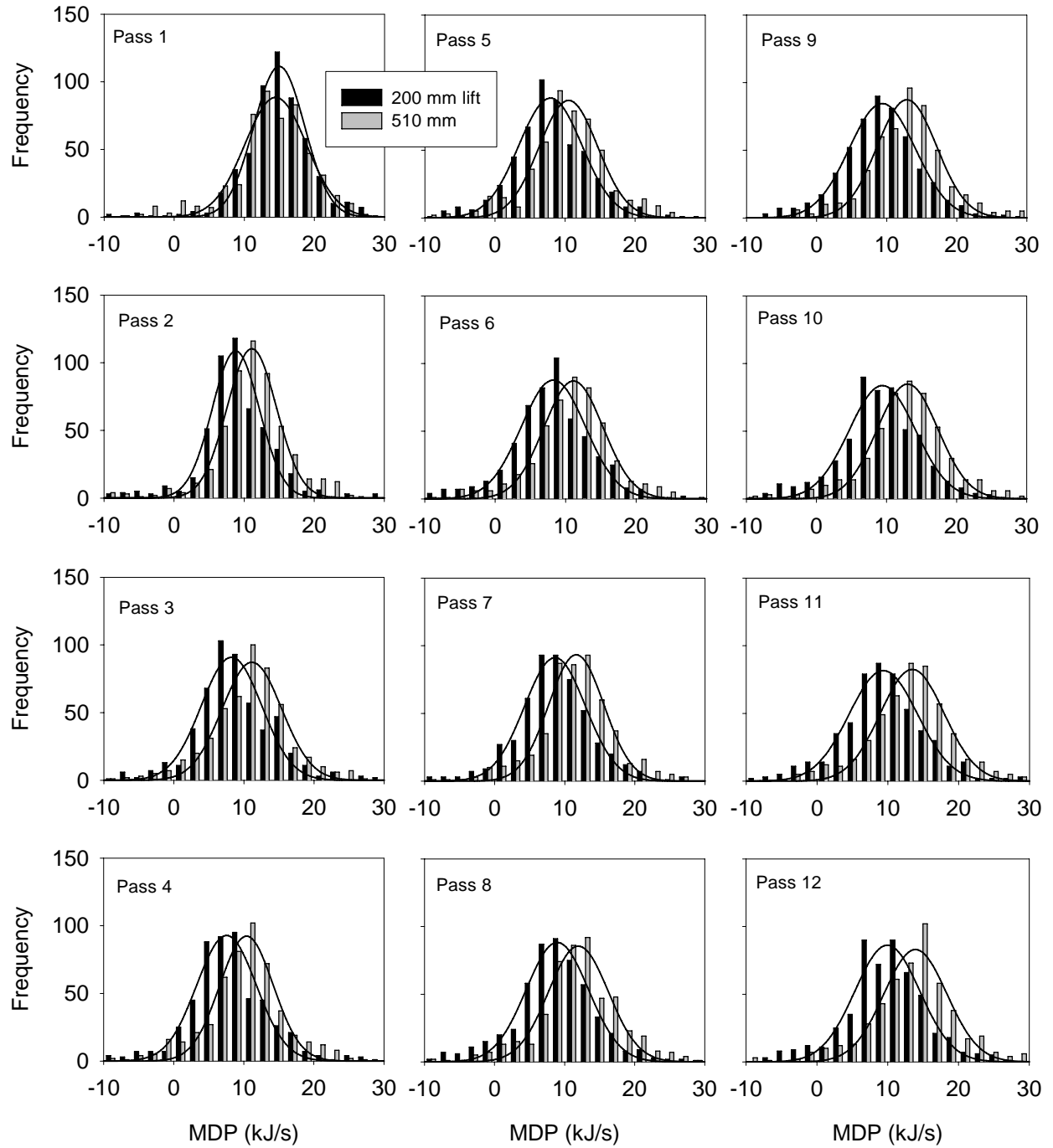


**Figure 95. Distribution plots of MDP for 200 mm and 510 mm lift thicknesses (all passes)**

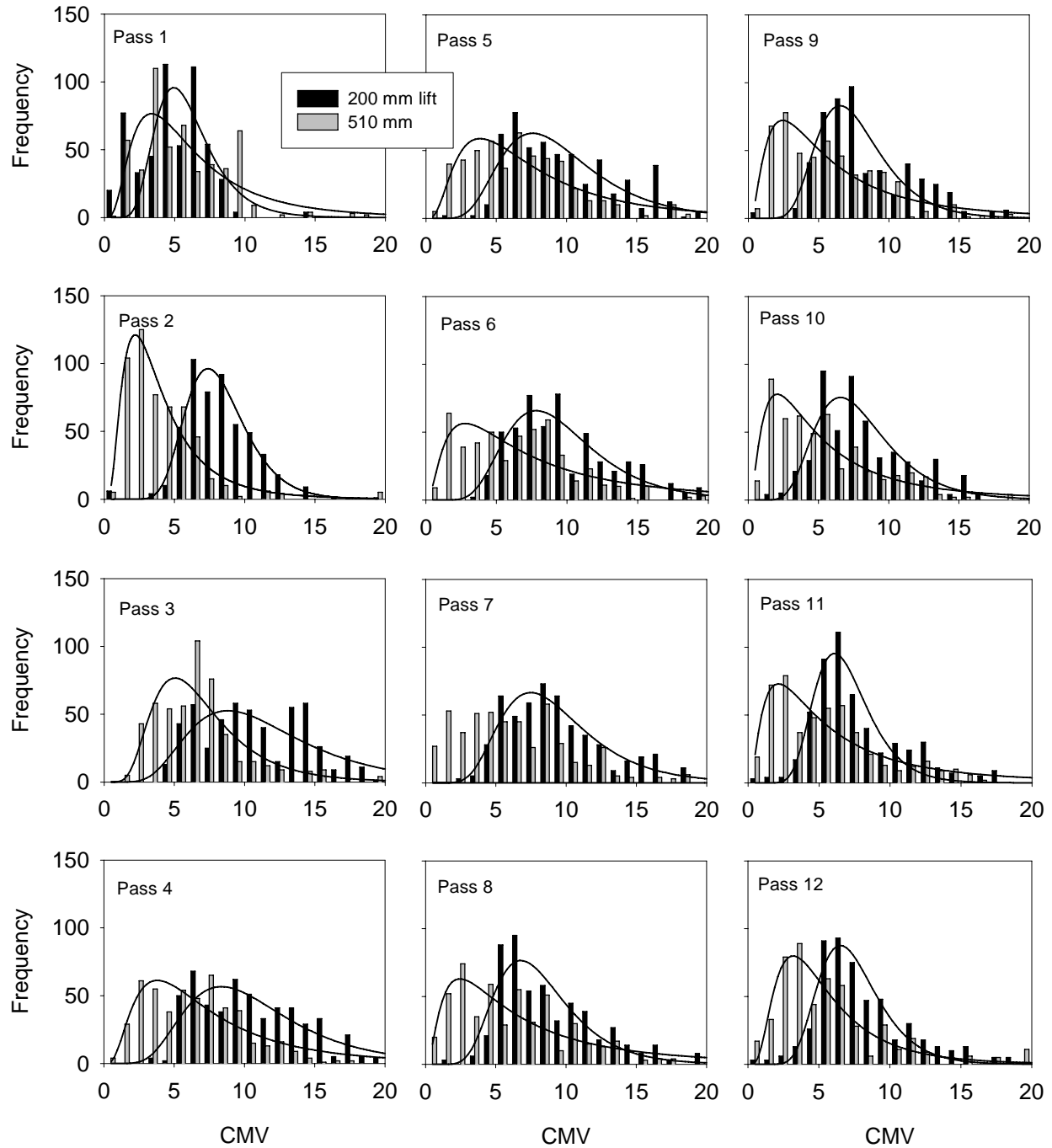


**Figure 96. Distribution plots of CMV for 200 mm and 510 mm lift thicknesses (all passes)**

## *Machine Output*

MDP is shown from Figure 97 to Figure 99 for all roller passes over the test area. CMV is shown from Figure 100 to Figure 102. The difference in roller elevation from that of Pass 1 is shown from Figure 103 to Figure 105. The data at a particular location within a given roller path is assumed to be constant along the entire width of the roller drum, since no method has yet to account for variation of soil properties along the width of the roller. Further, dashed lines are provided in the figures to demarcate areas of nominal 200 mm and 510 mm lift thickness.

For Pass 2, which is when soil properties were measured, MDP results were observed to be locally variable, ranging from nearly 0 kJ/s (stiff material) to greater than 20 kJ/s (soft material) over a distance of less than 1 m. Still, the global trend of the data is that high MDP values are observed in regions of 510 mm lift thickness and lower MDP values are observed in regions of 200 mm lift thickness. Recognizing that rolling resistance and sinkage are affected by surficial soil characteristics, MDP measurements provide only a subtle indication of differential lift thickness over the test region at two roller passes.

CMV, a measure of roller drum behavior, depends on soil characteristics well below the soil surface, with measurement influence depths reportedly ranging from 0.4 to 0.6 m for a 2-ton roller to 0.8 to 1.5 m for a 12-ton roller (ISSMGE 2005). CMV compaction monitoring technology identified the regions of 510 mm lift thickness. In these areas for Pass 2, CMV ranged from 0 to about 6 (red to green). In regions of 200 mm lift thickness, CMV ranged from about 5 to about 15 (green to violet). CMV measurements even identified localized areas of thick lift on the south (left) side of the test area, every area except those from 2 to 12 m in the y-direction in the first roller path (x ranging from 0 to 2.16 m). At these locations, the excavated areas have dimensions smaller than the drum width, such that the drum can bridge the comparatively soft area. Still, CMV provides accurate mapping capabilities for areas nearly as wide as the roller drum and with lengths greater than about 1 m.

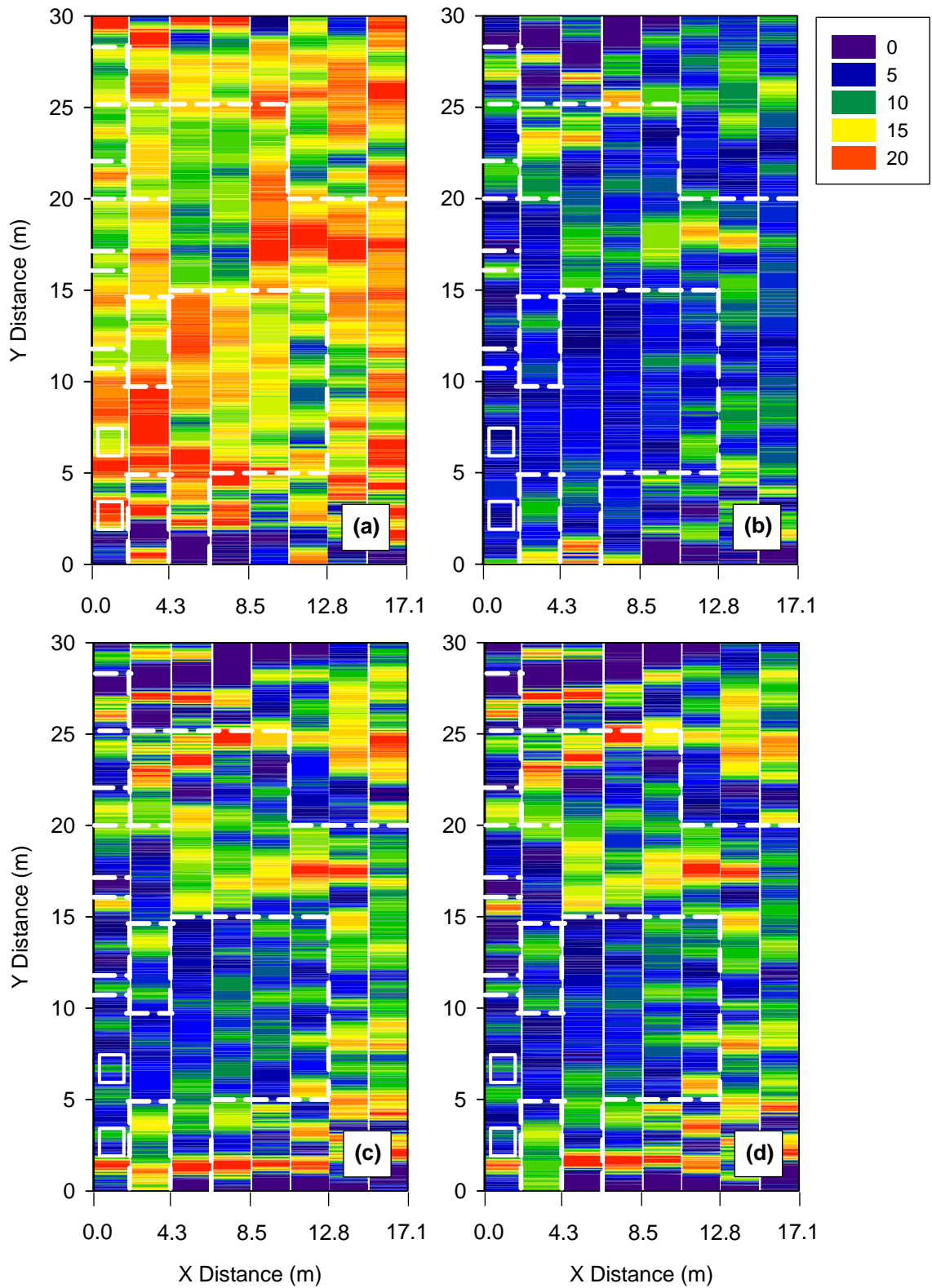


**Figure 97. MDP (kJ/s) output at (a) Pass 1, (b) Pass 2, (c) Pass 3, and (d) Pass 4**

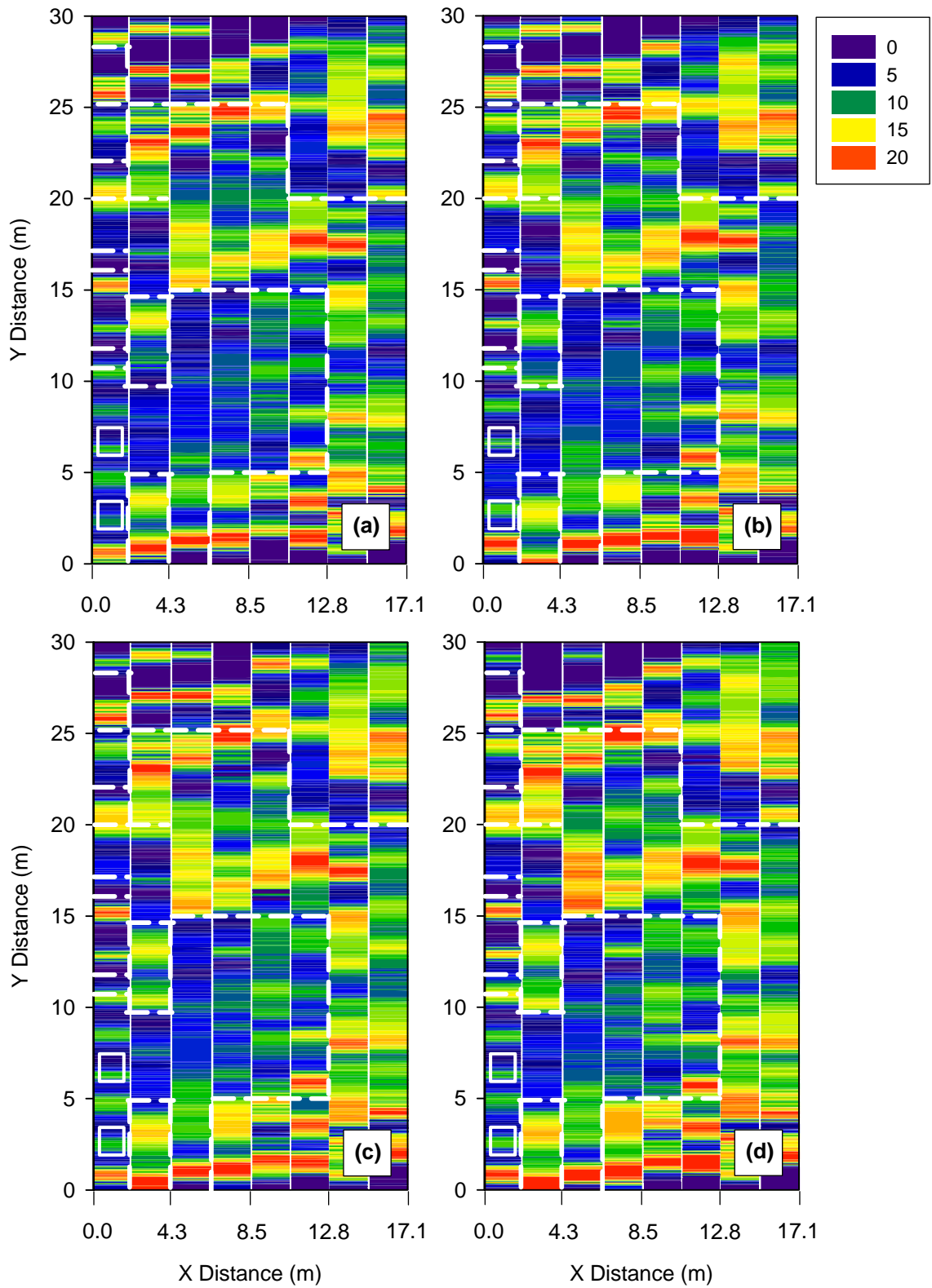


**Figure 98. MDP (kJ/s) output at (a) Pass 5, (b) Pass 6, (c) Pass 7, and (d) Pass 8**

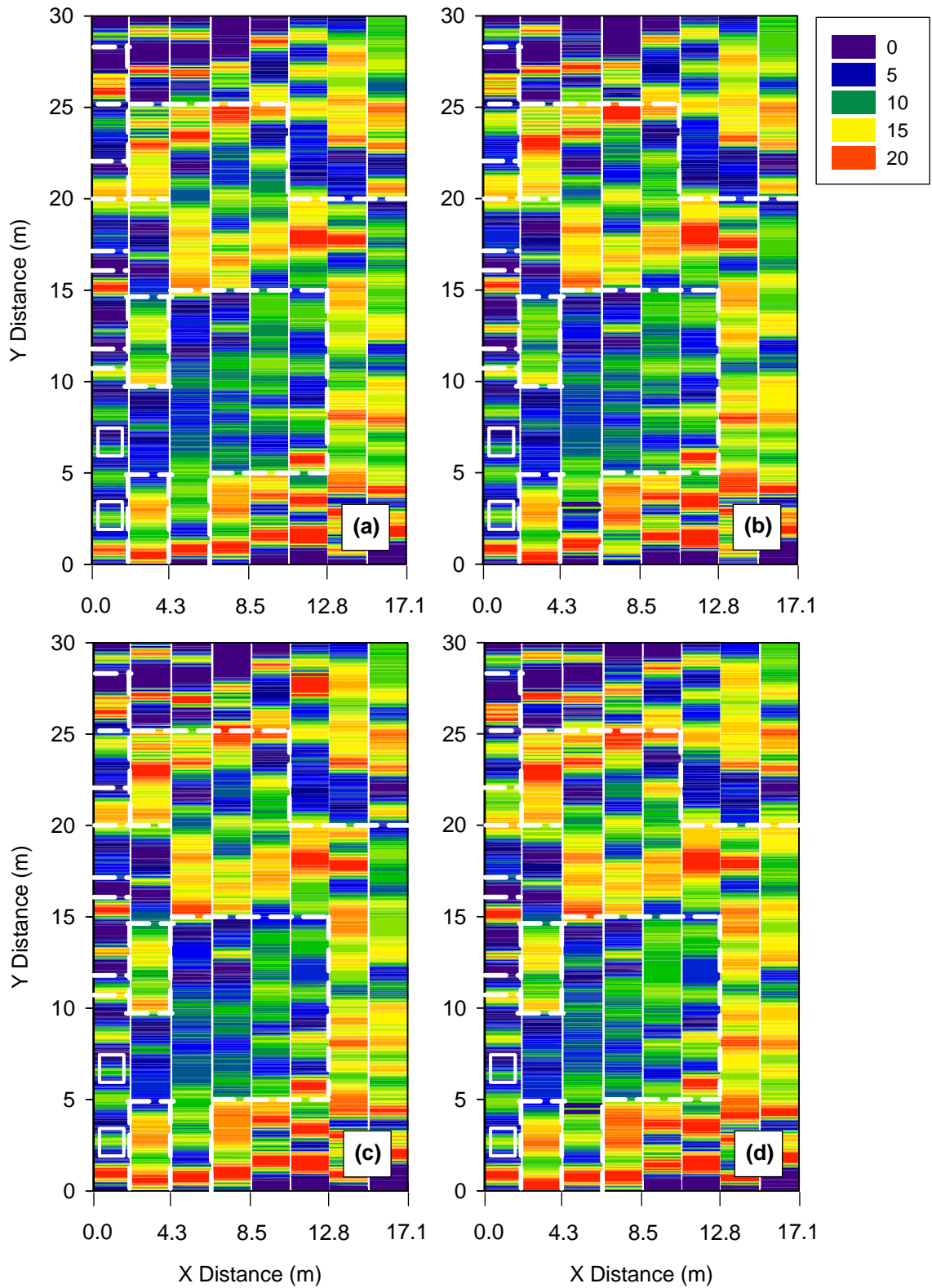


**Figure 99. MDP (kJ/s) output at (a) Pass 9, (b) Pass 10, (c) Pass 11, and (d) Pass 12**

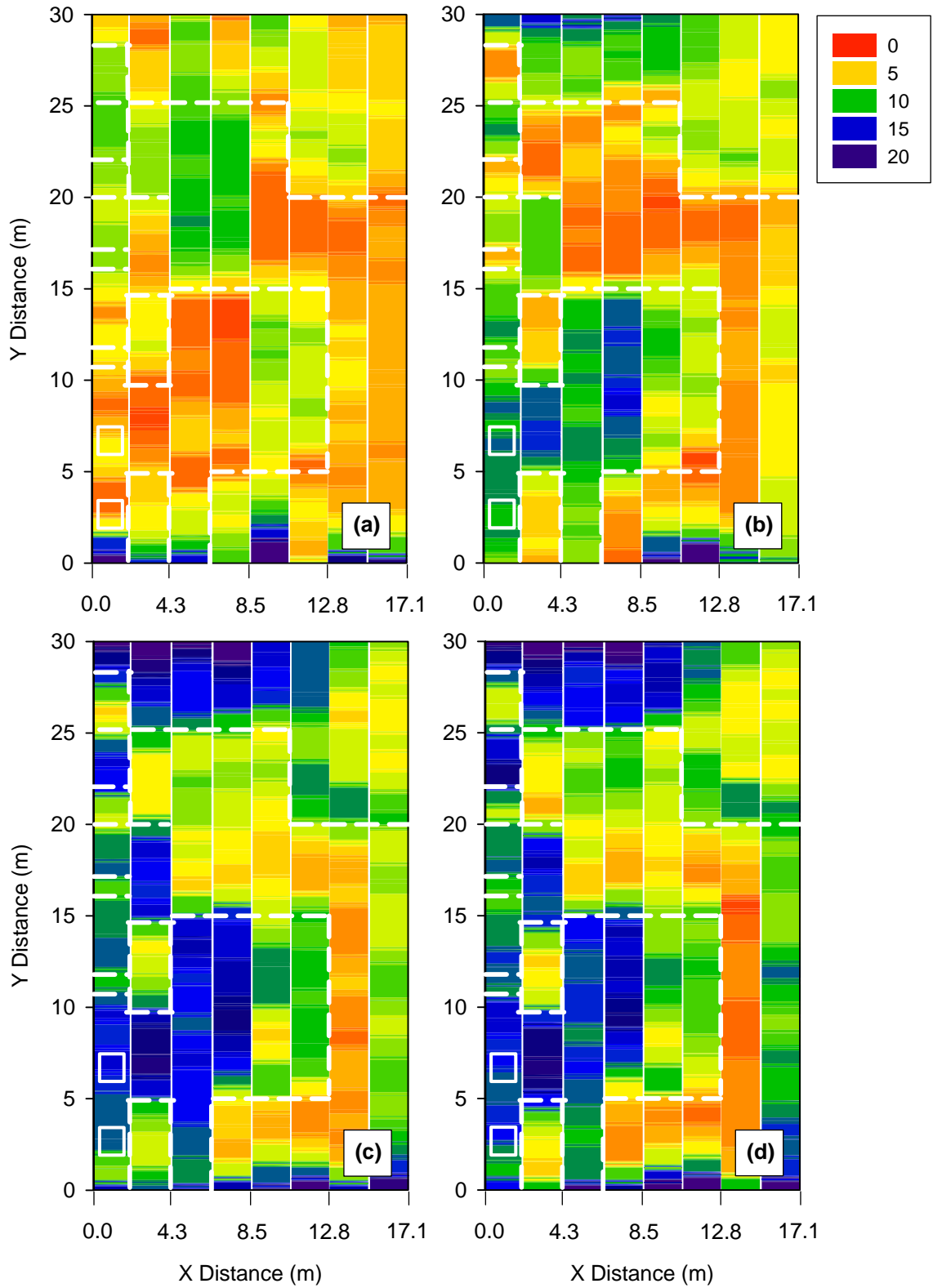


**Figure 100. CMV output at (a) Pass 1, (b) Pass 2, (c) Pass 3, and (d) Pass 4**

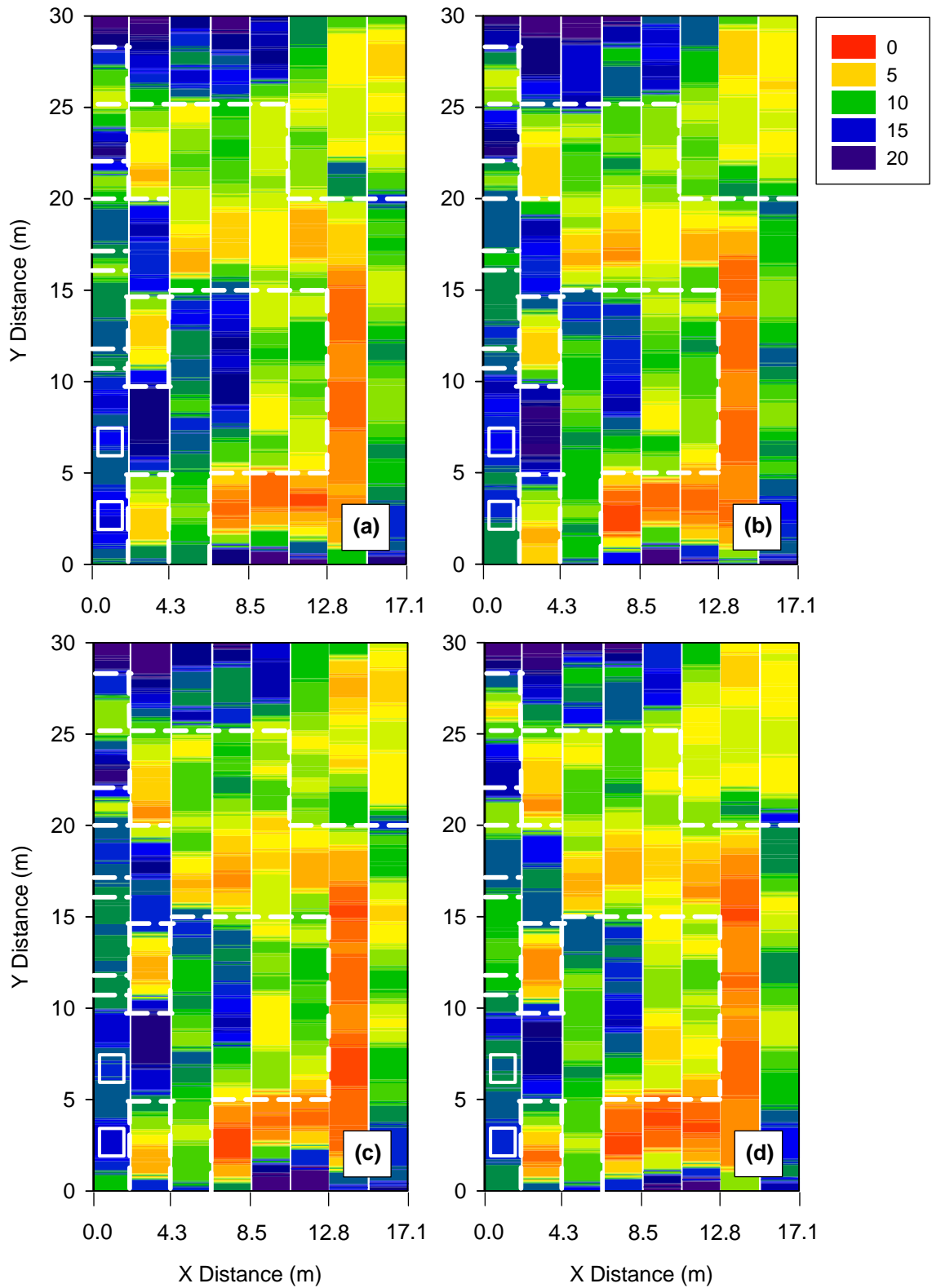


**Figure 101. CMV output at (a) Pass 5, (b) Pass 6, (c) Pass 7, and (d) Pass 8**

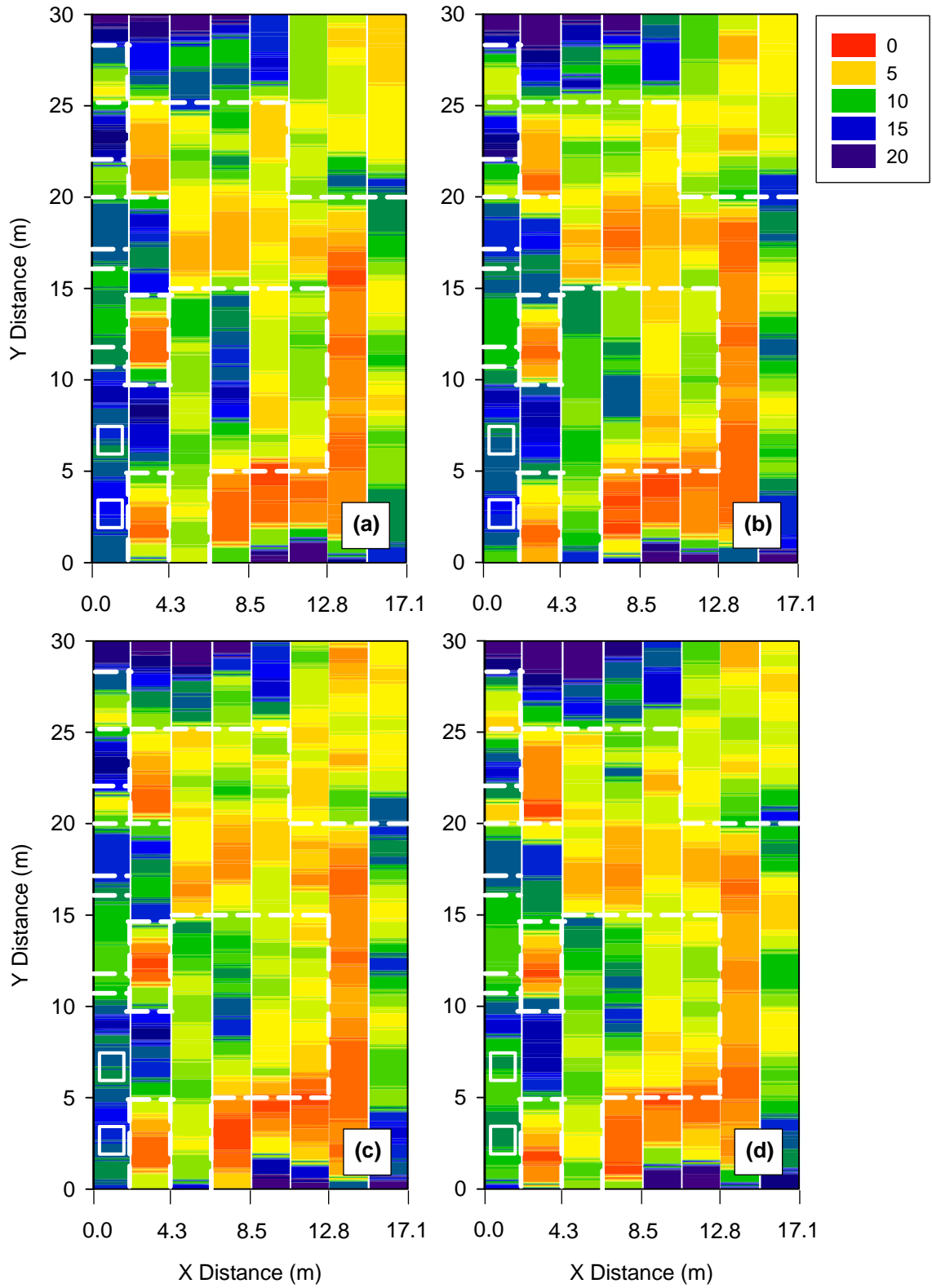


**Figure 102. CMV output at (a) Pass 9, (b) Pass 10, (c) Pass 11, and (d) Pass 12**

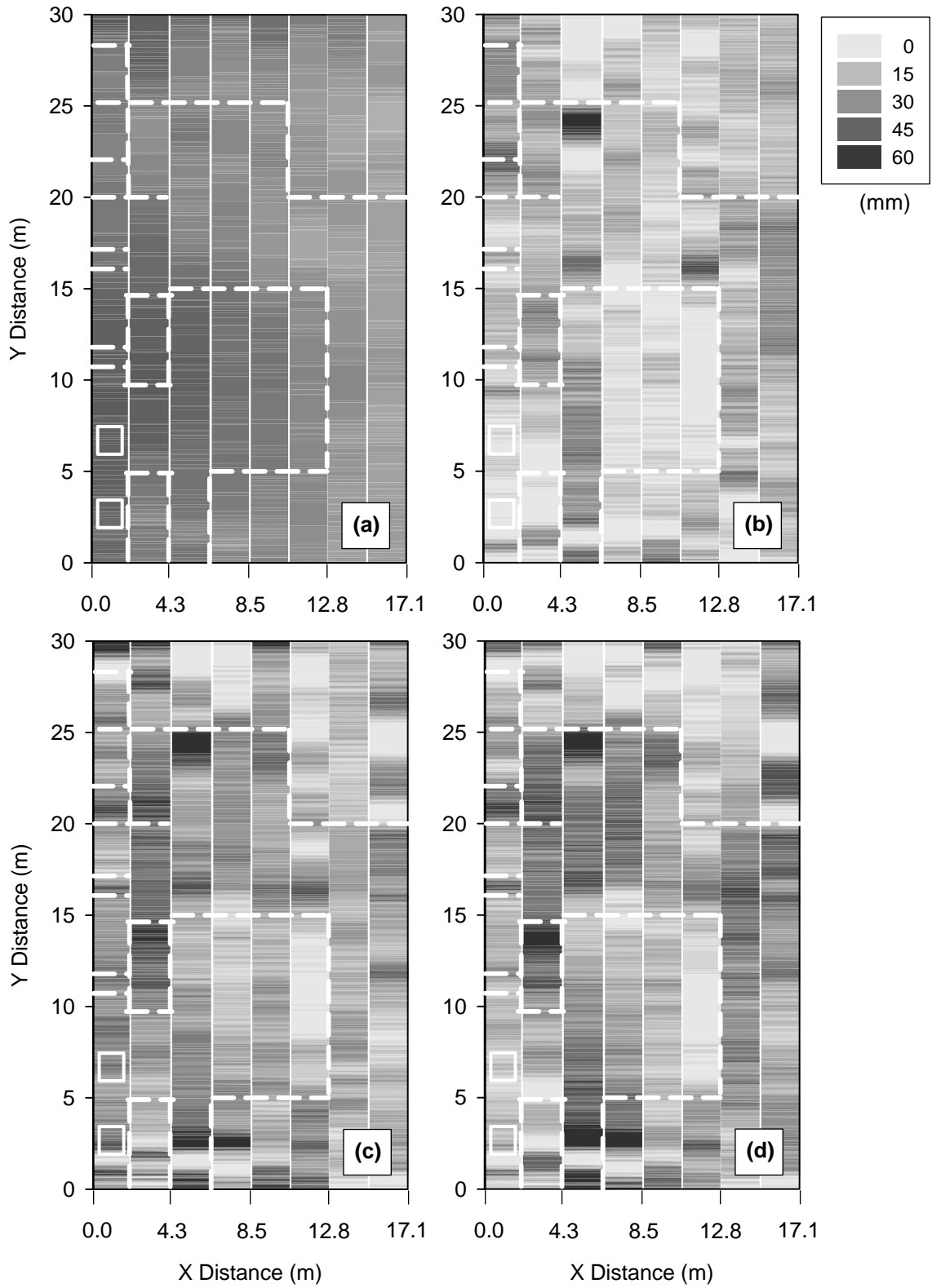


**Figure 103. Roller elevation difference at (a) Pass 1, (b) Pass 2, (c) Pass 3, and (d) Pass 4**

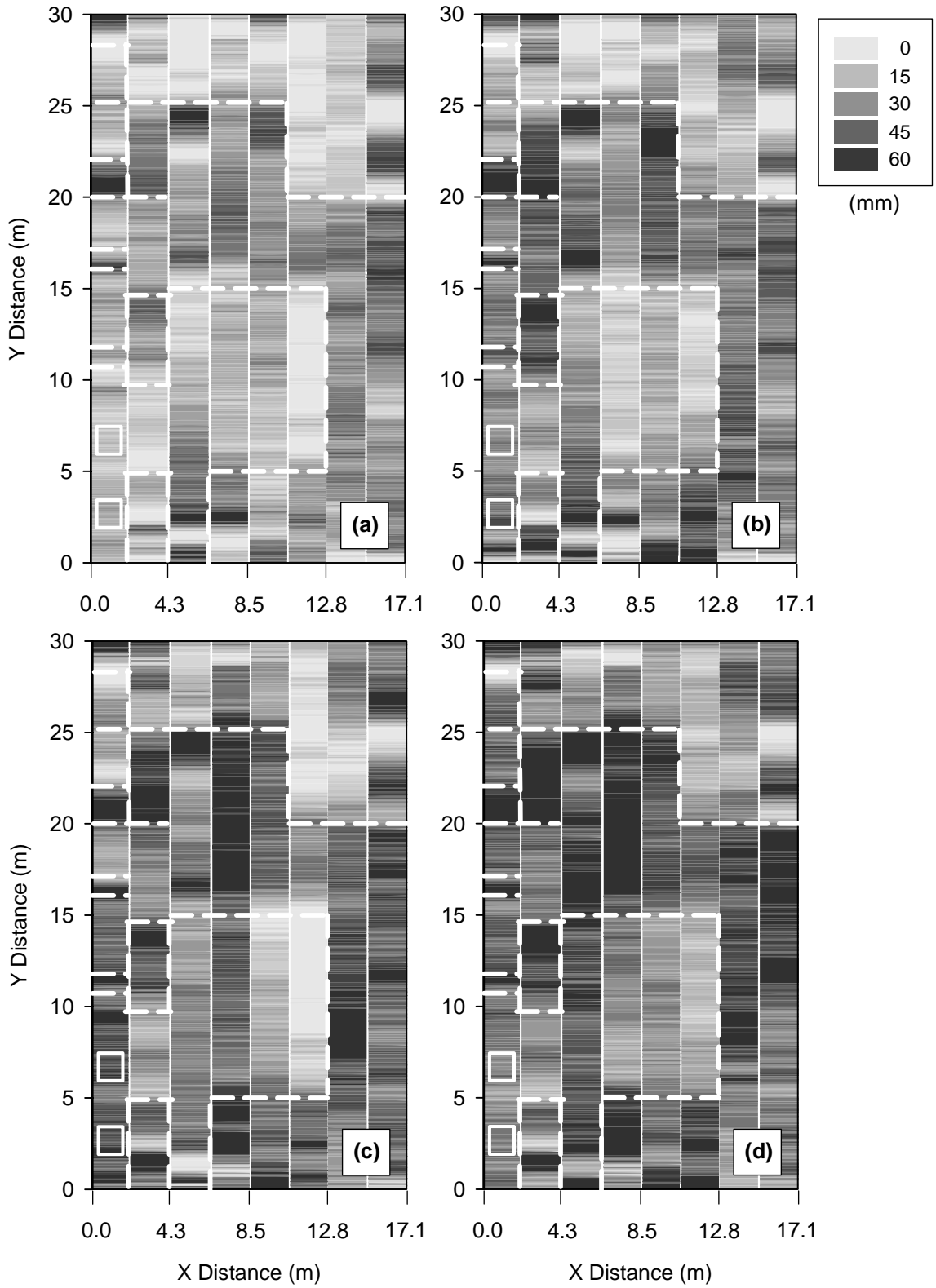


**Figure 104. Roller elevation difference at (a) Pass 5, (b) Pass 6, (c) Pass 7, and (d) Pass 8**

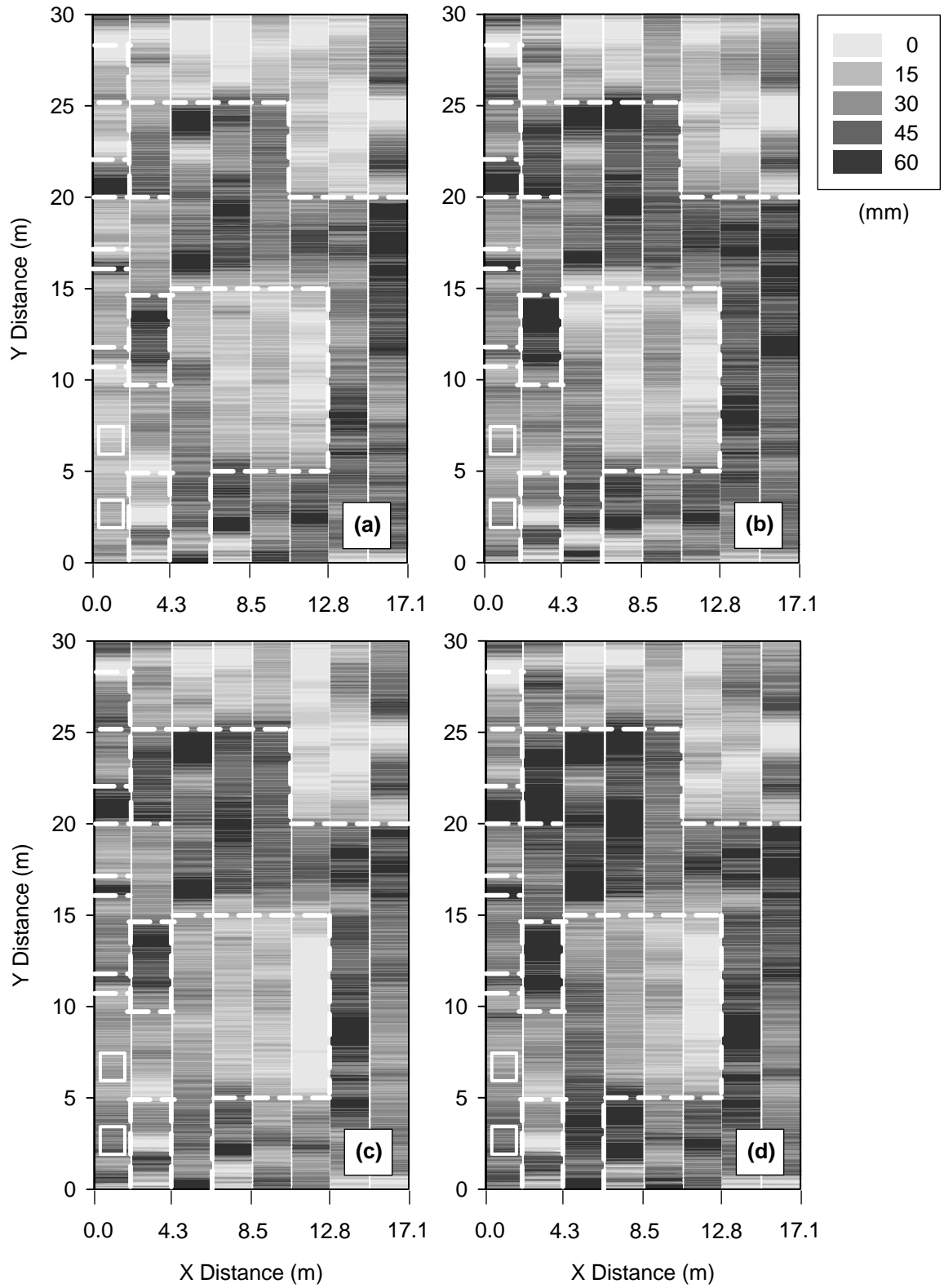


**Figure 105. Roller elevation difference at (a) Pass 9, (b) Pass 10, (c) Pass 11, and (d) Pass 12**

*Spatial Analysis of Compaction Monitoring Measurements*

The semivariogram remains a standard method to quantify spatial structure of soil properties. Spatial variability of each compaction monitoring measurement was thus described by an experimental variogram derived from measurements taken on the spatial test area. The CMV semivariograms did not fluctuate around a constant value, indicating that the measurements were correlated at the scale of sampling. The ability to observe the spatial structure of the data is the principal prerequisite for performing reliable geostatistical analyses; many gridding methods requiring only that a continuous function (or model) be used to express the semivariance as a function of lag distance. The semivariogram models that produced the cross-validation results of the highest accuracy were retained for further geostatistical analysis. Based on visual observation of the experimental variogram, either exponential or spherical models were fitted to the experimental semivariograms for each soil measurement system of this project.

Based on recommendations (Golden Software 2002), maximum lag distance was established as one-third of the maximum spacing interval, calculated to be 12 m. The default number of lag bins (25) was used, giving lag bin widths of 0.48 m. A summary of MDP variogram models and their fit parameters is provided in Table 10. The experimental variograms and model variograms for MDP are shown in Figure 106, with cross-validation results shown in Figure 107. A summary of CMV variogram models and their fit parameters is provided in Table 11. The experimental variograms and model variograms for CMV are shown in Figure 108, with cross-validation results shown in Figure 109.

**Table 10. Summary of MDP variogram modeling**

roller pass	Model	Model Parameters			Cross Validation			
		Scale (kJ <sup>2</sup> /s <sup>2</sup> )	Length (m)	Nugget (kJ <sup>2</sup> /s <sup>2</sup> )	Mean <sup>a</sup>	S.E.M. <sup>b</sup>	Slope <sup>c</sup>	R <sup>2</sup> <sup>c</sup>
1	Spherical	20.5	1.4	2.6	0.025	0.097	0.67	0.73
2	Spherical	17.6	2.4	0.0	0.022	0.121	0.78	0.89
3	Spherical	95.8	1.1	0.0	0.024	0.437	0.21	0.08
4	Spherical	30.5	1.0	3.0	0.031	0.103	0.64	0.82
5	Spherical	36.0	0.9	0.0	0.016	0.102	0.66	0.85
6	Spherical	35.0	1.0	0.0	0.033	0.114	0.64	0.77
7	Spherical	81.0	1.0	0.0	0.028	0.113	0.65	0.77
8	Spherical	36.0	1.1	0.0	0.021	0.116	0.68	0.77
9	Spherical	39.5	1.1	0.0	0.038	0.121	0.67	0.77
10	Spherical	69.8	0.5	0.0	0.003	0.313	0.15	0.20
11	Spherical	45.5	1.0	0.0	0.037	0.129	0.66	0.78
12	Spherical	42.3	1.1	0.0	0.067	0.118	0.67	0.77

<sup>a</sup> Mean of residuals (estimated observation – measured observation)

<sup>b</sup> Standard error of the mean

<sup>c</sup> For plots of estimated versus measured MDP

<sup>d</sup> Models assume isotropy

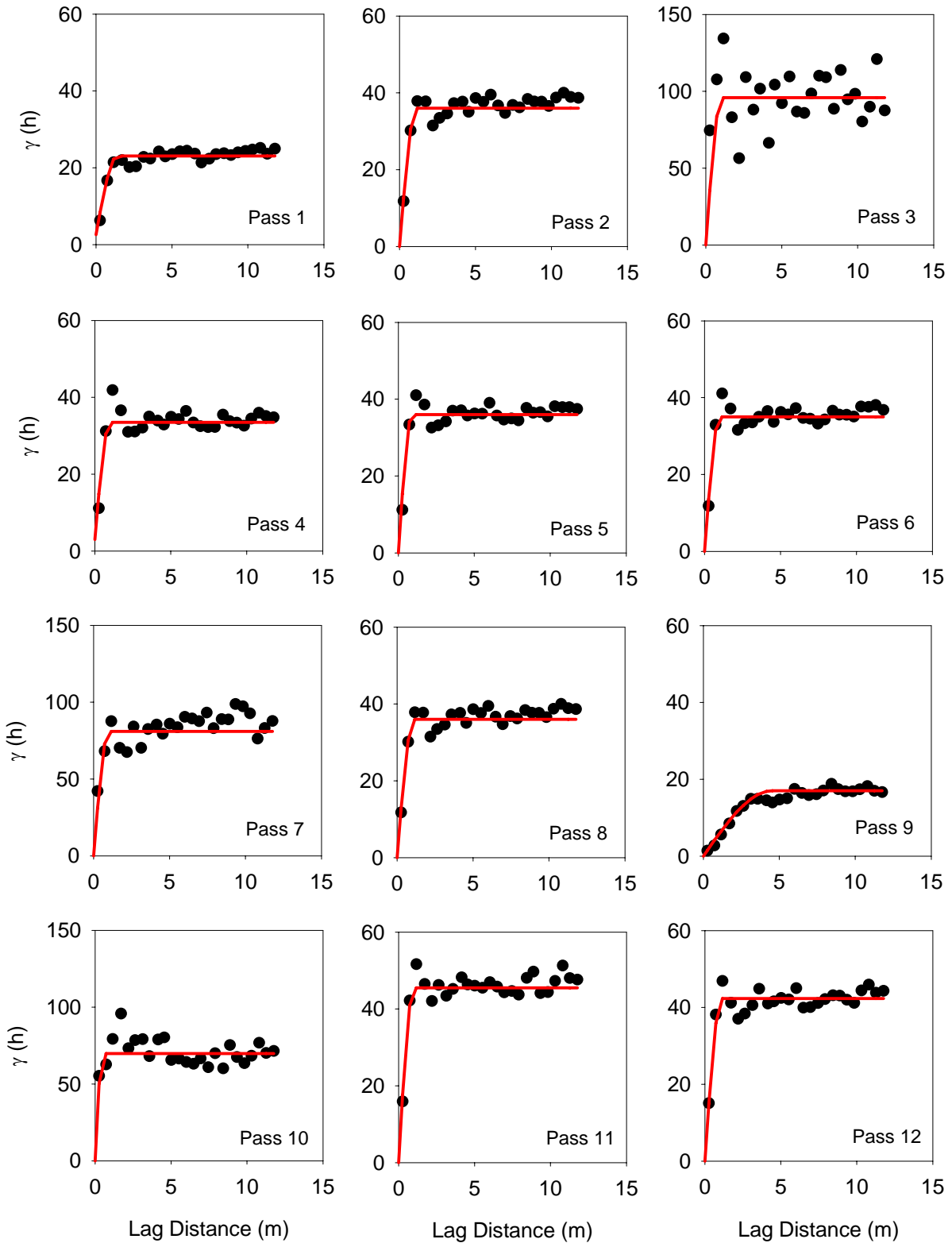


**Figure 106. Experimental variograms (points) and variogram models (lines) for MDP**

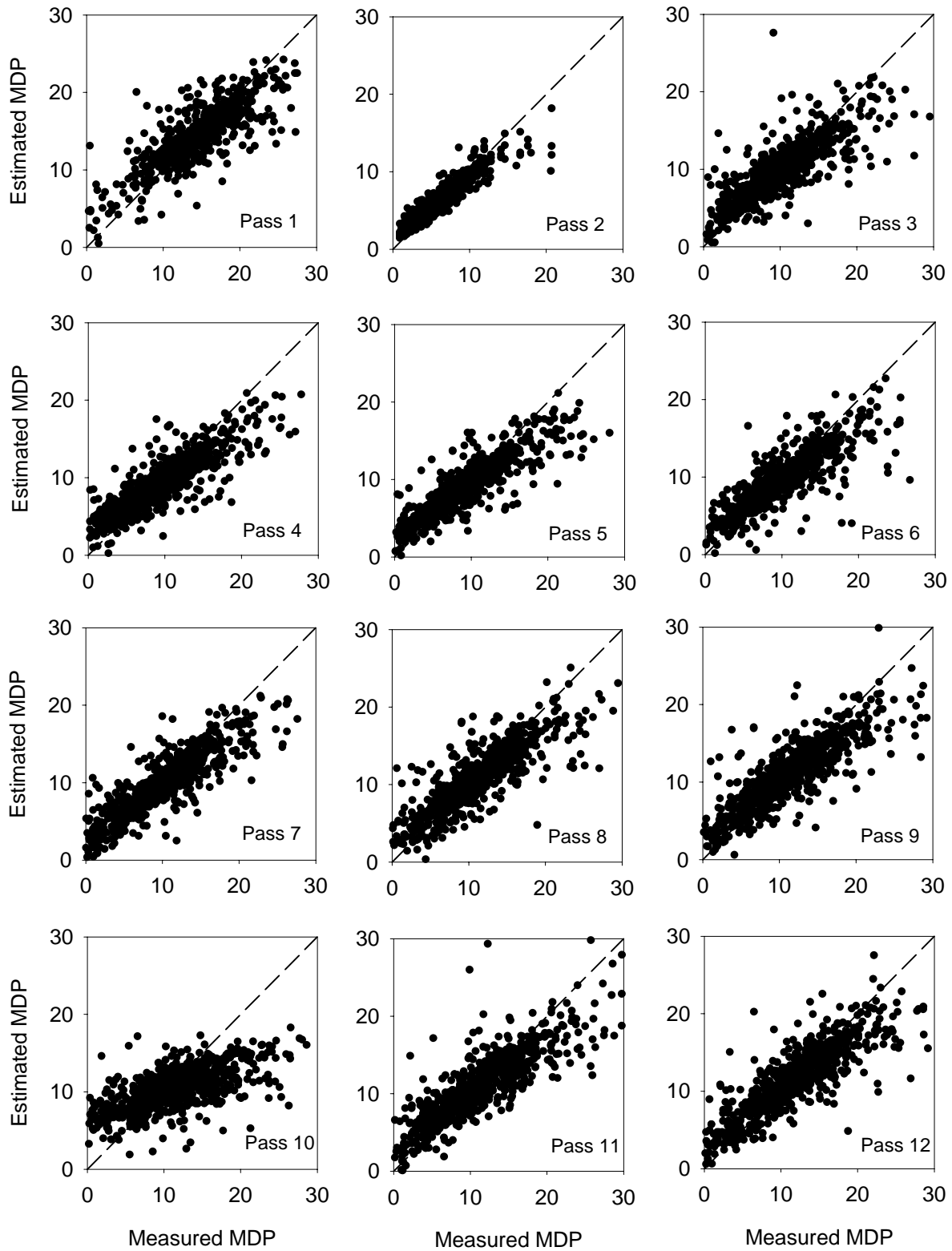


**Figure 107. MDP cross-validation results (measured versus estimated observations)**

**Table 11. Summary of CMV variogram modeling**

roller pass	Model	Model Parameters			Cross Validation			
		Scale	Length (m)	Nugget	Mean <sup>a</sup>	S.E.M. <sup>b</sup>	Slope <sup>c</sup>	R <sup>2c</sup>
1	Exponential	10.3	3.2	0.0	-0.000	0.030	0.92	0.94
2	Exponential	18.5	3.0	0.0	-0.021	0.042	0.90	0.93
3	Exponential	23.0	5.0	0.0	-0.016	0.040	0.93	0.93
4	Exponential	21.5	3.2	0.0	-0.003	0.041	0.92	0.94
5	Exponential	20.0	3.3	0.0	-0.005	0.040	0.92	0.93
6	Exponential	21.0	4.3	0.0	-0.014	0.042	0.92	0.93
7	Exponential	23.0	3.0	0.0	-0.024	0.057	0.88	0.90
8	Exponential	18.5	3.3	0.0	-0.002	0.043	0.91	0.92
9	Exponential	18.5	3.0	0.0	-0.022	0.046	0.90	0.91
10	Exponential	21.5	3.0	0.0	-0.001	0.047	0.91	0.92
11	Exponential	22.5	2.6	0.0	-0.018	0.054	0.89	0.91
12	Exponential	27.0	3.3	0.0	-0.021	0.059	0.90	0.91

<sup>a</sup> Mean of residuals (estimated observation – measured observation)

<sup>b</sup> Standard error of the mean

<sup>c</sup> For plots of estimated versus measured MDP

<sup>d</sup> Models assume isotropy

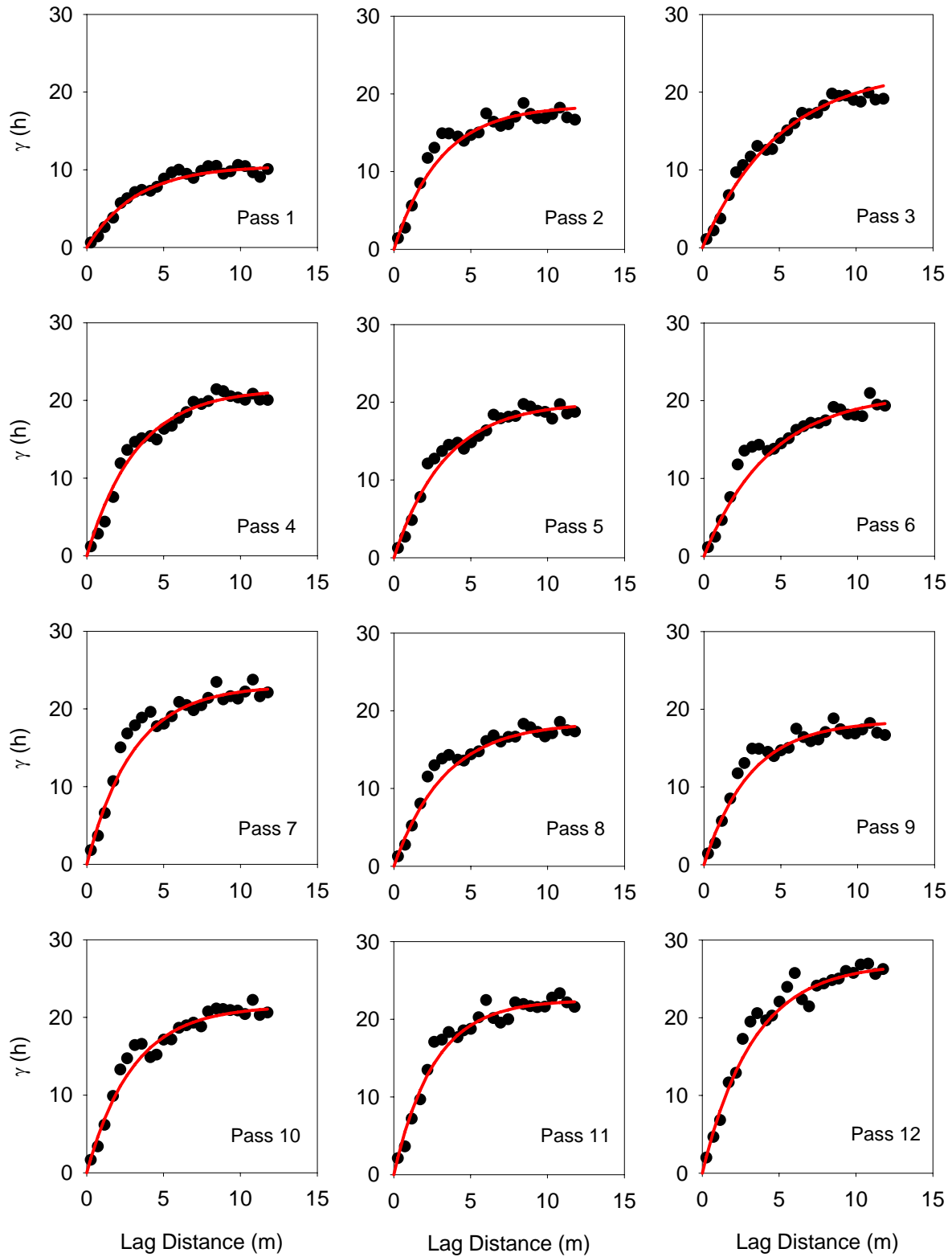


**Figure 108. Experimental variograms (points) and variogram models (lines) for CMV**

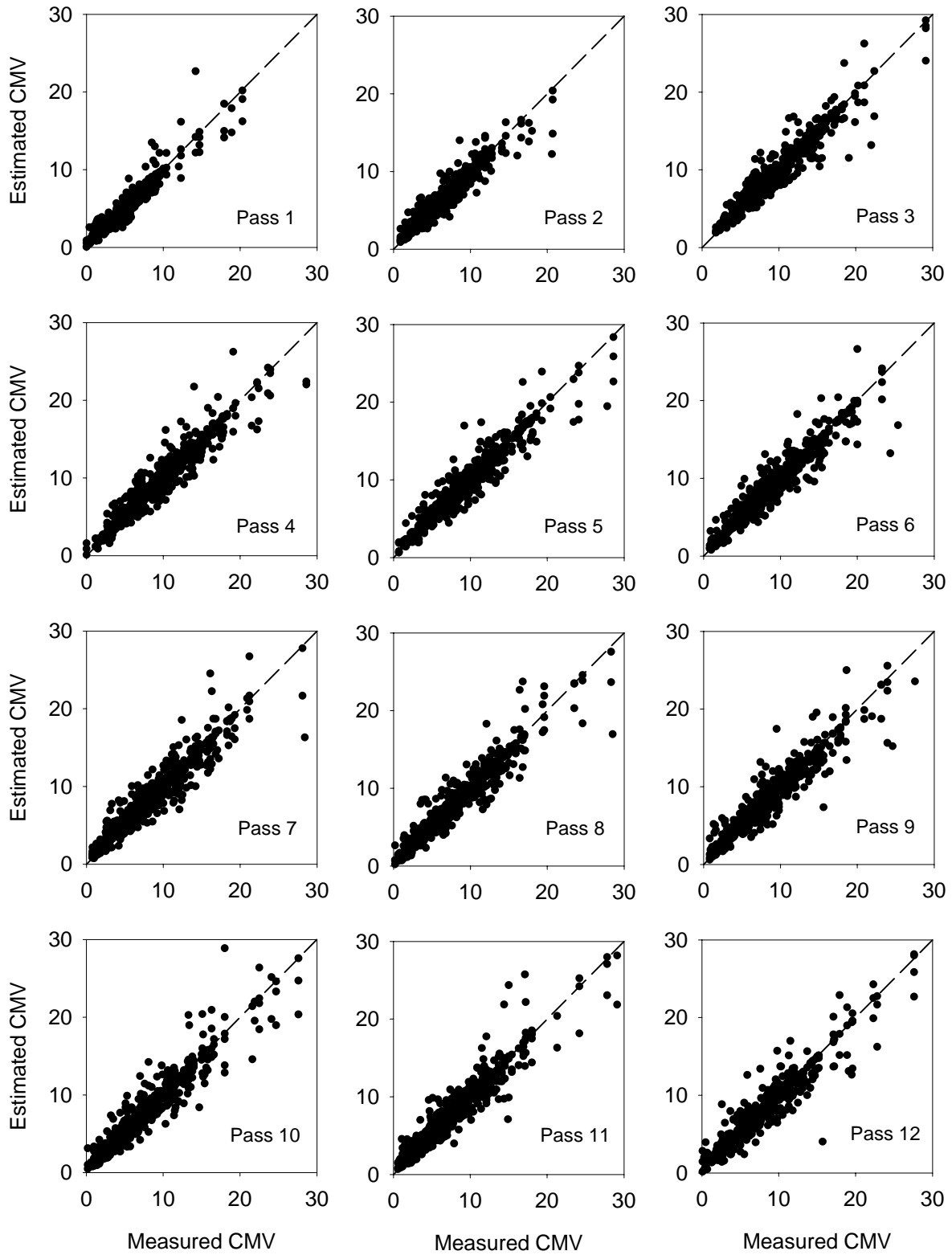


**Figure 109. CMV cross-validation results (measured versus estimated observations)**

Kriging is an interpolation method of geostatistics that uses spatial dependence and spatial structure of a measured property to predict values of that property at unsampled locations. Because the method was originally developed for the mining industry (Journel and Huijbregts 1978), kriging is particularly common in geosciences such as geotechnical engineering. Further, kriging provides the least bias in predictions from all linear interpolation methods because the interpolated or kriged values are computed from equations that minimize the variance of the estimated value. Kriging is an exact interpolation method, in which the measured values will always be returned when interpolating to measurement locations. For this project, compaction monitoring data were analyzed using kriging operations in Surfer 8 (Golden Software 2002) and spatial modeling results.

Kriged MDP results are shown from Figure 110 to Figure 112 for all passes. Since the spatial structure of MDP measurements was relatively weak, the kriging operation had the effect of smoothing the data (i.e., mitigating the local variability of MDP). Thus, the areas of thicker lift are shown more clearly than the raw data.

Kriged CMV results are shown from Figure 113 to Figure 115 for all passes. For this measurement system, relatively strong spatial structure was observed. Since the measurements were applied to the discrete points of the roller drum, however, the interpolation still had the effect of smoothing data. The areas of thicker lift are still observed in the kriged surface, but these areas appear to be less accurate than the raw data, which were plotted using simple polygons.

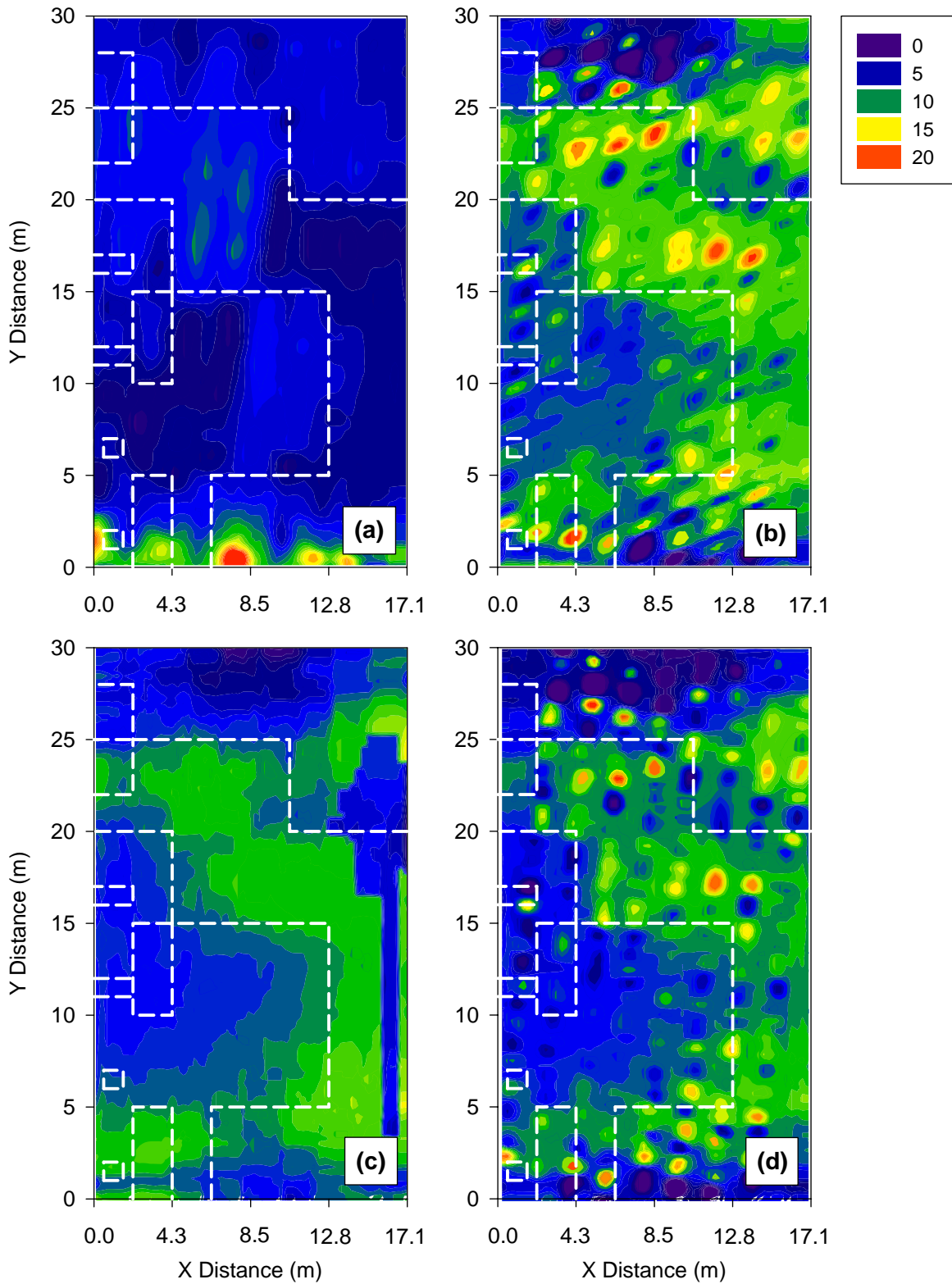


**Figure 110. Kriged MDP (kJ/s) for (a) Pass 1, (b) Pass 2, (c) Pass 3, (d) Pass 4**

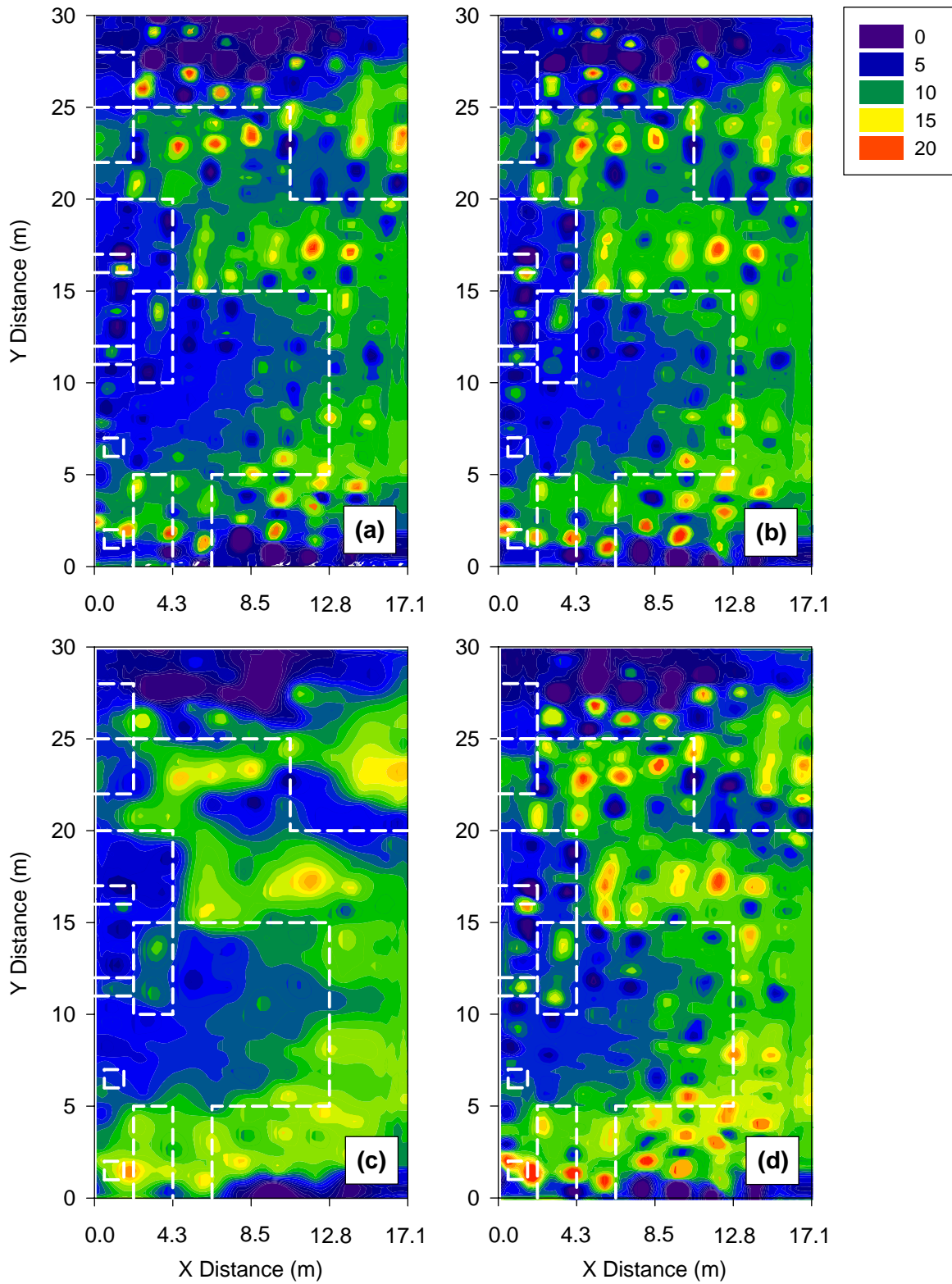


**Figure 111. Kriged MDP (kJ/s) for (a) Pass 5, (b) Pass 6, (c) Pass 7, (d) Pass 8**

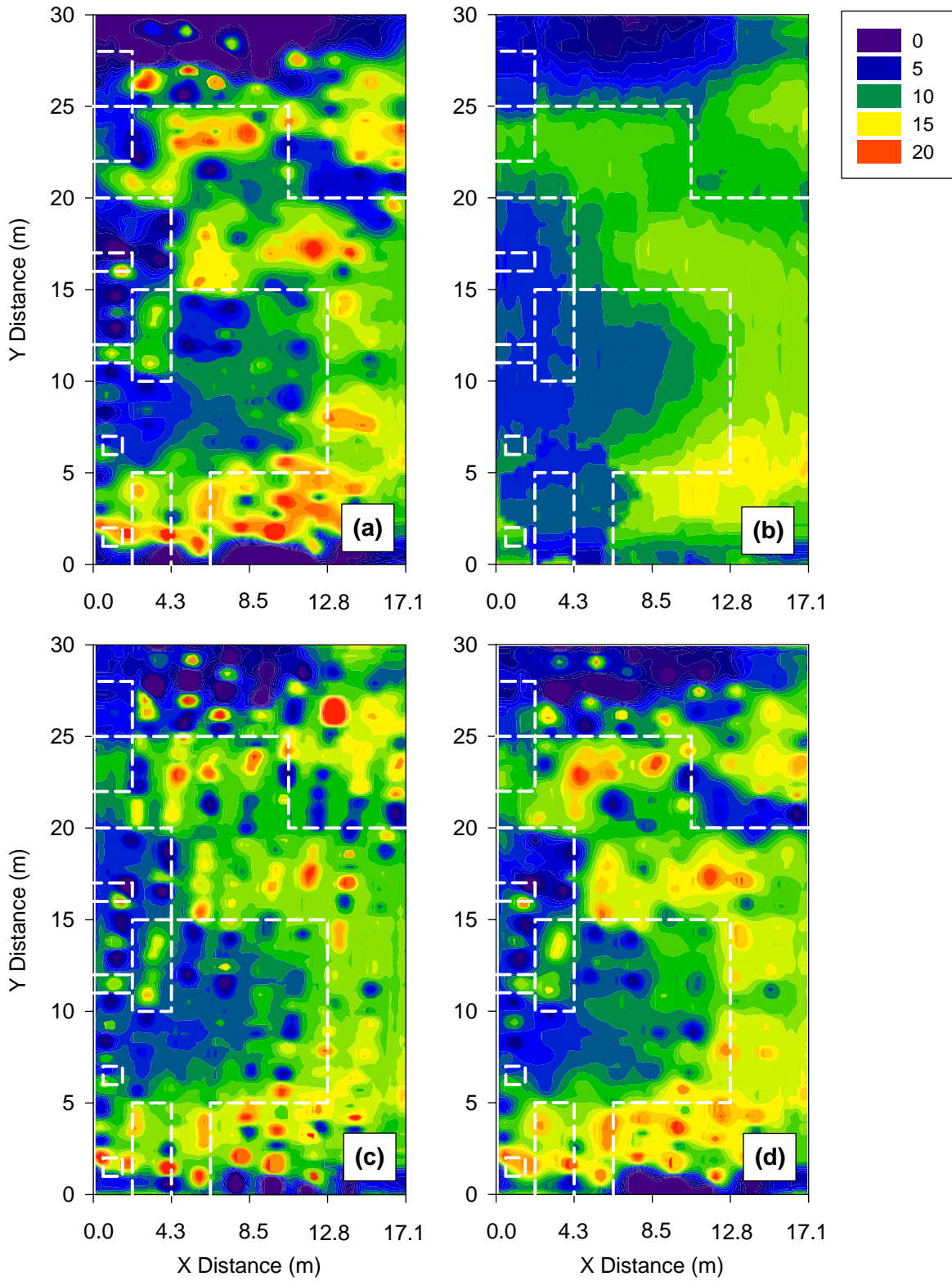


**Figure 112. Kriged MDP (kJ/s) for (a) Pass 9, (b) Pass 10, (c) Pass 11, (d) Pass 12**

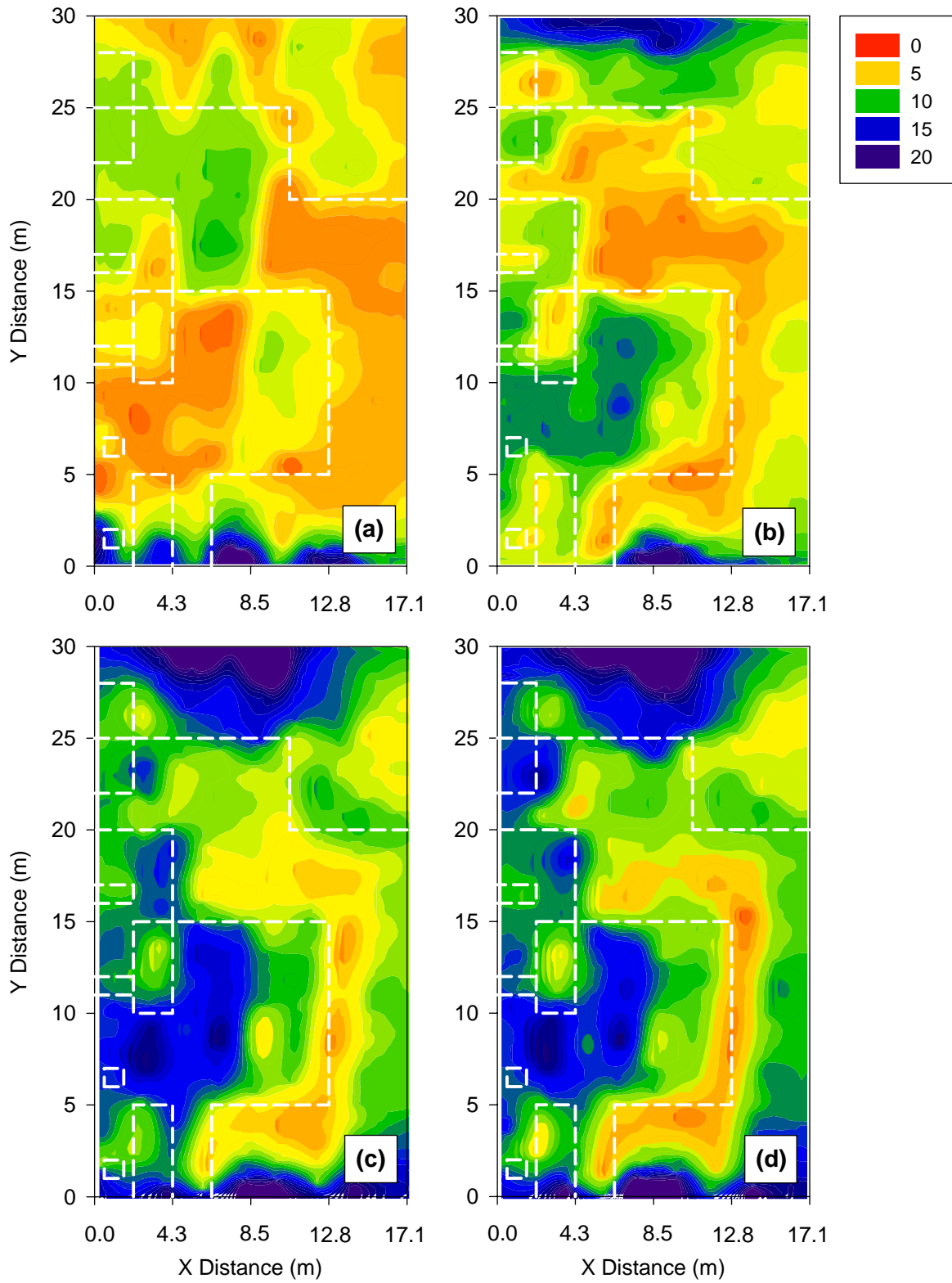


**Figure 113. Kriged CMV for (a) Pass 1, (b) Pass 2, (c) Pass 3, (d) Pass 4**

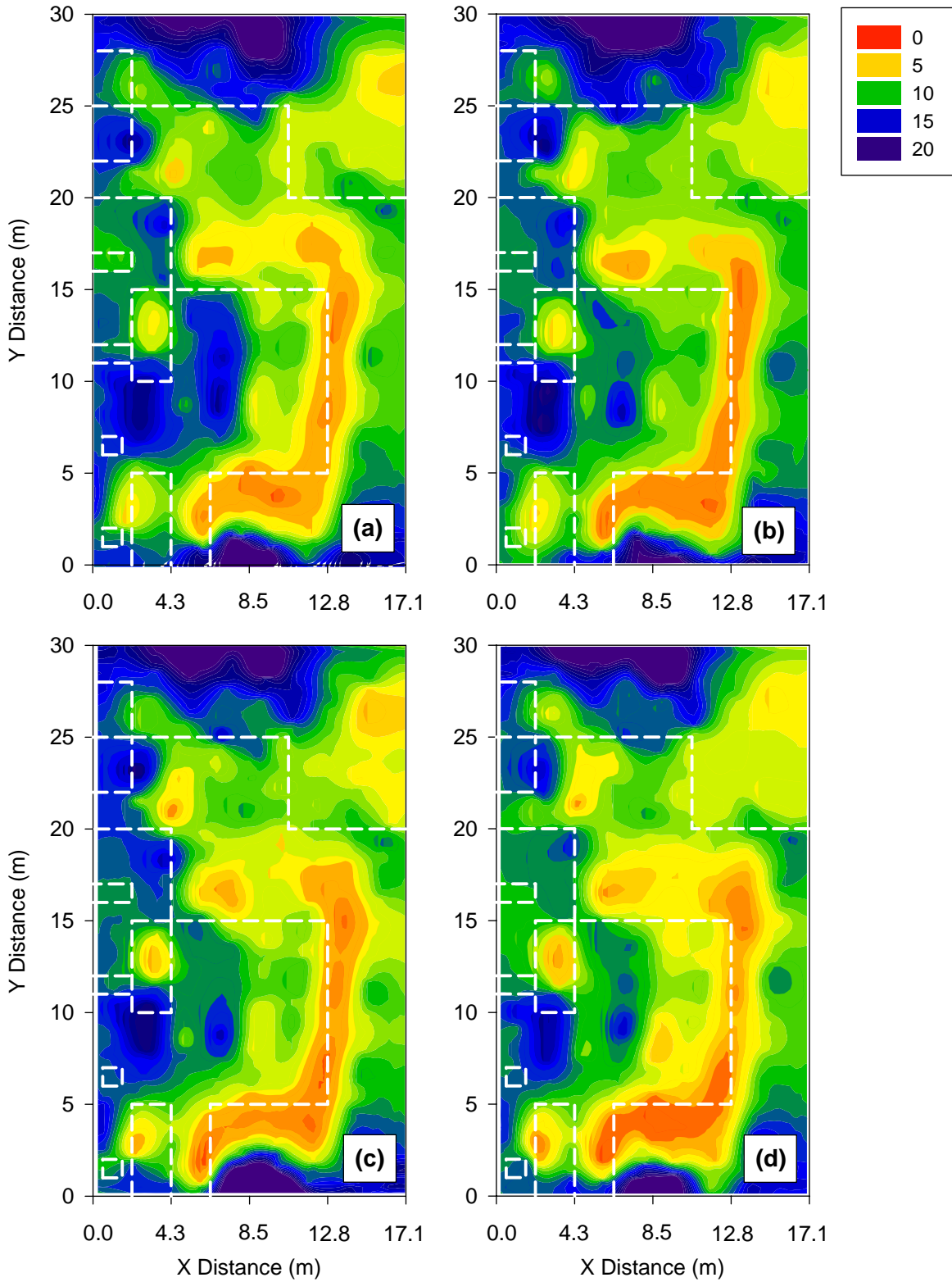


**Figure 114. Kriged CMV for (a) Pass 5, (b) Pass 6, (c) Pass 7, (d) Pass 8**

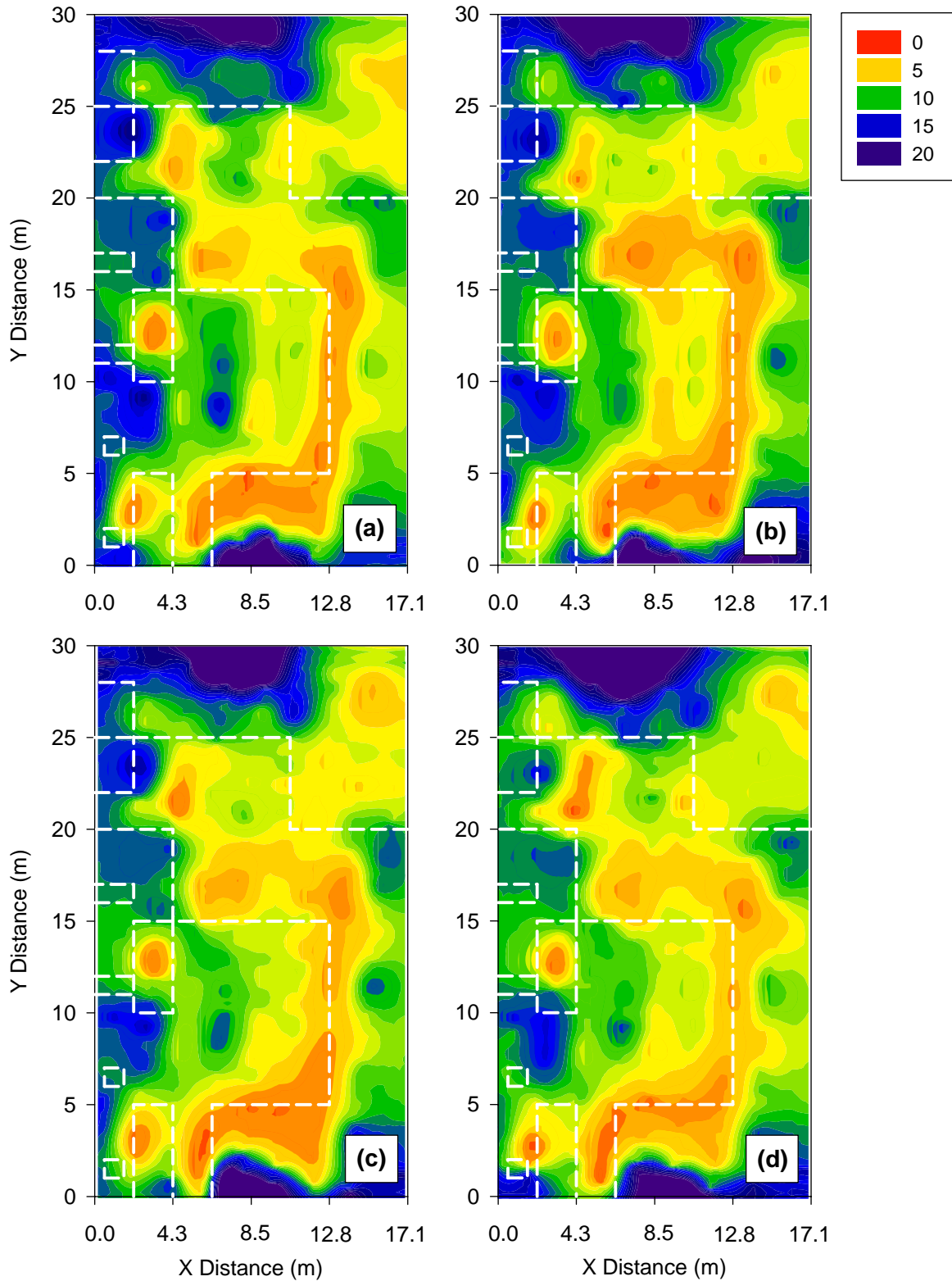


**Figure 115. Kriged CMV for (a) Pass 9, (b) Pass 10, (c) Pass 11, (d) Pass 12**

### *Spatial Analysis of In Situ Measurements*

Spatial variability of each in situ measurement was described by an experimental variogram derived from 192 measurements taken on the spatial test area. These semivariograms generally did not fluctuate around a constant value, indicating that the measurements were correlated at the scale of the sampling plan. As with compaction monitoring measurements, the semivariogram models that produced the most accurate cross-validation results were retained for further geostatistical analysis. Either exponential or spherical models were fitted to the experimental semivariograms for each soil measurement system of this project. The experimental variograms and model variograms for in situ measurements for Spatial 2 are shown in Figure 116, with cross validation results provided in Figure 117. The summary of variogram parameters are provided in Table 12.

After modeling the semivariogram for each in situ measurement, kriging was performed using Surfer 8.0. Single, nominal moisture content (optimum) was intended for the test area. The contour plot of moisture content (Figure 118) shows that, in fact, moisture content was within  $\pm 1\%$  of optimum moisture content (8%). However, inherent variation in moisture content with strong spatial structure resulting from construction operations was present and impacted measurements of soil stability. The soil moisture content approached 9% in the southeast (lower-left), center, and northwest (upper-right) regions of the test area. The moisture content was as low as 7% in the southern portion of the test area. Moisture variability on large-scale production areas is generally unavoidable. The moisture variation observed for this project, which was relatively uniform, clearly affected the compaction results, as discussed later.

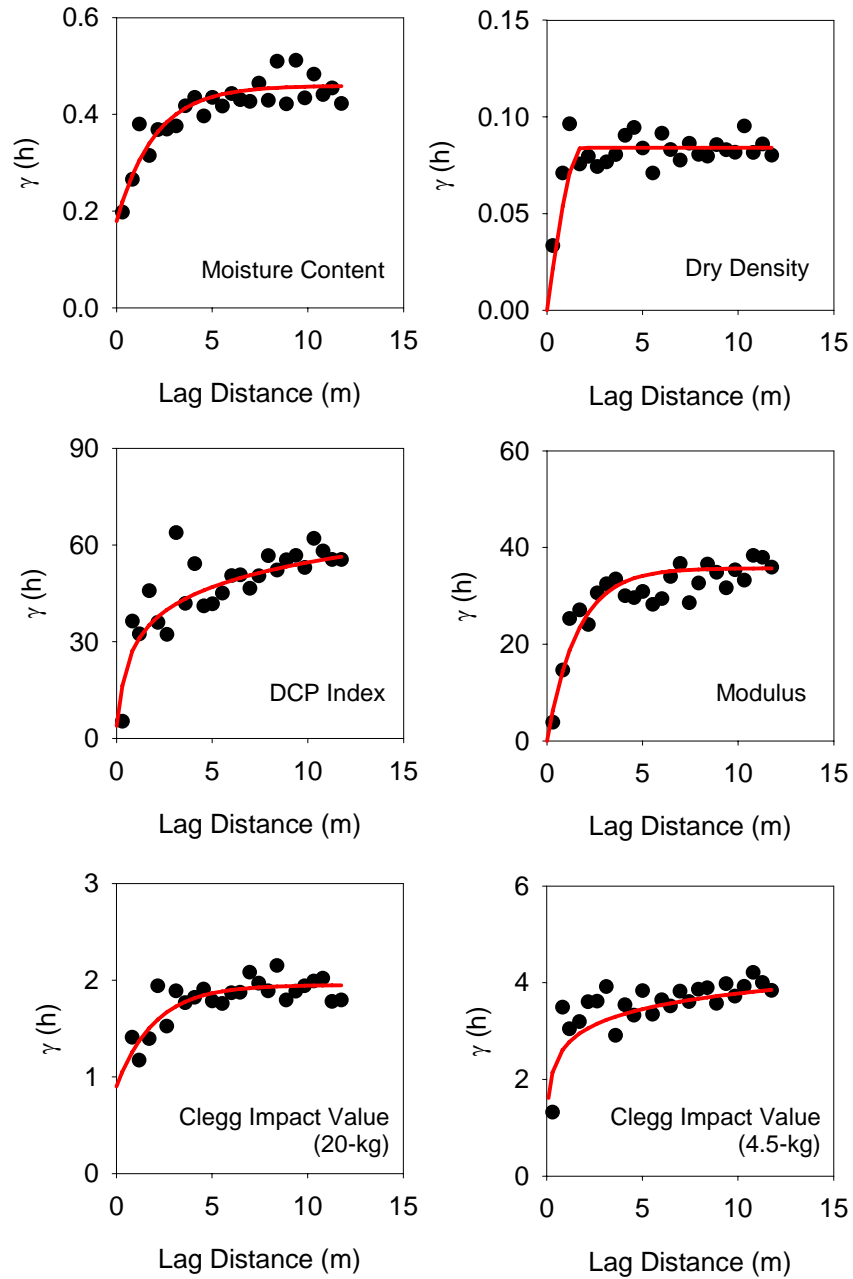


**Figure 116. Experimental (points) and model (lines) variograms for in situ measurements of Spatial 2**

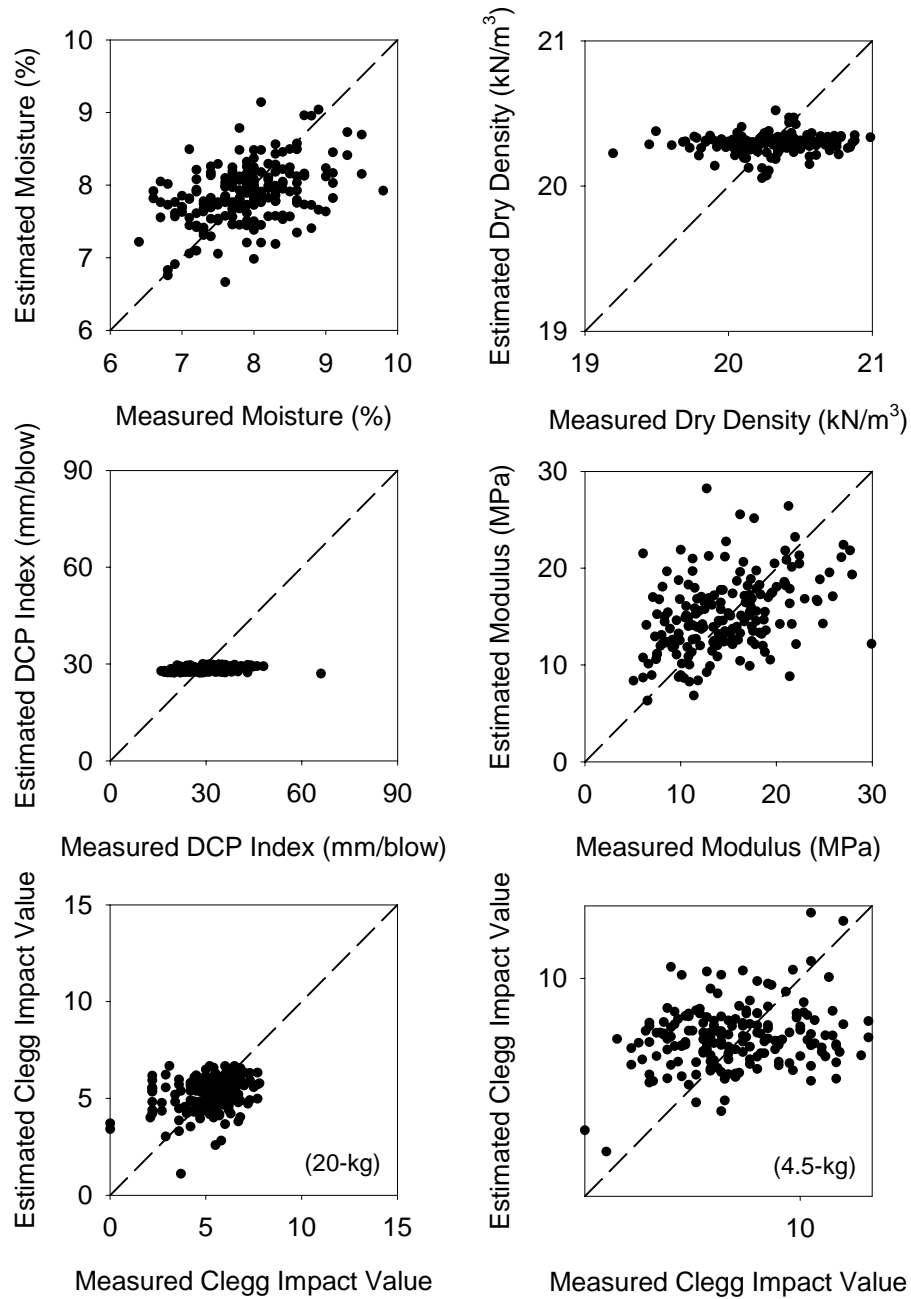


**Figure 117. Cross validation results (measured versus estimated observations) for in situ properties at Spatial 2**

**Table 12. Summary of in situ measurement variogram modeling**

Soil Property	Model	Model Parameters			Cross Validation			
		Scale	Length (m)	Nugget	Mean <sup>a</sup>	S.E.M. <sup>b</sup>	Slope <sup>c</sup>	R <sup>2c</sup>
Moisture	Exponential	0.28	4.5	0.18	-0.001	0.954	0.27	0.19
Density	Spherical	0.08	1.8	0.00	-0.104	9.177	0.02	0.01
DCP	Exponential	61.5	6.8	0.00	-0.104	9.177	0.05	0.19
Modulus	Exponential	35.70	3.5	0.00	0.046	14.817	0.34	0.24
CIV (20)	Exponential	1.05	3.2	0.90	0.008	1.747	0.17	0.09
CIV (4.5)	Exponential	2.5	1.0	1.20	-0.032	1.944	0.11	0.06

<sup>a</sup> Mean of residuals (estimated observation – measured observation)

<sup>b</sup> Standard error of the mean

<sup>c</sup> For plots of estimated versus measured in situ measurements

<sup>d</sup> Models assume isotropy

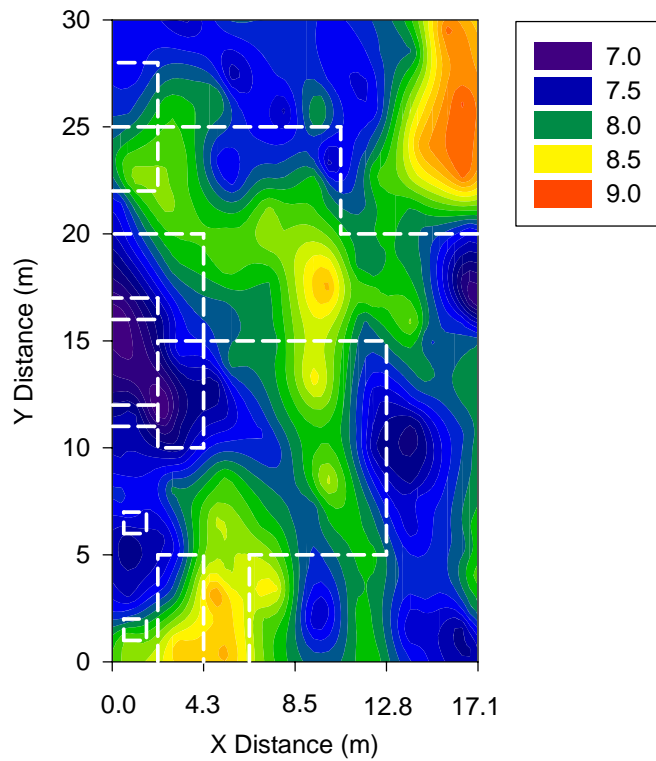


**Figure 118. Moisture content for Spatial 2 at Pass 2**

The contours of in situ soil properties (e.g., dry density, modulus, DCP index, CIV) are provided in Figure 119. Dashed lines are again provided for the boundaries of 200 mm and 510 mm lifts. Dry unit weight ranged from about 19 to 21 kN/m<sup>3</sup>, but was relatively uniform over the test area. The contour plot appears “spotty,” which is a result of kriging procedures necessarily producing measured values at measurement locations. In terms of uniformity, the spatial variation observed in dry density is preferred over variation that contains more global trends.

Soil strength and modulus measurements have previously been shown to decrease rapidly with increasing moisture content (White et al. 2005). Soil modulus determined using a PFWD and soil strength determined using a 20-kg Clegg Impact Tester, in particular, show the influence of moisture content. The comparatively high moisture observed in the southeast, center, and northwest regions of the test area are mirrored by lower modulus (less than 8 MPa) and Clegg impact value (less than 4) results.

Mean DCP index results from constant-penetration-depth (500 mm) tests are affected by both moisture content and lift thickness. DCP index over the western (upper) portion of the test area (y greater than 15 m) strongly reflects the observed moisture content, with higher moisture content producing higher DCP index (lower strength). DCP index over the eastern (lower) portion of the test area (y from 0 to 15 m) reflects the artificially imposed variation in lift thickness. In regions of 200 mm lift thickness, the DCP index begins to decrease at a depth of 200 mm, the depth of a stiff subgrade layer. In a similar trend, the regions of 510 mm lift thickness also show higher DCP index values for the full depth of the compaction layer. The DCP index contour very clearly identifies regions of variable lift thickness, as the measurement interpretation is essentially a measurement of lift thickness. Even localized regions of thick loose lifts (second roller path from 0 to 5 m and from 10 to 15 m) are identified.

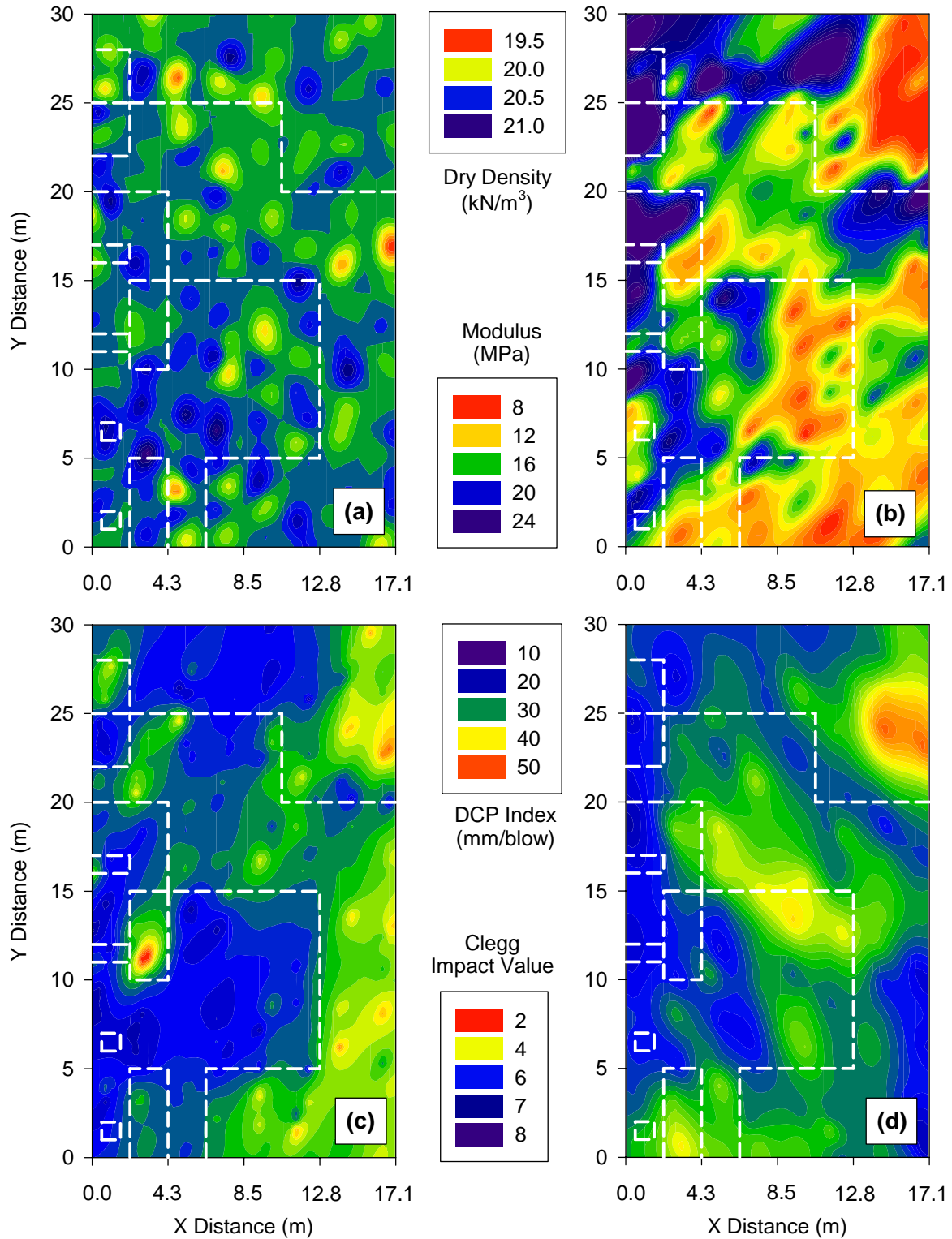


**Figure 119. In situ measurement results: (a) dry density, (b)  $E_{PFW}$ , (c) DCP index, and (d) Clegg impact value**

## Compaction Monitoring Use for Quality Control and Acceptance

The capabilities of a roller for identifying the in situ characteristics of unbound materials can be separated into three levels of compaction monitoring technology use, as diagrammed in Figure 120. The most basic of these levels (Level 1) may be the mapping of an area to obtain some compaction value that relates to the density, strength, or stiffness of the area. This capability was demonstrated from Figure 97 to Figure 102, where MDP and CMV measurements showed differential stiffness over a two-dimensional area.

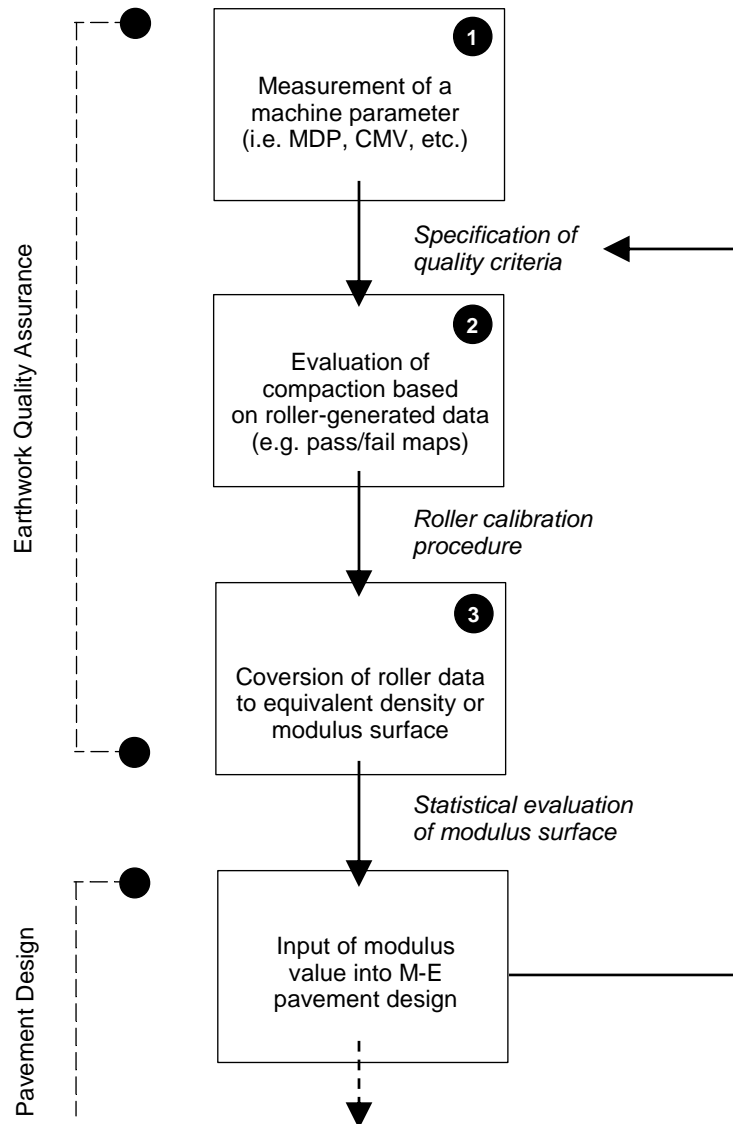


**Figure 120. Levels of compaction monitoring technology use**

By specifying a target compaction value for a particular compaction monitoring technology, the next level of compaction monitoring technology use (Level 2) may be achieved. In this case, the areas that fail to meet the prescribed specification can easily be identified and differentiated from

areas that do meet the quality criterion. Spatial plots that show pass/fail regions of the test area based on dry density quality criteria are provided in Figure 121 for MDP and CMV. This presentation of pass/fail regions of a spatial area demonstrates the use of compaction monitoring technology as a quality control and acceptance tool. In Figure 121 (a), the test area with MDP exceeding 8.3 kJ/s is shaded black to indicate a failing condition. This is done for CMV in Figure 121 (b), with 8.0 as the quality criterion. The figures coincidentally show failing soil conditions in many of the same regions, including those of 510 mm lift thickness. Recognizing that MDP is more locally variable and that this system is more sensitive to surficial characteristics, the failing regions of Figure 121 (a) appear to be more scattered. For the maps, only 35% and 30% of the test area achieved a passing condition according to MDP and CMV, respectively. Additionally, 47% of the test area achieved 95% compaction, which was the quality criterion for which the technologies were calibrated. Using the same quality criteria and the kriged MDP and CMV maps, pass/fail maps are shown in Figure 121 (c) and (d), respectively. The kriging procedure for MDP served as a smoothing operation that more clearly identified areas of variable lift thickness. Spatial analysis also smoothed CMV data; however, little difference is seen in pass/fail maps using raw and kriged data.

The kriged in situ measurements and quality criteria based on Pass 4 data from Strip 2 were used to create another set of pass/fail maps. These plots are shown in Figure 122. Quality criteria for dry unit weight,  $E_{PFWD}$ , mean DCP index, and CIV were 20.35 kN/m<sup>3</sup>, 32.0 MPa, 23 mm/blow, and 7.1, respectively. The pass/fail maps show the entire spatial area failing. Because measurements were taken after only two passes, this result was expected.

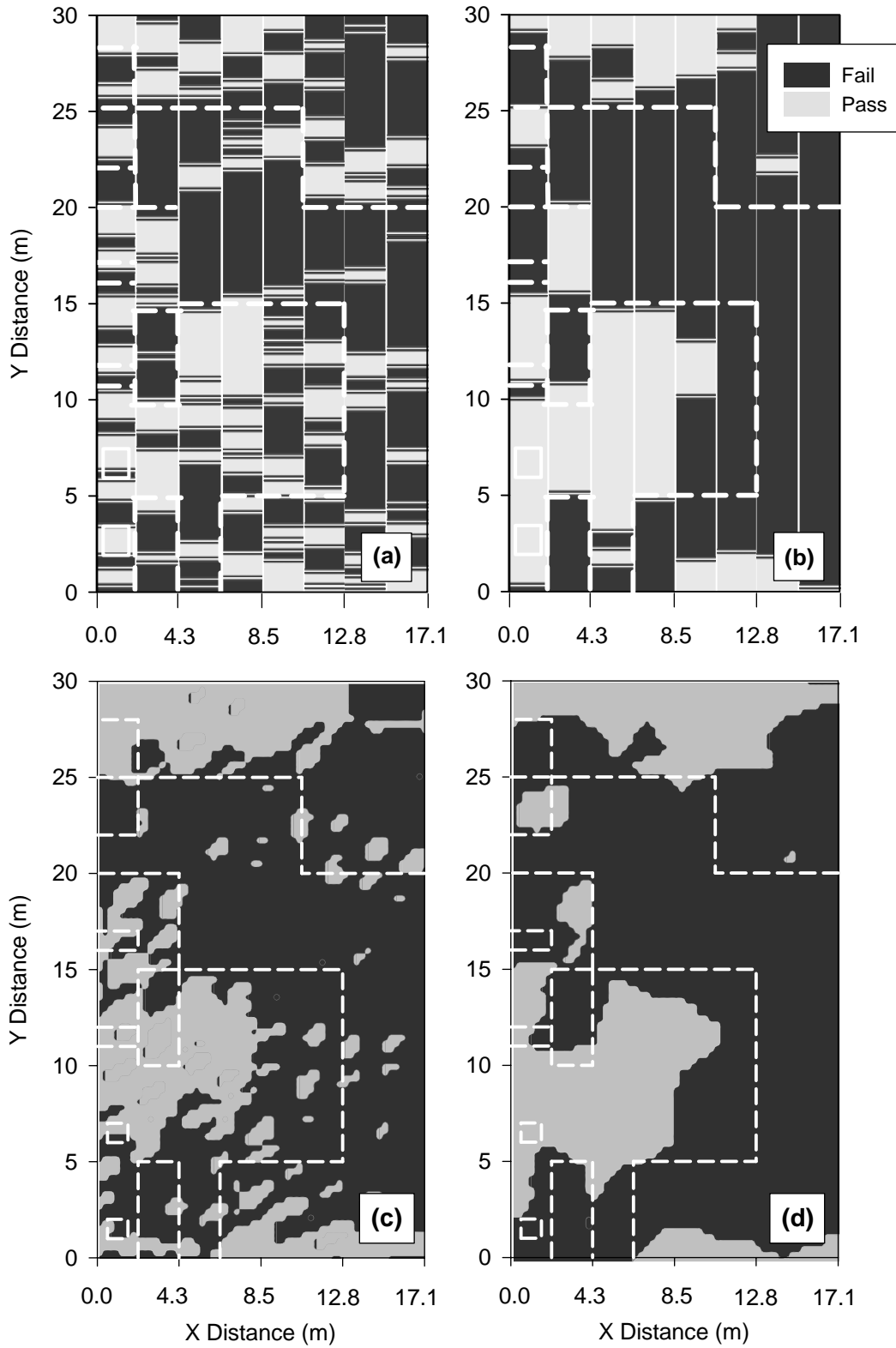


**Figure 121. Quality acceptance maps based on calibration for (a) MDP data, (b) CMV data, (c) MDP kriged surface, and (d) CMV kriged surface**

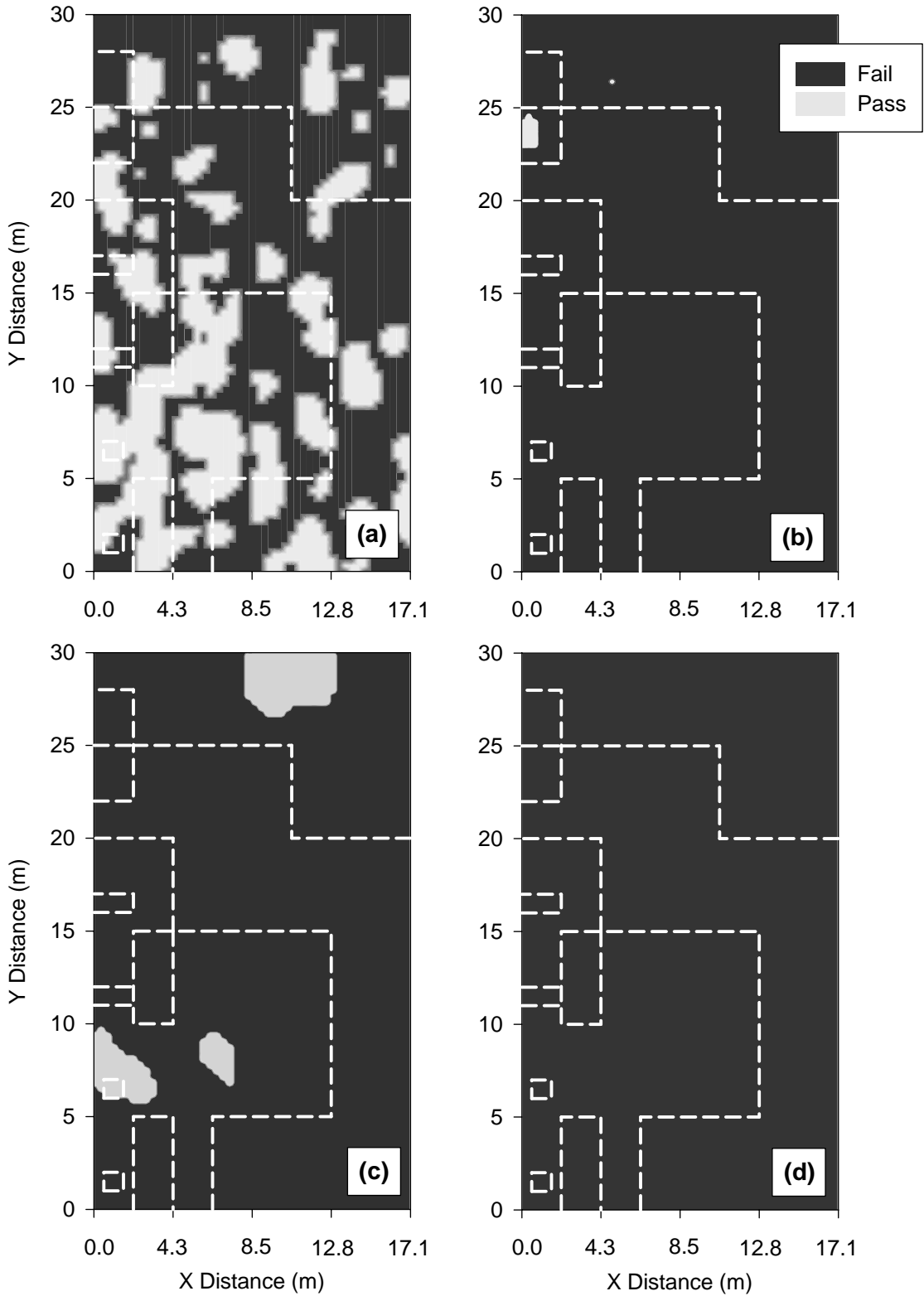


**Figure 122. Quality acceptance maps based on calibration for (a) dry unit weight, (b)  $E_{PFWD}$ , (c) DCP index, and (d) 20-kg CIV**

### Spatial Area 3

#### *Machine Output and Spatial Analysis of Machine Measurements*

MDP data for Spatial 3 is shown in Figure 123 for Passes 1 and 4. For Pass 1, the 17.1 m wide test area was compacted without overlapping (eight roller widths). For Pass 2, the area was compacted with overlapping to give 23 “widths” of data. The latter mapping process resulted in a more detailed identification of the soil properties. The dashed lines in Figure 123 represent the boundary between subgrade and subbase materials (at y equal to 5 m) and demarcation between areas of thin and thick lifts.

As was done for Spatial 2 data, the spatial distribution of MDP was investigated. The variogram was modeled and data were kriged to give MDP surfaces, which are provided in Figure 124. MDP ranges from 0 to 5 kJ/s for the subgrade material, which indicates a stiff soil condition. Higher MDP is observed for subbase material, ranging from about 0 to 10 kJ/s in areas of thin lift and from 5 to 20 kJ/s in areas of thick lift.

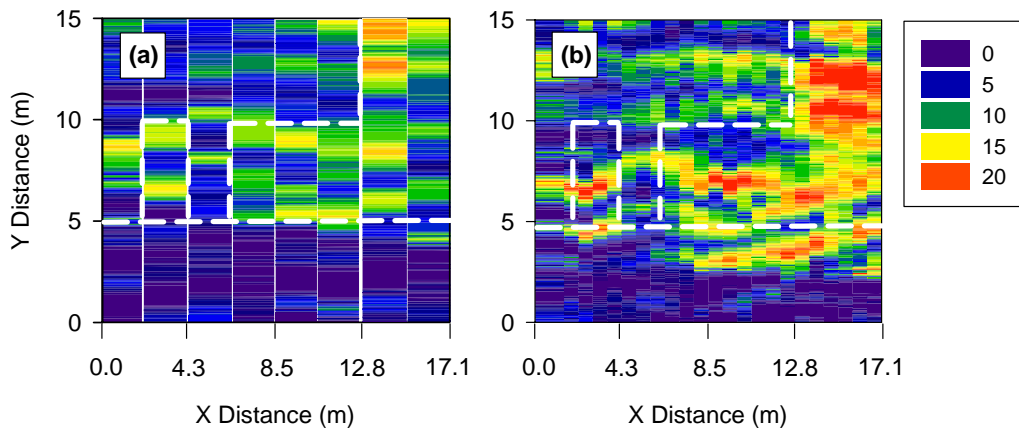


**Figure 123. MDP (kJ/s) output for Spatial 3 at (a) Pass 1 and (b) Pass 4**

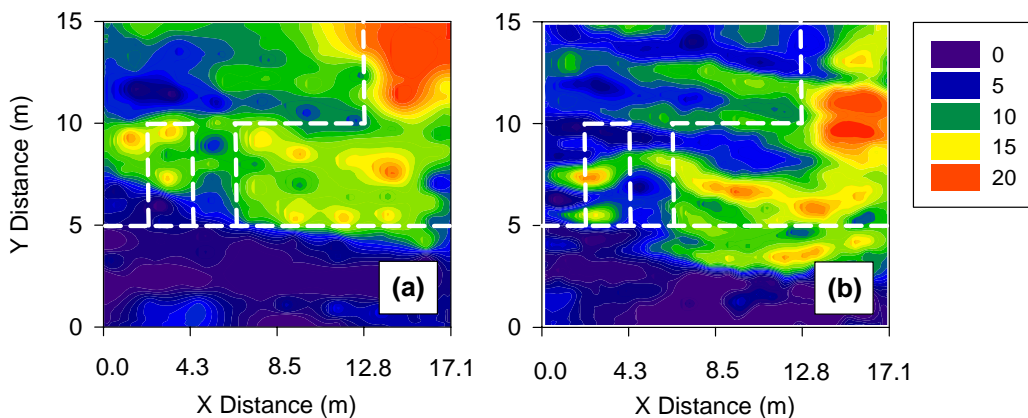


**Figure 124. Kriged MDP (kJ/s) at (a) Pass 1 (n = 592) and (b) Pass 4 (n = 1725)**

CMV was investigated in the same manner as MDP. The compaction monitoring data are shown in Figure 125 for Passes 1 and 4. Kriged surfaces for CMV are shown in Figure 126. CMV clearly shows the subgrade material to be stiffer than the subbase material, with CMV ranging from about 10 to greater than 20. CMV ranges from 0 to 10 for subbase material with only slight indication of differential lift thickness.

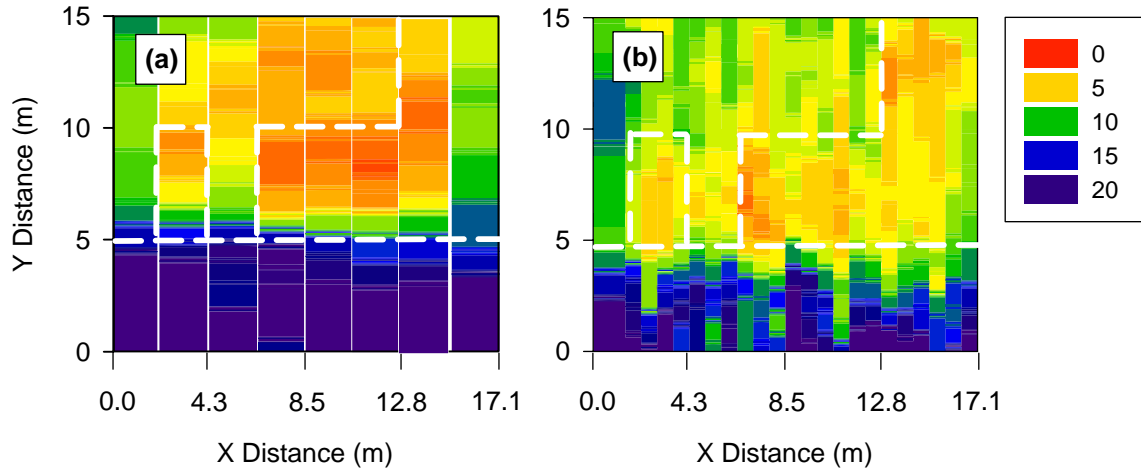


**Figure 125. CMV output for Spatial 3 at (a) Pass 1 and (b) Pass 4**

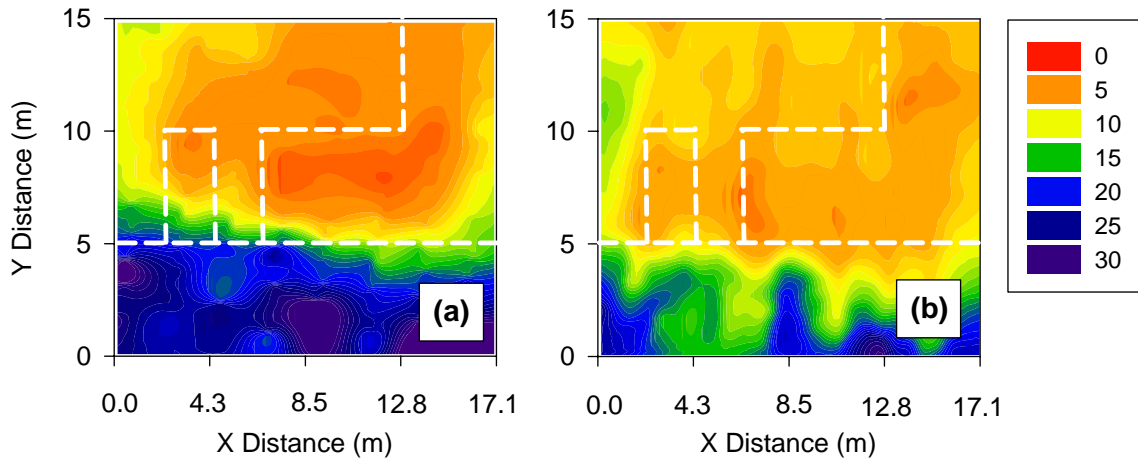


**Figure 126. Kriged CMV at (a) Pass 1 (n = 592) and (b) Pass 4 (n = 1725)**

*Spatial Analysis of In Situ Measurements*

Spatial analysis of 144 in situ measurements for Spatial 2 was performed as it was for Spatial 1. First, the spatial structure of the measurements was investigated by modeling the semivariograms. Variogram parameters are listed in Table 13. The experimental and model variograms are provided in Figure 127. Moisture content, DCP index, modulus, and CIV (20 kg) showed the strongest spatial correlation. Cross-validation results for the model variograms are provided in Figure 128.

**Table 13. Summary of variogram parameters for in situ measurements**

Soil Property	Model	Model Parameters			Cross Validation			
		Scale	Length (m)	Nugget	Mean <sup>a</sup>	S.E.M. <sup>b</sup>	Slope <sup>c</sup>	R <sup>2</sup> <sup>c</sup>
Moisture	Linear	0.49	---	0.47	-0.001	0.079	0.85	0.82
Density	Linear	0.52	---	0.38	0.013	0.055	0.41	0.50
DCP	Linear	31.93	---	79.30	-0.108	0.764	0.71	0.71
Modulus	Linear	64.14	---	201.0	0.047	1.239	0.80	0.75
CIV (20)	Linear	1.36	---	1.61	0.008	0.146	0.79	0.75
CIV (4.5)	Linear	3.02	---	10.59	0.023	0.821	0.11	0.06

<sup>a</sup> Mean of residuals (estimated observation – measured observation)

<sup>b</sup> Standard error of the mean

<sup>c</sup> For plots of estimated versus measured in situ measurements

<sup>d</sup> Models assume isotropy

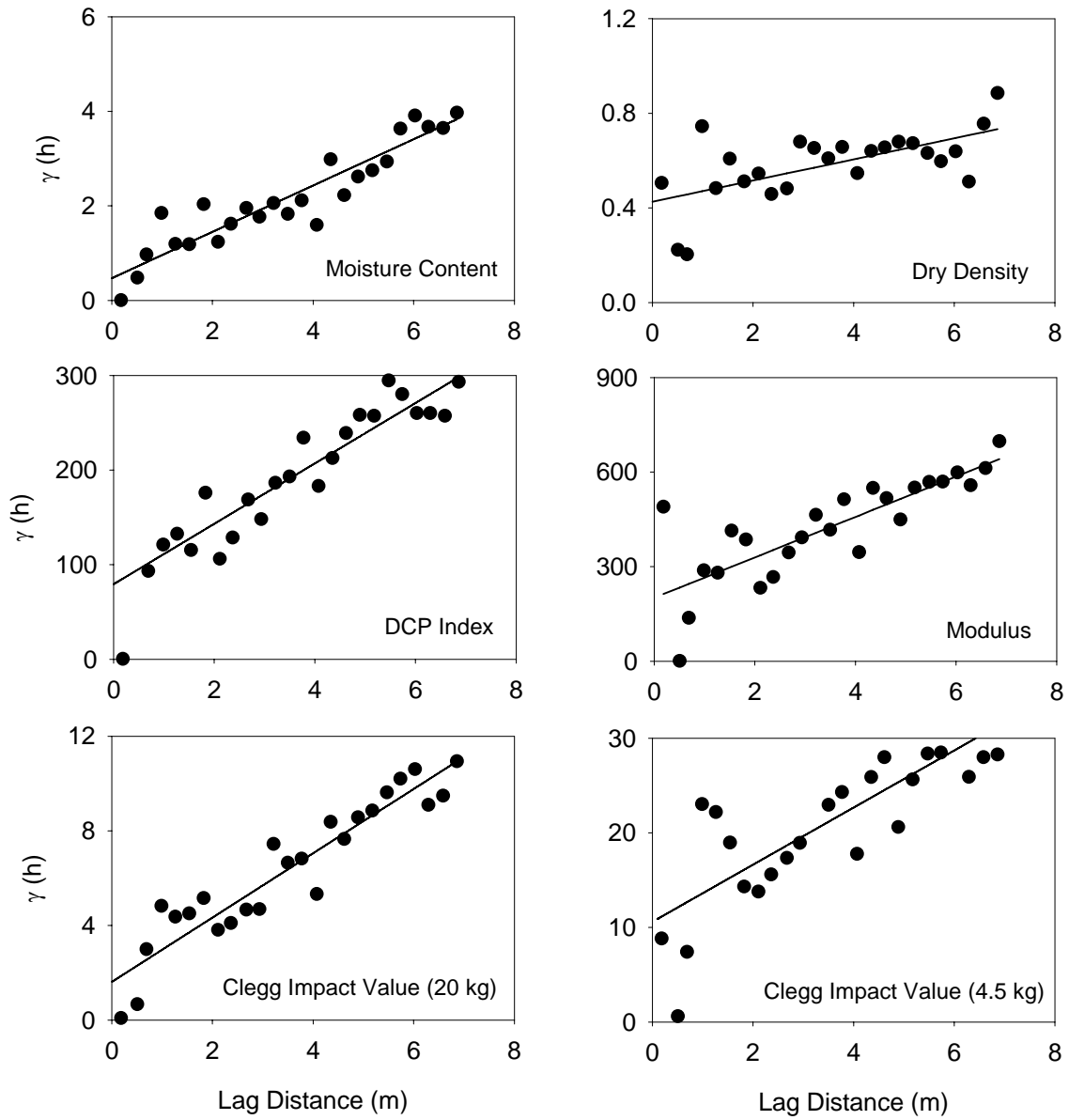


**Figure 127. Experimental (points) and model (lines) variograms for in situ measurements of Spatial 2**

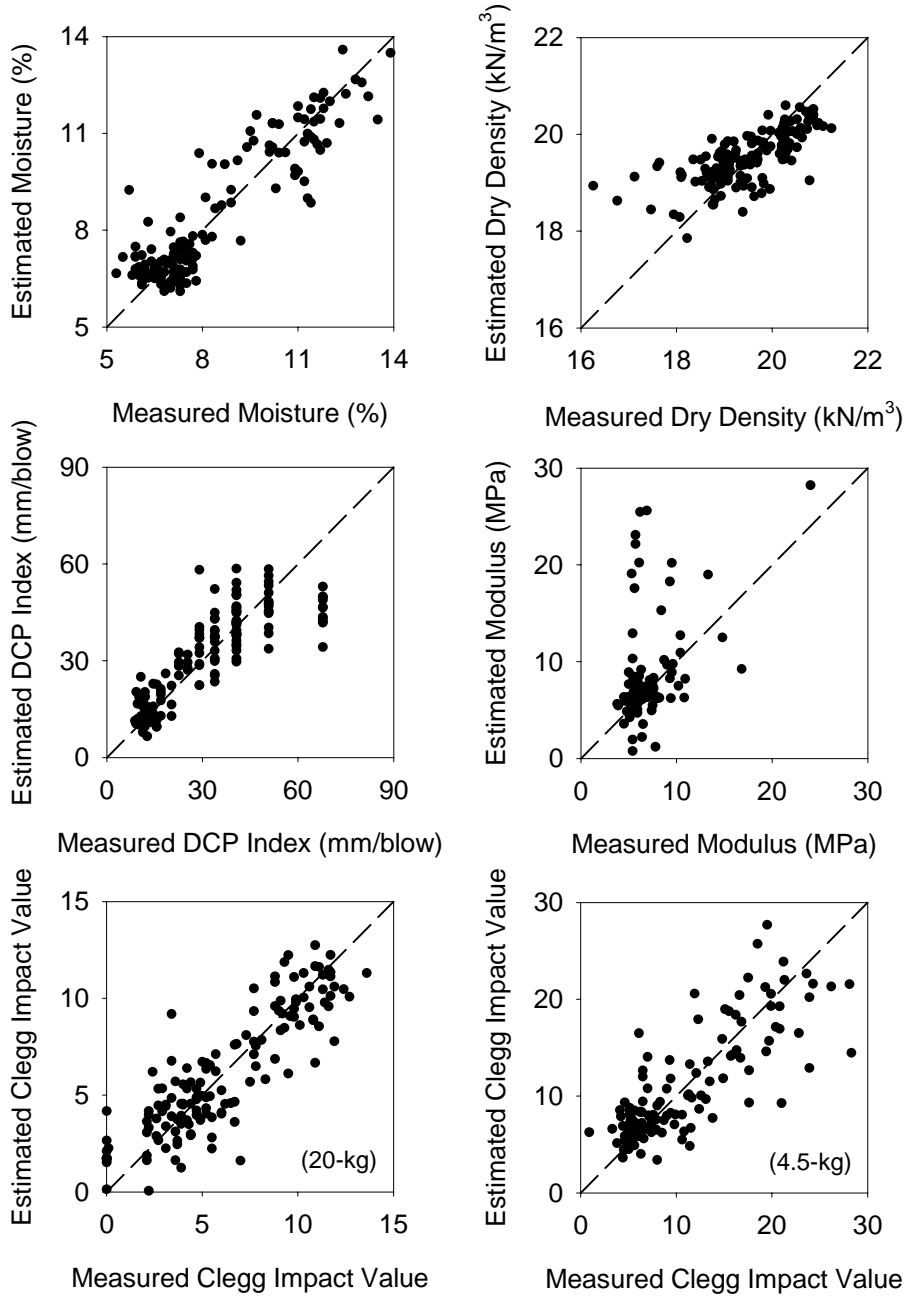


**Figure 128. In situ measurement cross-validation results (estimated versus measured observations)**

The spatial distribution of moisture content for Spatial 2 is shown in Figure 129 for Pass 1. The bottom third of the test area (Y from 0 to 5 m), which is comprised of subgrade material, shows moisture content ranging from 11% to 13%. Moisture content ranging from 5% to 7% is observed for the subbase material. Within the separate, nominal regions, some spatial variability of moisture content is observed. Higher moisture content is generally observed at the north (increasing X) side of the test area.

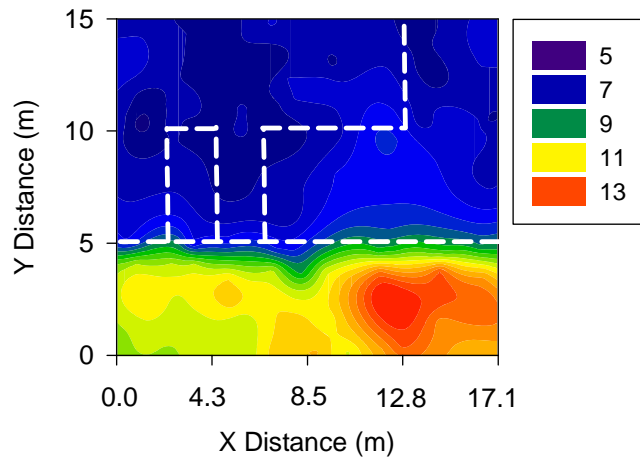


**Figure 129. Moisture content for Spatial 2 at Pass 1**

Kriged in situ measurements (Figure 130) show dry density ranging from about 18 to 22 kN/m<sup>3</sup> over the test area. The lowest density is observed in the subgrade material, despite higher stiffness than subbase material. Also, the top third of the test area (Y from 10 to 15 m) shows higher density than the middle third. Prior to testing, this soil was compacted with two roller passes (see Figure 73).

Modulus of the test area reflects the variation in deformation characteristics between the subgrade and subbase materials. Within the subbase material, modulus indicates variable deformation characteristics resulting from differential lift thickness (from excavations for Spatial 1).

Soil strength measurement using DCP index and CIV show that the existing subgrade material was stiffer than the subbase material. The spatial variation of soil strength for a given soil does not appear to be supported by the spatial distribution of moisture content or differential lift thickness.

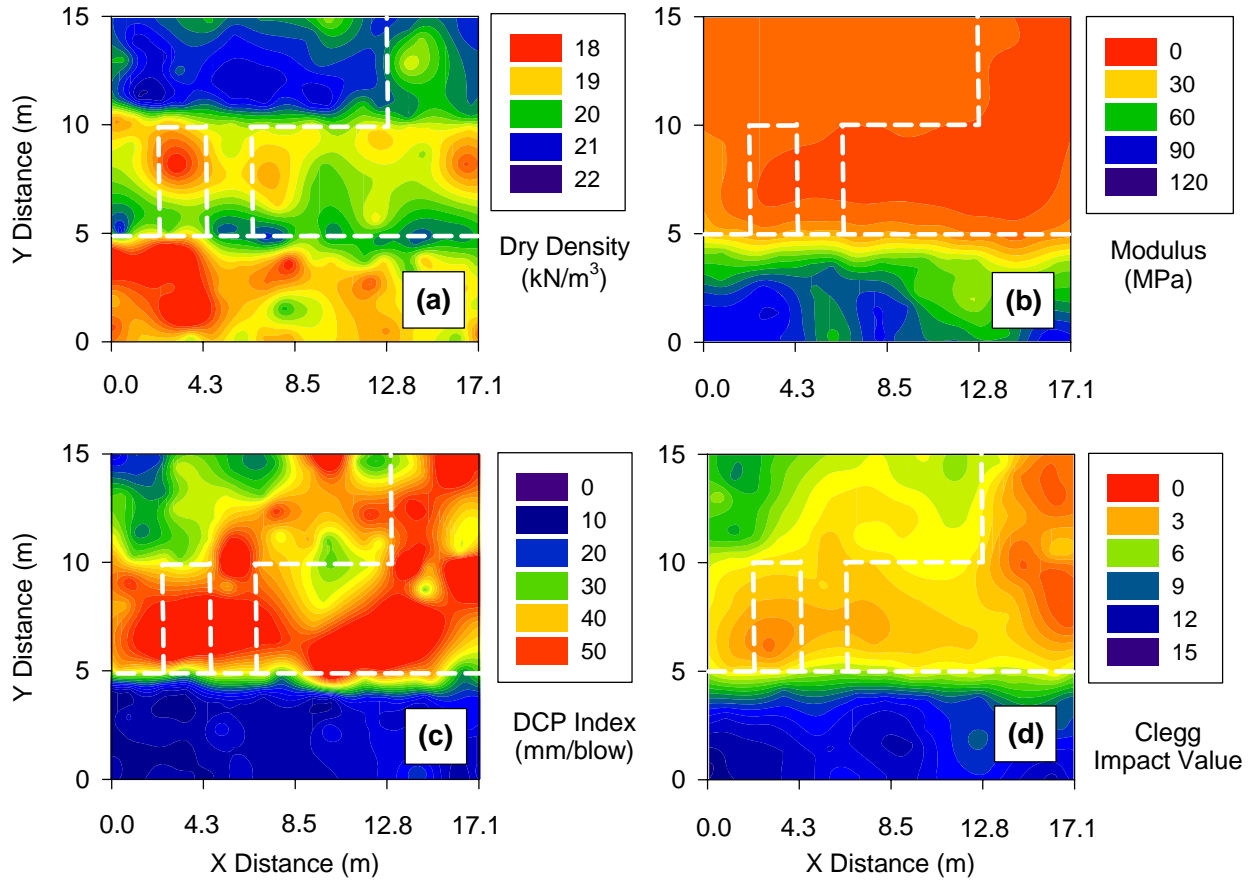


**Figure 130. Field measurement results: (a) dry density, (b)  $E_{PFWD}$ , (c) surface DCP index, and (d) 20-kg Clegg impact value**

## **Application of Findings to Technology Verification and Specification Development**

### *Evaluation of Pass/Fail Maps*

To evaluate the calibration procedure described above, the fraction of the test area that fails based on the results of traditional testing techniques (e.g., density, modulus) can be compared to the fraction of the test area that fails based on compaction monitoring results. Ideally, compaction monitoring results would indicate the same failing regions as field measurements. By using the regression analysis results from strip testing, however, the same pass/fail regions could not be created for density, modulus, CIV, or DCP index. The inability to quantifiably link soil properties with roller measurements for the spatial area, despite achieving very high correlation for test strip results, is attributed to the following: (1) the different factors, many of which have already been identified, affecting compaction monitoring and in situ compaction control measurements and (2) the relatively high variation observed for the compaction monitoring measurements.

The limited measurement influence depths of in situ quality control tests (e.g., nuclear moisture-density, PFWD) resulted in the inability of these devices to differentiate between regions of variable lift thickness. Rather, variation in soil modulus and surface strength measurements resulted only from variable moisture content. Alternatively, the measurement influence depth for the roller was much longer, particularly since the roller was operated at the “high” amplitude setting (measurement influence depth is proportional to vibration amplitude). For this reason, CMV accurately identified regions of 510 mm lift thickness. Because DCP index additionally captured the variable stiffness of the spatial area, the compaction monitoring technologies are anticipated to be correlated with this soil strength measurement. These correlations are an area of ongoing study, with focus on characterizing both measurement influence depth and the effect of underlying layers on machine response. Because the depth of influence of PLTs depend on plate size, future testing may also incorporate plate testing with 762 mm diameter plates.

### *Machine Calibration Design Considerations*

The empirical relationships between soil properties and compaction monitoring output are influenced by roller size, vibration amplitude and frequency, operating velocity, soil type, and stratigraphy underlying the compaction layer. Machine calibration procedures must therefore be conducted under the same conditions (e.g., moisture content, lift thickness, subgrade stiffness) as may be expected during earthwork production. Considering the variation of construction operations and environmental conditions on a project site, however, calibration with in situ tests for every condition is likely not feasible. The implications of this reality are that current calibration procedures, including the protocols followed in Europe, may need revision prior to implementation in the United States. For example, regression models that relate compaction monitoring results and moisture content to in situ soil properties are particularly sensitive to moisture content. Moisture content must therefore remain as a key calibration parameter. Additionally, the influence of the stiffness of underlying layers (and how it varies) must be addressed. Instead of 30 m or 60 m control strips, 300 m strips or calibration *areas* may be used in an attempt to incorporate more variation into the calibration operation; this measure would likely reduce correlation precision, but increase the robustness and statistical validity of the calibration.

For now, as compaction monitoring technologies continue to be implemented, the technologies must simply be used with special consideration for what the results may actually be measuring and indicating about the soil.

### **Project Observations**

The ability of two compaction monitoring technologies (CMV and MDP) to identify soil properties over spatial test areas was investigated with particular emphasis on demonstrating how the technology may be implemented as a QC/QA tool. Testing was first conducted on test strips with variable moisture to collect data for performing regression analyses and developing calibration (i.e., correlation) equations for the machine data. The use of moisture content as a regression parameter yielded correlation coefficients ranging from 0.85 to 0.95 for predicting soil strength and modulus from either MDP or CMV. MDP predicted soil density ( $R^2$  of 0.92) better than CMV ( $R^2$  of 0.62). A two-dimensional test area with variable lift thickness and moisture content was then constructed and tested using both compaction monitoring technology and in situ measurement devices. Classical statistical parameters were calculated from the compaction data; the spatial distribution of the data was subsequently investigated. MDP, shown to be locally variable, provided some indication of differential lift thickness and variable moisture content. CMV identified the regions of thick compaction layer. At the same time, in situ tests for soil engineering properties showed that moisture content significantly influenced soil stability.

Levels of compaction monitoring technology use were described, with the field study serving as an example. The first and second of these levels, measuring machine behavior to indicate soil condition and applying some criteria for evaluating the results, were successfully demonstrated with the experimental results from this study. Several challenges in generating a precise and reliable map of a soil engineering property based on compaction monitoring data and a calibration equation was noted, however, with the intention of identifying barriers to technology implementation. As the promise of compaction monitoring technologies continues to be documented, additional study should be conducted with the technologies to better guide specification development and technology implementation and use.

## PROJECT SUMMARY

Compaction monitoring technology applied to Caterpillar 825G impact and CS-533 vibratory smooth drum rollers was investigated with experimental testing and statistical analysis methods. To evaluate MDP and CMV technology, three projects were performed at the Caterpillar Edwards Facility near Peoria, Illinois.

The first project investigated MDP applied to a Caterpillar 825G roller. The following observations were made from Project 1 testing and analysis:

- Validation of MDP technology for alternative roller configurations has broad implications for earthwork construction practice.
- Variation of MDP measurements observed for a test strip was attributed to variable subgrade conditions, as in situ measurements did not show the same trends.
- The mean MDP measurement decreased with increasing roller passes, which is consistent with the decreasing rolling resistance during the soil compaction process. The standard deviation of MDP increased with roller passes, as the soil condition deviated from a uniform initial condition.
- Similar compaction was achieved by both the left- and right-side wheels of the impact roller, evidenced by similar density and strength measurements at the various stages of compaction. MDP is derived from machine-ground interaction from all wheels.
- A moderately strong ( $R^2 = 0.87$ ) correlation was observed between MDP and dry unit weight. The relationship, however, was strongly influenced by a single data point. A strong relationship ( $R^2 = 0.96$ ) was observed between MDP and DCP index.

The second project evaluated both MDP and CMV applied to a vibratory smooth drum roller for five different cohesionless base materials. The following conclusions were drawn from the data and analysis from this study:

- Testing a single test point does not provide a high level of confidence for representing the average material characteristics, particularly when dealing with variable intelligent compaction data and variable soil conditions. In the case of comparing intelligent compaction results to field measurements, soil property variation and measurement influence area must be considered. To perform statistical analyses, data were averaged over the test strip area at each stage of compaction.
- The effect of soil compaction on roller machine-ground interaction is to decrease machine power (rolling resistance) and increase CMV (soil stiffness response). The change in intelligent compaction data with each roller pass can be described in terms of physical soil properties through linear relationships observed with dry unit weight, soil strength, and soil modulus. Correlation coefficients (i.e.,  $R^2$  values) for the regressions generally exceed 0.90.
- The local variation in MDP is greater than that of CMV for four of the five soil types tested during this field study. Coefficients of variation and standard deviations for CMV and MDP, respectively, vary between test strips (soil types), despite being within a relatively narrow range for an individual test strip.

- Logarithmic relationships are generally observed between MDP and CMV compaction results, with different measurement influence depths acting for the two systems.
- For predicting physical soil properties independent of soil type, both intelligent compaction results (CMV or MDP) and nominal moisture content are statistically significant. The limited dataset, however, did not provide a consistent model to improve the prediction of soil properties using soil indices as regression parameters to represent soil type.

The final project was performed to identify the spatial distribution of soil characteristics and compaction monitoring data. The following conclusions were drawn from the data and analysis from this study:

- In terms of predicting soil strength and modulus from either MDP or CMV, testing conducted on several test strips with different nominal moisture contents produced correlations with correlation coefficients ranging from 0.85 to 0.95.
- MDP was shown to be locally variable and affected primarily by surficial soil characteristics. MDP provided some indication of differential lift thickness from compaction monitoring on a two-dimensional test area.
- CMV accurately identified the regions of thick lift on a two-dimensional test area with variable lift thickness and moisture content.
- Several challenges in generating a precise and reliable map of a soil engineering property based on compaction monitoring data and a calibration equation were identified, including (1) measurement influence depth, (2) variable compaction monitoring measurements, and (3) influences of underlying soil layers on machine response.

## **RECOMMENDATIONS FOR FUTURE RESEARCH**

For this research study, MDP technology was evaluated on a Caterpillar 825G roller to indicate compaction of Edwards till material. The ability of the roller to identify the state of the soil was verified with in situ testing. The feasibility of using this compaction monitoring technology for alternative roller configurations should continue to be studied, because such an effort would have broad implications for earthwork construction. Specifically, the mechanical performance of various machines should be investigated to identify machine internal loss coefficients for correcting gross power output for net power. Then, more calibration strip testing may be performed to identify the relationships between MDP and soil engineering properties for the various machines. The regression coefficients of these relationships can be compared to show how different rollers overcome rolling resistance during soil compaction operations.

Developing tools for managing and analyzing compaction monitoring data is an ongoing effort. These tools will be particularly important and necessary for inspectors of earthwork construction. Geostatistics have recently been used to analyze and view compaction monitoring data. Further investigation should be conducted to evaluate whether this approach to interpreting near-continuous data is appropriate and valid. Other methods for representing spatial data should be investigated. Roller manufacturers may participate in this effort. Such tools may include software for handheld computers, such that inspectors may see what roller operators see on the onboard compaction monitor. The software may also include features for performing statistical analyses using raw data without the need for an engineer to post-process data.



## REFERENCES

- Adam, D. 1997. Continuous compaction control (CCC) with vibratory rollers. In *GeoEnvironment 97: Proceedings of 1<sup>st</sup> Australia-New Zealand Conference on Environmental Geotechnics*. Rotterdam, Netherlands: A.A. Balkema, 245–250.
- ISSMGE. 2005. Roller-Integrated continuous compaction control (CCC): Technical Contractual Provisions, Recommendations. *TC3: Geotechnics for Pavements in Transportation Infrastructure*. International Society for Soil Mechanics and Geotechnical Engineering. <http://egweb.mines.edu/IntelligentCompaction/files/ISSMGE1.pdf>
- Journel, A.G. and C.J. Huijbregts. 1978. *Mining Geostatistics*. London: Academic Press.
- Sandstrom, A. and C. Pettersson. Intelligent systems for QC/QA in soil compaction. In *Proceedings of the Annual Transportation Research Board Meeting*. Washington, DC: Transportation Research Board, 2004. CD-ROM.
- Turner, H. and A. Sandstrom. 1980. A new device for instant compaction control. In *Proceedings of the International Conference on Compaction*. Volume 2. Paris, 611–614.
- White, D., E. Jaselskis, V. Schaefer, T. Cackler, I. Drew, and L. Li. 2004. *Field Evaluation of Compaction Monitoring Technology: Phase I*. Final report. Iowa DOT Project TR-495. Ames, IA: Center for Transportation Research and Education.
- White, D., M. Thompson, K. Jovaag, M. Morris. 2006. *Field Evaluation of Compaction Monitoring Technology: Phase II*. Final report. Iowa DOT Project TR-495. Ames, IA: Center for Transportation Research and Education.



## APPENDIX A. PROJECT 1 IN SITU TEST DATA

**Table 14. In situ measurement summary of Edwards till, 0 roller passes**

Test Point	Coordinates			Nuclear Gauge (kN/m <sup>3</sup> , %)						DCP
	Lat (40° 45')	Long (89° 46')	Elevation (ft)	$\gamma_d^1$	$w_g^1$	$\gamma_d^2$	$w_g^2$	$\gamma_d$	$w_g$	DCPI
1A	---	---	---	---	---	---	---	---	---	182
3A	---	---	---	11.18	10.2	11.37	11.3	11.28	10.8	---
3B	---	---	---	11.42	11.0	10.63	11.7	11.03	11.4	164
5A	---	---	---	10.16	10.1	9.94	11.3	10.05	10.7	248
5B	---	---	---	10.30	10.4	10.27	14.5	10.29	12.5	---
7A	---	---	---	10.19	10.5	10.49	10.9	10.34	10.7	---
7B	---	---	---	10.57	9.4	10.74	8.7	10.66	9.1	216
9A	---	---	---	10.12	12.2	10.59	11.9	10.35	12.1	186
9B	---	---	---	10.51	10.0	9.93	11.0	10.22	10.5	---
11A	---	---	---	9.99	12.5	10.70	9.1	10.34	10.8	---
11B	---	---	---	9.68	12.3	9.58	12.1	9.63	12.2	300
13A	---	---	---	10.19	11.7	10.21	11.8	10.20	11.8	206
13B	---	---	---	10.62	10.5	9.80	12.9	10.21	11.7	---
15A	---	---	---	11.01	8.4	9.65	13.2	10.33	10.8	---
15B	---	---	---	10.70	11.2	10.48	10.8	10.59	11.0	308
17A	---	---	---	10.51	11.7	9.68	14.3	10.09	13.0	226
17B	---	---	---	10.84	9.2	10.85	9.2	10.85	9.2	---
19A	---	---	---	10.54	10.5	10.34	11.3	10.44	10.9	---
19B	---	---	---	11.78	9.2	11.37	10.0	11.58	9.6	261

**Table 15. In situ measurement summary of Edwards till, 1 roller pass**

Test Point	Coordinates			Nuclear Gauge (kN/m <sup>3</sup> , %)						DCP
	Lat (40° 45')	Long (89° 46')	Elevation (ft)	$\gamma_d^1$	$w_g^1$	$\gamma_d^2$	$w_g^2$	$\gamma_d$	$w_g$	DCPI
1A	51.27442	16.00766	519.342	---	---	---	---	---	---	121
3A	51.28118	16.11985	519.612	12.43	12.8	12.60	13.1	12.51	13.0	---
3B	---	---	---	---	---	---	---	---	---	131
5A	51.29144	16.25671	519.612	12.49	13.0	12.24	12.5	12.36	12.8	129
7A	---	---	---	11.69	11.0	11.73	11.7	11.71	11.4	---
7B	51.29127	16.38370	519.476	---	---	---	---	---	---	141
9A	---	---	---	12.33	13.3	13.02	15.3	12.68	14.3	164
11A	51.29775	16.50648	519.187	12.10	12.7	13.02	12.4	12.56	12.6	---
11B	---	---	---	---	---	---	---	---	---	148
13A	51.31318	16.64018	519.126	11.80	12.0	11.78	14.2	11.79	13.1	151
13B	---	---	---	11.67	13.1	12.03	13.9	11.85	13.5	---
15A	51.30737	16.78256	519.085	13.35	10.7	12.21	13.2	12.78	12.0	---
15B	---	---	---	11.95	13.5	12.65	12.9	12.30	13.2	122
17A	51.31282	16.90345	519.050	11.37	13.9	12.49	13.1	11.93	13.5	107
17B	---	---	---	11.89	13.8	11.97	13.5	11.93	13.7	---
19A	51.32092	17.04433	518.816	13.45	12.2	12.50	13.3	12.98	12.8	---
19B	---	---	---	12.87	13.1	12.49	14.0	12.68	13.6	88

**Table 16. In situ measurement summary of Edwards till, 2 roller passes**

Test Point	Coordinates			Nuclear Gauge (kN/m <sup>3</sup> , %)						DCP
	Lat (40° 45')	Long (89° 46')	Elevation (ft)	$\gamma_d^1$	$w_g^1$	$\gamma_d^2$	$w_g^2$	$\gamma_d$	$w_g$	DCPI
2B	---	---	---	---	---	---	---	---	---	115
4A	---	---	---	---	---	---	---	---	---	109
6B	---	---	---	---	---	---	---	---	---	125
8A	---	---	---	---	---	---	---	---	---	129
10B	---	---	---	---	---	---	---	---	---	134
12A	---	---	---	---	---	---	---	---	---	115
14B	---	---	---	---	---	---	---	---	---	114
16A	---	---	---	---	---	---	---	---	---	107
18B	---	---	---	---	---	---	---	---	---	108
20B	---	---	---	---	---	---	---	---	---	85

**Table 17. In situ measurement summary of Edwards till, 4 roller passes**

Test Point	Coordinates			Nuclear Gauge (kN/m <sup>3</sup> , %)						DCP
	Lat (40° 45')	Long (89° 46')	Elevation (ft)	$\gamma_d^1$	$w_g^1$	$\gamma_d^2$	$w_g^2$	$\gamma_d$	$w_g$	DCPI
1B	51.36208	15.99646	519.151	---	---	---	---	---	---	29
3A	---	---	---	17.01	11.2	16.87	10.6	16.94	10.9	102
5B	51.37307	16.24282	519.665	17.23	12.0	17.33	12.5	17.28	12.3	97
7A	---	---	---	17.53	10.3	18.69	10.6	18.11	10.5	121
9B	51.38524	16.50833	519.055	18.03	11.0	17.47	12.9	17.75	12.0	96
11A	---	---	---	17.59	11.3	15.88	12.5	16.74	11.9	121
13B	51.39469	16.77227	518.964	17.17	12.9	17.09	12.8	17.13	12.9	113
15A	---	---	---	16.81	12.2	16.82	11.8	16.82	12.0	80
17B	51.40035	17.02881	518.817	17.61	12.3	17.34	12.0	17.48	12.2	77
19A	---	---	---	17.00	12.7	17.58	12.8	17.29	12.8	63

**Table 18. In situ measurement summary of Edwards till, 8 roller passes**

Test Point	Coordinates			Nuclear Gauge (kN/m <sup>3</sup> , %)						DCP
	Lat (40° 45')	Long (89° 46')	Elevation (ft)	$\gamma_d^1$	$w_g^1$	$\gamma_d^2$	$w_g^2$	$\gamma_d$	$w_g$	DCPI
3B	---	---	---	18.10	11.4	18.18	11.0	18.14	11.2	11
5A	---	---	---	18.03	11.3	17.91	12.3	17.97	11.8	12
7B	---	---	---	18.27	11.9	18.25	12.7	18.26	12.3	17
9A	---	---	---	18.24	12.3	18.32	11.8	18.28	12.1	17
11B	---	---	---	16.78	11.9	15.94	12.3	16.36	12.1	15
13A	---	---	---	18.24	10.4	25.18	12.6	21.71	11.5	15
15B	---	---	---	18.16	10.8	18.11	11.0	18.14	10.9	14
17A	---	---	---	17.81	11.3	17.91	12.5	17.86	11.9	17
19B	---	---	---	17.83	10.9	18.13	10.7	17.98	10.8	13

**Table 19. In situ measurement summary of Edwards till, 12 roller passes**

Test Point	Coordinates			Nuclear Gauge (kN/m <sup>3</sup> , %)						DCP
	Lat (40° 45')	Long (89° 46')	Elevation (ft)	$\gamma_d^1$	$w_g^1$	$\gamma_d^2$	$w_g^2$	$\gamma_d$	$w_g$	DCPI
2B	---	---	---	18.03	10.5	17.70	11.2	17.87	10.9	13
4A	---	---	---	19.60	10.9	19.29	12.1	19.45	11.5	14
6B	---	---	---	18.54	12.9	18.27	12.1	18.40	12.5	13
8A	---	---	---	17.92	11.9	18.21	12.4	18.07	12.2	15
10B	---	---	---	18.22	12.5	18.60	12.1	18.41	12.3	16
12A	---	---	---	19.04	10.8	18.83	12.1	18.94	11.5	12
14B	---	---	---	17.94	14.2	18.08	14.7	18.01	14.5	14
16A	---	---	---	18.38	12.4	19.07	11.8	18.72	12.1	15
18B	---	---	---	18.79	12.1	19.05	10.9	18.92	11.5	13



## APPENDIX B. PROJECT 1 DCP PROFILES

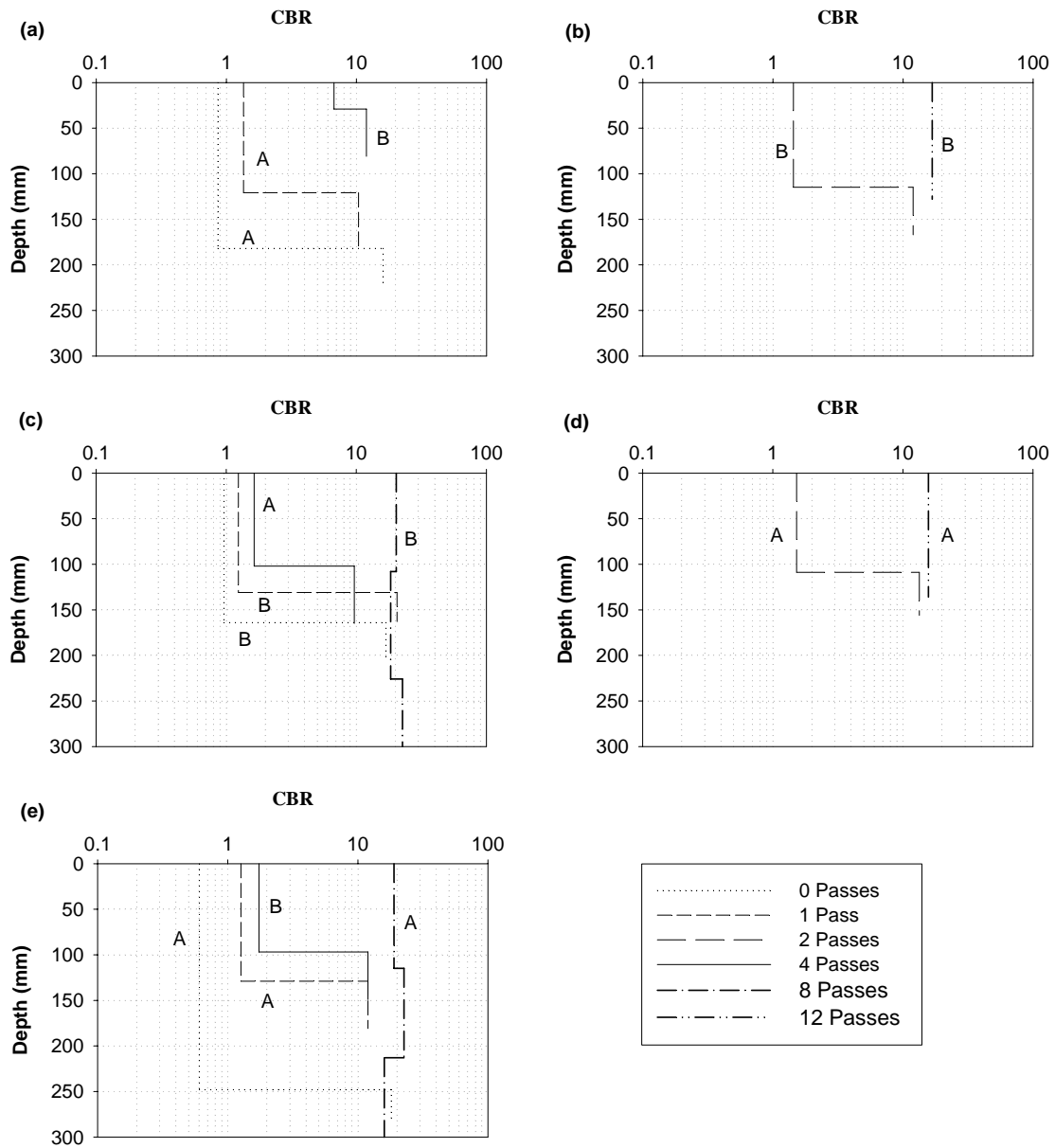
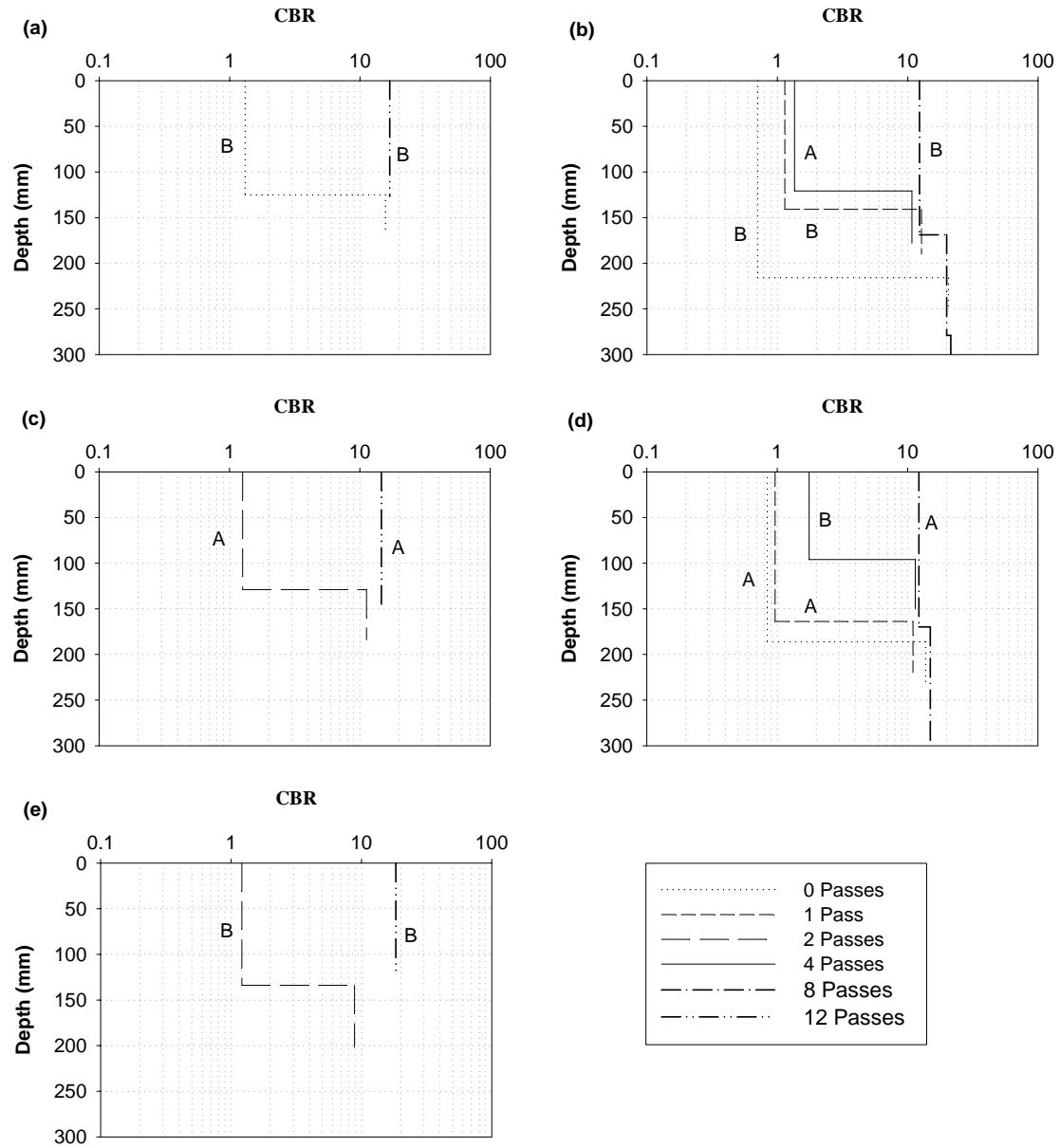


Figure 131. Edwards till: (a) Pt 1, (b) Pt 2, (c) Pt 3, (d) Pt 4, (e) Pt 5



**Figure 132. Edwards till: (a) Pt 6, (b) Pt 7, (c) Pt 8, (d) Pt 9, (e) Pt 10**

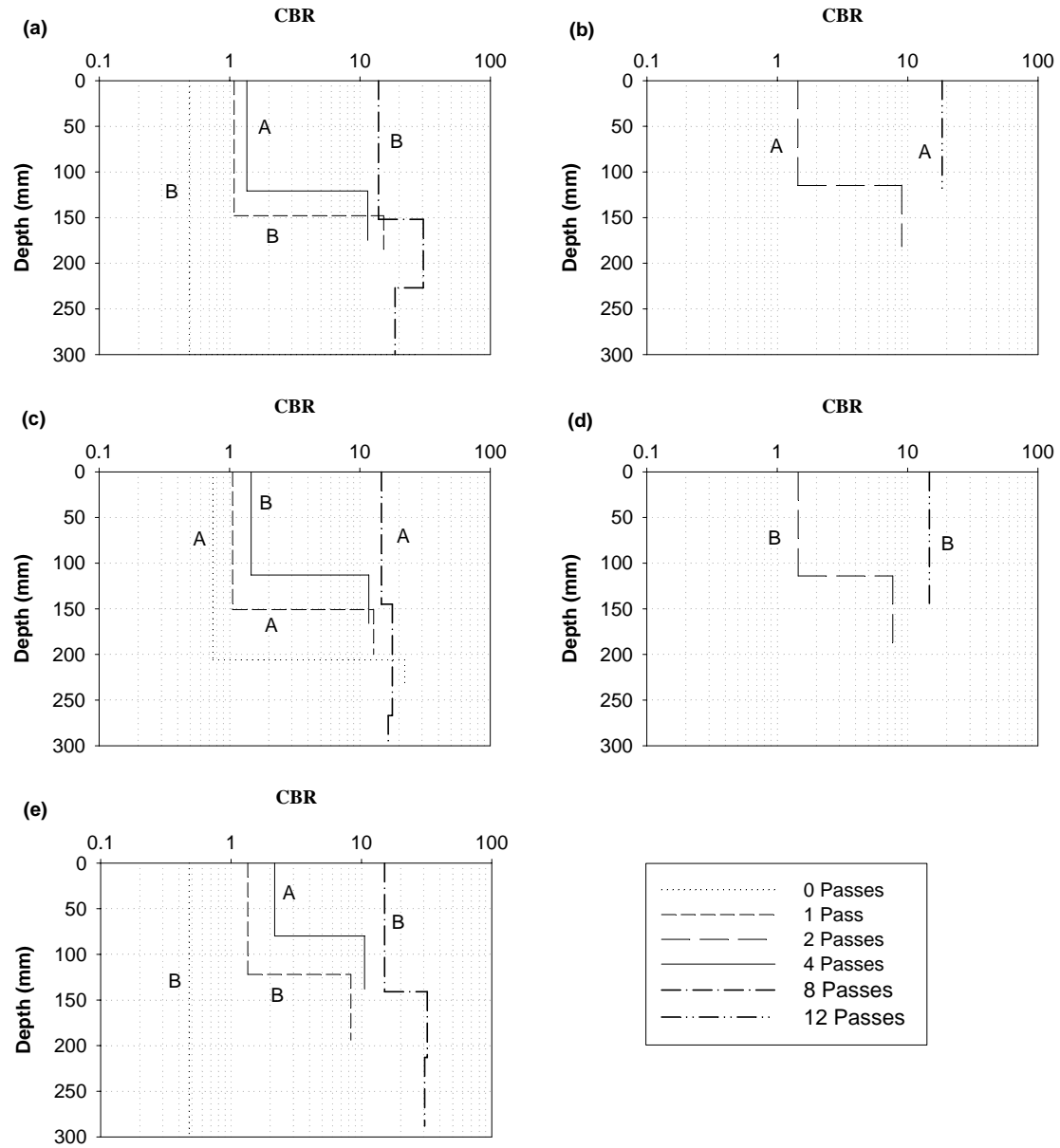
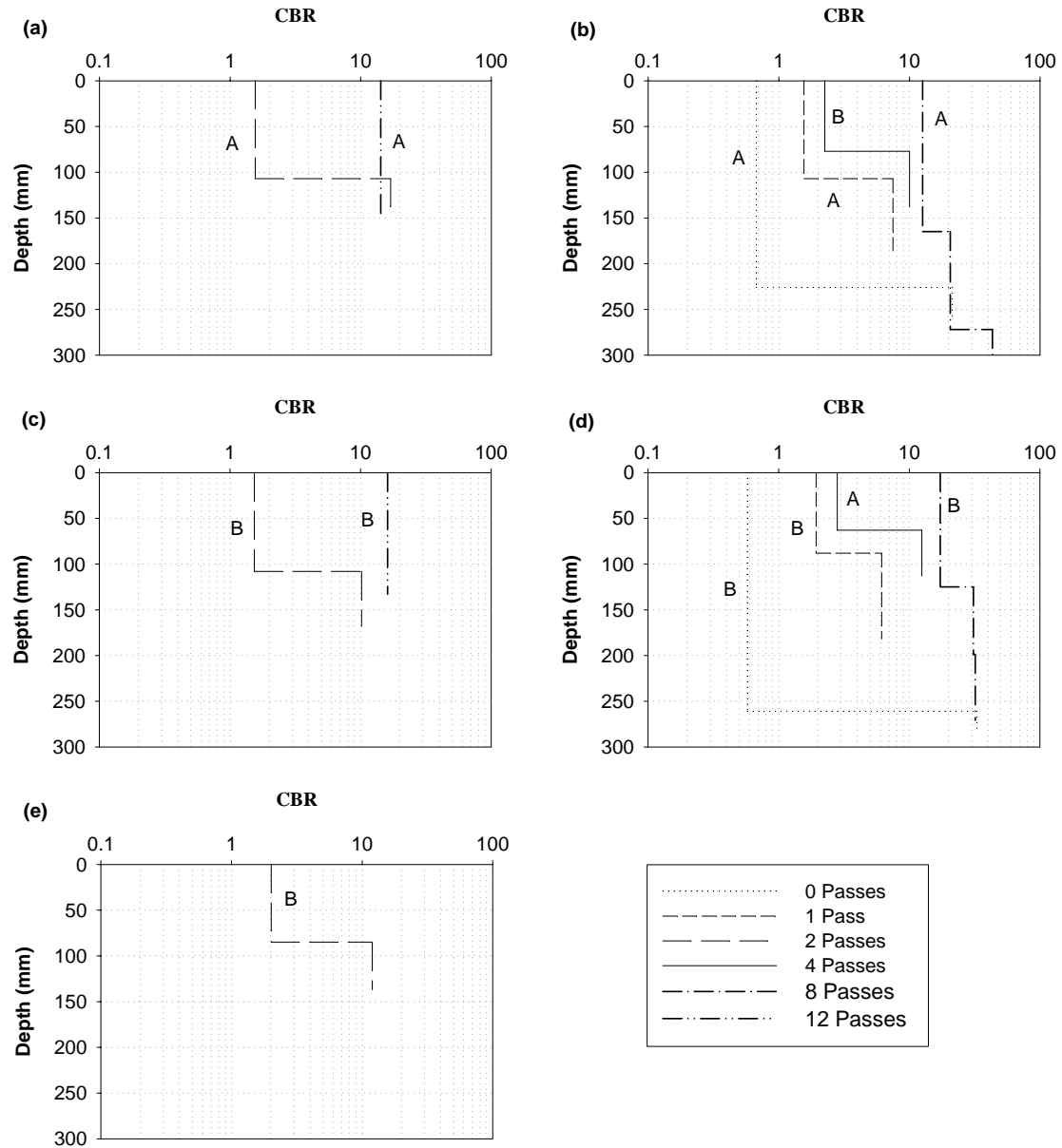


Figure 133. Edwards till: (a) Pt 11, (b) Pt 12, (c) Pt 13, (d) Pt 14, (e) Pt 15



**Figure 134. Edwards till: (a) Pt 16, (b) Pt 17, (c) Pt 18, (d) Pt 19, (e) Pt 20**

## APPENDIX C. PROJECT 2 IN SITU TEST DATA

**Table 20. Moisture and density summary of RAP, Strip 1, 0 roller passes**

Test Point	Coordinates (degrees, ft)			Nuclear Gauge (kN/m <sup>3</sup> , %)				Drive Core (kN/m <sup>3</sup> , %)			
	X	Y	Elevation	$\gamma_d^1$	$w_g^1$	$\gamma_d^2$	$w_g^2$	$\gamma_d$	$w_g$	$\gamma_d$	$w_g$
1	---	---	---	15.83	6.0	15.55	7.0	15.69	6.5	---	---
2	---	---	---	15.19	7.4	15.11	7.3	15.15	7.4	---	---
3	---	---	---	15.85	7.1	15.61	8.2	15.73	7.7	---	---
4	---	---	---	13.60	9.0	13.57	9.8	13.59	9.4	---	---
5	---	---	---	14.78	8.0	14.56	7.8	14.67	7.9	---	---
6	---	---	---	14.50	8.9	14.39	9.7	14.44	9.3	---	---
7	---	---	---	14.86	7.7	14.73	8.6	14.80	8.2	---	---
8	---	---	---	13.92	9.4	13.90	9.4	13.91	9.4	---	---
9	---	---	---	15.11	9.6	15.57	9.1	15.34	9.4	---	---
10	---	---	---	15.52	9.3	15.49	8.1	15.50	8.7	---	---

**Table 21. Stiffness and strength summary of RAP, Strip 1, 0 roller passes**

Test Point	GeoGauge		Clegg Impact Test			DCP	Portable FWD: E (MPa)			
	M (MPa)	S (MN/m)	CIV <sup>1</sup>	CIV <sup>2</sup>	CIV	DCPI	1	2	3	4
1	---	---	6.0	---	6.0	70	129.0	139.0	53.0	---
2	---	---	8.1	---	8.1	71	75.0	85.0	46.0	---
3	---	---	7.5	---	7.5	65	15.0	22.0	22.0	---
4	---	---	8.9	---	8.9	90	28.0	25.0	22.0	---
5	---	---	6.2	---	6.2	60	6.0	13.0	14.0	---
6	---	---	0.8	---	0.8	130	8.0	13.0	13.0	---
7	---	---	3.4	---	3.4	170	10.0	15.0	15.0	---
8	---	---	4.6	---	4.6	137	7.0	11.0	12.0	---
9	---	---	4.6	---	4.6	103	10.0	14.0	14.0	---
10	---	---	6.2	---	6.2	130	10.0	16.0	17.0	---

**Table 22. Moisture and density summary of RAP, Strip 1, 1 roller pass**

Test Point	Coordinates (degrees, ft)			Nuclear Gauge (kN/m <sup>3</sup> , %)				Drive Core (kN/m <sup>3</sup> , %)			
	X	Y	Elevation	$\gamma_d^1$	$w_g^1$	$\gamma_d^2$	$w_g^2$	$\gamma_d$	$w_g$	$\gamma_d$	$w_g$
1	---	---	---	15.58	5.7	15.28	6.6	15.43	6.2	---	---
2	---	---	---	15.76	7.4	16.20	6.4	15.98	6.9	---	---
3	---	---	---	16.73	7.6	16.49	9.0	16.61	8.3	---	---
4	---	---	---	15.85	7.5	16.29	6.8	16.07	7.2	---	---
5	---	---	---	16.27	8.3	16.57	7.2	16.42	7.8	---	---
6	---	---	---	15.79	9.2	15.55	9.2	15.67	9.2	---	---
7	---	---	---	16.15	7.3	16.16	7.8	16.16	7.6	---	---
8	---	---	---	15.88	8.6	15.98	8.2	15.93	8.4	---	---
9	---	---	---	16.38	9.6	16.01	10.1	16.20	9.9	---	---
10	---	---	---	16.51	7.6	16.23	8.8	16.37	8.2	---	---

**Table 23. Stiffness and strength summary of RAP, Strip 1, 1 roller pass**

Test Point	GeoGauge		Clegg Impact Test			DCP	Portable FWD: E (MPa)			
	M (MPa)	S (MN/m)	CIV <sup>1</sup>	CIV <sup>2</sup>	CIV	DCPI	1	2	3	4
1	---	---	13.6	---	13.6	36	11.0	21.0	23.0	---
2	---	---	14.2	---	14.2	44	6.0	17.0	21.0	---
3	---	---	11.0	---	11.0	42	10.0	19.0	23.0	---
4	---	---	7.4	---	7.4	35	34.0	36.0	34.0	---
5	---	---	11.7	---	11.7	31	18.0	26.0	27.0	---
6	---	---	9.6	---	9.6	36	39.0	35.0	30.0	---
7	---	---	9.0	---	9.0	32	21.0	25.0	31.0	---
8	---	---	8.0	---	8.0	61	6.0	20.0	21.0	---
9	---	---	10.6	---	10.6	39	9.0	15.0	17.0	---
10	---	---	8.0	---	8.0	48	8.0	15.0	16.0	---

**Table 24. Moisture and density summary of RAP, Strip 1, 2 roller passes**

Test Point	Coordinates (degrees, ft)			Nuclear Gauge (kN/m <sup>3</sup> , %)				Drive Core (kN/m <sup>3</sup> , %)			
	X	Y	Elevation	$\gamma_d^1$	$w_g^1$	$\gamma_d^2$	$w_g^2$	$\gamma_d$	$w_g$	$\gamma_d$	$w_g$
1	---	---	---	15.87	7.1	15.82	6.3	15.84	6.7	---	---
2	---	---	---	17.69	6.5	17.01	6.8	17.35	6.7	---	---
3	---	---	---	16.84	9.4	16.57	10.0	16.71	9.7	---	---
4	---	---	---	16.78	7.0	16.13	8.3	16.45	7.7	---	---
5	---	---	---	16.56	8.3	16.10	9.0	16.33	8.7	---	---
6	---	---	---	16.60	9.3	16.90	8.4	16.75	8.9	---	---
7	---	---	---	16.46	7.9	16.42	7.7	16.44	7.8	---	---
8	---	---	---	15.76	8.0	15.96	9.0	15.86	8.5	---	---
9	---	---	---	16.48	9.0	16.64	9.0	16.56	9.0	---	---
10	---	---	---	15.76	8.3	15.65	7.5	15.70	7.9	---	---

**Table 25. Stiffness and strength summary of RAP, Strip 1, 2 roller passes**

Test Point	GeoGauge		Clegg Impact Test			DCP	Portable FWD: E (MPa)			
	M (MPa)	S (MN/m)	CIV <sup>1</sup>	CIV <sup>2</sup>	CIV	DCPI	1	2	3	4
1	---	---	19.2	---	19.2	32	37.0	36.0	33.0	---
2	---	---	10.7	---	10.7	25	17.0	27.0	29.0	---
3	---	---	13.3	---	13.3	28	26.0	30.0	30.0	---
4	---	---	14.7	---	14.7	32	14.0	24.0	26.0	---
5	---	---	11.2	---	11.2	34	19.0	28.0	30.0	---
6	---	---	11.9	---	11.9	33	17.0	25.0	37.0	---
7	---	---	10.7	---	10.7	14	50.0	43.0	35.0	---
8	---	---	10.1	---	10.1	28	9.0	17.0	19.0	---
9	---	---	11.1	---	11.1	32	18.0	22.0	25.0	---
10	---	---	11.2	---	11.2	50	20.0	22.0	21.0	---

**Table 26. Moisture and density summary of RAP, Strip 1, 3 roller passes**

Test Point	Coordinates (degrees, ft)			Nuclear Gauge (kN/m <sup>3</sup> , %)				Drive Core (kN/m <sup>3</sup> , %)			
	X	Y	Elevation	$\gamma_d^1$	$w_g^1$	$\gamma_d^2$	$w_g^2$	$\gamma_d$	$w_g$	$\gamma_d$	$w_g$
1	---	---	---	16.21	5.8	16.42	5.7	16.31	5.8	---	---
2	---	---	---	16.53	8.0	16.97	6.6	16.75	7.3	---	---
3	---	---	---	16.92	8.2	17.11	8.5	17.01	8.4	---	---
4	---	---	---	17.41	7.2	16.81	7.0	17.11	7.1	---	---
5	---	---	---	16.68	7.9	17.14	7.2	16.91	7.6	---	---
6	---	---	---	17.22	7.6	17.09	8.0	17.15	7.8	---	---
7	---	---	---	15.94	9.1	16.27	9.5	16.11	9.3	---	---
8	---	---	---	16.32	9.2	16.54	8.5	16.43	8.9	---	---
9	---	---	---	16.53	9.8	17.19	8.6	16.86	9.2	---	---
10	---	---	---	17.52	7.6	17.50	7.7	17.51	7.7	---	---

**Table 27. Stiffness and strength summary of RAP, Strip 1, 3 roller passes**

Test Point	GeoGauge		Clegg Impact Test			DCP	Portable FWD: E (MPa)			
	M (MPa)	S (MN/m)	CIV <sup>1</sup>	CIV <sup>2</sup>	CIV	DCPI	1	2	3	4
1	---	---	14.8	---	14.8	24	12.0	22.0	26.0	---
2	---	---	14.0	---	14.0	21	20.0	29.0	31.0	---
3	---	---	14.9	---	14.9	24	12.0	22.0	26.0	---
4	---	---	17.0	---	17.0	40	16.0	26.0	30.0	---
5	---	---	13.1	---	13.1	40	23.0	33.0	35.0	---
6	---	---	13.8	---	13.8	28	14.0	25.0	29.0	---
7	---	---	14.1	---	14.1	31	12.0	22.0	25.0	---
8	---	---	14.2	---	14.2	30	20.0	25.0	24.0	---
9	---	---	13.9	---	13.9	26	13.0	17.0	18.0	---
10	---	---	12.5	---	12.5	22	7.0	15.0	17.0	---

**Table 28. Moisture and density summary of RAP, Strip 1, 4 roller passes**

Test Point	Coordinates (degrees, ft)			Nuclear Gauge (kN/m <sup>3</sup> , %)				Drive Core (kN/m <sup>3</sup> , %)			
	X	Y	Elevation	$\gamma_d^1$	$w_g^1$	$\gamma_d^2$	$w_g^2$	$\gamma_d$	$w_g$	$\gamma_d$	$w_g$
1	---	---	---	17.04	7.8	16.76	8.1	16.90	8.0	---	---
2	---	---	---	17.72	6.8	17.72	6.8	17.72	6.8	---	---
3	---	---	---	17.58	8.4	17.53	8.3	17.55	8.4	---	---
4	---	---	---	17.78	8.3	17.80	7.9	17.79	8.1	---	---
5	---	---	---	17.20	7.9	17.19	8.2	17.19	8.1	---	---
6	---	---	---	17.48	7.6	17.89	7.3	17.69	7.5	---	---
7	---	---	---	16.92	8.3	17.03	7.7	16.97	8.0	---	---
8	---	---	---	17.44	8.0	16.98	8.9	17.21	8.5	---	---
9	---	---	---	16.45	10.0	16.92	8.9	16.68	9.5	---	---
10	---	---	---	16.62	8.1	16.20	9.1	16.41	8.6	---	---

**Table 29. Stiffness and strength summary of RAP, Strip 1, 4 roller passes**

Test Point	GeoGauge		Clegg Impact Test			DCP	Portable FWD: E (MPa)			
	M (MPa)	S (MN/m)	CIV <sup>1</sup>	CIV <sup>2</sup>	CIV	DCPI	1	2	3	4
1	---	---	11.4	---	11.4	23	32.0	31.0	30.0	---
2	---	---	15.1	---	15.1	23	29.0	28.0	26.0	---
3	---	---	14.5	---	14.5	21	19.0	29.0	32.0	---
4	---	---	16.2	---	16.2	22	14.0	26.0	32.0	---
5	---	---	17.1	---	17.1	22	23.0	36.0	38.0	---
6	---	---	13.1	---	13.1	22	22.0	31.0	32.0	---
7	---	---	16.9	---	16.9	25	22.0	43.0	38.0	---
8	---	---	17.4	---	17.4	29	12.0	20.0	21.0	---
9	---	---	12.6	---	12.6	26	15.0	19.0	20.0	---
10	---	---	14.9	---	14.9	40	16.0	20.0	18.0	---

**Table 30. Moisture and density summary of RAP, Strip 1, 8 roller passes**

Test Point	Coordinates (degrees, ft)			Nuclear Gauge (kN/m <sup>3</sup> , %)				Drive Core (kN/m <sup>3</sup> , %)			
	X	Y	Elevation	$\gamma_d^1$	$w_g^1$	$\gamma_d^2$	$w_g^2$	$\gamma_d$	$w_g$	$\gamma_d$	$w_g$
1	---	---	---	17.25	6.6	17.17	6.9	17.21	6.8	---	---
2	---	---	---	17.61	7.3	17.83	6.3	17.72	6.8	---	---
3	---	---	---	18.30	7.8	18.14	8.5	18.22	8.2	---	---
4	---	---	---	17.39	7.1	17.08	7.6	17.23	7.4	---	---
5	---	---	---	17.34	9.3	17.69	9.3	17.52	9.3	---	---
6	---	---	---	17.55	8.7	17.63	9.2	17.59	9.0	---	---
7	---	---	---	17.00	8.7	17.74	7.4	17.37	8.1	---	---
8	---	---	---	16.59	7.7	16.65	8.5	16.62	8.1	---	---
9	---	---	---	17.36	8.1	17.20	9.6	17.28	8.9	---	---
10	---	---	---	17.19	8.3	17.20	7.8	17.19	8.1	---	---

**Table 31. Stiffness and strength summary of RAP, Strip 1, 8 roller passes**

Test Point	GeoGauge		Clegg Impact Test			DCP	Portable FWD: E (MPa)			
	M (MPa)	S (MN/m)	CIV <sup>1</sup>	CIV <sup>2</sup>	CIV	DCPI	1	2	3	4
1	---	---	17.2	---	17.2	24	18.0	29.0	33.0	---
2	---	---	22.1	---	22.1	18	17.0	30.0	34.0	---
3	---	---	25.6	---	25.6	22	17.0	29.0	33.0	---
4	---	---	21.6	---	21.6	16	17.0	29.0	33.0	---
5	---	---	21.5	---	21.5	18	31.0	45.0	48.0	---
6	---	---	18.5	---	18.5	31	19.0	33.0	36.0	---
7	---	---	17.8	---	17.8	19	20.0	34.0	35.0	---
8	---	---	20.1	---	20.1	22	18.0	25.0	24.0	---
9	---	---	15.4	---	15.4	20	24.0	26.0	24.0	---
10	---	---	19.5	---	19.5	36	20.0	26.0	23.0	---

**Table 32. Moisture and density summary of RAP, Strip 1, 12 roller passes**

Test Point	Coordinates (degrees, ft)			Nuclear Gauge (kN/m <sup>3</sup> , %)				Drive Core (kN/m <sup>3</sup> , %)			
	X	Y	Elevation	$\gamma_d^1$	$w_g^1$	$\gamma_d^2$	$w_g^2$	$\gamma_d$	$w_g$	$\gamma_d$	$w_g$
1	---	---	---	17.00	6.6	17.30	6.1	17.15	6.4	---	---
2	---	---	---	17.55	8.9	17.96	7.9	17.75	8.4	---	---
3	---	---	---	18.52	8.2	18.16	8.4	18.34	8.3	---	---
4	---	---	---	17.23	8.5	18.03	7.4	17.63	8.0	---	---
5	---	---	---	17.85	8.0	17.72	8.1	17.78	8.1	---	---
6	---	---	---	16.82	9.1	17.31	8.0	17.07	8.6	---	---
7	---	---	---	16.43	9.1	16.42	8.2	16.42	8.7	---	---
8	---	---	---	16.87	8.6	16.89	9.3	16.88	9.0	---	---
9	---	---	---	16.53	9.9	16.42	8.6	16.47	9.3	---	---
10	---	---	---	16.24	8.1	16.65	8.3	16.45	8.2	---	---

**Table 33. Stiffness and strength summary of RAP, Strip 1, 12 roller passes**

Test Point	GeoGauge		Clegg Impact Test			DCP	Portable FWD: E (MPa)			
	M (MPa)	S (MN/m)	CIV <sup>1</sup>	CIV <sup>2</sup>	CIV	DCPI	1	2	3	4
1	---	---	22.3	---	22.3	19	35.0	32.0	31.0	---
2	---	---	18.7	---	18.7	15	21.0	33.0	37.0	---
3	---	---	23.4	---	23.4	14	20.0	34.0	38.0	---
4	---	---	23.7	---	23.7	16	84.0	78.0	70.0	---
5	---	---	21.8	---	21.8	14	21.0	41.0	49.0	---
6	---	---	20.9	---	20.9	15	21.0	30.0	33.0	---
7	---	---	19.0	---	19.0	18	31.0	41.0	43.0	---
8	---	---	18.4	---	18.4	15	55.0	43.0	35.0	---
9	---	---	18.5	---	18.5	19	24.0	22.0	21.0	---
10	---	---	14.3	---	14.3	26	8.0	18.0	20.0	---

**Table 34. Moisture and density summary of CA6-C, Strip 2, 0 roller passes**

Test Point	Coordinates (degrees, ft)			Nuclear Gauge (kN/m <sup>3</sup> , %)				Drive Core (kN/m <sup>3</sup> , %)			
	X	Y	Elevation	$\gamma_d^1$	$w_g^1$	$\gamma_d^2$	$w_g^2$	$\gamma_d$	$w_g$	$\gamma_d$	$w_g$
1	-59	11	---	16.67	2.4	16.84	2.9	16.75	2.7	---	---
2	-69	12	---	15.65	3.5	15.17	4.5	15.41	4.0	---	---
3	-79	14	---	15.55	4.0	15.25	4.1	15.40	4.1	---	---
4	-88	16	---	15.98	3.1	16.15	3.3	16.06	3.2	---	---
5	-98	18	---	16.24	3.5	15.77	4.0	16.01	3.8	---	---
6	-108	20	---	15.55	4.5	15.65	4.1	15.60	4.3	---	---
7	-118	21	---	16.20	4.3	16.07	4.7	16.13	4.5	---	---
8	-128	23	---	15.11	5.5	14.89	5.2	15.00	5.4	---	---
9	-138	24	---	15.13	5.3	15.68	4.9	15.40	5.1	---	---
10	-147	26	---	15.76	4.7	15.82	4.9	15.79	4.8	---	---

**Table 35. Stiffness and strength summary of CA6-C, Strip 2, 0 roller passes**

Test Point	GeoGauge		Clegg Impact Test			DCP	Portable FWD: E (MPa)			
	M (MPa)	S (MN/m)	CIV <sup>1</sup>	CIV <sup>2</sup>	CIV	DCPI	1	2	3	4
1	---	---	3.6	---	3.6	79	2.0	4.0	7.0	---
2	---	---	4.3	---	4.3	87	3.0	11.0	11.0	---
3	---	---	4.2	---	4.2	100	3.0	11.0	13.0	---
4	---	---	4.3	---	4.3	75	3.0	7.0	10.0	---
5	---	---	3.2	---	3.2	77	5.0	25.0	18.0	---
6	---	---	4.0	---	4.0	71	2.0	10.0	11.0	---
7	---	---	3.8	---	3.8	69	3.0	17.0	12.0	---
8	---	---	3.5	---	3.5	73	12.0	34.0	26.0	---
9	---	---	4.7	---	4.7	77	21.0	28.0	16.0	---
10	---	---	4.5	---	4.5	67	3.0	12.0	13.0	---

**Table 36. Moisture and density summary of CA6-C, Strip 2, 1 roller pass**

Test Point	Coordinates (degrees, ft)			Nuclear Gauge (kN/m <sup>3</sup> , %)				Drive Core (kN/m <sup>3</sup> , %)			
	X	Y	Elevation	$\gamma_d^1$	$w_g^1$	$\gamma_d^2$	$w_g^2$	$\gamma_d$	$w_g$	$\gamma_d$	$w_g$
1	-59	11	---	17.48	4.4	17.64	4.6	17.56	4.5	---	---
2	-69	12	---	17.09	4.2	17.31	4.3	17.20	4.3	---	---
3	-79	14	---	16.79	3.5	17.01	3.5	16.90	3.5	---	---
4	-88	16	---	17.96	3.0	17.99	3.2	17.97	3.1	---	---
5	-98	18	---	17.58	4.3	18.10	3.7	17.84	4.0	---	---
6	-108	20	---	18.00	4.2	18.32	4.6	18.16	4.4	---	---
7	-118	21	---	18.13	3.7	18.05	4.5	18.09	4.1	---	---
8	-128	23	---	17.48	4.2	17.88	4.0	17.68	4.1	---	---
9	-138	24	---	17.88	5.1	17.61	4.6	17.74	4.9	---	---
10	-147	26	---	17.33	5.2	17.70	5.2	17.52	5.2	---	---

**Table 37. Stiffness and strength summary of CA6-C, Strip 2, 1 roller pass**

Test Point	GeoGauge		Clegg Impact Test			DCP	Portable FWD: E (MPa)			
	M (MPa)	S (MN/m)	CIV <sup>1</sup>	CIV <sup>2</sup>	CIV	DCPI	1	2	3	4
1	---	---	6.5	---	6.5	57	4.0	19.0	20.0	---
2	---	---	7.3	---	7.3	69	4.0	18.0	20.0	---
3	---	---	6.6	---	6.6	59	3.0	14.0	17.0	---
4	---	---	8.3	---	8.3	57	9.0	23.0	23.0	---
5	---	---	7.4	---	7.4	61	5.0	21.0	21.0	---
6	---	---	8.5	---	8.5	48	9.0	19.0	21.0	---
7	---	---	6.8	---	6.8	67	6.0	21.0	23.0	---
8	---	---	7.5	---	7.5	55	7.0	23.0	25.0	---
9	---	---	7.3	---	7.3	50	8.0	25.0		---
10	---	---	6.5	---	6.5	56	20.0	30.0	25.0	---

**Table 38. Moisture and density summary of CA6-C, Strip 2, 2 roller passes**

Test Point	Coordinates (degrees, ft)			Nuclear Gauge (kN/m <sup>3</sup> , %)						Drive Core (kN/m <sup>3</sup> , %)	
	X	Y	Elevation	$\gamma_d^1$	$w_g^1$	$\gamma_d^2$	$w_g^2$	$\gamma_d$	$w_g$	$\gamma_d$	$w_g$
1	-59	11	---	18.19	3.0	18.10	3.3	18.14	3.2	---	---
2	-69	12	---	18.21	4.0	18.27	3.8	18.24	3.9	---	---
3	-79	14	---	18.54	4.1	18.66	4.2	18.60	4.2	---	---
4	-88	16	---	18.38	4.4	18.60	4.0	18.49	4.2	---	---
5	-98	18	---	18.05	3.9	18.27	3.9	18.16	3.9	---	---
6	-108	20	---	18.30	4.0	18.30	4.5	18.30	4.3	---	---
7	-118	21	---	18.18	3.3	18.38	2.8	18.28	3.1	---	---
8	-128	23	---	18.32	4.6	18.13	5.3	18.22	5.0	---	---
9	-138	24	---	17.78	5.4	17.45	4.6	17.62	5.0	---	---
10	-147	26	---	17.96	5.4	18.24	6.3	18.10	5.9	---	---

**Table 39. Stiffness and strength summary of CA6-C, Strip 2, 2 roller passes**

Test Point	GeoGauge		Clegg Impact Test			DCP	Portable FWD: E (MPa)			
	M (MPa)	S (MN/m)	CIV <sup>1</sup>	CIV <sup>2</sup>	CIV	DCPI	1	2	3	4
1	---	---	8.8	---	8.8	55	4.0	22.0	2.0	---
2	---	---	9.2	---	9.2	53	3.0	19.0	22.0	---
3	---	---	8.3	---	8.3	50	4.0	19.0	21.0	---
4	---	---	8.4	---	8.4	49	9.0	25.0	26.0	---
5	---	---	9.5	---	9.5	47	4.0	20.0	22.0	---
6	---	---	10.2	---	10.2	44	4.0	18.0	24.0	---
7	---	---	8.6	---	8.6	45	12.0	28.0	30.0	---
8	---	---	8.1	---	8.1	54	7.0	38.0	34.0	---
9	---	---	9.3	---	9.3	54	7.0	23.0	24.0	---
10	---	---	9.9	---	9.9	45	7.0	21.0	29.0	---

**Table 40. Moisture and density summary of CA6-C, Strip 2, 4 roller passes**

Test Point	Coordinates (degrees, ft)			Nuclear Gauge (kN/m <sup>3</sup> , %)						Drive Core (kN/m <sup>3</sup> , %)	
	X	Y	Elevation	$\gamma_d^1$	$w_g^1$	$\gamma_d^2$	$w_g^2$	$\gamma_d$	$w_g$	$\gamma_d$	$w_g$
1	-59	11	---	19.29	4.4	19.05	5.2	19.17	4.8	---	---
2	-69	12	---	19.20	3.7	18.33	4.1	18.76	3.9	---	---
3	-79	14	---	19.01	4.0	18.47	4.4	18.74	4.2	---	---
4	-88	16	---	18.38	4.0	18.74	3.7	18.56	3.9	---	---
5	-98	18	---	18.68	5.2	18.79	5.2	18.73	5.2	---	---
6	-108	20	---	18.83	5.3	19.23	4.7	19.03	5.0	---	---
7	-118	21	---	18.46	4.7	18.33	4.3	18.39	4.5	---	---
8	-128	23	---	18.57	4.0	18.74	5.0	18.65	4.5	---	---
9	-138	24	---	17.99	5.6	18.72	4.6	18.36	5.1	---	---
10	-147	26	---	18.25	4.5	18.27	4.0	18.26	4.3	---	---

**Table 41. Stiffness and strength summary of CA6-C, Strip 2, 4 roller passes**

Test Point	GeoGauge		Clegg Impact Test			DCP	Portable FWD: E (MPa)			
	M (MPa)	S (MN/m)	CIV <sup>1</sup>	CIV <sup>2</sup>	CIV	DCPI	1	2	3	4
1	76.3	10.3	12.2	---	12.2	28	10.0	37.0	39.0	---
2	80.0	10.8	12.5	---	12.5	26	16.0	34.0	31.0	---
3	74.9	10.1	11.9	---	11.9	30	43.0	51.0	43.0	---
4	74.4	10.0	12.3	---	12.3	26	6.0	27.0	26.0	---
5	75.4	10.2	12.8	---	12.8	34	6.0	25.0	26.0	---
6	78.1	10.5	12.5	---	12.5	25	5.0	25.0	28.0	---
7	70.0	9.5	12.9	---	12.9	28	11.0	30.0	29.0	---
8	79.6	10.7	13.8	---	13.8	30	5.0	25.0	30.0	---
9	77.8	10.5	14.0	---	14.0	31	6.0	23.0	25.0	---
10	76.6	10.3	13.0	---	13.0	26	20.0	28.0	23.0	---

**Table 42. Moisture and density summary of CA6-C, Strip 2, 8 roller passes**

Test Point	Coordinates (degrees, ft)			Nuclear Gauge (kN/m <sup>3</sup> , %)				Drive Core (kN/m <sup>3</sup> , %)			
	X	Y	Elevation	$\gamma_d^1$	$w_g^1$	$\gamma_d^2$	$w_g^2$	$\gamma_d$	$w_g$	$\gamma_d$	$w_g$
1	-59	11	---	19.54	3.0	19.43	3.7	19.49	3.4	---	---
2	-69	12	---	19.76	4.4	19.90	4.7	19.83	4.6	---	---
3	-79	14	---	19.71	3.9	19.78	3.3	19.75	3.6	---	---
4	-88	16	---	19.53	2.9	19.31	3.0	19.42	3.0	---	---
5	-98	18	---	19.16	4.6	19.27	4.4	19.22	4.5	---	---
6	-108	20	---	19.09	5.2	19.02	4.9	19.05	5.1	---	---
7	-118	21	---	19.46	3.9	19.01	5.0	19.24	4.5	---	---
8	-128	23	---	19.45	5.2	19.81	4.7	19.63	5.0	---	---
9	-138	24	---	18.44	4.2	18.60	3.7	18.52	4.0	---	---
10	-147	26	---	18.93	5.0	19.86	5.5	19.39	5.3	---	---

**Table 43. Stiffness and strength summary of CA6-C, Strip 2, 8 roller passes**

Test Point	GeoGauge		Clegg Impact Test			DCP	Portable FWD: E (MPa)			
	M (MPa)	S (MN/m)	CIV <sup>1</sup>	CIV <sup>2</sup>	CIV	DCPI	1	2	3	4
1	68.7	9.3	21.4	---	21.4	21	11.0	33.0	36.0	---
2	79.8	10.8	18.1	---	18.1	21	11.0	33.0	37.0	---
3	68.1	9.2	17.1	---	17.1	22	6.0	26.0	27.0	---
4	69.0	9.3	18.0	---	18.0	21	7.0	27.0	28.0	---
5	73.5	9.9	16.7	---	16.7	21	6.0	25.0	26.0	---
6	74.4	10.0	17.8	---	17.8	21	15.0	35.0	30.0	---
7	74.6	10.1	15.4	---	15.4	23	10.0	36.0	33.0	---
8	70.8	9.5	17.6	---	17.6	23	17.0	33.0	32.0	---
9	67.7	9.1	15.0	---	15.0	21	10.0	24.0	31.0	---
10	66.8	9.0	16.7	---	16.7	24	9.0	25.0	25.0	---

**Table 44. Moisture and density summary of CA6-C, Strip 2, 12 roller passes**

Test Point	Coordinates (degrees, ft)			Nuclear Gauge (kN/m <sup>3</sup> , %)						Drive Core (kN/m <sup>3</sup> , %)	
	X	Y	Elevation	$\gamma_d^1$	$w_g^1$	$\gamma_d^2$	$w_g^2$	$\gamma_d$	$w_g$	$\gamma_d$	$w_g$
1	-59	11	---	20.01	4.4	20.20	4.1	20.11	4.3	---	---
2	-69	12	---	19.65	3.1	20.03	3.3	19.84	3.2	---	---
3	-79	14	---	18.72	5.1	19.27	5.0	19.00	5.1	---	---
4	-88	16	---	19.59	3.9	20.01	3.4	19.80	3.7	---	---
5	-98	18	---	1.98	4.2	19.92	4.4	10.95	4.3	---	---
6	-108	20	---	19.20	4.9	19.32	4.8	19.26	4.9	---	---
7	-118	21	---	19.18	4.8	19.73	3.8	19.46	4.3	---	---
8	-128	23	---	19.62	3.6	19.62	3.7	19.62	3.7	---	---
9	-138	24	---	18.85	4.4	18.99	4.3	18.92	4.4	---	---
10	-147	26	---	18.22	5.2	18.36	5.1	18.29	5.2	---	---

**Table 45. Stiffness and strength summary of CA6-C, Strip 2, 12 roller passes**

Test Point	GeoGauge		Clegg Impact Test			DCP	Portable FWD: E (MPa)			
	M (MPa)	S (MN/m)	CIV <sup>1</sup>	CIV <sup>2</sup>	CIV	DCPI	1	2	3	4
1	76.2	10.3	23.5	---	23.5	14	8.0	33.0	34.0	---
2	82.5	11.1	18.8	---	18.8	17	9.0	35.0	39.0	---
3	67.3	9.1	17.4	---	17.4	18	23.0	58.0	48.0	---
4	71.8	9.7	18.5	---	18.5	18	15.0	39.0	31.0	---
5	78.8	10.6	18.7	---	18.7	17	22.0	42.0	37.0	---
6	73.6	9.9	21.7	---	21.7	16	16.0	37.0	35.0	---
7	66.2	8.9	16.8	---	16.8	17	14.0	35.0	33.0	---
8	70.7	9.5	18.8	---	18.8	18	8.0	33.0	33.0	---
9	78.0	10.5	18.3	---	18.3	19	10.0	27.0	26.0	---
10	79.2	10.7	17.1	---	17.1	20	9.0	25.0	27.0	---

**Table 46. Moisture and density summary of CA5-C, Strip 3, 0 roller passes**

Test Point	Coordinates (degrees, ft)			Nuclear Gauge (kN/m <sup>3</sup> , %)						Drive Core (kN/m <sup>3</sup> , %)	
	X	Y	Elevation	$\gamma_d^1$	$w_g^1$	$\gamma_d^2$	$w_g^2$	$\gamma_d$	$w_g$	$\gamma_d$	$w_g$
1	-103	16	---	12.61	3.4	12.41	3.1	12.51	3.3	---	---
2	-113	18	---	12.50	3.3	12.36	3.7	12.43	3.5	---	---
3	-123	20	---	11.89	2.0	12.49	2.0	12.19	2.0	---	---
4	-132	21	---	12.50	2.7	12.38	3.1	12.44	2.9	---	---
5	-142	24	---	11.45	2.3	12.35	2.5	11.90	2.4	---	---
6	-152	25	---	12.06	2.7	11.91	3.3	11.99	3.0	---	---
7	-162	27	---	11.75	2.9	12.33	2.5	12.04	2.7	---	---
8	-172	29	---	11.18	3.9	11.45	4.7	11.32	4.3	---	---
9	-182	21	---	12.05	3.2	12.08	4.2	12.06	3.7	---	---
10	-192	31	---	11.15	3.9	11.14	3.4	11.15	3.7	---	---

**Table 47. Stiffness and strength summary of CA5-C, Strip 3, 0 roller passes**

Test Point	GeoGauge		Clegg Impact Test			DCP	Portable FWD: E (MPa)			
	M (MPa)	S (MN/m)	CIV <sup>1</sup>	CIV <sup>2</sup>	CIV	DCPI	1	2	3	4
1	42.9	5.8	15.3	---	15.3	127	3.0	10.0	18.0	---
2	36.9	5.0	20.2	---	20.2	59	21.0	26.0	19.0	---
3	44.9	6.1	17.0	---	17.0	76	13.0	14.0	13.0	---
4	35.2	4.8	11.7	---	11.7	65	8.0	15.0	18.0	---
5	40.1	5.4	6.1	---	6.1	76	13.0	50.0	21.0	---
6	41.1	5.6	9.7	---	9.7	52	3.0	10.0	16.0	---
7	42.1	5.7	12.1	---	12.1	87	5.0	12.0	12.0	---
8	44.2	6.0	16.0	---	16.0	49	28.0	14.0	15.0	---
9	45.7	6.2	8.0	---	8.0	42	3.0	9.0	12.0	---
10	50.8	6.9	7.1	---	7.1	46	2.0	7.0	9.0	---

**Table 48. Moisture and density summary of CA5-C, Strip 3, 1 roller pass**

Test Point	Coordinates (degrees, ft)			Nuclear Gauge (kN/m <sup>3</sup> , %)						Drive Core (kN/m <sup>3</sup> , %)	
	X	Y	Elevation	$\gamma_d^1$	$w_g^1$	$\gamma_d^2$	$w_g^2$	$\gamma_d$	$w_g$	$\gamma_d$	$w_g$
1	-103	16	---	12.65	2.7	12.77	2.5	12.71	2.6	---	---
2	-113	18	---	0.96	1.9	12.90	2.2	6.93	2.1	---	---
3	-123	20	---	12.83	3.1	12.30	3.6	12.57	3.4	---	---
4	-132	21	---	13.37	1.9	13.01	2.7	13.19	2.3	---	---
5	-142	24	---	13.67	2.5	13.43	2.5	13.55	2.5	---	---
6	-152	25	---	13.40	2.1	13.15	2.7	13.27	2.4	---	---
7	-162	27	---	13.32	2.5	13.10	2.7	13.21	2.6	---	---
8	-172	29	---	12.44	3.0	12.55	3.4	12.50	3.2	---	---
9	-182	21	---	13.12	2.2	12.85	2.6	12.98	2.4	---	---
10	-192	31	---	12.17	2.8	11.67	3.1	11.92	3.0	---	---

**Table 49. Stiffness and strength summary of CA5-C, Strip 3, 1 roller pass**

Test Point	GeoGauge		Clegg Impact Test			DCP	Portable FWD: E (MPa)			
	M (MPa)	S (MN/m)	CIV <sup>1</sup>	CIV <sup>2</sup>	CIV	DCPI	1	2	3	4
1	34.9	4.7	17.7	---	17.7	45	3.0	18.0	22.0	---
2	43.4	5.9	12.4	---	12.4	54	4.0	22.0	16.0	---
3	35.3	4.8	9.0	---	9.0	55	4.0	16.0	24.0	---
4	29.4	4.0	12.6	---	12.6	47	3.0	12.0	15.0	---
5	33.1	4.5	7.8	---	7.8	52	3.0	12.0	15.0	---
6	39.3	5.3	7.8	---	7.8	42	4.0	16.0	19.0	---
7	36.5	4.9	6.5	---	6.5	48	3.0	15.0	17.0	---
8	40.6	5.5	13.7	---	13.7	48	14.0	36.0	35.0	---
9	41.7	5.6	9.9	---	9.9	46	8.0	25.0	26.0	---
10	38.7	5.2	10.1	---	10.1	52	3.0	31.0	20.0	---

**Table 50. Moisture and density summary of CA5-C, Strip 3, 2 roller passes**

Test Point	Coordinates (degrees, ft)			Nuclear Gauge (kN/m <sup>3</sup> , %)						Drive Core (kN/m <sup>3</sup> , %)	
	X	Y	Elevation	$\gamma_d^1$	$w_g^1$	$\gamma_d^2$	$w_g^2$	$\gamma_d$	$w_g$	$\gamma_d$	$w_g$
1	-103	16	---	12.52	3.2	13.82	2.4	13.17	2.8	---	---
2	-113	18	---	12.88	2.1	13.02	2.1	12.95	2.1	---	---
3	-123	20	---	13.79	1.9	13.32	3.2	13.56	2.6	---	---
4	-132	21	---	13.65	2.0	13.73	2.2	13.69	2.1	---	---
5	-142	24	---	13.48	1.8	13.43	2.0	13.45	1.9	---	---
6	-152	25	---	13.56	2.3	13.23	3.1	13.39	2.7	---	---
7	-162	27	---	13.18	2.0	13.31	1.3	13.24	1.7	---	---
8	-172	29	---	13.27	2.3	13.37	3.1	13.32	2.7	---	---
9	-182	21	---	12.77	3.5	12.94	4.0	12.86	3.8	---	---
10	-192	31	---	14.50	2.1	14.73	2.6	14.62	2.4	---	---

**Table 51. Stiffness and strength summary of CA5-C, Strip 3, 2 roller passes**

Test Point	GeoGauge		Clegg Impact Test			DCP	Portable FWD: E (MPa)			
	M (MPa)	S (MN/m)	CIV <sup>1</sup>	CIV <sup>2</sup>	CIV	DCPI	1	2	3	4
1	37.1	5.0	13.6	---	13.6	58	4.0	26.0	35.0	---
2	41.2	5.6	12.1	---	12.1	50	3.0	12.0	14.0	---
3	32.1	4.3	13.5	---	13.5	51	5.0	17.0	17.0	---
4	34.7	5.0	13.9	---	13.9	46	12.0	43.0	30.0	---
5	41.1	5.6	11.1	---	11.1	46	9.0	39.0	37.0	---
6	40.0	5.4	11.6	---	11.6	48	6.0	44.0	32.0	---
7	34.3	4.6	10.8	---	10.8	81	5.0	22.0	21.0	---
8	48.9	6.6	13.6	---	13.6	42	12.0	38.0	40.0	---
9	42.1	5.7	11.4	---	11.4	47	8.0	35.0	35.0	---
10	42.5	5.7	15.3	---	15.3	37	3.0	19.0	26.0	---

**Table 52. Moisture and density summary of CA5-C, Strip 3, 4 roller passes**

Test Point	Coordinates (degrees, ft)			Nuclear Gauge (kN/m <sup>3</sup> , %)						Drive Core (kN/m <sup>3</sup> , %)	
	X	Y	Elevation	$\gamma_d^1$	$w_g^1$	$\gamma_d^2$	$w_g^2$	$\gamma_d$	$w_g$	$\gamma_d$	$w_g$
1	-103	16	---	13.42	2.9	13.62	3.6	13.52	3.3	---	---
2	-113	18	---	13.32	1.5	13.21	1.5	13.27	1.5	---	---
3	-123	20	---	13.79	0.4	13.93	2.6	13.86	1.5	---	---
4	-132	21	---	13.51	2.0	13.45	2.0	13.48	2.0	---	---
5	-142	24	---	13.38	2.0	13.18	1.6	13.28	1.8	---	---
6	-152	25	---	13.62	2.5	13.40	3.2	13.51	2.9	---	---
7	-162	27	---	13.67	2.5	14.06	2.1	13.86	2.3	---	---
8	-172	29	---	13.46	2.9	13.71	2.9	13.59	2.9	---	---
9	-182	21	---	14.37	3.3	14.11	2.7	14.24	3.0	---	---
10	-192	31	---	15.32	1.8	15.02	2.3	15.17	2.1	---	---

**Table 53. Stiffness and strength summary of CA5-C, Strip 3, 4 roller passes**

Test Point	GeoGauge		Clegg Impact Test			DCP	Portable FWD: E (MPa)			
	M (MPa)	S (MN/m)	CIV <sup>1</sup>	CIV <sup>2</sup>	CIV	DCPI	1	2	3	4
1	35.5	4.8	14.7	---	14.7	37	4.0	24.0	31.0	---
2	37.1	5.0	13.8	---	13.8	41	19.0	35.0	37.0	---
3	31.8	4.3	14.8	---	14.8	44	6.0	25.0	31.0	---
4	37.3	5.0	13.1	---	13.1	42	37.0	30.0	29.0	---
5	37.5	5.1	12.6	---	12.6	44	6.0	11.0	30.0	---
6	51.5	6.9	13.2	---	13.2	42	12.0	46.0	40.0	---
7	40.4	5.5	7.1	---	7.1	32	3.0	16.0	13.0	---
8	44.3	6.0	13.2	---	13.2	25	3.0	52.0	56.0	---
9	52.7	7.1	15.3	---	15.3	32	11.0	38.0	44.0	---
10	42.9	5.8	10.2	---	10.2	32	7.0	31.0	34.0	---

**Table 54. Moisture and density summary of CA5-C, Strip 3, 8 roller passes**

Test Point	Coordinates (degrees, ft)			Nuclear Gauge (kN/m <sup>3</sup> , %)						Drive Core (kN/m <sup>3</sup> , %)	
	X	Y	Elevation	$\gamma_d^1$	$w_g^1$	$\gamma_d^2$	$w_g^2$	$\gamma_d$	$w_g$	$\gamma_d$	$w_g$
1	-103	16	---	14.51	2.8	14.62	2.5	14.57	2.7	---	---
2	-113	18	---	14.09	1.1	14.36	1.5	14.22	1.3	---	---
3	-123	20	---	14.29	3.3	14.59	4.0	14.44	3.7	---	---
4	-132	21	---	14.31	2.2	14.59	2.0	14.45	2.1	---	---
5	-142	24	---	14.42	2.0	14.36	2.4	14.39	2.2	---	---
6	-152	25	---	14.14	3.2	14.23	2.7	14.18	3.0	---	---
7	-162	27	---	13.42	3.1	13.31	2.8	13.36	3.0	---	---
8	-172	29	---	14.39	3.5	14.48	2.6	14.44	3.1	---	---
9	-182	21	---	15.02	3.2	14.92	3.4	14.97	3.3	---	---
10	-192	31	---	16.27	3.0	16.54	2.7	16.41	2.9	---	---

**Table 55. Stiffness and strength summary of CA5-C, Strip 3, 8 roller passes**

Test Point	GeoGauge		Clegg Impact Test			DCP	Portable FWD: E (MPa)			
	M (MPa)	S (MN/m)	CIV <sup>1</sup>	CIV <sup>2</sup>	CIV	DCPI	1	2	3	4
1	44.0	5.9	12.8	---	12.8	37	10.0	36.0	41.0	---
2	47.8	6.4	10.1	---	10.1	35	9.0	30.0	28.0	---
3	43.4	5.9	11.6	---	11.6	41	9.0	50.0	50.0	---
4	40.7	5.5	13.6	---	13.6	32	6.0	33.0	42.0	---
5	55.2	7.4	12.1	---	12.1	30	5.0	35.0	39.0	---
6	37.0	5.0	11.3	---	11.3	35	8.0	96.0	62.0	---
7	39.3	5.3	17.8	---	17.8	46	22.0	134.0	44.0	---
8	43.5	5.9	16.1	---	16.1	33	4.0	54.0	62.0	---
9	51.7	7.0	11.4	---	11.4	28	4.0	49.0	51.0	---
10	43.2	5.8	14.8	---	14.8	21	4.0	53.0	54.0	---

**Table 56. Moisture and density summary of CA5-C, Strip 3, 12 roller passes**

Test Point	Coordinates (degrees, ft)			Nuclear Gauge (kN/m <sup>3</sup> , %)						Drive Core (kN/m <sup>3</sup> , %)	
	X	Y	Elevation	$\gamma_d^1$	$w_g^1$	$\gamma_d^2$	$w_g^2$	$\gamma_d$	$w_g$	$\gamma_d$	$w_g$
1	-103	16	---	14.99	2.4	15.05	2.6	15.02	2.5	---	---
2	-113	18	---	14.50	1.8	14.36	2.0	14.43	1.9	---	---
3	-123	20	---	14.66	2.5	14.34	3.6	14.50	3.1	---	---
4	-132	21	---	15.83	2.7	15.11	2.4	15.47	2.6	---	---
5	-142	24	---	14.20	2.2	14.08	2.4	14.14	2.3	---	---
6	-152	25	---	14.72	2.7	14.29	3.1	14.51	2.9	---	---
7	-162	27	---	14.26	2.4	14.39	2.7	14.33	2.6	---	---
8	-172	29	---	14.64	2.7	14.59	3.3	14.62	3.0	---	---
9	-182	21	---	15.58	3.1	15.54	3.2	15.56	3.2	---	---
10	-192	31	---	16.98	2.3	17.30	2.8	17.14	2.6	---	---

**Table 57. Stiffness and strength summary of CA5-C, Strip 3, 12 roller passes**

Test Point	GeoGauge		Clegg Impact Test			DCP	Portable FWD: E (MPa)			
	M (MPa)	S (MN/m)	CIV <sup>1</sup>	CIV <sup>2</sup>	CIV	DCPI	1	2	3	4
1	---	---	---	---	---	---	---	---	---	---
2	---	---	---	---	---	---	---	---	---	---
3	---	---	---	---	---	---	---	---	---	---
4	---	---	---	---	---	---	---	---	---	---
5	---	---	---	---	---	---	---	---	---	---
6	---	---	---	---	---	---	---	---	---	---
7	---	---	---	---	---	---	---	---	---	---
8	---	---	---	---	---	---	---	---	---	---
9	---	---	---	---	---	---	---	---	---	---
10	---	---	---	---	---	---	---	---	---	---

**Table 58. Moisture and density summary of FA6, Strip 4, 0 roller passes**

Test Point	Coordinates (degrees, ft)			Nuclear Gauge (kN/m <sup>3</sup> , %)						Drive Core (kN/m <sup>3</sup> , %)	
	X	Y	Elevation	$\gamma_d^1$	$w_g^1$	$\gamma_d^2$	$w_g^2$	$\gamma_d$	$w_g$	$\gamma_d$	$w_g$
1	-50	8	---	15.03	6.4	14.99	5.5	15.01	6.0	---	---
2	-60	10	---	14.11	4.3	14.48	3.9	14.29	4.1	---	---
3	-70	12	---	14.22	5.3	14.51	4.7	14.37	5.0	---	---
4	-80	12	---	13.93	4.5	14.26	4.3	14.10	4.4	---	---
5	-90	14	---	14.17	4.3	14.51	4.2	14.34	4.3	---	---
6	-100	15	---	14.22	6.1	14.78	4.7	14.50	5.4	---	---
7	-109	17	---	14.78	5.3	14.40	5.5	14.59	5.4	---	---
8	-119	18	---	13.92	6.4	13.79	5.8	13.86	6.1	---	---
9	-129	19	---	13.64	5.6	13.81	4.9	13.72	5.3	---	---
10	-139	20	---	14.06	5.6	14.06	6.0	14.06	5.8	---	---

**Table 59. Stiffness and strength summary of FA6, Strip 4, 0 roller passes**

Test Point	GeoGauge		Clegg Impact Test			DCP	Portable FWD: E (MPa)			
	M (MPa)	S (MN/m)	CIV <sup>1</sup>	CIV <sup>2</sup>	CIV	DCPI	1	2	3	4
1	14.2	1.9	---	---	---	252	---	---	---	---
2	16.1	2.2	---	---	---	290	---	---	---	---
3	16.9	2.3	---	---	---	280	---	---	---	---
4	12.9	1.7	---	---	---	267	---	---	---	---
5	16.2	2.2	---	---	---	268	---	---	---	---
6	13.0	1.8	---	---	---	295	---	---	---	---
7	10.2	1.4	---	---	---	278	---	---	---	---
8	11.3	1.5	---	---	---	275	---	---	---	---
9	10.9	1.5	---	---	---	277	---	---	---	---
10	11.8	1.6	---	---	---	249	---	---	---	---

**Table 60. Moisture and density summary of FA6, Strip 4, 1 roller pass**

Test Point	Coordinates (degrees, ft)			Nuclear Gauge (kN/m <sup>3</sup> , %)						Drive Core (kN/m <sup>3</sup> , %)	
	X	Y	Elevation	$\gamma_d^1$	$w_g^1$	$\gamma_d^2$	$w_g^2$	$\gamma_d$	$w_g$	$\gamma_d$	$w_g$
1	-50	8	---	16.32	6.6	16.48	6.1	16.40	6.4	---	---
2	-60	10	---	15.91	4.5	16.06	5.0	15.99	4.8	---	---
3	-70	12	---	16.04	6.0	16.43	5.6	16.23	5.8	---	---
4	-80	12	---	16.16	5.6	16.05	6.2	16.11	5.9	---	---
5	-90	14	---	16.23	5.0	16.56	4.6	16.39	4.8	---	---
6	-100	15	---	17.41	7.6	17.14	7.2	17.27	7.4	---	---
7	-109	17	---	16.71	6.5	16.84	6.2	16.78	6.4	---	---
8	-119	18	---	17.23	5.9	17.30	6.0	17.26	6.0	---	---
9	-129	19	---	16.49	5.6	16.75	6.0	16.62	5.8	---	---
10	-139	20	---	17.14	6.3	17.15	6.8	17.15	6.6	---	---

**Table 61. Stiffness and strength summary of FA6, Strip 4, 1 roller pass**

Test Point	GeoGauge		Clegg Impact Test			DCP	Portable FWD: E (MPa)			
	M (MPa)	S (MN/m)	CIV <sup>1</sup>	CIV <sup>2</sup>	CIV	DCPI	1	2	3	4
1	15.3	2.1	---	---	---	236	---	---	---	---
2	15.8	2.1	---	---	---	282	---	---	---	---
3	16.3	2.2	---	---	---	246	---	---	---	---
4	16.6	2.2	---	---	---	250	---	---	---	---
5	15.7	2.1	---	---	---	246	---	---	---	---
6	18.0	2.4	---	---	---	226	---	---	---	---
7	15.0	2.0	---	---	---	220	---	---	---	---
8	17.1	2.3	---	---	---	217	---	---	---	---
9	19.0	2.6	---	---	---	235	---	---	---	---
10	13.9	1.9	---	---	---	217	---	---	---	---

**Table 62. Moisture and density summary of FA6, Strip 4, 2 roller passes**

Test Point	Coordinates (degrees, ft)			Nuclear Gauge (kN/m <sup>3</sup> , %)						Drive Core (kN/m <sup>3</sup> , %)	
	X	Y	Elevation	$\gamma_d^1$	$w_g^1$	$\gamma_d^2$	$w_g^2$	$\gamma_d$	$w_g$	$\gamma_d$	$w_g$
1	-50	8	---	18.10	6.4	18.08	6.3	18.09	6.4	---	---
2	-60	10	---	16.78	5.1	16.84	4.4	16.81	4.8	---	---
3	-70	12	---	16.84	6.1	17.25	5.8	17.04	6.0	---	---
4	-80	12	---	16.54	5.7	16.37	6.1	16.45	5.9	---	---
5	-90	14	---	16.90	4.9	17.15	4.9	17.03	4.9	---	---
6	-100	15	---	17.72	7.2	17.48	8.6	17.60	7.9	---	---
7	-109	17	---	17.23	6.1	17.34	6.4	17.29	6.3	---	---
8	-119	18	---	18.18	5.6	18.39	5.7	18.28	5.7	---	---
9	-129	19	---	17.44	5.8	17.20	6.6	17.32	6.2	---	---
10	-139	20	---	17.67	7.6	17.75	8.0	17.71	7.8	---	---

**Table 63. Stiffness and strength summary of FA6, Strip 4, 2 roller passes**

Test Point	GeoGauge		Clegg Impact Test			DCP	Portable FWD: E (MPa)			
	M (MPa)	S (MN/m)	CIV <sup>1</sup>	CIV <sup>2</sup>	CIV	DCPI	1	2	3	4
1	26.2	3.5	4.4	---	4.4	146	---	---	---	---
2	19.1	2.6	5.7	---	5.7	138	---	---	---	---
3	24.3	3.3	4.2	---	4.2	166	---	---	---	---
4	22.9	3.1	4.2	---	4.2	133	---	---	---	---
5	21.1	2.8	5.1	---	5.1	136	---	---	---	---
6	27.2	3.7	6.0	---	6.0	105	---	---	---	---
7	21.4	2.9	5.2	---	5.2	121	---	---	---	---
8	21.4	2.9	4.6	---	4.6	122	---	---	---	---
9	22.5	3.0	4.8	---	4.8	105	---	---	---	---
10	20.2	2.7	4.4	---	4.4	162	---	---	---	---

**Table 64. Moisture and density summary of FA6, Strip 4, 4 roller passes**

Test Point	Coordinates (degrees, ft)			Nuclear Gauge (kN/m <sup>3</sup> , %)						Drive Core (kN/m <sup>3</sup> , %)	
	X	Y	Elevation	$\gamma_d^1$	$w_g^1$	$\gamma_d^2$	$w_g^2$	$\gamma_d$	$w_g$	$\gamma_d$	$w_g$
1	-50	8	---	18.52	6.2	18.46	6.3	18.49	6.3	---	---
2	-60	10	---	17.69	5.1	17.28	5.0	17.48	5.1	---	---
3	-70	12	---	18.08	5.2	18.43	6.1	18.25	5.7	---	---
4	-80	12	---	17.67	5.5	17.58	5.9	17.63	5.7	---	---
5	-90	14	---	17.92	4.4	181.01	5.5	99.47	5.0	---	---
6	-100	15	---	18.36	8.7	18.61	8.2	18.49	8.5	---	---
7	-109	17	---	17.75	6.5	18.10	6.6	17.92	6.6	---	---
8	-119	18	---	18.10	6.2	18.07	7.0	18.08	6.6	---	---
9	-129	19	---	18.14	6.5	17.91	6.4	18.03	6.5	---	---
10	-139	20	---	18.49	5.9	18.22	6.5	18.36	6.2	---	---

**Table 65. Stiffness and strength summary of FA6, Strip 4, 4 roller passes**

Test Point	GeoGauge		Clegg Impact Test			DCP	Portable FWD: E (MPa)			
	M (MPa)	S (MN/m)	CIV <sup>1</sup>	CIV <sup>2</sup>	CIV	DCPI	1	2	3	4
1	30.3	4.1	6.2	---	6.2	124	5.0	12.0	14.0	---
2	26.5	3.6	5.5	---	5.5	206	---	---	---	---
3	31.6	4.3	6.1	---	6.1	145	3.0	11.0	13.0	---
4	33.1	4.5	5.2	---	5.2	155	3.0	10.0	11.0	---
5	38.8	5.2	6.3	---	6.3	137	3.0	12.0	13.0	---
6	37.1	5.0	6.6	---	6.6	117	10.0	18.0	17.0	---
7	30.6	4.1	6.6	---	6.6	123	4.0	14.0	16.0	---
8	33.6	4.5	7.0	---	7.0	110	3.0	12.0	14.0	---
9	31.7	4.3	6.6	---	6.6	121	5.0	14.0	15.0	---
10	32.5	4.4	4.9	---	4.9	131	7.0	13.0	14.0	---

**Table 66. Moisture and density summary of FA6, Strip 4, 8 roller passes**

Test Point	Coordinates (degrees, ft)			Nuclear Gauge (kN/m <sup>3</sup> , %)						Drive Core (kN/m <sup>3</sup> , %)	
	X	Y	Elevation	$\gamma_d^1$	$w_g^1$	$\gamma_d^2$	$w_g^2$	$\gamma_d$	$w_g$	$\gamma_d$	$w_g$
1	-50	8	---	18.91	6.5	18.96	6.0	18.94	6.3	---	---
2	-60	10	---	17.77	5.3	17.58	4.9	17.67	5.1	---	---
3	-70	12	---	17.72	5.9	18.03	5.6	17.88	5.8	---	---
4	-80	12	---	18.60	5.0	18.41	5.8	18.50	5.4	---	---
5	-90	14	---	17.99	5.8	17.75	6.1	17.87	6.0	---	---
6	-100	15	---	19.51	7.7	20.01	6.9	19.76	7.3	---	---
7	-109	17	---	18.14	6.6	18.08	7.4	18.11	7.0	---	---
8	-119	18	---	19.13	6.9	18.98	6.5	19.05	6.7	---	---
9	-129	19	---	18.39	6.3	18.18	5.1	18.28	5.7	---	---
10	-139	20	---	18.36	6.5	18.66	6.9	18.51	6.7	---	---

**Table 67. Stiffness and strength summary of FA6, Strip 4, 8 roller passes**

Test Point	GeoGauge		Clegg Impact Test			DCP	Portable FWD: E (MPa)			
	M (MPa)	S (MN/m)	CIV <sup>1</sup>	CIV <sup>2</sup>	CIV	DCPI	1	2	3	4
1	38.5	5.2	6.8	---	6.8	86	8.0	19.0	18.0	---
2	31.8	4.3	7.3	---	7.3	60	4.0	15.0	16.0	---
3	38.5	5.2	7.1	---	7.1	54	4.0	15.0	16.0	---
4	41.1	5.5	7.6	---	7.6	47	5.0	6.0	17.0	---
5	41.7	5.6	8.8	---	8.8	51	6.0	18.0	19.0	---
6	49.5	6.7	8.5	---	8.5	41	6.0	19.0	19.0	---
7	41.8	5.6	7.8	---	7.8	44	6.0	20.0	23.0	---
8	41.0	5.5	7.6	---	7.6	47	6.0	19.0	20.0	---
9	40.1	5.4	9.7	---	9.7	39	9.0	20.0	18.0	---
10	30.3	4.1	5.7	---	5.7	80	4.0	12.0	14.0	---

**Table 68. Moisture and density summary of FA6, Strip 4, 12 roller passes**

Test Point	Coordinates (degrees, ft)			Nuclear Gauge (kN/m <sup>3</sup> , %)						Drive Core (kN/m <sup>3</sup> , %)	
	X	Y	Elevation	$\gamma_d^1$	$w_g^1$	$\gamma_d^2$	$w_g^2$	$\gamma_d$	$w_g$	$\gamma_d$	$w_g$
1	-50	8	---	18.99	5.7	18.25	6.3	18.62	6.0	---	---
2	-60	10	---	17.33	4.5	17.61	4.9	17.47	4.7	---	---
3	-70	12	---	18.21	5.7	18.25	5.3	18.23	5.5	---	---
4	-80	12	---	18.22	6.6	18.87	6.2	18.54	6.4	---	---
5	-90	14	---	19.12	5.9	19.46	4.4	19.29	5.2	---	---
6	-100	15	---	19.73	5.4	19.68	6.2	19.71	5.8	---	---
7	-109	17	---	18.32	6.9	18.30	7.0	18.31	7.0	---	---
8	-119	18	---	19.29	6.5	19.01	7.1	19.15	6.8	---	---
9	-129	19	---	18.76	6.3	18.60	6.9	18.68	6.6	---	---
10	-139	20	---	18.68	6.7	18.36	8.2	18.52	7.5	---	---

**Table 69. Stiffness and strength summary of FA6, Strip 4, 12 roller passes**

Test Point	GeoGauge		Clegg Impact Test			DCP	Portable FWD: E (MPa)			
	M (MPa)	S (MN/m)	CIV <sup>1</sup>	CIV <sup>2</sup>	CIV	DCPI	1	2	3	4
1	42.3	5.7	8.0	---	8.0	49	6.0	20.0	21.0	---
2	41.5	5.6	7.8	---	7.8	43	5.0	21.0	20.0	---
3	41.8	5.6	7.4	---	7.4	46	6.0	18.0	18.0	---
4	43.8	5.9	6.9	---	6.9	51	8.0	20.0	19.0	---
5	49.5	6.7	8.1	---	8.1	41	6.0	20.0	20.0	---
6	46.0	6.2	10.1	---	10.1	41	21.0	29.0	24.0	---
7	49.9	6.7	9.7	---	9.7	38	12.0	32.0	30.0	---
8	50.1	6.8	9.1	---	9.1	36	15.0	43.0	34.0	---
9	45.9	6.2	7.8	---	7.8	40	18.0	32.0	27.0	---
10	30.6	4.1	5.9	---	5.9	68	6.0	17.0	17.0	---

**Table 70. Moisture and density summary of CA6-G, Strip 5, 0 roller passes**

Test Point	Coordinates (degrees, ft)			Nuclear Gauge (kN/m <sup>3</sup> , %)						Drive Core (kN/m <sup>3</sup> , %)	
	X	Y	Elevation	$\gamma_d^1$	$w_g^1$	$\gamma_d^2$	$w_g^2$	$\gamma_d$	$w_g$	$\gamma_d$	$w_g$
1	-57	10	---	14.23	8.0	14.17	8.5	14.20	8.3	---	---
2	-67	11	---	13.42	11.3	14.37	8.2	13.89	9.8	---	---
3	-77	12	---	14.70	7.0	15.11	6.6	14.91	6.8	---	---
4	-87	14	---	15.69	7.7	14.89	9.2	15.29	8.5	---	---
5	-96	15	---	13.98	10.1	13.98	8.4	13.98	9.3	---	---
6	-106	17	---	13.95	8.5	14.25	8.3	14.10	8.4	---	---
7	-116	19	---	14.95	8.0	15.32	7.4	15.14	7.7	---	---
8	-126	20	---	14.48	6.7	14.86	6.1	14.67	6.4	---	---
9	-136	21	---	14.39	7.5	15.02	6.8	14.70	7.2	---	---
10	-146	23	---	13.57	7.5	13.46	8.9	13.52	8.2	---	---

**Table 71. Stiffness and strength summary of CA6-G, Strip 5, 0 roller passes**

Test Point	GeoGauge		Clegg Impact Test			DCP	Portable FWD: E (MPa)			
	M (MPa)	S (MN/m)	CIV <sup>1</sup>	CIV <sup>2</sup>	CIV	DCPI	1	2	3	4
1	---	---	5.2	---	5.2	198	---	4.0	---	---
2	---	---	2.9	---	2.9	136	3.0	4.0	---	---
3	---	---	2.0	---	2.0	222	6.0	6.0	---	---
4	---	---	2.9	---	2.9	237	3.0	4.0	---	---
5	---	---	3.6	---	3.6	254	7.0	7.0	---	---
6	---	---	3.2	---	3.2	239	5.0	6.0	---	---
7	---	---	3.8	---	3.8	254	16.0	18.0	---	---
8	---	---	2.7	---	2.7	242	4.0	6.0	---	---
9	---	---	3.0	---	3.0	200	7.0	6.0	---	---
10	---	---	---	---	---	210	5.0	4.0	---	---

**Table 72. Moisture and density summary of CA6-G, Strip 5, 1 roller pass**

Test Point	Coordinates (degrees, ft)			Nuclear Gauge (kN/m <sup>3</sup> , %)						Drive Core (kN/m <sup>3</sup> , %)	
	X	Y	Elevation	$\gamma_d^1$	$w_g^1$	$\gamma_d^2$	$w_g^2$	$\gamma_d$	$w_g$	$\gamma_d$	$w_g$
1	-57	10	---	16.24	8.5	16.32	7.9	16.28	8.2	---	---
2	-67	11	---	15.77	9.5	15.80	9.0	15.79	9.3	---	---
3	-77	12	---	15.74	7.0	15.68	7.3	15.71	7.2	---	---
4	-87	14	---	15.44	9.0	15.46	8.3	15.45	8.7	---	---
5	-96	15	---	16.26	8.2	16.35	7.3	16.31	7.8	---	---
6	-106	17	---	15.46	9.0	15.71	7.7	15.58	8.4	---	---
7	-116	19	---	16.18	7.1	16.26	7.8	16.22	7.5	---	---
8	-126	20	---	15.80	8.0	16.29	7.7	16.05	7.9	---	---
9	-136	21	---	16.45	8.7	16.56	6.9	16.50	7.8	---	---
10	-146	23	---	15.57	6.7	15.65	5.1	15.61	5.9	---	---

**Table 73. Stiffness and strength summary of CA6-G, Strip 5, 1 roller pass**

Test Point	GeoGauge		Clegg Impact Test			DCP	Portable FWD: E (MPa)			
	M (MPa)	S (MN/m)	CIV <sup>1</sup>	CIV <sup>2</sup>	CIV	DCPI	1	2	3	4
1	---	---	5.4	---	5.4	73	13.0	22.0	18.0	---
2	---	---	4.2	---	4.2	77	12.0	14.0	13.0	---
3	---	---	4.4	---	4.4	64	---	19.0	17.0	---
4	---	---	5.7	---	5.7	49	24.0	32.0	26.0	---
5	---	---	4.4	---	4.4	72	19.0	22.0	18.0	---
6	---	---	4.1	---	4.1	68	8.0	14.0	13.0	---
7	---	---	6.8	---	6.8	52	16.0	20.0	19.0	---
8	---	---	5.6	---	5.6	61	10.0	14.0	12.0	---
9	---	---	5.4	---	5.4	29	4.0	12.0	12.0	---
10	---	---	5.0	---	5.0	68	8.0	20.0	17.0	---

**Table 74. Moisture and density summary of CA6-G, Strip 5, 2 roller passes**

Test Point	Coordinates (degrees, ft)			Nuclear Gauge (kN/m <sup>3</sup> , %)						Drive Core (kN/m <sup>3</sup> , %)	
	X	Y	Elevation	$\gamma_d^1$	$w_g^1$	$\gamma_d^2$	$w_g^2$	$\gamma_d$	$w_g$	$\gamma_d$	$w_g$
1	-57	10	---	17.15	7.7	16.62	7.3	16.89	7.5	---	---
2	-67	11	---	17.03	8.5	16.46	8.4	16.75	8.5	---	---
3	-77	12	---	16.90	6.6	16.86	6.3	16.88	6.5	---	---
4	-87	14	---	16.90	9.4	17.50	8.6	17.20	9.0	---	---
5	-96	15	---	16.59	6.4	16.89	6.8	16.74	6.6	---	---
6	-106	17	---	16.16	8.4	16.04	9.9	16.10	9.2	---	---
7	-116	19	---	16.70	8.2	17.28	7.4	16.99	7.8	---	---
8	-126	20	---	16.75	8.5	16.90	8.0	16.82	8.3	---	---
9	-136	21	---	16.90	7.2	16.97	6.8	16.93	7.0	---	---
10	-146	23	---	16.37	8.4	16.48	6.8	16.42	7.6	---	---

**Table 75. Stiffness and strength summary of CA6-G, Strip 5, 2 roller passes**

Test Point	GeoGauge		Clegg Impact Test			DCP	Portable FWD: E (MPa)			
	M (MPa)	S (MN/m)	CIV <sup>1</sup>	CIV <sup>2</sup>	CIV	DCPI	1	2	3	4
1	---	---	5.8	---	5.8	70	18.0	23.0	18.0	---
2	---	---	6.1	---	6.1	50	11.0	14.0	14.0	---
3	---	---	6.0	---	6.0	41	11.0	19.0	19.0	---
4	---	---	7.7	---	7.7	38	5.0	52.0	37.0	---
5	---	---	6.3	---	6.3	48	21.0	26.0	21.0	---
6	---	---	6.0	---	6.0	69	13.0	21.0	19.0	---
7	---	---	7.7	---	7.7	36	23.0	32.0	29.0	---
8	---	---	7.2	---	7.2	49	18.0	27.0	20.0	---
9	---	---	7.8	---	7.8	33	14.0	31.0	24.0	---
10	---	---	5.9	---	5.9	43	12.0	22.0	21.0	---

**Table 76. Moisture and density summary of CA6-G, Strip 5, 4 roller passes**

Test Point	Coordinates (degrees, ft)			Nuclear Gauge (kN/m <sup>3</sup> , %)						Drive Core (kN/m <sup>3</sup> , %)	
	X	Y	Elevation	$\gamma_d^1$	$w_g^1$	$\gamma_d^2$	$w_g^2$	$\gamma_d$	$w_g$	$\gamma_d$	$w_g$
1	-57	10	---	17.17	9.5	17.37	8.8	17.27	9.2	---	---
2	-67	11	---	16.82	8.8	17.56	8.9	17.19	8.9	---	---
3	-77	12	---	16.86	8.5	17.03	8.0	16.94	8.3	---	---
4	-87	14	---	18.14	8.9	18.16	9.3	18.15	9.1	---	---
5	-96	15	---	17.39	8.3	17.09	8.7	17.24	8.5	---	---
6	-106	17	---	16.60	7.6	17.06	6.7	16.83	7.2	---	---
7	-116	19	---	17.06	8.4	17.61	7.7	17.33	8.1	---	---
8	-126	20	---	17.55	7.2	17.15	7.8	17.35	7.5	---	---
9	-136	21	---	17.39	8.7	16.73	8.6	17.06	8.7	---	---
10	-146	23	---	17.44	8.9	17.42	7.3	17.43	8.1	---	---

**Table 77. Stiffness and strength summary of CA6-G, Strip 5, 4 roller passes**

Test Point	GeoGauge		Clegg Impact Test			DCP	Portable FWD: E (MPa)			
	M (MPa)	S (MN/m)	CIV <sup>1</sup>	CIV <sup>2</sup>	CIV	DCPI	1	2	3	4
1	---	---	9.3	---	9.3	41	56.0	39.0	24.0	---
2	---	---	8.1	---	8.1	48	7.0	20.0	19.0	---
3	---	---	10.6	---	10.6	27	28.0	28.0	25.0	---
4	---	---	10.2	---	10.2	26	67.0	78.0	54.0	---
5	---	---	10.6	---	10.6	22	15.0	31.0	25.0	---
6	---	---	8.9	---	8.9	40	33.0	37.0	27.0	---
7	---	---	11.2	---	11.2	31	45.0	65.0	56.0	---
8	---	---	9.8	---	9.8	31	42.0	69.0	34.0	---
9	---	---	10.1	---	10.1	20	16.0	38.0	30.0	---
10	---	---	9.7	---	9.7	32	24.0	32.0	28.0	---

**Table 78. Moisture and density summary of CA6-G, Strip 5, 8 roller passes**

Test Point	Coordinates (degrees, ft)			Nuclear Gauge (kN/m <sup>3</sup> , %)						Drive Core (kN/m <sup>3</sup> , %)	
	X	Y	Elevation	$\gamma_d^1$	$w_g^1$	$\gamma_d^2$	$w_g^2$	$\gamma_d$	$w_g$	$\gamma_d$	$w_g$
1	-57	10	---	17.47	8.3	17.45	8.5	17.46	8.4	---	---
2	-67	11	---	17.22	7.4	16.98	8.7	17.10	8.1	---	---
3	-77	12	---	18.14	7.8	18.24	8.0	18.19	7.9	---	---
4	-87	14	---	18.55	7.2	18.33	8.4	18.44	7.8	---	---
5	-96	15	---	18.05	7.3	18.63	7.3	18.34	7.3	---	---
6	-106	17	---	18.07	6.1	17.88	7.0	17.97	6.6	---	---
7	-116	19	---	18.33	8.0	18.54	6.4	18.43	7.2	---	---
8	-126	20	---	17.91	8.3	17.83	7.6	17.87	8.0	---	---
9	-136	21	---	18.22	7.9	18.14	7.6	18.18	7.8	---	---
10	-146	23	---	18.57	7.4	18.38	8.1	18.47	7.8	---	---

**Table 79. Stiffness and strength summary of CA6-G, Strip 5, 8 roller passes**

Test Point	GeoGauge		Clegg Impact Test			DCP	Portable FWD: E (MPa)			
	M (MPa)	S (MN/m)	CIV <sup>1</sup>	CIV <sup>2</sup>	CIV	DCPI	1	2	3	4
1	---	---	9.4	---	9.4	17	71.0	40.0	32.0	---
2	---	---	14.9	---	14.9	20	21.0	23.0	19.0	---
3	---	---	13.0	---	13.0	18	29.0	38.0	32.0	---
4	---	---	14.9	---	14.9	31	76.0	76.0	56.0	---
5	---	---	10.3	---	10.3	18	67.0	50.0	33.0	---
6	---	---	11.5	---	11.5	42	11.0	27.0	28.0	---
7	---	---	10.1	---	10.1	22	33.0	39.0	32.0	---
8	---	---	11.3	---	11.3	24	63.0	40.0	33.0	---
9	---	---	13.3	---	13.3	16	58.0	63.0	52.0	---
10	---	---	9.5	---	9.5	43	26.0	30.0	27.0	---

**Table 80. Moisture and density summary of CA6-G, Strip 5, 12 roller passes**

Test Point	Coordinates (degrees, ft)			Nuclear Gauge (kN/m <sup>3</sup> , %)						Drive Core (kN/m <sup>3</sup> , %)	
	X	Y	Elevation	$\gamma_d^1$	$w_g^1$	$\gamma_d^2$	$w_g^2$	$\gamma_d$	$w_g$	$\gamma_d$	$w_g$
1	-57	10	---	18.54	7.8	18.54	7.9	18.54	7.9	---	---
2	-67	11	---	18.00	10.3	18.46	10.3	18.23	10.3	---	---
3	-77	12	---	18.35	7.3	18.22	9.3	18.28	8.3	---	---
4	-87	14	---	18.80	8.2	19.04	9.2	18.92	8.7	---	---
5	-96	15	---	18.28	8.5	18.66	7.6	18.47	8.1	---	---
6	-106	17	---	18.39	7.7	18.21	7.9	18.30	7.8	---	---
7	-116	19	---	18.63	7.3	18.52	7.9	18.58	7.6	---	---
8	-126	20	---	18.00	8.0	18.25	8.1	18.13	8.1	---	---
9	-136	21	---	18.69	6.6	18.52	7.5	18.61	7.1	---	---
10	-146	23	---	19.57	8.4	18.46	8.9	19.02	8.7	---	---

**Table 81. Stiffness and strength summary of CA6-G, Strip 5, 12 roller passes**

Test Point	GeoGauge		Clegg Impact Test			DCP	Portable FWD: E (MPa)			
	M (MPa)	S (MN/m)	CIV <sup>1</sup>	CIV <sup>2</sup>	CIV	DCPI	1	2	3	4
1	---	---	8.9	---	8.9	26	24.0	30.0	28.0	---
2	---	---	14.4	---	14.4	18	28.0	32.0	25.0	---
3	---	---	13.5	---	13.5	14	37.0	51.0	40.0	---
4	---	---	13.8	---	13.8	13	212.0	128.0	86.0	---
5	---	---	10.7	---	10.7	30	35.0	22.0	19.0	---
6	---	---	10.5	---	10.5	15	13.0	26.0	26.0	---
7	---	---	12.3	---	12.3	22	27.0	34.0	31.0	---
8	---	---	11.3	---	11.3	17	50.0	53.0	41.0	---
9	---	---	14.6	---	14.6	14	53.0	63.0	48.0	---
10	---	---	12.4	---	12.4	25	40.0	67.0	56.0	---



## APPENDIX D. PROJECT 2 DCP PROFILES

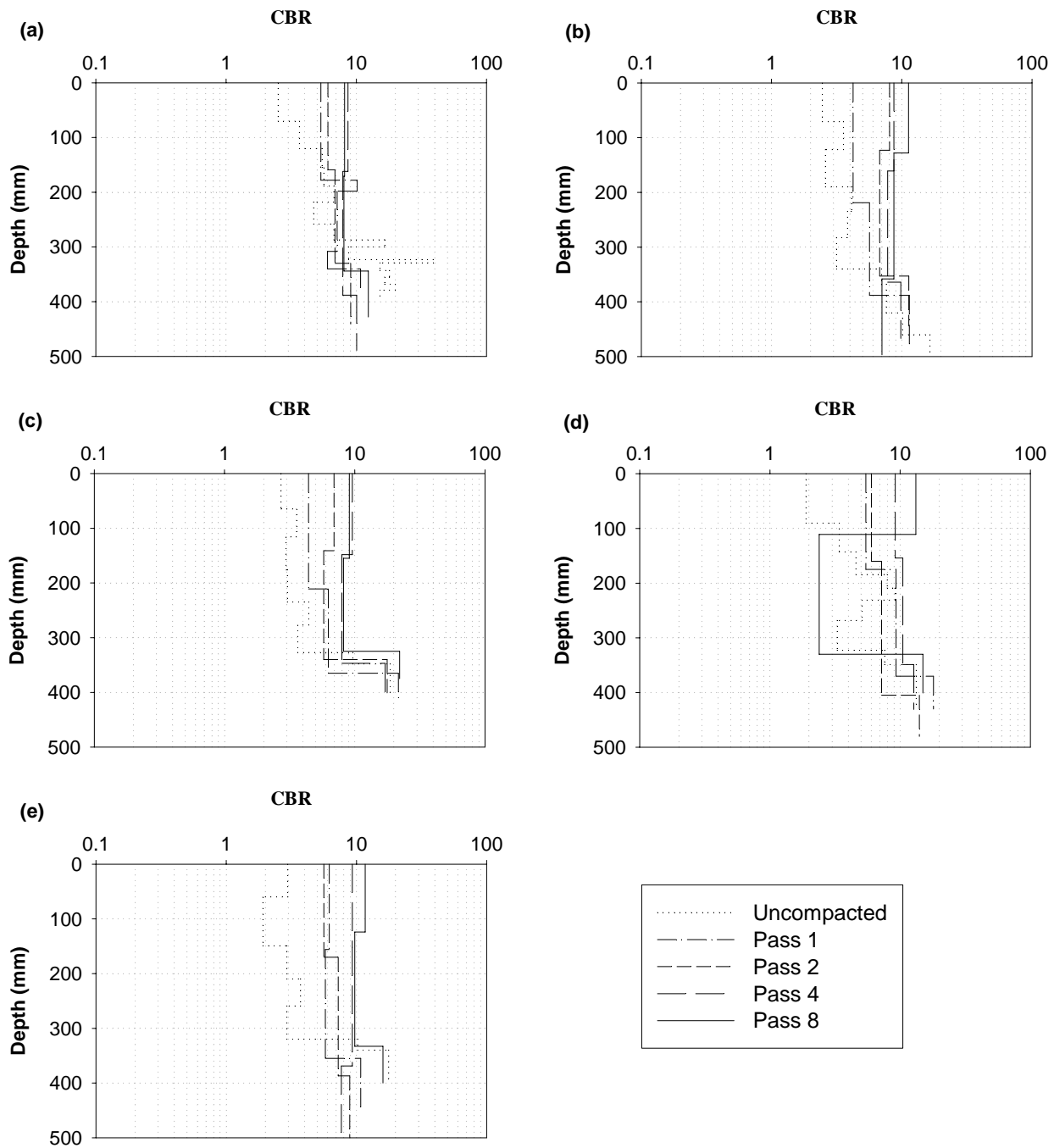
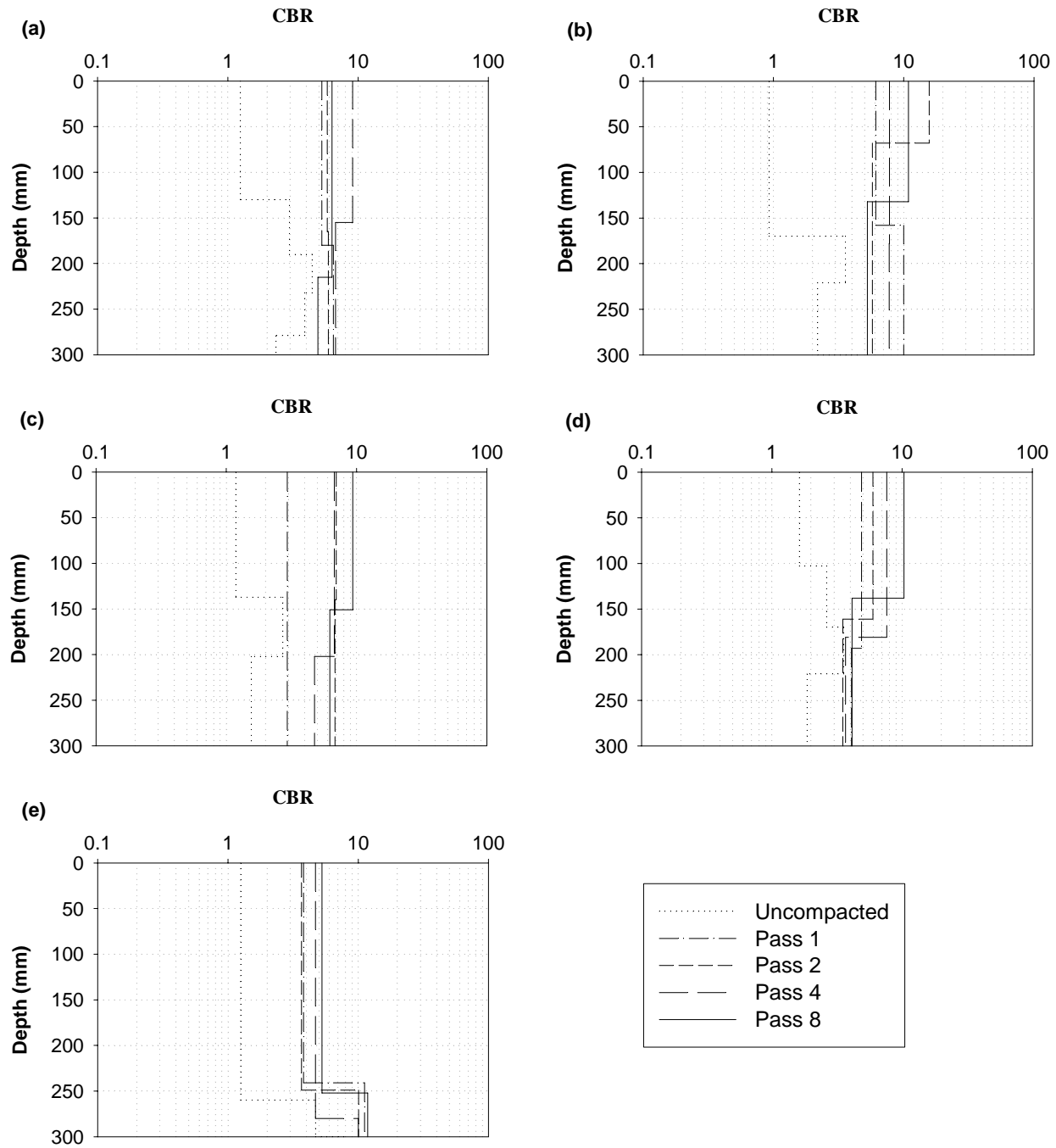
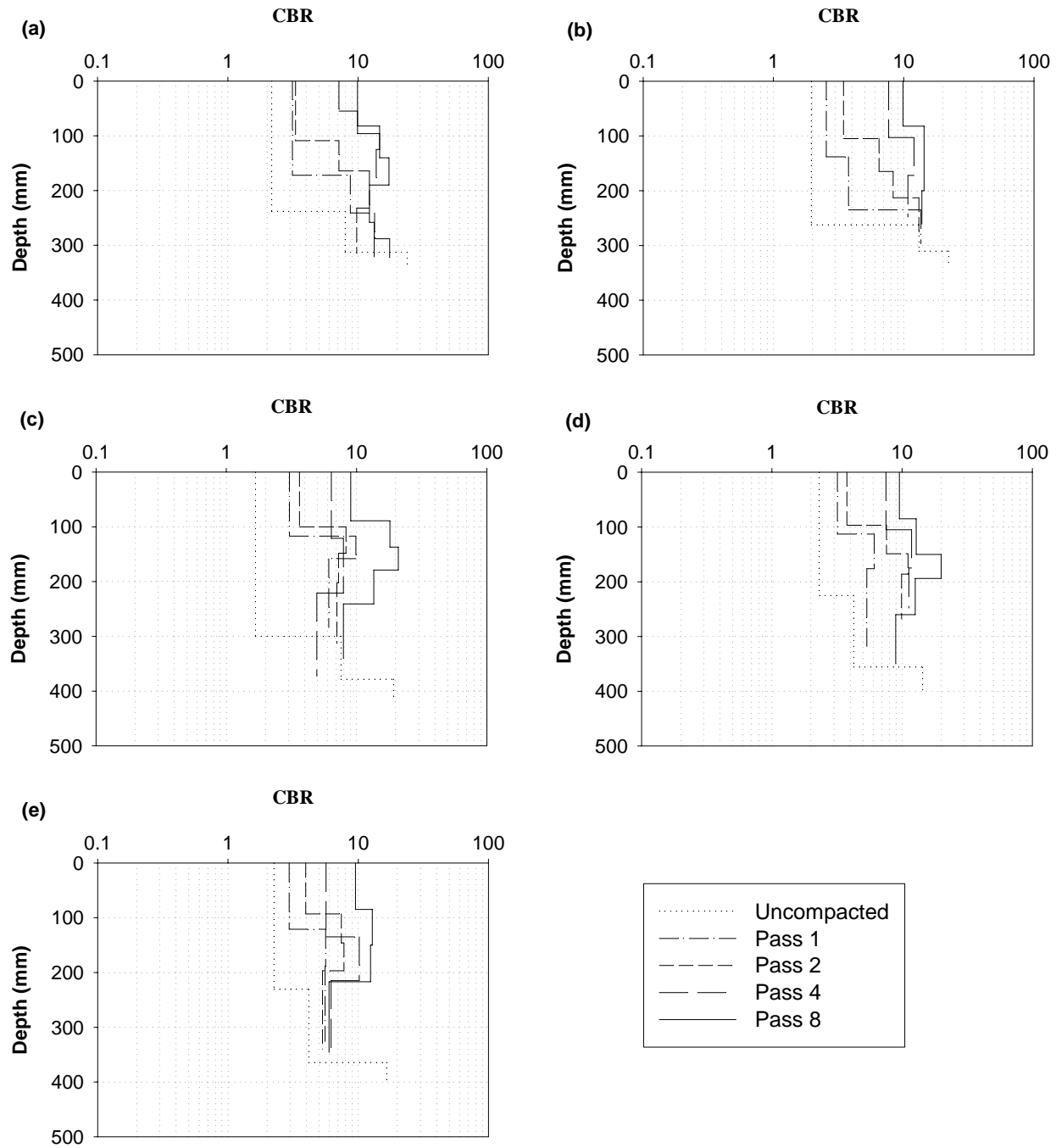


Figure 135. Strip 1: (a) Pt 1, (b) Pt 2, (c) Pt 3, (d) Pt 4, and (e) Pt 5



**Figure 136. Strip 1: (a) Pt 6, (b) Pt 7, (c) Pt 8, (d) Pt 9, and (e) Pt 10**



**Figure 137. Strip 2: (a) Pt 1, (b) Pt 2, (c) Pt 3, (d) Pt 4, and (e) Pt 5**

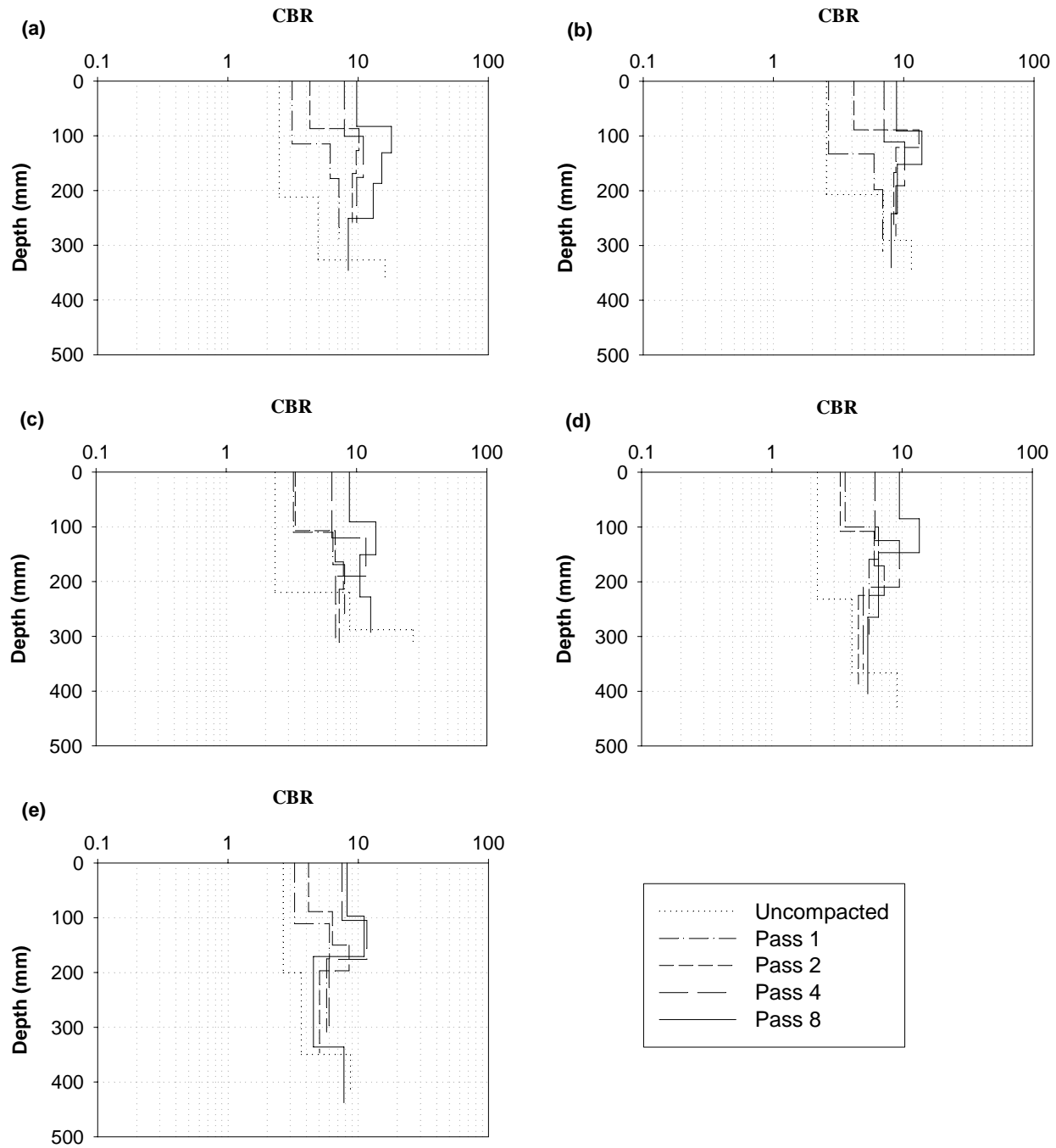


**Figure 138. Strip 2: (a) Pt 6, (b) Pt 7, (c) Pt 8, (d) Pt 9, and (e) Pt 10**

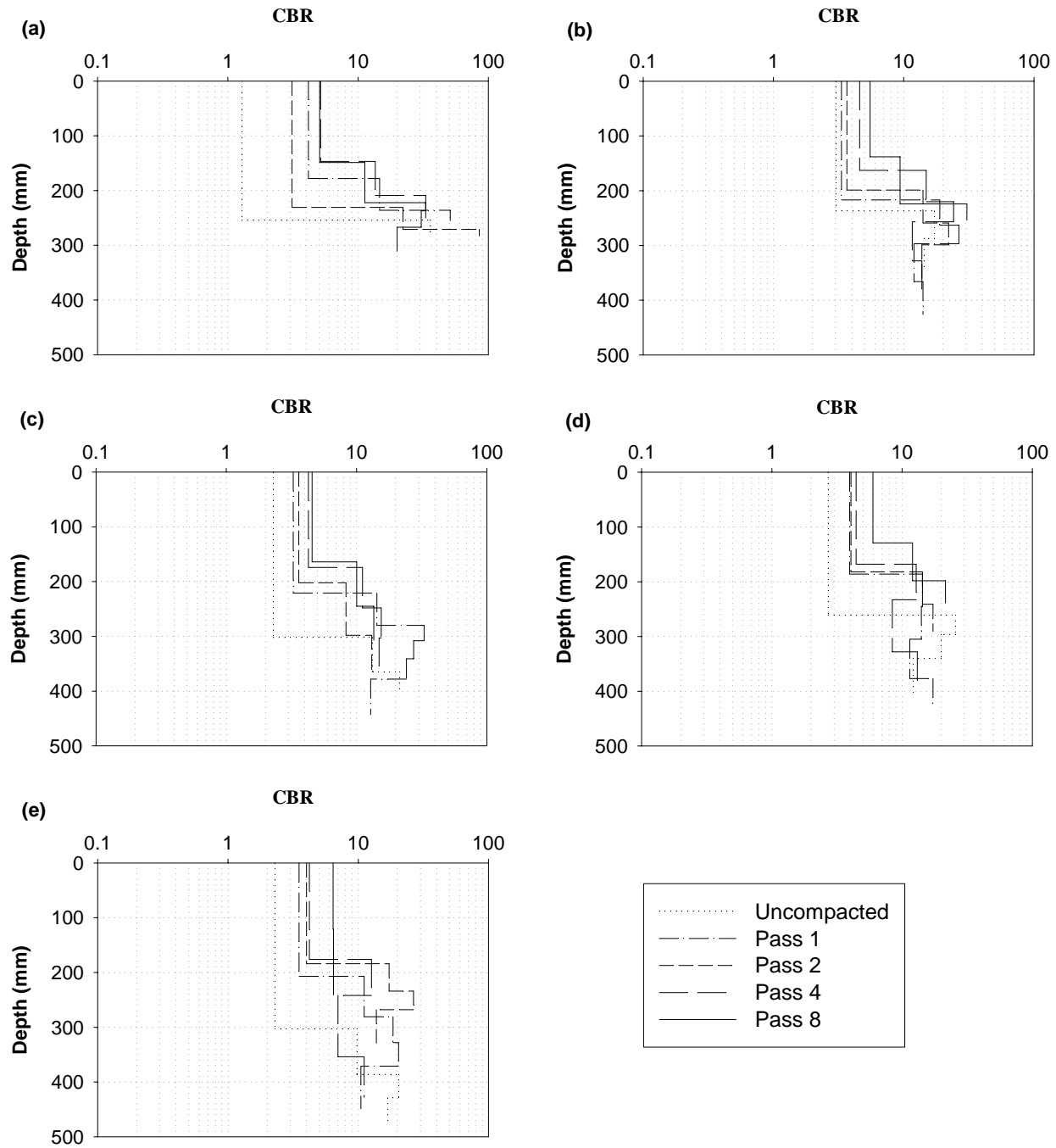


**Figure 139. Strip 3: (a) Pt 1, (b) Pt 2, (c) Pt 3, (d) Pt 4, and (e) Pt 5**

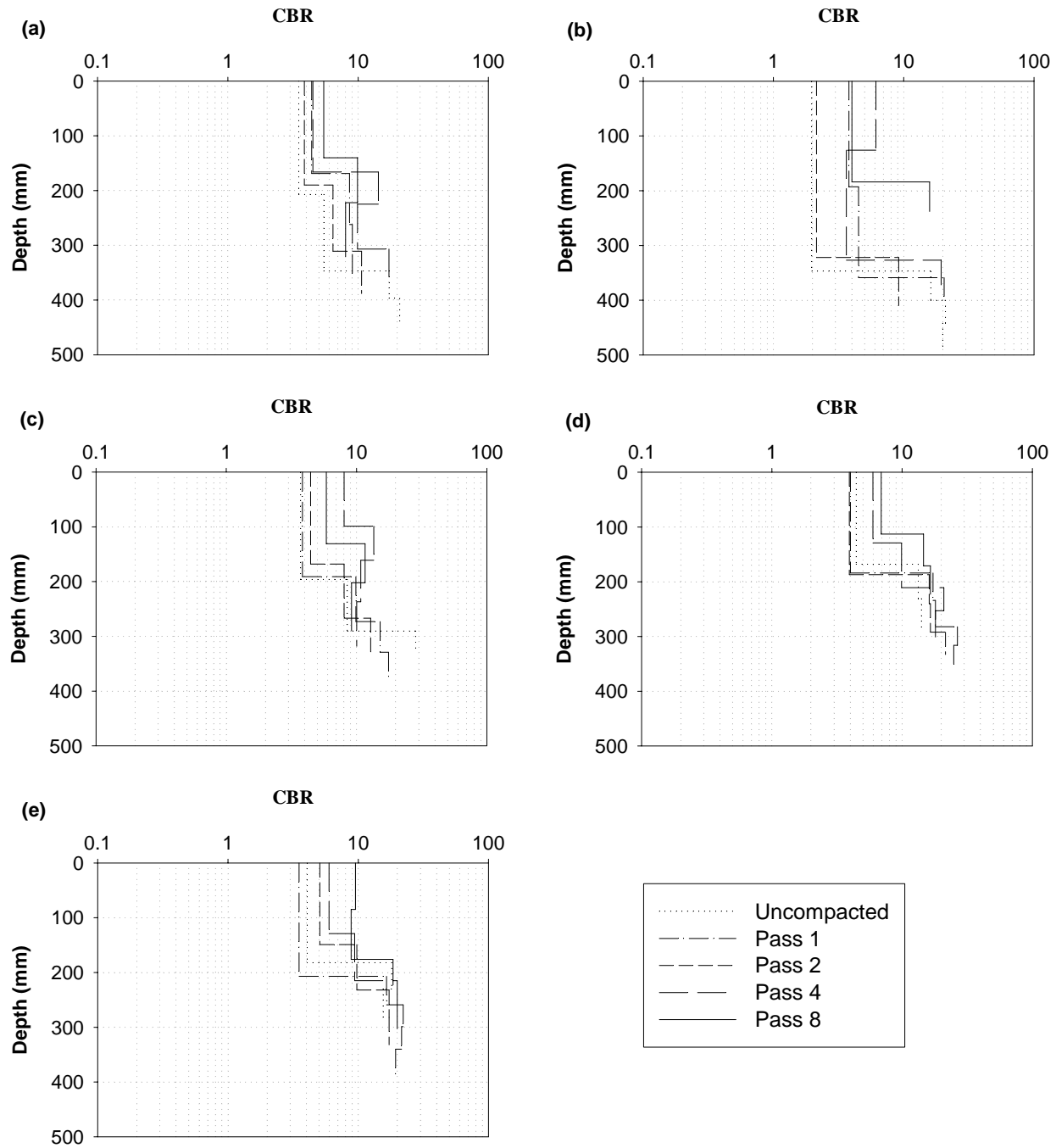


**Figure 140. Strip 3: (a) Pt 6, (b) Pt 7, (c) Pt 8, (d) Pt 9, and (e) Pt 10**

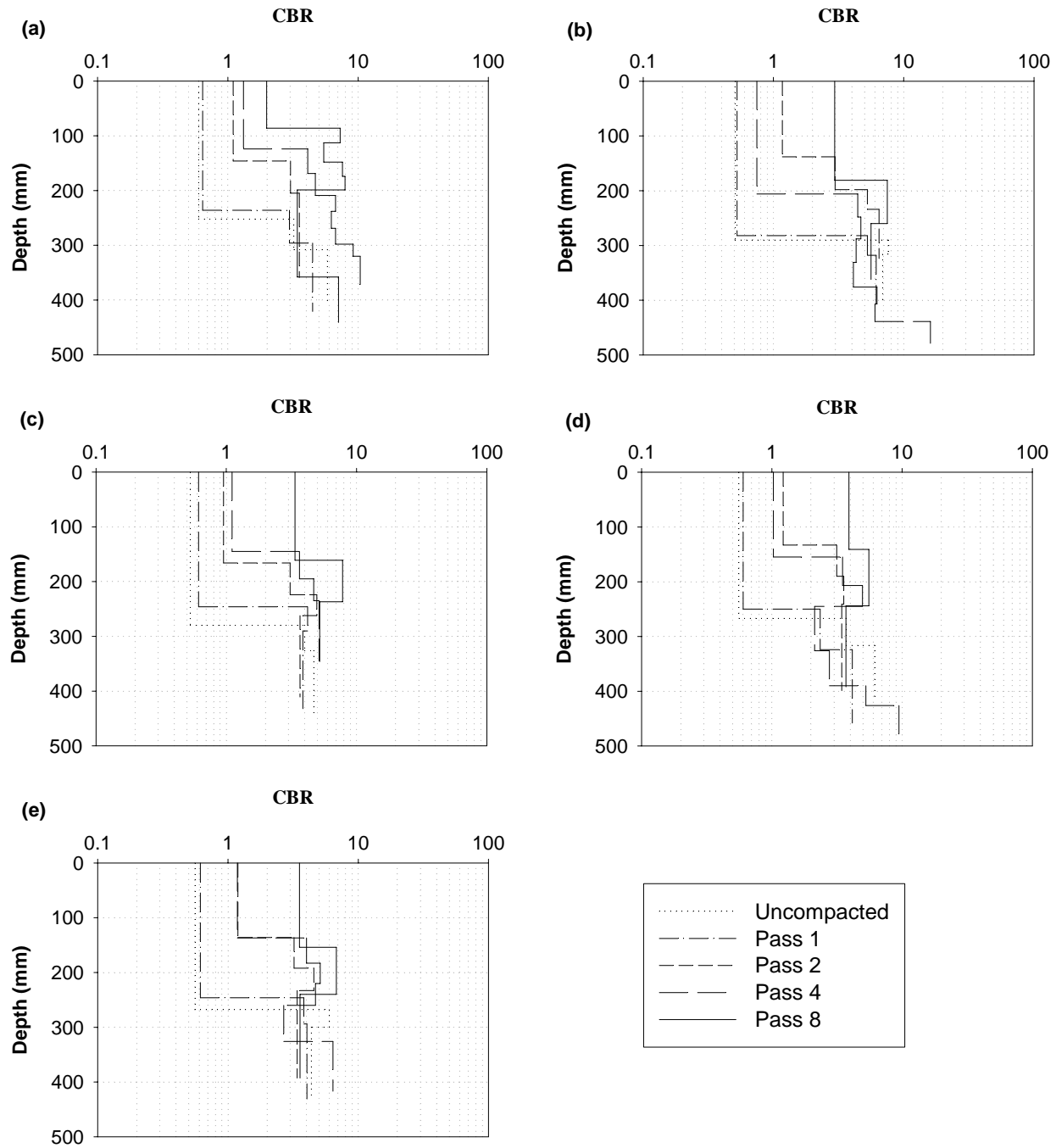


**Figure 141. Strip 4: (a) Pt 1, (b) Pt 2, (c) Pt 3, (d) Pt 4, and (e) Pt 5**

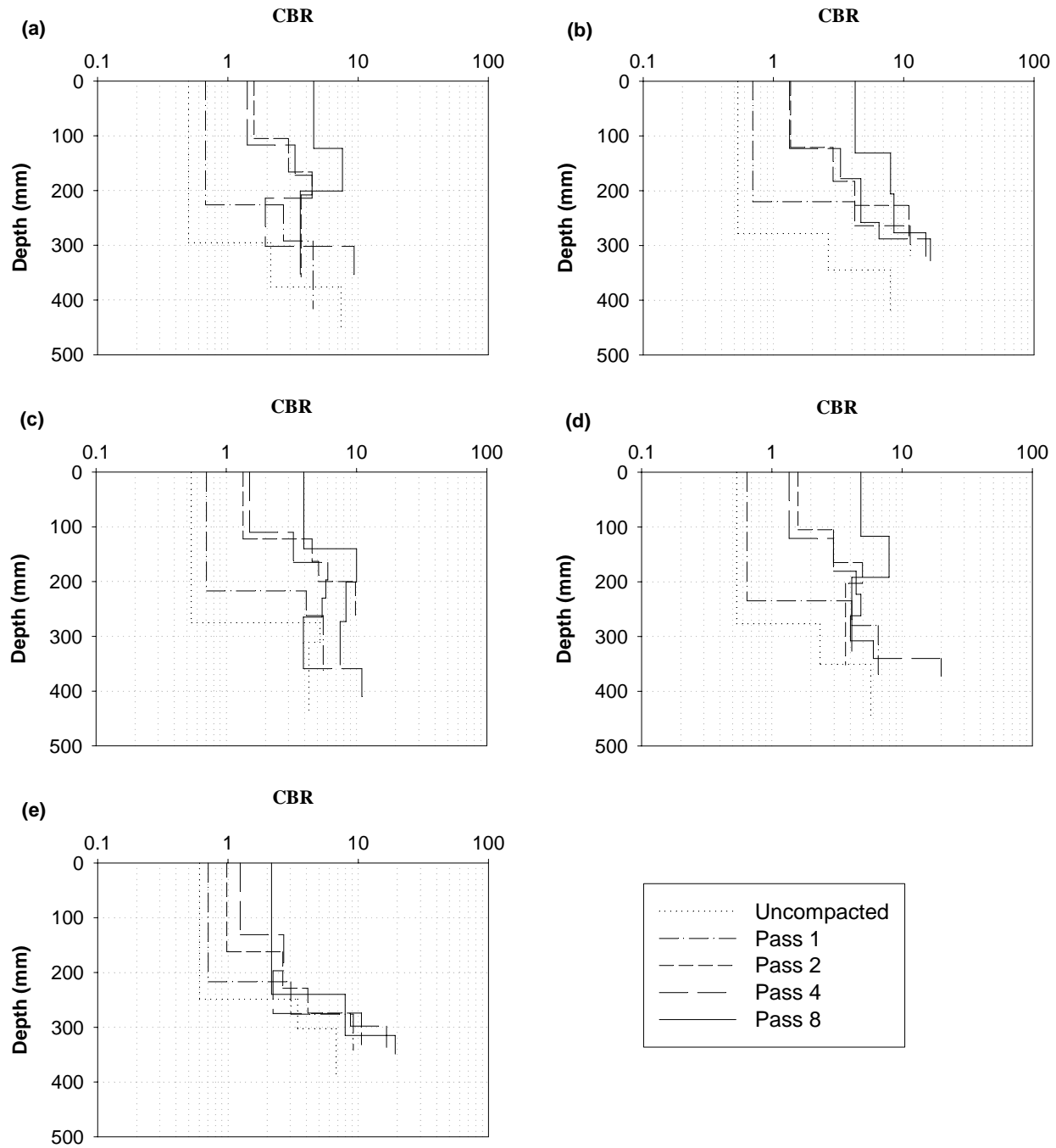


**Figure 142. Strip 4: (a) Pt 6, (b) Pt 7, (c) Pt 8, (d) Pt 9, and (e) Pt 10**

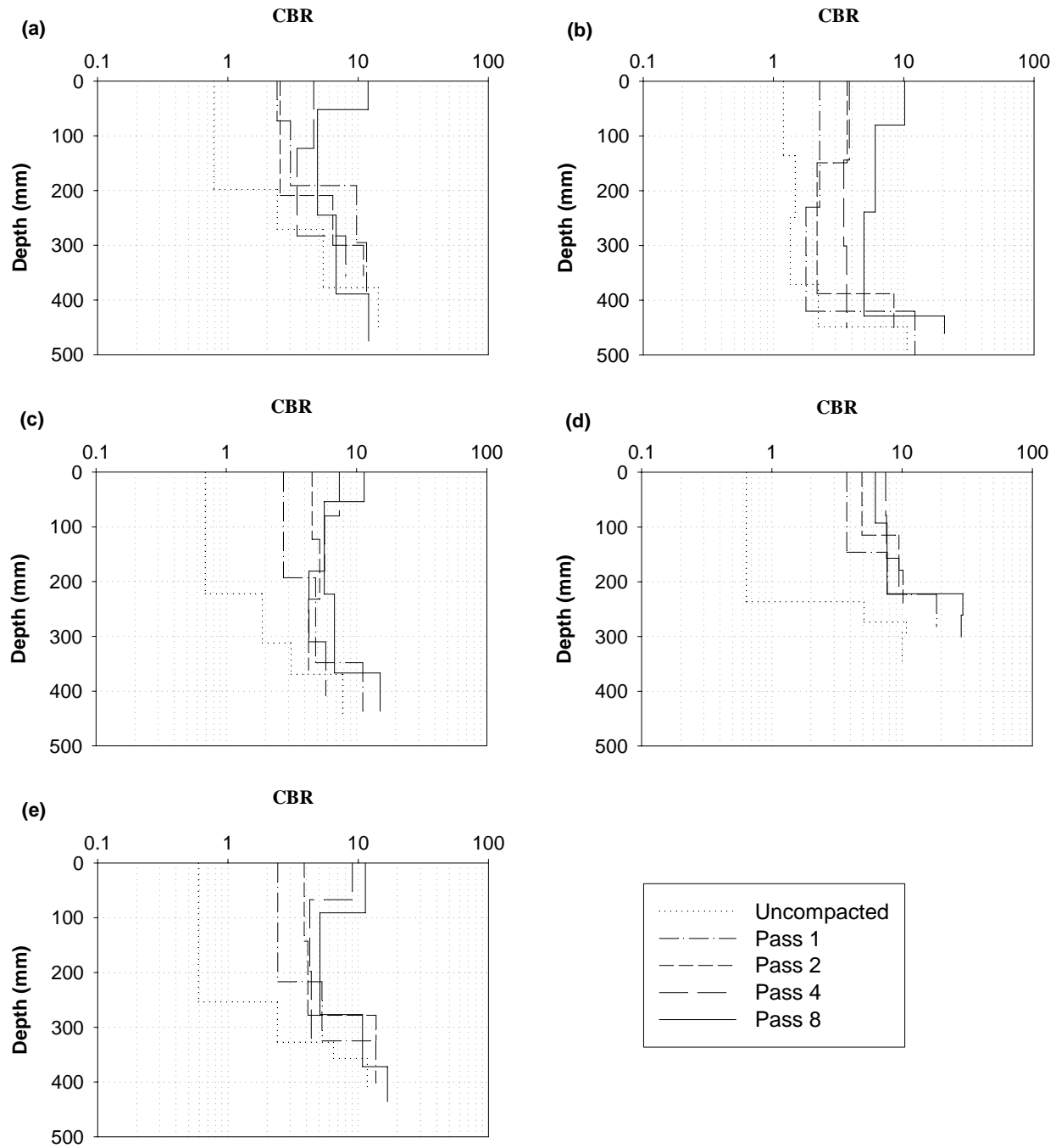


**Figure 143. Strip 5: (a) Pt 1, (b) Pt 2, (c) Pt 3, (d) Pt 4, and (e) Pt 5**

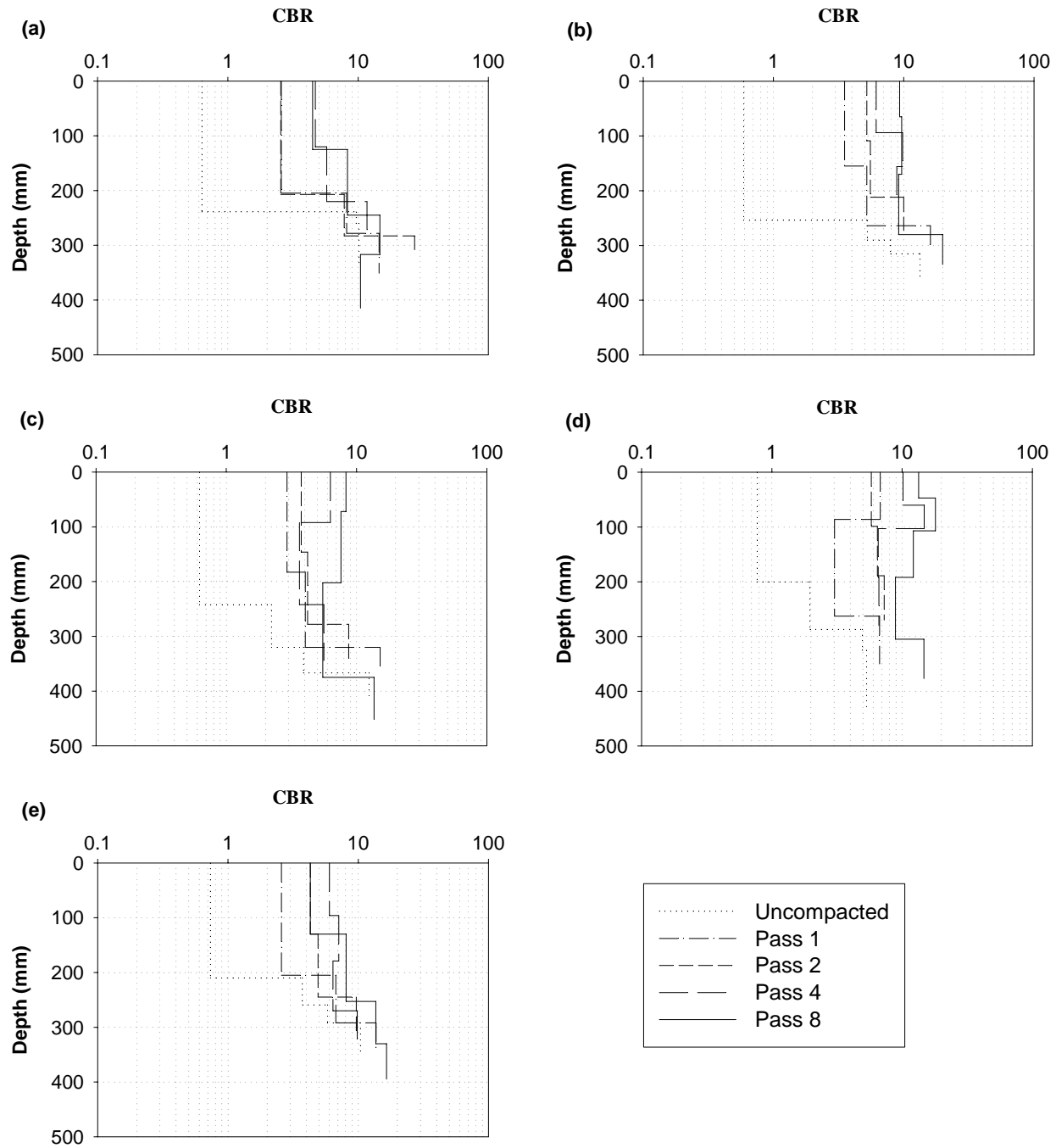


**Figure 144. Strip 5: (a) Pt 6, (b) Pt 7, (c) Pt 8, (d) Pt 9, and (e) Pt 10**

## APPENDIX E. PROJECT 2 PLATE LOAD TEST LOAD-DEFLECTION CURVES

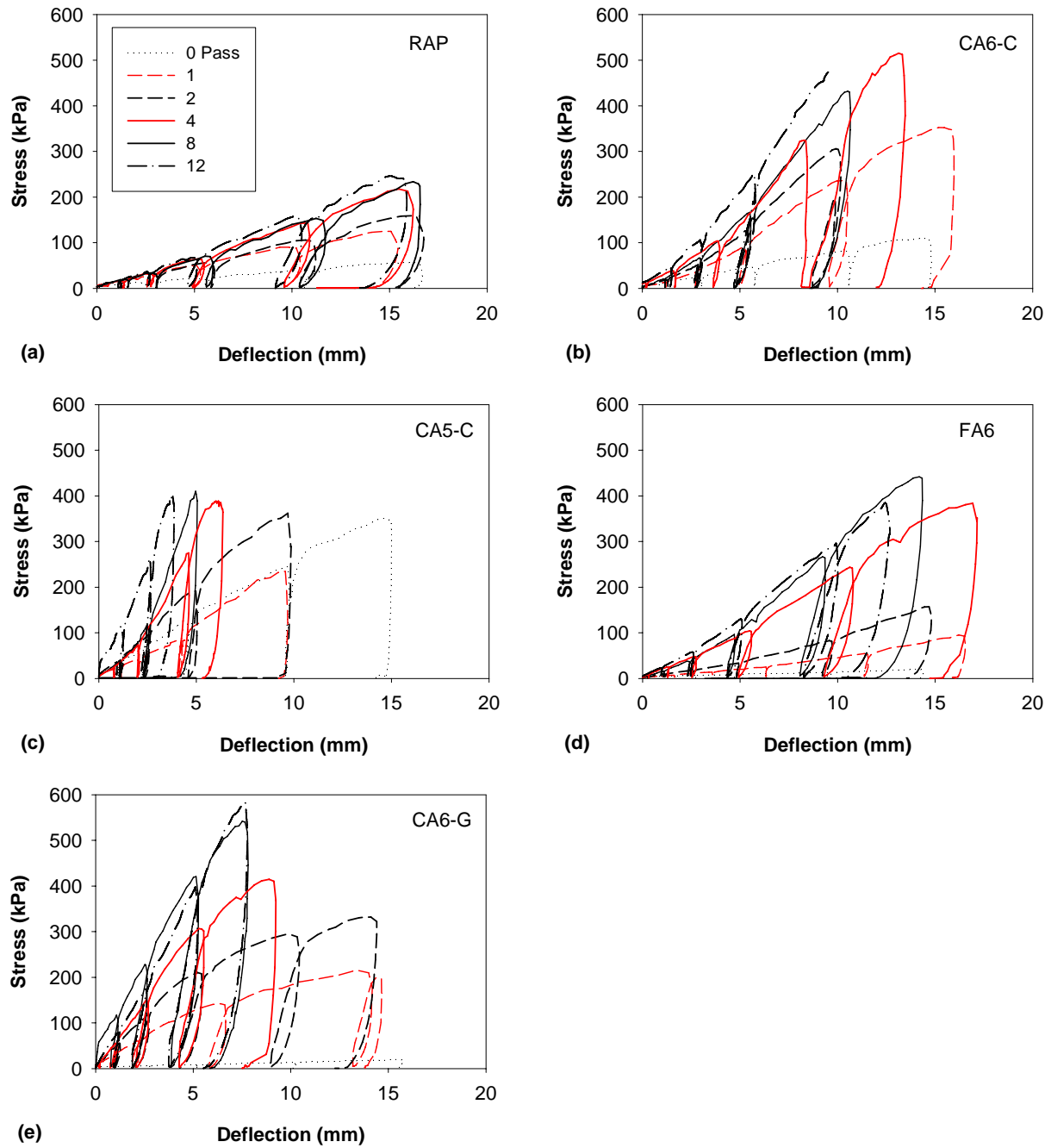


Figure 145. Plate load test load-deflection curves: (a) RAP, (b) CA6-C, (c) CA5-C, (d) FA6, and (e) CA6-G



## APPENDIX F. PROJECT 3 IN SITU TEST DATA

**Table 82. Summary of Spatial 2 in situ test data**

<b>Test Point</b>	<b>N</b>	<b>E</b>	<b>Dry Density</b>	<b>w (%)</b>	<b>CIV (20-kg)</b>	<b>CIV (4.5-kg)</b>	<b>DCPI (mm/blow)</b>	<b>E<sub>PFWD</sub> (MPa)</b>
1	4935.25	4811.94	19.98	9.5	3.7	5.3	42	7.5
2	4936.86	4819.42	20.22	8.7	4.4	6.4	31	7.4
3	4936.40	4823.31	20.50	9.3	3.6	7.1	33	11.4
4	4937.49	4825.62	20.39	8.8	2.9	5.8	41	6.6
5	4936.51	4833.06	20.06	8.9	0.0	4.0	48	5.1
6	4935.06	4833.89	20.33	9.5	3.7	4.6	46	6.5
7	4934.44	4839.05	20.31	8.2	4.5	6.2	30	8.6
8	4935.23	4842.58	20.23	7.1	5.2	10.3	21	29.9
9	4933.45	4849.69	19.90	6.8	5.4	12.7	34	16.2
10	4934.61	4852.62	19.20	5.9	6.5	9.1	39	18.9
11	4932.30	4855.26	20.04	8.0	5.7	8.2	32	8.3
12	4934.28	4858.86	20.08	8.4	4.7	9.0	36	9.3
13	4933.06	4865.02	20.34	8.0	4.9	6.8	44	9.1
14	4930.98	4866.47	20.47	8.0	5.4	7.3	32	13.4
15	4930.49	4872.28	20.15	7.6	7.0	7.6	31	18.5
16	4932.36	4874.87	20.15	8.1	7.0	8.6	34	14.4
17	4929.89	4880.12	20.25	7.9	5.5	8.4	43	9.6
18	4930.87	4886.35	20.61	8.3	7.0	8.4	35	13.8
19	4928.79	4888.99	20.23	7.5	6.0	8.0	29	11.1
20	4929.95	4893.31	20.50	8.6	5.7	5.5	39	8.4
21	4929.11	4898.87	20.58	8.4	6.5	8.0	34	12.0
22	4927.07	4900.77	20.25	6.7	7.3	8.4	35	11.9
23	4928.53	4904.85	20.11	7.1	7.8	11.0	35	17.2
24	4926.34	4906.14	19.81	7.4	5.2	6.7	39	17.9
25	4930.05	4815.05	19.92	7.2	5.7	6.0	30	9.9
26	4931.29	4815.82	20.23	8.3	5.7	7.8	35	10.0
27	4929.50	4819.93	20.41	8.2	5.4	6.3	24	10.1
28	4930.45	4822.47	20.25	8.5	2.2	5.9	38	7.0
29	4929.57	4828.94	20.39	9.1	0.0	5.8	44	6.1
30	4927.98	4833.89	20.04	8.5	3.6	4.9	35	8.0
31	4927.22	4838.32	20.67	7.7	5.5	10.6	22	16.8
32	4928.77	4841.43	20.23	7.8	5.2	9.9	21	24.3
33	4928.11	4846.42	20.14	8.0	7.3	7.7	29	19.8
34	4927.65	4852.18	20.04	7.9	4.5	9.7	29	17.2
35	4925.35	4855.18	19.60	9.0	4.7	7.8	31	17.2
36	4927.12	4858.01	20.26	7.1	4.5	7.2	30	16.2
37	4926.27	4862.62	20.25	8.3	4.0	13.5	41	10.6
38	4924.26	4866.88	20.39	8.0	3.6	7.6	33	15.0
39	4923.81	4870.37	20.55	6.7	5.4	7.5	32	15.9
40	4924.44	4874.19	20.88	7.2	7.0	7.8	33	13.3

**Table 83. Summary of Spatial 2 in situ test data**

Test Point	N	E	Dry Density	w (%)	CIV (20-kg)	CIV (4.5-kg)	DCPI (mm/blow)	E <sub>PFWD</sub> (MPa)
41	4922.58	4878.60	20.20	7.0	5.5	10.4	39	18.6
42	4923.43	4881.38	19.98	8.1	5.0	9.9	34	11.5
43	4921.60	4885.67	20.00	7.2	4.5	7.7	43	13.7
44	4922.66	4891.23	20.42	8.1	5.0	7.6	36	12.4
45	4922.32	4895.09	20.34	7.4	5.2	7.3	31	15.3
46	4920.57	4897.64	20.03	7.3	5.7	7.9	34	12.7
47	4919.68	4901.03	20.26	7.3	5.7	6.3	32	8.3
48	4920.92	4903.80	20.39	7.8	4.2	12.3	30	8.1
49	4919.90	4900.70	19.89	7.7	7.7	11.2	19	25.2
50	4925.26	4814.52	20.41	7.9	5.7	8.6	25	24.5
51	4922.66	4818.78	20.41	7.4	5.2	7.8	24	26.8
52	4923.30	4822.96	20.67	7.3	5.7	10.7	22	18.2
53	4921.42	4828.42	20.25	7.6	4.2	6.9	29	8.1
54	4922.55	4832.63	20.09	8.6	5.4	10.3	26	21.4
55	4920.29	4837.08	20.12	7.7	5.4	7.5	39	7.1
56	4921.92	4840.73	20.45	8.2	6.3	7.8	27	15.2
57	4918.58	4845.68	20.34	7.6	6.3	7.4	33	17.3
58	4920.68	4847.43	20.37	7.7	2.9	9.4	30	19.5
59	4919.67	4850.64	20.08	8.8	6.0	7.4	26	17.4
60	4918.47	4854.01	20.28	7.4	6.2	10.0	31	13.5
61	4917.82	4857.30	20.86	7.7	5.4	7.6	25	17.8
62	4918.77	4865.09	20.56	7.3	2.2	5.7	25	7.5
63	4916.06	4870.51	20.09	7.9	5.5	9.3	22	17.2
64	4918.00	4873.08	20.20	6.9	5.0	8.8	28	8.7
65	4915.08	4877.05	20.52	7.9	6.0	7.2	23	16.2
66	4916.07	4882.29	20.58	8.0	5.4	9.0	26	8.9
67	4914.33	4886.28	19.95	8.0	5.4	6.4	26	13.1
68	4915.84	4889.22	20.41	8.3	5.5	7.5	24	10.7
69	4915.43	4894.78	20.33	8.0	5.2	8.4	38	9.6
70	4912.97	4897.35	20.47	8.3	6.8	9.7	25	10.9
71	4912.57	4900.08	20.74	8.1	2.2	7.0	45	6.1
72	4913.58	4904.80	20.55	8.4	6.7	6.8	30	9.8
73	4918.59	4808.29	20.15	7.6	6.3	8.0	20	12.9
74	4917.93	4817.44	20.06	7.4	6.2	8.5	20	27.0
75	4916.10	4820.93	20.14	8.2	2.9	10.9	21	25.9
76	4915.17	4823.39	19.73	8.7	5.0	10.2	25	11.3
77	4916.66	4828.35	20.12	7.3	5.5	6.9	34	12.2
78	4916.00	4830.44	20.30	6.6	5.5	5.3	32	18.8
79	4914.04	4832.66	20.09	8.8	6.5	7.9	22	10.6
80	4914.33	4836.65	20.22	7.9	5.4	7.4	32	15.2

**Table 84. Summary of Spatial 2 in situ test data**

<b>Test Point</b>	<b>N</b>	<b>E</b>	<b>Dry Density</b>	<b>w (%)</b>	<b>CIV (20-kg)</b>	<b>CIV (4.5-kg)</b>	<b>DCPI (mm/blow)</b>	<b>E<sub>PFWD</sub> (MPa)</b>
81	4914.45	4845.01	19.98	8.6	4.7	6.7	26	17.6
82	4913.62	4848.51	20.17	9.3	5.2	5.6	28	11.9
83	4911.86	4851.02	20.55	8.6	4.9	7.8	40	13.8
84	4913.03	4854.49	20.34	8.3	2.7	8.9	30	11.6
85	4910.43	4862.17	20.12	9.0	2.1	6.0	27	7.3
86	4910.64	4865.12	19.79	8.4	4.2	8.8	25	11.8
87	4910.88	4868.54	19.98	8.0	4.9	8.5	24	7.9
88	4909.24	4871.20	20.50	7.9	6.8	10.2	22	10.9
89	4910.38	4877.26	20.06	9.1	4.2	9.4	30	7.5
90	4907.94	4881.23	20.55	7.4	4.0	8.0	19	10.8
91	4909.58	4884.57	20.33	8.1	3.4	8.9	28	6.4
92	4907.51	4887.90	20.55	7.6	5.0	10.4	22	19.4
93	4906.77	4892.77	20.75	7.7	5.2	7.3	40	11.7
94	4907.69	4895.96	20.06	7.1	6.0	6.3	32	16.0
95	4906.33	4898.28	20.08	7.0	5.0	11.0	37	14.4
96	4906.99	4902.38	20.42	7.9	3.9	7.6	31	9.8
97	4917.47	4805.39	20.59	7.3	6.7	7.9	22	18.1
98	4910.23	4816.49	20.85	7.8	6.0	8.5	24	14.6
99	4908.35	4819.56	19.89	7.9	5.2	8.8	22	24.2
100	4910.36	4821.99	20.06	6.8	6.3	6.9	22	19.6
101	4908.68	4830.09	20.23	7.7	5.5	9.4	23	12.5
102	4906.84	4836.20	19.70	8.6	2.2	7.8	28	14.2
103	4908.17	4838.90	20.09	8.0	5.2	8.2	28	16.7
104	4905.67	4839.74	20.61	8.6	5.0	6.1	24	16.3
105	4905.90	4846.63	20.03	7.7	5.0	9.4	26	15.4
106	4904.40	4850.31	20.45	7.8	4.5	7.7	30	11.3
107	4906.18	4852.15	20.09	8.1	4.7	6.6	27	10.5
108	4905.44	4856.21	20.36	7.8	2.7	6.5	31	18.2
109	4903.08	4862.23	20.55	7.9	5.5	10.6	17	20.0
110	4903.80	4867.36	20.09	8.0	4.7	7.3	25	17.0
111	4901.78	4869.24	20.77	7.5	5.7	8.0	23	19.1
112	4903.55	4872.46	19.76	7.5	4.7	6.8	21	17.9
113	4901.09	4878.16	20.56	8.0	6.2	10.0	19	13.5
114	4900.57	4882.66	20.99	7.9	6.8	7.5	24	7.8
115	4901.99	4884.85	20.45	8.2	6.0	8.2	20	17.4
116	4900.14	4888.66	20.61	8.3	5.5	7.4	23	22.1
117	4901.07	4892.47	19.92	9.1	5.4	9.8	28	10.8
118	4898.79	4894.12	20.28	8.7	5.4	6.7	30	8.2
119	4898.66	4896.43	20.53	7.8	6.5	7.1	30	10.4
120	4899.96	4901.48	19.97	8.0	3.4	6.3	30	9.1

**Table 85. Summary of Spatial 2 in situ test data**

<b>Test Point</b>	<b>N</b>	<b>E</b>	<b>Dry Density</b>	<b>w (%)</b>	<b>CIV (20-kg)</b>	<b>CIV (4.5-kg)</b>	<b>DCPI (mm/blow)</b>	<b>E<sub>PFWD</sub> (MPa)</b>
121	4904.45	4805.23	20.04	8.3	6.3	8.6	21	21.4
122	4903.73	4815.90	20.31	6.7	4.7	6.2	29	16.2
123	4900.92	4818.91	19.45	8.6	5.5	9.5	18	33.4
124	4902.44	4820.66	20.23	8.0	5.5	9.1	18	22.4
125	4900.29	4824.42	20.00	7.8	3.6	5.8	43	6.1
126	4900.71	4828.39	19.84	7.2	6.3	8.4	22	17.4
127	4901.79	4831.54	20.45	7.3	6.7	9.3	23	18.8
128	4899.51	4832.94	20.45	7.9	4.9	7.3	27	12.5
129	4900.41	4840.32	20.34	8.3	6.0	10.3	30	14.0
130	4899.58	4844.10	19.92	8.4	2.2	6.5	25	11.3
131	4897.50	4848.09	20.31	7.9	5.8	8.2	30	9.8
132	4898.63	4851.06	20.45	7.6	2.2	5.8	31	11.7
133	4898.42	4858.54	20.55	8.6	6.5	10.7	16	24.9
134	4896.03	4861.27	20.25	6.6	6.2	9.1	25	14.4
135	4897.06	4866.00	20.52	7.3	7.7	7.5	20	12.9
136	4894.97	4869.87	20.48	7.7	3.1	12.6	23	15.4
137	4895.94	4875.81	20.44	8.5	6.5	12.3	22	11.6
138	4895.37	4879.31	20.88	8.1	6.7	8.8	22	15.0
139	4894.02	4881.56	20.42	8.7	5.0	7.1	24	18.3
140	4895.05	4885.39	20.34	8.3	6.3	8.6	24	20.4
141	4894.57	4890.07	20.56	7.8	2.2	6.7	27	9.9
142	4892.24	4892.59	19.49	9.8	4.9	8.0	25	15.4
143	4891.62	4895.75	20.56	8.1	5.4	7.4	27	12.2
144	4893.04	4901.70	19.84	9.0	4.2	5.8	24	13.3
145	4898.00	4805.93	19.68	7.0	5.8	10.9	25	22.4
146	4896.86	4813.10	20.09	7.8	6.0	7.6	22	21.6
147	4895.36	4816.46	20.70	8.0	7.3	8.8	21	16.7
148	4893.90	4819.74	20.64	8.3	6.5	10.0	23	11.5
149	4894.48	4827.06	20.39	8.4	4.2	7.8	33	14.0
150	4893.95	4831.77	20.22	8.0	5.8	7.5	29	14.6
151	4892.24	4833.66	20.37	8.5	4.5	6.6	35	13.4
152	4891.63	4836.76	20.23	8.2	6.7	11.1	38	10.8
153	4891.98	4843.73	20.42	8.1	2.2	11.2	22	30.8
154	4890.16	4846.43	20.30	7.7	6.2	8.8	23	20.9
155	4889.58	4850.97	20.75	7.1	5.5	8.4	25	9.8
156	4891.08	4855.77	20.44	8.3	5.0	6.9	27	10.8
157	4888.19	4861.27	20.11	6.8	6.5	11.7	35	18.7
158	4887.84	4864.42	20.11	5.9	5.8	6.4	28	15.4
159	4889.81	4866.44	20.25	7.6	5.5	10.3	66	14.2
160	4889.45	4870.19	20.72	6.9	7.2	10.3	26	21.4

**Table 86. Summary of Spatial 2 in situ test data**

<b>Test Point</b>	<b>N</b>	<b>E</b>	<b>Dry Density</b>	<b>w (%)</b>	<b>CIV (20-kg)</b>	<b>CIV (4.5-kg)</b>	<b>DCPI (mm/blow)</b>	<b>E<sub>PFWD</sub> (MPa)</b>
161	4888.06	4876.44	20.78	8.5	3.6	13.4	20	20.9
162	4886.12	4879.14	20.58	7.6	5.7	11.2	18	16.5
163	4885.90	4883.16	20.42	7.2	6.0	16.5	19	23.0
164	4887.75	4885.46	21.14	7.3	7.5	10.3	19	17.9
165	4884.83	4889.82	20.56	7.5	5.7	11.9	29	17.9
166	4886.21	4891.87	20.33	7.7	2.2	8.3	33	17.2
167	4886.54	4892.10	20.53	7.8	5.5	6.2	30	14.2
168	4886.26	4899.94	20.61	9.1	2.2	15.5	30	8.3
169	4888.62	4810.52	20.15	7.6	5.7	11.0	26	27.9
170	4889.50	4813.82	19.97	7.4	5.7	7.4	40	21.0
171	4888.32	4816.26	20.28	7.7	4.4	11.0	34	17.7
172	4887.81	4819.52	19.78	7.6	6.5	8.4	34	30.4
173	4886.47	4823.70	20.70	7.8	7.7	11.9	20	33.1
174	4886.64	4827.20	20.06	8.4	5.4	9.6	19	35.6
175	4887.45	4829.91	20.34	8.7	6.2	9.1	20	31.4
176	4885.37	4833.71	20.63	7.2	6.5	8.1	31	12.7
177	4886.24	4839.89	20.83	7.7	6.8	8.3	25	21.9
178	4883.43	4841.46	19.87	7.2	7.7	9.1	25	32.1
179	4885.39	4848.43	20.36	7.1	6.5	12.2	20	27.7
180	4882.63	4850.38	20.00	6.4	6.0	9.2	36	21.3
181	4884.32	4855.87	20.34	6.9	6.2	8.8	18	25.5
182	4881.44	4860.48	20.45	6.9	6.7	10.1	17	20.8
183	4883.73	4864.36	20.37	8.0	6.3	9.8	19	15.9
184	4881.14	4866.58	20.39	7.5	6.7	13.7	29	14.7
185	4880.61	4871.87	20.25	7.2	6.5	10.8	17	31.6
186	4880.03	4876.26	20.58	8.2	5.0	10.1	18	10.0
187	4881.48	4879.82	20.78	7.9	6.5	7.8	20	12.3
188	4880.85	4883.68	20.69	6.8	6.2	8.6	22	14.5
189	4880.25	4889.07	20.25	7.5	5.5	6.4	28	11.3
190	4880.07	4891.17	20.47	7.0	6.2	7.5	19	21.6
191	4878.08	4894.66	20.58	7.4	5.8	7.1	20	20.9
192	4878.99	4898.34	20.30	8.9	4.4	6.5	22	17.3

**Table 87. Summary of Spatial 3 in situ test data**

Test Point	N	E	Dry Density	w (%)	CIV (20-kg)	CIV (4.5-kg)	DCPI (mm/blow)	E <sub>PFWD</sub> (MPa)
1	4931.21	4879.94	20.53	7.5	2.2	6.6	4	5.1
2	4929.08	4879.15	20.36	7.1	0.0	5.1	3	3.8
3	4929.41	4884.13	20.19	7.1	0.0	7.1	5	5.2
4	4930.13	4887.63	20.22	6.6	2.2	7.6	6	5.6
5	4929.88	4891.33	20.15	5.9	5.5	7.4	5	5.2
6	4927.93	4891.33	19.89	7.5	5.5	10.8	6	5.9
7	4929.32	4893.29	19.01	7.2	0.0	3.3	3	4.8
8	4927.46	4893.31	19.12	7.2	0.0	5.6	3	3.9
9	4928.10	4898.43	18.11	6.7	0.0	4.5	4	5.6
10	4928.89	4901.93	18.82	6.9	0.0	5.6	5	6.5
11	4928.62	4909.16	19.97	8.6	6.5	9.0	7	6.2
12	4926.19	4908.51	20.20	8.1	2.4	5.1	9	10.4
13	4927.94	4912.61	19.54	11.0	10.1	13.3	12	53.8
14	4926.34	4912.59	19.20	12.3	9.3	14.9	12	52.4
15	4926.02	4916.40	18.96	13.0	7.7	12.3	12	52.0
16	4927.10	4919.11	19.34	12.5	10.8	19.4	17	55.6
17	4926.84	4922.87	18.35	11.7	9.5	16.6	13	79.6
18	4923.84	4923.23	19.57	11.0	12.7	20.4	21	99.7
19	4923.98	4879.54	19.56	6.9	0.0	7.6	5	7.5
20	4922.32	4877.80	20.31	6.0	7.0	10.6	6	6.8
21	4921.68	4883.04	19.20	6.3	2.1	5.3	4	4.5
22	4923.34	4885.13	19.70	6.2	3.9	5.1	4	5.1
23	4922.98	4890.03	19.82	7.8	0.0	6.2	4	5.9
24	4920.77	4890.41	20.22	5.9	2.1	5.7	4	4.6
25	4923.01	4892.74	19.10	7.1	0.0	4.6	5	6.0
26	4920.71	4892.24	19.05	7.3	2.1	4.8	3	5.5
27	4922.15	4896.05	19.48	7.4	3.6	5.0	7	7.4
28	4920.32	4899.50	19.38	7.7	4.4	6.1	3	4.5
29	4921.39	4908.76	20.20	8.7	6.2	6.4	5	5.0
30	4919.35	4908.84	20.33	9.1	5.2	5.2	6	5.4
31	4920.21	4911.38	18.74	14.5	6.8	11.6	13	24.0
32	4918.27	4912.54	19.82	12.4	9.1	12.1	16	42.9
33	4918.44	4916.13	19.01	12.8	9.0	15.9	13	48.1
34	4919.18	4918.16	19.62	11.7	9.9	15.5	17	90.4
35	4919.60	4918.54	18.61	11.8	10.3	19.7	16	59.1
36	4918.03	4922.15	19.07	12.0	10.6	15.1	10	45.5
37	4917.72	4876.98	20.52	6.7	5.0	9.9	8	7.2
38	4915.02	4876.67	20.14	6.5	6.7	7.2	7	7.1
39	4916.88	4881.31	20.42	7.1	5.4	6.6	5	7.5
40	4915.47	4884.60	20.59	7.3	5.2	5.2	4	6.7

**Table 88. Summary of Spatial 3 in situ test data**

<b>Test Point</b>	<b>N</b>	<b>E</b>	<b>Dry Density</b>	<b>w (%)</b>	<b>CIV (20-kg)</b>	<b>CIV (4.5-kg)</b>	<b>DCPI (mm/blow)</b>	<b>E<sub>PFWD</sub> (MPa)</b>
41	4916.40	4888.62	20.28	7.5	5.5	11.5	6	8.2
42	4914.10	4888.25	19.79	7.6	4.2	8.0	5	7.6
43	4916.33	4892.45	18.83	8.0	3.1	7.9	5	5.5
44	4914.53	4891.83	19.02	8.3	4.9	5.6	6	4.9
45	4913.86	4898.64	19.42	7.7	3.9	11.4	4	6.4
46	4914.01	4904.79	19.07	8.1	3.1	4.7	3	5.4
47	4914.19	4907.88	20.25	8.9	4.2	4.4	5	5.7
48	4911.97	4907.65	19.81	8.3	4.9	5.4	6	5.7
49	4914.35	4910.83	18.94	11.8	11.9	12.4	12	67.5
50	4911.62	4910.48	19.79	13.5	9.6	12.6	12	56.9
51	4911.96	4913.68	18.08	14.5	9.1	7.0	14	49.1
52	4913.08	4916.55	18.93	13.9	7.7	13.5	14	20.0
53	4913.60	4920.89	18.54	13.2	8.8	16.3	14	46.7
54	4910.79	4921.36	18.72	11.5	9.8	14.8	15	78.5
55	4910.84	4872.76	19.48	7.3	3.4	4.6	3	5.8
56	4908.05	4877.06	20.36	6.5	6.7	10.6	5	5.7
57	4908.84	4881.16	20.26	6.1	4.4	7.6	5	6.3
58	4907.27	4884.18	20.81	7.7	2.7	7.1	5	6.2
59	4909.10	4887.37	20.94	7.0	5.2	9.8	7	6.9
60	4906.55	4887.28	20.75	6.8	4.0	7.9	5	5.5
61	4908.44	4890.45	19.57	6.7	4.7	5.8	7	6.9
62	4906.40	4890.49	19.01	6.6	4.7	4.9	6	7.7
63	4907.38	4896.37	19.68	7.6	3.4	5.4	6	5.8
64	4905.55	4899.12	19.68	7.4	3.7	5.0	5	5.4
65	4907.11	4906.23	20.25	8.9	3.9	4.1	3	6.1
66	4904.98	4905.89	19.57	8.4	2.9	5.1	4	9.3
67	4906.69	4910.04	18.98	11.2	11.1	23.9	19	78.1
68	4904.06	4909.55	19.24	11.2	10.6	19.9	17	57.4
69	4905.59	4914.27	18.88	11.5	9.3	11.9	13	18.6
70	4903.63	4916.26	19.34	10.2	12.4	20.8	16	92.9
71	4905.86	4921.31	19.01	9.7	9.8	16.8	17	61.6
72	4901.52	4920.49	19.07	11.9	11.9	20.8	19	55.4
73	4902.92	4875.46	20.28	6.9	3.6	6.4	8	6.3
74	4900.79	4874.58	20.22	7.4	6.0	7.8	9	10.8
75	4900.52	4879.88	20.70	5.5	3.9	0.9	7	7.9
76	4902.09	4882.33	20.86	7.5	3.1	4.9	4	5.8
77	4902.26	4885.76	20.58	7.3	6.0	7.4	6	6.4
78	4899.96	4885.96	20.97	6.2	5.2	6.6	5	6.4
79	4901.01	4889.90	19.43	6.1	2.9	5.5	5	6.5
80	4899.18	4889.54	19.23	6.1	3.6	4.6	5	6.1

**Table 89. Summary of Spatial 3 in situ test data**

Test Point	N	E	Dry Density	w (%)	CIV (20-kg)	CIV (4.5-kg)	DCPI (mm/blow)	E <sub>PFWD</sub> (MPa)
81	4899.14	4896.87	18.60	7.3	2.7	3.8	4	5.2
82	4899.84	4901.09	18.90	6.4	2.1	6.3	4	5.4
83	4899.91	4905.88	20.41	7.3	5.7	9.0	9	13.3
84	4897.48	4905.71	20.52	7.3	5.4	7.0	6	5.6
85	4900.49	4909.50	17.64	7.9	11.4	22.8	14	68.5
86	4896.77	4908.45	18.94	11.4	10.8	16.7	17	32.6
87	4896.67	4912.42	18.40	11.2	10.9	17.5	17	75.0
88	4899.00	4915.96	19.95	11.4	11.6	23.9	20	88.5
89	4899.16	4920.35	18.63	11.4	10.3	19.3	17	99.3
90	4895.52	4919.75	18.76	11.5	9.9	19.9	19	65.1
91	4896.57	4875.49	20.59	6.7	4.7	8.5	8	6.0
92	4893.57	4873.71	19.97	5.9	6.0	6.3	7	6.1
93	4895.44	4879.01	20.77	6.8	4.0	6.8	6	5.7
94	4893.13	4882.44	20.86	6.0	4.7	9.4	6	5.8
95	4895.00	4885.57	20.74	6.9	2.2	8.7	4	5.7
96	4891.97	4885.35	20.25	6.2	4.9		6	6.7
97	4894.58	4888.80	19.24	7.0	2.6		3	6.9
98	4892.27	4888.70	19.34	6.4	4.3		5	7.0
99	4893.80	4892.28	19.43	6.3	4.4		5	6.4
100	4891.86	4896.61	18.94	6.3	2.6		3	7.8
101	4892.85	4903.77	20.26	7.8	4.7		5	10.4
102	4890.79	4903.85	20.28	7.0	5.0		5	9.5
103	4893.26	4909.07	18.76	10.4	9.8		17	95.5
104	4890.31	4908.79	18.77	11.7	9.2		18	71.8
105	4890.20	4912.40	18.76	11.6	8.8		13	55.6
106	4891.59	4915.43	18.68	9.5	11.6		17	54.0
107	4892.21	4919.47	19.40	10.2	8.8		15	36.3
108	4887.95	4918.91	18.66	10.1	11.3		21	79.2
109	4888.85	4874.44	20.26	6.7	5.7	8.3	6	6.1
110	4886.14	4872.97	20.39	6.5	7.8	11.3	11	10.2
111	4886.38	4877.86	20.86	6.7	7.8	11.2	9	9.4
112	4887.83	4880.22	20.28	6.5	5.2	6.5	6	5.7
113	4887.99	4884.77	20.63	7.3	4.2	13.8	7	7.5
114	4884.62	4884.15	21.07	6.7	7.5	11.4	8	7.2
115	4887.38	4887.29	19.07	5.9	4.2	6.2	7	9.3
116	4885.25	4886.99	18.94	7.3	3.4	5.1	6	9.5
117	4885.89	4893.78	17.59	7.2	3.1	8.0	4	5.0
118	4884.50	4900.38	19.70	7.7	0.1	4.4	3	5.8
119	4885.90	4903.44	18.99	5.7	2.7	6.4	7	5.3
120	4883.62	4902.90	19.78	9.2	3.7	4.2	5	5.4

**Table 90. Summary of Spatial 3 in situ test data**

<b>Test Point</b>	<b>N</b>	<b>E</b>	<b>Dry Density</b>	<b>w (%)</b>	<b>CIV (20-kg)</b>	<b>CIV (4.5-kg)</b>	<b>DCPI (mm/blow)</b>	<b>E<sub>PFWD</sub> (MPa)</b>
121	4885.86	4906.39	17.47	11.3	10.9	15.7	19	56.9
122	4882.69	4905.98	16.76	10.6	7.3	17.6	17	29.7
123	4882.85	4911.23	18.22	10.2	11.3	24.3	18	97.7
124	4884.61	4914.99	16.26	10.1	11.7	23.6	22	94.6
125	4884.75	4918.64	19.38	10.9	11.1	21.3	20	71.9
126	4880.59	4918.72	18.93	9.6	11.7	21.2	19	83.8
127	4880.10	4918.64	20.52	7.2	8.1	9.3	10	8.7
128	4880.04	4871.74	20.45	6.4	6.7	13.1	14	10.9
129	4882.32	4875.26	20.97	7.1	9.5	17.6	10	7.6
130	4880.15	4877.61	19.92	7.7	3.4	6.1	7	6.0
131	4881.62	4883.18	21.24	5.8	8.8	21.0	9	7.9
132	4878.64	4883.03	20.30	7.1	8.3	9.4	6	5.4
133	4880.56	4886.26	18.87	5.3	4.0	6.5	7	9.0
134	4878.12	4886.01	18.50	7.0	4.4	5.7	5	9.6
135	4879.65	4890.08	19.37	6.5	3.7	5.5	4	14.8
136	4878.53	4893.34	19.34	6.8	4.4	5.4	5	16.8
137	4878.40	4902.07	19.70	7.4	2.2	6.0	5	8.4
138	4876.59	4902.12	20.78	6.3	3.9	6.5	5	6.9
139	4877.62	4905.45	18.07	11.0	7.7	16.2	20	69.9
140	4875.00	4905.15	17.12	10.3	7.7	28.3	22	53.9
141	4876.90	4909.11	17.94	11.3	11.7	18.5	16	41.9
142	4874.21	4911.77	18.77	10.4	11.7	28.1	23	88.0
143	4877.22	4916.19	18.80	10.9	10.9	26.2	22	81.7
144	4873.82	4915.70	18.10	9.4	13.6	19.5	19	80.2